Essays in International Trade and Spatial Economics

by

Elliot Kang

A dissertation submitted in partial fulfillment
of the requirements for the degree of
Doctor of Philosophy
(Economics)
in the University of Michigan
2025

Doctoral Committee:

Professor Andrei A. Levchenko, Co-Chair
Associate Professor Sebastian Sotelo, Co-Chair
Professor Costas Arkolakis, Yale University
Professor Jagadeesh Sivadasan

Elliot Kang
emkang@umich.edu
ORCID iD: 0000-0003-3071-9641

© Elliot Kang 2025

DEDICATION

This dissertation is dedicated to everyone who supported me throughout this academic journey.

ACKNOWLEDGEMENTS

I would like to express my sincere appreciation to those who have contributed to my academic journey and the completion of this dissertation. The path to completing a PhD is rarely traveled alone, and I have been fortunate to have had exceptional support throughout this challenging yet rewarding process.

I am especially grateful to my chairs, Andrei A. Levchenko and Sebastian Sotelo, whose guidance and support have been essential in shaping my research and career. They dedicated countless hours to discussing my research, patiently providing insightful feedback that fundamentally improved my work. Their willingness to share their expertise, challenge my thinking, and encourage my intellectual growth has made a significant difference in my academic development. The rigorous training I received under their mentorship has equipped me with invaluable skills that will benefit me throughout my career.

I extend my thanks to my committee members Jagadeesh Sivadasan and Costas Arkolakis for their valuable criticism and constructive feedback. Their perspectives broadened my understanding of the field and pushed me to consider alternative approaches that I might otherwise have overlooked. Their insights have substantially improved this dissertation and helped me refine my ideas and approach.

I appreciate my coauthors for the opportunity to explore new perspectives together, and I thank the faculty at the University of Michigan for their helpful comments during presentations and meetings, which have enhanced the quality of my work. The vibrant intellectual environment fostered by the Economics Department provided fertile ground for developing ideas.

My time in Ann Arbor was enriched by my fellow PhD students and friends, whose companionship made these years both productive and enjoyable. I cherish the friendship we shared throughout this challenging period.

I am very thankful to my parents and parents-in-law for their consistent support during my studies. Their encouragement has been a source of strength throughout this process. They not only provided emotional support but also practical assistance in numerous ways that allowed me to focus on my research.

My daughter Audrey has been the greatest joy in this journey. Her arrival in the midst of my doctoral studies brought perspective to my life, reminding me daily of what truly matters.

Finally, I reserve special gratitude for my wife Susie. Her patience, understanding, and unwavering support have been essential to my graduation, and words cannot adequately express my appreciation for her presence in my life. Her love and support have been the foundation upon which this work was built. This achievement is as much hers as it is mine, for without her partnership, this journey would have been immeasurably more difficult, if not impossible.

TABLE OF CONTENTS

DEDICATION ii

ACKNOWLEDGEMENTS iii

LIST OF FIGURES vii

LIST OF TABLES ix

LIST OF APPENDICES xi

ABSTRACT xii

CHAPTER

1 Global Fisheries: Quantifying the Externalities from Open Access 1

1.1 Introduction 1
1.2 Data 6
1.3 Empirical Patterns 9
1.4 A Model of Global Fishery 13
1.4.1 Environment 14
1.4.2 Decentralized Equilibrium 17
1.4.3 Planner's Problem 20
1.4.4 Optimal Policy 22
1.5 Taking the Model to Data 23
1.5.1 Calibration of Elasticities of Substitutions 23
1.5.2 Calibration of Remaining Parameters 28
1.5.3 Model Fit 29
1.6 Quantitative Results 29
1.6.1 Decentralized Equilibrium (Business As Usual) and Planner 30
1.6.2 Policy Counterfactual: Eliminating Fuel Subsidies 32
1.7 Conclusion 35

2 Deforestation: A Global and Dynamic Perspective 37

2.1 Introduction 37
2.2 Data sources 42
2.3 Empirical Patterns about Global Deforestation 43
2.4 Theory 48

2.4.1 Environment . . . 49
2.4.2 Expenditures and Market Clearing Conditions. . . . 53
2.4.3 Evolution of Labor, Land and Forest Area . . . 54
2.4.4 Equilibrium . . . 54
2.5 Analytical Results . . . 55
2.6 Taking the Model to Data . . . 58
2.6.1 Calibration of the Baseline Static Equilibrium . . . 59
2.6.2 Calibration of Dynamics-related Parameters . . . 59
2.6.3 Calibration of the Land-producing Technology . . . 59
2.6.4 Components of Trade Costs . . . 61
2.7 Counterfactual Analysis . . . 61
2.7.1 The Path of Forests . . . 61
2.7.2 The Roles of Structural Change and Comparative Advantage . . . 63
2.7.3 Incorporating Population Growth . . . 65
2.7.4 The Deforestation Impact of Raising Trade Costs . . . 67
2.7.5 Carbon Heterogeneity, Dynamics, and Reforestation. . . . 68
2.8 Conclusion . . . 70

3 Playing with Blocs: Quantifying Decoupling . . . 72

3.1 Introduction . . . 72
3.2 Data, Basic Facts, and Bloc Classification . . . 77
3.2.1 Data . . . 77
3.2.2 Bloc Classification . . . 77
3.3 Quantitative Framework . . . 79
3.3.1 Setup . . . 79
3.3.2 Calibration . . . 83
3.3.3 Baseline Trade Cost Change Scenario . . . 84
3.3.4 Counterfactuals . . . 86
3.3.5 Robustness and Sensitivity . . . 89
3.3.6 Determinants of Trade Changes . . . 92
3.4 Conclusion . . . 95

APPENDICES . . . 96

BIBLIOGRAPHY . . . 148

LIST OF FIGURES

FIGURE

1.1 Global Catch and Stock of Big Eye Tuna (2018, in tonnes) . . . 7
1.2 Global Fishery Stock over Time (1980-2018) . . . 10
1.3 Declaration of EEZ and Fishery Stock . . . 11
1.4 Model Fit . . . 30
1.5 Dynamic Path of Outcomes: BAU and Planner . . . 32
1.6 Average Stock to Capacity Ratio (BAU and Planner) . . . 33
1.7 Average Stock to Capacity Ratio (Counterfactual SS relative to BAU SS) . . . 35

2.1 Forest and Deforestation across the World (1990-2020) . . . 44
2.2 Change in Share of Land in Forest versus Share of Land in Agriculture (1990-2020) 45
2.3 Change in Agricultural Land and Forest Area against Comparative Advantage in Agriculture . . . 46
2.4 Change in Forest and Agricultural Area on Population Growth . . . 47
2.5 Multilateral versus Unilateral Trade Cost Reduction: Change in Global Forest Area relative to Baseline . . . 62
2.6 Multilateral versus Unilateral Trade Cost Reduction: Select Countries . . . 63
2.7 The Role of the Elasticity of Substitution, σ . . . 64
2.8 The Role of Comparative Advantage . . . 65
2.9 The Role of Population Growth . . . 66
2.10 Change in Forest Share versus Population . . . 67

3.1 Trade/GDP Ratios . . . 73
3.2 Change in Trade Costs with the US and China (2015-2023) . . . 79
3.3 Baseline Change in Trade Costs (2015-2023) . . . 85
3.4 Baseline Change in Real GDP and Real Income (2015-2023) . . . 87
3.5 Counterfactual Real GDP Changes (2015-2023) . . . 90
3.6 Bilateral Trade Flows and Political Alignment: Coefficient on UN Agreement (β_t^{UN}) 94

A.1 Relationship between κ and β_1 . . . 100
A.2 Dynamic Path of Outcomes: BAU and Counterfactual . . . 100
A.3 Average Stock to Capacity Ratio . . . 101

B.1 Carbon Stock per Hectare across the World . . . 132
B.2 Model Fit . . . 132
B.3 Multilateral vs Unilateral Trade Cost Increase: Change in Global Forest Area . . . 133

C.1 Counterfactual Real Income Changes (2015-2023) . . . 140
C.2 Bilateral Tariff Changes, 2021-2015 . . . 141

C.3 Density of Percentages, Leiden Algorithm 142
C.4 Model implied Trade Cost and Head-Ries Trade Cost 147

LIST OF TABLES

TABLE

1.1 Fishery Subsidies and High Sea Production (2002-2018) . . . 13
1.2 Estimation of η . . . 25
1.3 Estimation of ν . . . 27
1.4 Parameter Calibration . . . 29
1.5 Quantitative Results: BAU and Planner . . . 31
1.6 Quantitative Results: BAU and Counterfactual . . . 34

2.1 The Relationship between Population Growth and Forest Area (30 Years Interval) . . . 48
2.2 Parameter Calibration . . . 58
2.3 Social Costs of Deforestation under Different Trade Integration Scenarios . . . 70

3.1 Change in Trade (2015-2023) . . . 74
3.2 Log Change in Average Trade Cost between Blocs (187 countries, 2015-2023) . . . 78
3.3 Parameter Values . . . 83
3.4 Log Change in Average Trade Costs between Blocs (2015-2023) . . . 86
3.5 Baseline Change in Real GDP and Real Income, Percentage Points (2015-2023) . . . 86
3.6 Counterfactual GDP and Real Income, Percentage Points (2015-2023) . . . 91
3.7 Explanatory Variables for Trade Flow Changes . . . 93

A.1 List of Fishing Location . . . 96
A.2 List of Fishery Species . . . 96
A.3 List of Countries . . . 97
A.4 Summary Statistics of Fishery Stock . . . 98
A.5 Summary Statistics of Fuel Subsidies . . . 99

B.1 Mapping of Countries to Regions . . . 126
B.2 Summary Statistics by Regions (1990-2020) . . . 127
B.3 Counterfactual Changes in Forest Area . . . 128
B.4 Summary Statistics by Country (1990-2020) - First Part . . . 129
B.5 Summary Statistics by Country (1990-2020) - Second Part . . . 130
B.6 Summary Statistics by Country (1990-2020) - Third Part . . . 131

C.1 Country List . . . 134
C.2 Sector Key . . . 135
C.3 Bloc Assignment, 187 Countries (2015-2023) . . . 136
C.4 Bloc Assignment, 66 Model Countries (2015-2023) . . . 139
C.5 Bloc Comparison, Community Detection Algorithm and Baseline Classification . . . 143
C.6 Bloc Comparison, Baseline 2015 versus Baseline 2016 (All Countries) . . . 143

C.7 Bloc Comparison, Baseline 2015 versus Baseline 2016 (Model Countries) 144
C.8 Log Change in Average Trade Cost between Blocs (Model Countries, 2016-2023) . . . 144
C.9 Baseline Change in GDP and Real Income (2016-2023) 144
C.10 Bloc Comparison, Baseline 2015 versus Baseline 2002 (Model Countries) 145
C.11 Log Change in Average Trade Cost between Blocs (Model Countries, 2002-2007) . . . 145
C.12 Log Change in Average Trade Costs between 2015 Blocs (Model Countries, 2002-2007) 146
C.13 Model implied Trade Cost and Head-Ries Trade Cost 147

LIST OF APPENDICES

A Appendix to Chapter 1 96

B Appendix to Chapter 2 111

C Appendix to Chapter 3 134

ABSTRACT

This dissertation examines international trade and spatial economics with a focus on natural resources and geopolitical tensions.

In the first chapter, I use a novel geospatial dataset of global fishery catch and develop a quantitative dynamic spatial model to quantify the externalities from open access in global fishing. I first show that assigning property rights leads to larger fishery stock and fuel subsidies to vessels are positively correlated with high sea fishing. Then, I build a dynamic spatial model of global fisheries and compare two polar cases of open access: the decentralized equilibrium, where atomistic firms have open access to the fishery, and the socially optimal allocation, where the social planner has exclusive property rights. Taking the model to the data in 2018, I find that in the socially optimal allocation, the average global fishery stock at the steady state increases by 88%, and the net present value of global welfare increases by 0.11%, compared to the decentralized equilibrium. The counterfactual analysis shows that fuel subsidies are globally welfare-reducing and decrease the average global fishery stock at the steady state by 3.2%.

The second chapter, co-authored with Farid Farrokhi, Heitor S. Pellegrina, and Sebastian Sotelo, investigates the relationship between international trade and deforestation. Using the data on forest and agricultural land use from 1990-2020, we document that deforestation is strongly associated with agricultural land expansion and is more severe in countries with comparative advantage in agriculture. We show analytically and quantitatively that global reductions in trade costs reduce global deforestation when agriculture is complementary in demand to other sectors. Using the calibrated model, we demonstrate that multilateral reductions in agricultural trade costs reduce global deforestation by 0.5 percentage points. We find that countries with comparative advantage in agriculture also tend to have absolute advantage, making trade liberalization globally land-saving.

The third chapter, co-authored with Barthélémy Bonadio, Zhen Huo, Andrei A. Levchenko, Nitya Pandalai-Nayar, Hiroshi Toma, and Petia Topalova, analyzes how recent geopolitical tensions have reshaped global trade patterns. Using bilateral trade data from 2015-2023, we document evidence of trade fragmentation rather than deglobalization, with countries sorting into US-aligned and China-aligned blocs. Contrary to conventional wisdom, we find that the median country experienced a 0.6% increase in real income due to these changing trade patterns, as within-bloc trade costs decreased while cross-bloc costs increased. We also discover that bloc alignment often does not follow economic interests, suggesting that geopolitical considerations increasingly influence

trade relationships.

Together, these chapters advance our understanding of the complex interconnections between international trade and spatial economics in a changing global landscape.

CHAPTER 1

Global Fisheries: Quantifying the Externalities from Open Access

Abstract

This paper uses a novel geospatial dataset of global fishery catch and develops a quantitative dynamic spatial model to quantify the externalities from open access in global fishing. I first show that (i) the average global fishery stock decreased by 35% between 1980 and 2018, (ii) assigning property rights leads to larger fishery stock, and (iii) fuel subsidies to vessels are positively correlated with high sea fishing. Then, I build a dynamic spatial model of global fisheries and compare two polar cases of open access: the decentralized equilibrium, where atomistic firms have open access to the fishery, and the socially optimal allocation, where the social planner has exclusive property rights. Taking the model to the data in 2018, I find that in the socially optimal allocation, the average global fishery stock at the steady state increases by 88%, and the net present value of global welfare increases by 0.11%, compared to the decentralized equilibrium. The counterfactual analysis shows that fuel subsidies are globally welfare-reducing and decrease the average global fishery stock at the steady state by 3.2%.

1.1 Introduction

The tragedy of the commons, a market failure to internalize the social cost under open access, has long been studied in economics [Hardin, 1968, Ostrom, 1990], but quantifying its economic impact remains challenging. Global fisheries present a prominent example of the tragedy of commons. Since 1980, the proportion of over-fished species has risen from 20% to 35%, underscoring the increasing pressure on marine resources [FAO, 2022]. Fish are not only essential for marine biodiversity but also play a critical role in human diets, accounting for 20% of total animal protein intake globally [FAO, 2024b]. For some developing countries, the share of fish in total animal protein intake is much higher, for example 52% in Indonesia, emphasizing its significance in food

security.[1] Recognizing the importance of fisheries, multilateral global initiatives have sought to preserve fishery stocks by establishing the Exclusive Economic Zones (EEZs) or designating protected areas [UN, 1982, 2023].[2] Despite these efforts, individual countries unilaterally continue to subsidize fishing activities [Sala et al., 2018].

This paper quantifies the externalities in global fisheries arising from open access and investigates how global fishery policies impact the spatial distribution of fishery activities and global welfare. I compile a novel geospatial dataset on fishery catch, fishery stock, and international trade. Guided by the stylized facts about the patterns of global fisheries with open access and subsidies, I develop a dynamic spatial model of global fisheries featuring multiple fishing locations, exporters, and importers, along with the evolution of fish stocks. To quantify the externalities from open access, I compare the outcomes from two polar cases: a decentralized equilibrium, where atomistic firms have open access to the fishery, and the optimal allocation, where a social planner has exclusive property rights. I analytically characterize the difference in outcomes between the two, where the social planner fully internalizes the externalities of fishery production while the atomistic firms do not. The quantitative results show that in the social planner allocation, the average global fishery stock at the steady state increases by 88%, and the net present value of global welfare increases by 0.11% compared to the decentralized equilibrium. To understand policy impacts, I conduct a counterfactual analysis of permanently eliminating fuel subsidies and find that fuel subsidies are globally welfare-reducing and decrease the average global fishery stock at the steady state by 3.2%.

I begin by compiling a novel comprehensive geospatial dataset, consisting of global fishery catch, global fishery stocks, international trade, and other complementary statistics. First, the geospatial dataset on global fishery catch from Sea Around Us provides detailed information on catch weights by countries and species at the grid-level $(0.5^\circ \times 0.5^\circ \approx 60km \times 60km)$. Second, the fishery stocks are estimated at the grid level using the estimation package from natural science literature, taking the fishery catch data as one of the inputs. Third, I construct a fishery trade dataset with domestic consumption by harmonizing bilateral fishery trade flows with FAO food balance sheets. Fourth, I collect other complementary statistics on fishery such as fishery habitat suitability, ex-vessel prices, employment, and subsidies, which I use for model calibration and estimation. By combining the geospatial catch dataset ("production flows") with the international trade dataset ("trade flows"), I track the flow of fisheries from fishing locations to final destinations, offering a

[1] The reliance on fish as a protein source varies substantially across countries, ranging from Indonesia's 52% to Japan's 34%, China's 25%, and the USA's 7% [FAO, 2024b].

[2] A landmark initiative was the declaration of Exclusive Economic Zones (EEZs) in 1994 under the United Nations Convention on the Law of the Sea. By providing coastal nations with property rights over marine resources within 200 nautical miles of their shores, the EEZ framework aimed to foster responsible management of marine resources [UN, 1982]. More recently, attention has shifted to preserving fish stocks beyond national jurisdiction. The 2023 High Seas Treaty aims to protect 30% of the global ocean through the designation of marine protected areas [UN, 2023].

valuable resource for quantitative analysis.

Using this dataset, I present three empirical findings that motivate my quantitative model of global fisheries. First, in the past 40 years, global fishery stocks have decreased by 35% on average, and the number of overfished species has more than doubled. Second, the assignment of property rights is associated with larger fishery stock. Taking the declaration of EEZ in 1994 as a quasi-experiment, I show that the fishery stock increased in the EEZ relative to the high sea after the declaration. Third, government subsidies to the fishing industry, such as fuel subsidies toward vessels, are correlated with high seas fishing. This finding suggests that understanding the spatial dimension of the global fishery is crucial to examining the impact of fishery policies. In addition, this finding is informative about the key elasticity of substitution across fishing locations at the calibration.

I then develop a dynamic spatial model of global fisheries that incorporates the evolution of fishery stocks under a global trade system. The quantitative model accounts for multiple exporters and importers, multiple fishing locations, and two industries with outside good and fishery sectors. The fishery output is consumed as nested constant elasticity of substitution (CES), where fish are differentiated by the order of species, exporters, and fishing locations at each tier of the nests.[3] The fishery stocks evolve according to a law of motion governed by ecological growth function and anthropogenic activity, closely following the literature from natural science on population dynamics. Firms in the fishery sector are subject to two frictions: iceberg commuting costs to reach fishing locations from home countries and iceberg trade costs to ship fish from home countries to final destinations.

The quantitative model features two key characteristics. First, fishing productivity is an increasing function of fishery stocks. Fishery production today results in the fishery sector becoming less productive in the future, implying an additional cost of fishing. I refer the loss of future productivity from fishing as the dynamic social cost. Second, the only dynamic force in the decentralized equilibrium is the evolution of fishery stock. The atomistic firms ignore the impact of harvesting on future stock and solve a static optimization problem, not accounting for the dynamic social cost. As a result, the decentralized equilibrium allocation equalizes the marginal utility of fishery consumption with the static marginal cost of fishing, which is the input cost per unit of output.

To quantify the externalities, I compare the decentralized equilibrium with the optimal allocation by the social planner. I begin with characterizing the planner's problem that directly chooses the allocation of labor and consumption. In contrast to atomistic firms in the decentralized equilibrium, the planner fully internalizes the dynamic social cost of fishery production. From the planner's first-order conditions, I show that the planner allocation equalizes the marginal utility

[3] An example of differentiation across fishing locations at the bottom tier is the Tuna from the Pacific Ocean caught by China versus the Tuna from the Atlantic Ocean caught by the USA.

of fishery with the total cost of fishing, which includes both the static marginal cost and the dynamic social cost. The dynamic social cost of fishing that the decentralized equilibrium fails to internalize becomes the source of the externality. Since the dynamic social cost is positive and the marginal utility of fishery consumption diminishes, the planner allocates fewer inputs to the fishery and keeps a larger fishery stock than in the decentralized equilibrium.

Then, I take the quantitative model to data. I disaggregate the world into 30 countries, comprising 25 individual countries and 5 continental groups, chosen based on the size of fishery industries and overall economies. Additionally, I divide the high seas into 16 regions as defined by FAO fishing regions, resulting in a total of 46 fishing locations. I group fish species into 10 broader species following the ISSCAAP classification. By calibrating the model to data in 2018, I estimate the elasticities of substitution from IV regression that uses the exogenous variations in the geographical proximity to fishery habitat as a supply-side shock. Finally, I recover the fundamentals from model inversion.

I use the calibrated model to quantitatively address the two questions of this paper. First, I compare the baseline decentralized equilibrium with the optimal allocation by the social planner. This comparison allows me to measure the inefficiencies associated with the externalities in global fisheries. Second, I examine a counterfactual scenario where I permanently eliminate all fuel subsidies. This exercise allows me to quantify the effect of fishery policy on the spatial distribution of fishing activities and global welfare.

In the baseline decentralized equilibrium, I find that the average global fishery stock decreases by 32% at the steady state compared to the initial year of 2018. With the fishery stock becoming scarce, the fishery sector becomes less productive and the fish becomes more expensive, resulting in lower fishery consumption at the steady state. In contrast, in the socially optimal allocation, the average global fishery stock increases by 27% at the steady state compared to the initial year of 2018. Comparing steady states, the average global fishery stock in the socially optimal allocation is 88% larger than the average global fishery stock in the decentralized equilibrium. In the socially optimal allocation, the net present value of global welfare increases by 0.11% compared to the decentralized equilibrium. The reason is that the planner internalizes the effect that fishing today has on the productivity of fishing tomorrow, and consequently allocates fewer workers toward fishery than in the decentralized equilibrium. While less fish is consumed in the earlier periods, fishery consumption exceeds the level of the decentralized equilibrium over time since the accumulated stock increases fishery productivity and allows for more fishery consumption even with less labor. Moreover, since more labor is allocated to the outside good sector, the consumption of outside good is larger than in the decentralized equilibrium.

Lastly, I turn to examine the impact of fuel subsidies. In a scenario where all such subsidies are permanently eliminated, I find the average global fishery stock at the steady state increases by 3.2%

compared to the steady state of the baseline. The net present value of global welfare increases by 0.004%. While the magnitude is small, the result implies that fuel subsidies are welfare-reducing from a global perspective. By eliminating fuel subsidies, as in the case of the planner, fishery consumption decreases in the earlier periods but increases as the stock accumulates.

Related Literature. This paper contributes to three major strands of literature. First, this study contributes to the growing body of work at the intersection of trade, spatial economics, and the environment. Copeland and Taylor [2004] and Copeland et al. [2022] provide comprehensive overviews. Recent advances, as noted by Desmet and Rossi-Hansberg [2024], have incorporated spatial dimensions into quantitative models. Several recent studies have focused on climate change and air pollution [Desmet and Rossi-Hansberg, 2015, Costinot et al., 2016, Shapiro, 2016, Gouel and Laborde, 2021, Conte et al., 2021]. Recent work has also started studying the quantitative relationship between trade and natural resources. These papers include Farrokhi [2020] on global oil markets, Dominguez-Iino [2023] on environmental policies in South American supply chains, Farrokhi et al. [2024] on global deforestation, Hsiao [2024] on international cooperation in the palm oil market and Carleton et al. [2024] on the agricultural trade and the spatial allocation of global water use. My paper is unique in characterizing the optimal allocation by the planner and quantifying the externalities from open access to natural resources in the context of global fisheries. To my knowledge, this is the first paper to apply a dynamic spatial quantitative model to global fisheries.

Second, I build upon the literature examining optimal environmental policies in open economies. Early theoretical work includes Markusen [1975], Copeland [1996], and Hoel [1996]. Recent studies by Kortum and Weisbach [2021] and Weisbach et al. [2023] analyze unilaterally-optimal carbon tax policies in two-country models. Elliott et al. [2010] and Shapiro [2021] develop quantitative analyses of environmental policies. More recently, Farrokhi and Lashkaripour [2024] characterize optimal climate and trade policies in a multi-country general equilibrium model and quantitatively assess the performance of these policies. The contribution of my paper lies in the quantitative analysis of optimal allocation in dynamic settings.

Lastly, I contribute to the extensive literature on the extraction of natural resources and fisheries. Building on the seminal work by Hotelling [1931], natural resource extraction has been widely studied [Chichilnisky, 2017, Brander and Taylor, 1997, 1998, Copeland and Taylor, 2009, Anderson et al., 2018, Arkolakis and Walsh, 2023, Noack and Costello, 2024]. While early works on fisheries were primarily theoretical [Gordon, 1954, Smith, 1969], recent empirical studies have focused on specific regions or species [Costello and Polasky, 2008, Huang and Smith, 2014, Kroodsma et al., 2018, Fenichel et al., 2020]. I complement these studies by linking the global fishery catch data with international trade and offering a global general equilibrium quantification of externalities from open access to fishery.

The rest of the paper proceeds as follows. Section 1.2 describes the data sources used in the paper. Section 2.3 establishes empirical facts to motivate the main framework in the paper. Section 2.4 builds the dynamic spatial model of global fishery. Section 1.4.3 describes the planner's problem and discusses the comparison with the decentralized equilibrium. Section 2.6 calibrates the model by taking the model to data. Section 2.7 shows the quantitative results from the decentralized equilibrium, the social planner, and the counterfactual scenario. Section 1.7 concludes.

1.2 Data

This section describes a novel dataset that combines geospatial datasets of global fishery catch and stock with international trade flows and other fishery datasets.

Fishery Catch. The fishery catch dataset is sourced from Sea Around Us.[4] The dataset spans annually since 1980 for approximately 200 countries, covering 1,100 species worldwide. This dataset provides the catch quantity in tonnes for each species by individual country at the grid level of fishing location $(0.5^\circ \times 0.5^\circ \approx 60km \times 60km)$. The grid level estimation process integrates information from several sources, including grid-level natural habitat conditions, national statistics by individual countries, and the Food and Agriculture Organization fishery database [Zeller and Pauly, 2015].[5] To give a graphical illustration of the catch dataset, Figure 1.1 panel (a) displays a map of the catch of Big Eye Tuna in 2018.

Fishery Stock. I employ the CMSY++ package provided by the Sea Around Us to estimate fishery stock levels. The package takes historical catch data and biological information of species as inputs and estimates the time series of fishery stock.[6] The estimation also allows me to infer the carrying capacity, which is the maximum population of species that can be attained in the given geography. The carrying capacity suggests the level of fishery stock that would be attained without any anthropogenic activity. Taking the inputs as given, the model infers the stock and

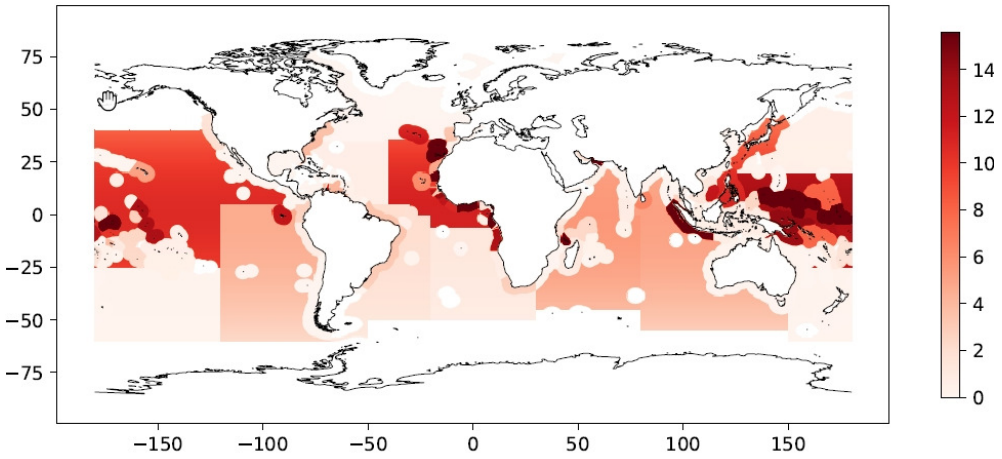
[4]Sea Around Us is the research initiative at the University of British Columbia, specializing in quantifying the impact of fisheries on marine environments.

[5]The FAO publishes the annual global fisheries statistics with fishing location information based on individual country surveys [FAO, 2024a]. However, the FAO dataset's geographic units are much broader than the Sea Around Us dataset, classifying the global ocean into 19 FAO major fishing areas. The primary benefit of the granular dataset from Sea Around Us is that it allows me to distinguish between EEZ and high sea.

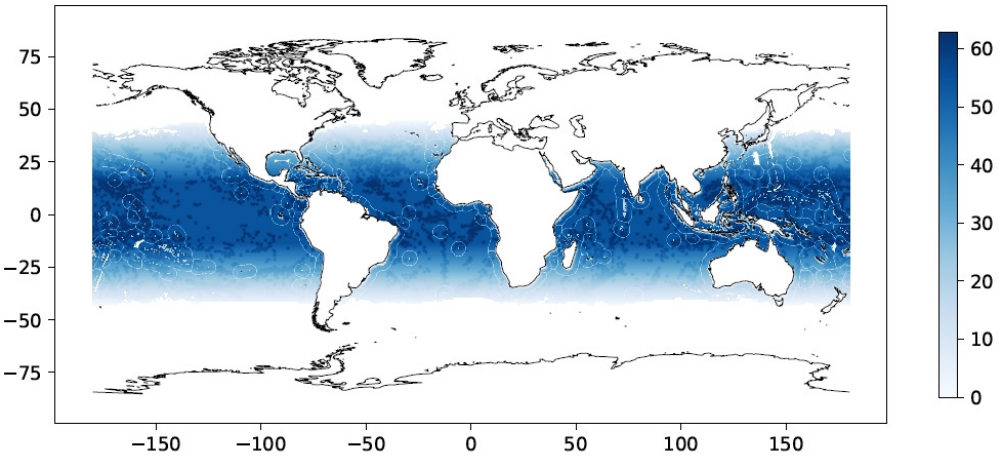
[6]Estimating fishery stock is inherently more complicated than estimating fishery catch. Broadly, there are two methods of measuring fishery stock in the literature: direct estimation via research vessels, which is limited in scope and commonly conducted by developed countries, and indirect estimation from historical catch and biological data. The indirect method, while broader and longitudinal, relies on assumptions about the model of stock growth. CMSY++ package combines the indirect method with a machine learning algorithm.

Figure 1.1: Global Catch and Stock of Big Eye Tuna (2018, in tonnes)

(a) Global Catch of Big Eye Tuna (2018, in tonnes)



(b) Global Stock of Big Eye Tuna (2018, in tonnes)



Notes: Panel (a) shows the spatial distribution for the global catch of Big Eye Tuna in 2018. Panel (b) shows the spatial distribution for the global stock of Big Eye Tuna in 2018.

carrying capacity that best rationalizes the time series of observed catch.[7] The machine learning algorithm, trained on direct observation data, enhances the estimation accuracy.[8] Inputting the fishery catch dataset to the CMSY++ package, I obtain the time series of fishery stock since 1980 and the carrying capacity for 1,100 species at the grid-level. To give a graphical illustration of the stock dataset, Figure 1.1 panel (b) displays a map of the stock of Big Eye Tuna in 2018.

[7]The Schaefer growth model from CMSY++ is consistent with the growth model used in this paper.

[8]Froese et al. [2023] validate this methodology, demonstrating that stock levels for 91% of species in the training set fall within the model's 95% confidence interval in cross-validation.

Fishery Trade. I construct a fishery trade dataset by combining bilateral trade flows with domestic consumption, both sourced from FAO. The FAO dataset on fishery trade provides the bilateral trade flows, both in quantity and value, between 240 countries for over 1,000 products since 2019.[9] Dealing with domestic consumption has often been problematic in international trade literature. I overcome this difficulty by complementing the bilateral trade dataset with the FAO food balance sheet.[10] The FAO food balance sheet provides information on total production, domestic consumption, total exports, and total imports by type of commodities after 2010. I merge the food balance sheet data with bilateral trade flows and infer the domestic consumption so that the trade patterns are consistent in the two datasets.

Other Fishery Datasets. Other fishery datasets used in the paper include fishery habitat suitability, fishery ex-vessel prices, fishery subsidies, and fishery employment. The fishery habitat suitability, provided by Sea Around Us, measures the time-invariant habitat suitability of overall geographic conditions at the grid for over 1,000 species.[11] The fishery ex-vessel prices, also published by Sea Around Us, measure the landed value of fishery at the port for over 1,000 species, expressed in nominal USD per tonne since 1980.[12] While the fishery ex-vessel prices do not vary across fishing locations, they provide a consistent comparison of landed value across countries and species [Sumaila et al., 2015]. The country-level fishery subsidies data, sourced from Sumaila et al. [2019], are available from 2002 to 2018. Lastly, fishery employment data are from the OECD since 2010.

Geographic Boundaries. I use the geographic boundary shapefiles to assign $0.5^\circ \times 0.5^\circ$ grids into EEZs and high seas. To assign the grids into EEZs, I use the shapefile of EEZ boundaries from the version 12 of Flanders Marine Institute.[13] To assign the grids into high seas, I use the shapefile from FAO major fishing area boundaries.[14]

Other Country-level Datasets. I use data on GDP and total employment from World Economic Outlook and UN-ILO, respectively. I also obtain the coordinates of global ports from World Port Index, covering more than 3,500 major ports worldwide.

[9] For instance, I observe how much tuna was exported from China to USA from the FAO dataset on fishery trade.

[10] The purpose of FAO food balance sheet is to understand the current status of food consumption and security by each country.

[11] The geographic conditions include but are not limited to depth, distance from the coast, and the existence of coral reefs [Zeller and Pauly, 2015].

[12] The dataset is constructed by compiling various data sources including FAO, OECD, the European Commission, etc.

[13] The shapefile of EEZ boundaries can be downloaded at https://www.vliz.be/en/imis?dasid=8394&doiid=911.

[14] The shapefile of FAO major fishing area boundaries can be downloaded at https://www.fao.org/fishery/en/area/search

Harmonization of Datasets. For the rest of the paper, I harmonize the dataset in the following way. First, I classify countries into 30 countries, consisting of 25 individual countries and 5 regional aggregates. 25 individual countries are picked based on the national GDP and fishery output, covering 78% of global GDP and 84% of global fishery output. The remaining countries are regrouped into 5 regional aggregates based on their continents. Appendix Table A.3 provides the mapping of countries.

Second, I classify $0.5^\circ \times 0.5^\circ$ grids of the global ocean into 46 fishing locations, consisting of 30 EEZs and 16 high seas. Each EEZ maps to the EEZ of each country, picked earlier based on the size of the overall economy and fishery industry. Each high sea corresponds to each of FAO major fishing areas that are exclusive of EEZs. By overlaying the shapefile of EEZs with the shapefile of FAO major fishing areas, I define each high sea as the grids belonging to each of FAO major fishing areas but not to any of EEZs. Appendix Table A.1 provides the list of 46 fishing locations.

Lastly, I aggregate individual species into 10 species. While the fishery catch dataset covers more than 1,100 species and the fishery trade dataset covers about 1,000 products, I harmonize the dataset by mapping them into 10 species from the International Standard Statistical Classification of Aquatic Animals and Plants (ISSCAAP). Appendix Table A.2 provides the list of 10 species. As a result, the harmonized dataset consists of 30 countries, 46 fishing locations, and 10 species.

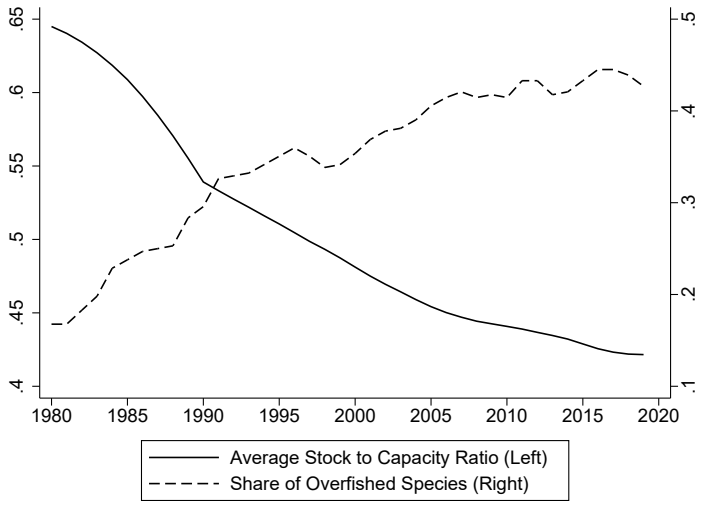
1.3 Empirical Patterns

In this section, I document three empirical patterns of global fishery that motivate the quantitative model. First, I show the decline in fishery stock between 1980 and 2020. Second, I find that the lack of property rights is associated with lower fishery stock. Third, I document that fishery subsidies are correlated with fishing on high seas.

Pattern 1. Global fishery stock has been decreasing

Figure 1.2 shows the trend in global fishery stock between 1980 and 2018. The solid line refers to the average stock to capacity ratio across species and fishing locations. The stock to capacity ratio measures a stock level of fishery relative to its carrying capacity for a given species and fishing location. This ratio serves as an indicator of anthropogenic impact on fishery stock since it approaches 1 in the absence of harvest and approaches 0 as the stock nears complete depletion. During this period, the average stock to capacity ratio decreased from 0.65 to 0.42, implying a 35% decrease on average. The dotted line refers to the proportion of overfished species. Following the criteria from FAO, the species are defined to be overfished if the stock level falls below 40% of carrying capacity. I find that the proportion of overfished species increased from 17% to 43%

Figure 1.2: Global Fishery Stock over Time (1980-2018)



Notes: Species and fishing locations are aggregated into 10 species and 46 fishing locations. A species by region is defined to be overfished if the stock is below 40% of carrying capacity, following the criteria from FAO [FAO, 2022].

during this period. Appendix Table A.4 provides detailed descriptive statistics of fishery stock changes by species.[15]

Pattern 2. Assigning property rights lead to larger fishery stock

Next, I examine the relationship between property rights and fishery stock. To do so, I employ the following event-study framework, taking the declaration of EEZ in 1994 as a quasi-experiment. The declaration of EEZ in 1994 provided coastal nations with property rights over marine resources within 200 nautical miles of their shores.[16] I argue that the declaration of EEZ was exogenous to the fishery stock, as the focus of the introduction of EEZ was primarily on energy and mineral resources due to the relative size of sectors [Osherenko, 2006].

Taking the declaration of EEZ in 1994 as a quasi-experiment, I estimate equation (1.1) to study the effect of property rights on fishery stock

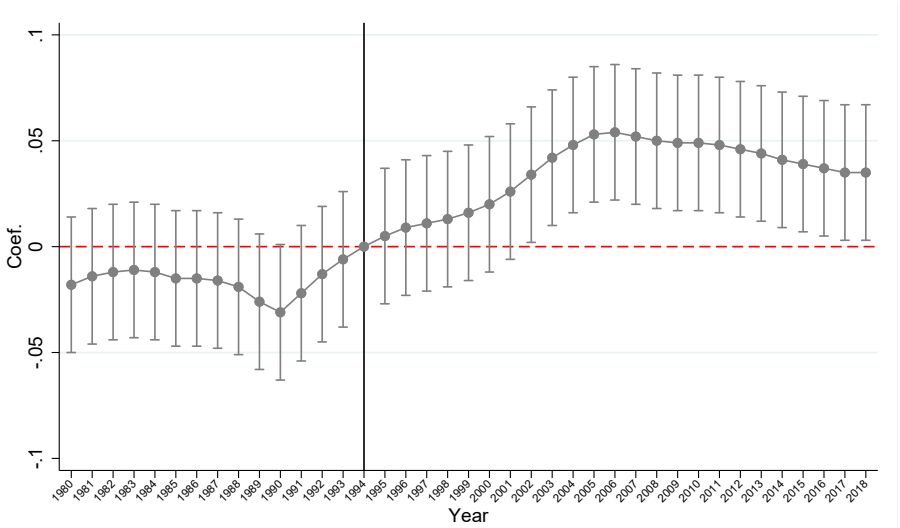
$$x_{k,st}/M_{k,s} = \beta_0 + \sum_{\tau=1980}^{2018} \beta_\tau EEZ_k \times \mathbb{1}\{t = \tau\} + \delta_{k,s} + \delta_t + \varepsilon_{k,st} \tag{1.1}$$

where $x_{k,st}/M_{k,s}$ is the stock to capacity ratio at fishing location k for species s in year t, EEZ_k is the indicator variable for whether fishing location k belongs within the boundaries of EEZ,

[15] Appendix Table A.4 suggests the heterogeneity in stock changes across species. Some stocks, such as squids, experienced more than 40% decrease in stock, while some stocks, such as codes, only decreased by 6%.

[16] While EEZs were first defined in the 1982 United Nations Convention on the Law of the Sea, they were formally declared and became effective in 1994.

Figure 1.3: Declaration of EEZ and Fishery Stock



Notes: The figure shows the coefficients for the event study regression of equation (1.1). Each dot indicates the point estimate of β_τ and each range refers to the 95% confidence interval, where β_τ captures the difference in the average stock to capacity ratio at the EEZ relative to the high sea in year τ compared to the year of EEZ declaration.

$\mathbb{1}\{t = \tau\}$ is the indicator variable for whether year $t = \tau$, $\delta_{k,s}$ is the fishing location-species fixed effect, δ_t is the year fixed effect, and $\varepsilon_{k,st}$ is the error term. Using 1994 as a base year, the coefficient β_τ measures the difference in the average stock to capacity ratio at the EEZ relative to the high sea in year τ compared to the base year. Given that the stocks should not have been disproportionately affected before the declaration of EEZ, I expect the coefficient β_τ to be zero for $\tau < 1994$.

Figure 1.3 presents the estimates of β_τ from equation (1.1). Prior to the EEZ declaration in 1994, the coefficient β_τ is not statistically different from zero, validating the absence of differential trends in fishery stocks between the EEZ and high sea. The coefficient β_τ becomes significantly positive after 2002, indicating that the EEZ experienced a differential increase in fishery stocks. The delayed emergence of significant effects suggests a temporal lag in the realization of fishery stock increase. Quantitatively, in the years after 2002, the stock to capacity ratio in the EEZ increased by approximately 5 percentage points relative to the high sea, compared to the base year 1994. Given that the average stock to capacity ratio in 1994 was 0.52 from Figure 1.2, 5 percentage points increase account for about 10% increase in average fishery stock.

This pattern motivates a model in which a lack of property rights leads to exploiting fishery stock. Thus, I compare two polar cases of property rights in the model: the decentralized equilibrium, where firms are atomistic with open access, and the socially optimal allocation, where the planner has globally exclusive property rights.

Pattern 3. Fishery subsidies are correlated with high sea production

Finally, I investigate the impact of fishery subsidies on the location of fishing. Despite global efforts to preserve fishery stocks [UN, 1982, 2023], individual countries continue to promote fishing activities, mainly through subsidies. While the first discussion to regulate fishery subsidies began in the 2001 Doha Round [Chang, 2003], effective global regulation has not been achieved. Consequently, the fishery remains highly subsidized, with subsidies accounting for 10% of global fishery output [Sala et al., 2018].[17]

Among the major types of fishery subsidies, fuel subsidies are important for the following reasons.[18] First, they constitute the largest single category of subsidies, representing 21% of total subsidies in the fishing industry in 2018. Second, they have become the primary target for global regulation due to their role in facilitating the exploitation of resources in the high sea by extending the operational range of fishing fleets [Sumaila et al., 2019]. Appendix Table A.5 shows the summary statistics of fuel subsidies between 2002 and 2018.[19]

I consider equation (1.2) to explore the relationship between subsidies and the location of fishing:

$$\Delta \ln(Y_{i,t}^{HS}/Y_{i,t}^{EEZ}) = \beta_0 + \beta_1 \Delta \ln S_{i,t} + \Delta X_{i,t} + \varepsilon_{i,t} \tag{1.2}$$

where $Y_{i,t}^{HS}$ and $Y_{i,t}^{EEZ}$ are the high sea and EEZ production for country i at year t, $S_{i,t}$ is the fishery subsidy, $X_{i,t}$ is other controls, and $\varepsilon_{i,t}$ denotes the error term. The operator Δ refers to the change between 2002 and 2018. The coefficient β_1 captures the correlation between fishery subsidies and the relative production at the high sea.

There could be a concern about the confounding factors that affect the incentives to provide subsidies and the fishing locations. For example, if EEZs were fully exploited due to higher demand for fishery, governments could have larger incentives to provide subsidies, affecting the amount of subsidies and the relative production at the high sea. To address the endogeneity issue, I control for population growth and GDP growth.

Table 1.1 shows the estimates of equation (1.2) for different types of subsidies. Columns (1) and (2) include all types of fishery subsidies as the regressor, while Columns (3) and (4) restrict the regressor to fuel subsidies. The results suggest that countries that increase their fishery subsidies tend to disproportionately expand their fishery output in high seas. After controlling for population growth and GDP growth, column (2) suggests that a 10 percent increase in fishery subsidies is associated with a 3 percent increase in the output from high sea relative to EEZ. Column (4)

[17] Following the continued concern, the WTO has recently made another agreement to prohibit subsidies that promote fishing [WTO, 2023].

[18] The major types of subsidies include fuel, infrastructure, and management subsidies [Sumaila et al., 2019].

[19] China has more than doubled its fuel subsidies during this period, accounting for more than 40% of total fuel subsidies in 2018.

Table 1.1: Fishery Subsidies and High Sea Production (2002-2018)

	(1)	(2)	(3)	(4)
$\Delta \ln S_{i,t}$	0.346*	0.323*	0.117**	0.112**
	(0.158)	(0.163)	(0.040)	(0.042)
Other Controls	N	Y	N	Y
Type of Subsidies	All	All	Fuel	Fuel
R^2	0.132	0.176	0.187	0.268
N	30	30	30	30

Notes: The regression is weighted by log output in the initial year 2002. Columns "All" refer to the regression where the regressor includes all fishery subsidies. Columns "Fuel" refer to the regression where the regressor includes fishery subsidies. Other controls include log differences of population and GDP per capita.

implies that a 10 percent increase in fuel subsidies is correlated with an 1.1 percent increase in the output from high sea relative to EEZ.

Motivated by this empirical fact, I examine the impact of fuel subsidies on global welfare and the spatial distribution of fishing activities in the quantitative exercise. Moreover, the regression is informative about the elasticity of substitution across fishing locations. The idea is that if the fishery goods are more substitutable across locations, the effect of subsidies on relative production would be larger. In Section 2.6, I simulate the model and estimate equation (1.2) using the simulated results to discipline the parameter governing the elasticity of substitution across fishing locations.

1.4 A Model of Global Fishery

In this section, I develop a dynamic spatial model of global fishery, where each country produces from fishing locations and exports to another country. I compare two polar cases: a decentralized equilibrium, where atomistic firms have open access to the fishery, and the socially optimal allocation, where a social planner has exclusive property rights. While the atomistic firms solve a static problem, the global social planner solves a dynamic problem, fully internalizing the social cost.[20] I describe the environment and characterize the decentralized equilibrium and the planner's problem.

[20]The status quo can be interpreted as in-between two polar cases, where individual countries internalize some dynamic costs within their EEZs.

1.4.1 Environment

The economy consists of I countries indexed by i or j. There are H high sea locations, which are the sea locations that are beyond any country's jurisdiction. Since I and H are disjoint, there are in total $K = I + H$ fishing locations, indexed by k. Time is discrete and indexed by t. The economy has two sectors: fishery, f, and outside good, o. The fishery sector is disaggregated into $s \in S$ species. Outside good is freely traded and serves as numeraire. The frictions in the economy are iceberg commuting costs $\tau_{ik,s}$ and iceberg trade costs $d_{ij,s}$. The iceberg commuting costs $\tau_{ik,s}$ are the frictions that exporters face upon harvesting at fishing locations and bringing back the output to their ports. The iceberg trade costs $d_{ij,s}$ are the frictions that exporters face upon shipping fishery to importers. The economy is endowed with the initial fishery stock $x_{k,s0}$, distinguished by fishing location k and species s, and the total labor force $\tilde{L}_i$. For expositional purposes, I suppress the subscript f for the fishery sector.

1.4.1.1 Preferences

The representative household in importer j has quasi-linear preferences between outside good and fishery bundle:

$$U_{j,t} = C^o_{j,t} + b_j \ln C_{j,t} \tag{1.3}$$

where $U_{j,t}$ is the household welfare at time t, $C^o_{j,t}$ is the consumption of outside good, $C_{j,t}$ is the consumption of fishery bundle, and b_j is the demand shifter of the fishery bundle. One advantage of quasi-linear preferences is that the equilibrium at the fishery sector is independent of income effects.

The fishery bundle is comprised of three tiers of CES aggregators. In the upper tier, varieties of fishery goods are differentiated by species s, for example, tuna and squid. Consumers in importer j combine the varieties from every species s according to CES preferences with the elasticity of substitution ν and the demand shifters b_s:

$$C_{j,t} = \left(\sum_{s \in S} b_s C_{j,st}^{\frac{\nu-1}{\nu}} \right)^{\frac{\nu}{\nu-1}} \tag{1.4}$$

where $C_{j,st}$ is the consumption of fishery species s.

In the middle tier, varieties of species s are differentiated by exporter i, for example, tuna exported by China and tuna exported by Chile. Consumers in country j consuming species s combine the varieties from every exporter i according to CES preferences with the elasticity of substitution η and the demand shifters b_{ij}:

$$C_{j,st} = \left(\sum_{i \in I} b_{ij} C_{ij,st}^{\frac{\eta-1}{\eta}} \right)^{\frac{\eta}{\eta-1}} \tag{1.5}$$

where $C_{ij,st}$ is the consumption of fishery species s from exporter i.

Finally, in the lower tier, varieties of species s from exporter i are differentiated by fishing location k, for example, tuna exported by China caught from Pacific ocean and tuna exported by China caught from Atlantic ocean. Consumers in importer j consuming species s by exporter i combine the varieties from every fishing location k according to CES preferences with the elasticity of substitution κ and the demand shifters $b_{k,s}$:

$$C_{ij,st} = \left(\sum_{k \in K} b_{k,s} C_{ijk,st}^{\frac{\kappa-1}{\kappa}} \right)^{\frac{\kappa}{\kappa-1}} \tag{1.6}$$

where $C_{ijk,st}$ is the consumption of fishery species s from exporter i at fishing location k.

1.4.1.2 Technology

In the fishery sector, each variety of fish is produced under the constant to returns to scale technology:

$$Q_{ijk,st} = \frac{z_i \left(x_{k,st-1} / M_{k,s} \right)^{\xi}}{d_{ij,s} \tau_{ik,s}} L_{ijk,st} \tag{1.7}$$

where $Q_{ijk,st}$ is the output quantity of fishery by exporter i to importer j at fishing location k for species s, $x_{k,st-1}$ is the fishery stock from previous period, $M_{k,s}$ is the carrying capacity, $d_{ij,s}$ is the iceberg trade cost, $\tau_{ik,s}$ is the iceberg commuting cost, z_i is the country-specific productivity shifter, ξ is the stock elasticity of output, and $L_{ijk,st}$ is the labor input.

Since the output $Q_{ijk,st}$ represents the quantity delivered to the importer, the fishery technology is subject to the iceberg trade and commuting costs. Specifically, delivering one unit of fish to importer j requires exporter i to ship $d_{ij,s}$ units of fish under the iceberg trade cost. Additionally, shipping $d_{ij,s}$ units of fish requires exporter i to harvest $d_{ij,s}\tau_{ik,s}$ units of fish from the fishing location k under the iceberg commuting cost.

Moreover, the fishery productivity is an increasing function of the stock to capacity ratio $x_{k,st-1}/M_{k,s}$. This captures the efficiency gains in the harvest from stock abundance with an elasticity of ξ.

In the outside good sector, outside good is produced under the constant to returns to scale

technology:

$$Q^o_{i,t} = z^o_i L^o_{i,t} \tag{1.8}$$

where z^o_i is the productivity shifter, and $L^o_{i,t}$ is the labor input. I assume that the outside sector is large enough to be produced at every country.

1.4.1.3 Nature

Following the standard literature on population dynamics [Gordon, 1954, Schaefer, 1954, Clark, 1990, Smith, 2009], the evolution of fishery stock is determined by two competing forces: ecological growth function and anthropogenic activity such that

$$x_{k,st+1} - x_{k,st} = G(x_{k,st}) - H(x_{k,st}) \tag{1.9}$$

where $x_{k,st}$ is the fishery stock, $G(x_{k,st})$ is the natural regrowth, and $H(x_{k,st})$ is the total harvest.

The natural regrowth $G(x_{k,st})$ follows a logistic equation capturing two fundamental biological mechanisms in fishery dynamics:

$$G(x_{k,st}) = \gamma_{k,s} x_{k,st}(1 - \frac{x_{k,st}}{M_{k,s}}) \tag{1.10}$$

where $\gamma_{k,s}$ is the intrinsic growth rate and $M_{k,s}$ is the carrying capacity. First, at low stock levels, population grows proportionally at the intrinsic growth rate $\gamma_{k,s}$, reflecting the reproductive ability of species. Second, at high stock levels, population growth is bounded by the carrying capacity $M_{k,s}$, representing environmental constraints to species.[21]

The total harvest $H(x_{k,st})$ equals the sum of harvests across all bilateral trade pairs adjusted for trade and commuting frictions:

$$H(x_{k,st}) = \sum_{i \in I} \sum_{j \in I} d_{ij,s} \tau_{ik,s} Q_{ijk,st} \tag{1.11}$$

where $d_{ij,s}$ is the iceberg trade cost, $\tau_{ik,s}$ is the iceberg commuting cost, and $Q_{ijk,st}$ is the output quantity. The total harvest is obtained by multiplying the output by the iceberg trade and commuting frictions and summing over all importers and exporters, since the output $Q_{ijk,st}$ represents the quantity delivered to importer j.

[21] Given these features, the stock to capacity ratio $x_{k,st}/M_{k,s}$ ranges from 0 to 1. The first partial derivative of fishery growth is a decreasing function of $x_{k,st}$ and the second partial derivative is negative, with the fishery growth being maximized at $x_{k,st}/M_{k,s} = 0.5$.

1.4.2 Decentralized Equilibrium

In this subsection, I characterize the decentralized equilibrium where fishery firms are atomistic under open access to the fishery. All markets are perfectly competitive. The outside good is freely traded and serves as numeraire. Each atomistic firm solves a static problem, ignoring the impact of its harvest on future stock. The only dynamic factor is the evolution of fishery stock in the decentralized equilibrium. The details are provided in Appendix The details are provided in Appendix A.3.1.

1.4.2.1 Utility Maximization

Given equations (1.3), (1.4), (1.5), and (1.6), the representative household in country j maximizing its utility allocates a fixed amount of its expenditure b_j on fishery bundle and the rest to the outside good such that

$$X_{j,t} = b_j, \quad X^o_{j,t} = E_{j,t} - b_j$$

where $X_{j,t}$ is the fishery expenditure and $E_{j,t}$ is the household income.

From the upper tier of CES, the expenditure share of species s in all fishery expenditure by country j, $\pi_{j,st}$, and the consumer price index in country j for aggregate fishery bundle, $P_{j,t}$, are given by

$$\pi_{j,st} = \frac{b_s P_{j,st}^{1-\nu}}{P_{j,t}^{1-\nu}}, \quad P_{j,t} = \left[\sum_{s\in S} b_s P_{j,st}^{1-\nu}\right]^{\frac{1}{1-\nu}}$$

Then, from the middle tier of CES, the expenditure share of country i in all expenditure by country j for species s, $\pi_{ij,st}$, and the consumer price index in country j for species s, $P_{j,st}$, are given by

$$\pi_{ij,st} = \frac{b_{ij} P_{ij,st}^{1-\eta}}{P_{j,st}^{1-\eta}}, \quad P_{j,st} = \left[\sum_{i\in I} b_{ij} P_{ij,st}^{1-\eta}\right]^{\frac{1}{1-\eta}}$$

Finally, from the bottom tier of CES, the expenditure share of fishing location k in all expenditure by country j for species s from country i, $\pi_{ijk,st}$, and the consumer price index in country j for species s from country i, $P_{ij,st}$, are given by

$$\pi_{ijk,st} = \frac{b_{k,s} p_{ijk,st}^{1-\kappa}}{P_{ij,st}^{1-\kappa}}, \quad P_{ij,st} = \left[\sum_{k\in K} b_{k,s} p_{ijk,st}^{1-\kappa}\right]^{\frac{1}{1-\kappa}}$$

where $p_{ijk,st}$ equals the marginal cost of production for species s from exporter i to importer j at fishing location k.

1.4.2.2 Profit Maximization

Given equation (1.7), for each variety of fish, a representative firm in the fishery sector chooses its labor inputs, thus its output, to maximize the profit. I assume that each firm is atomistic under open access. Instead of solving a dynamic problem, each atomistic firm solves a static problem, ignoring the impact of its harvest on future stock. The price of fishery $p_{ijk,st}$ equals the marginal cost of production such that

$$p_{ijk,st} = \frac{d_{ij,s}\tau_{ik,s}}{(x_{k,st-1}/M_{k,s})^{\xi}} \frac{w_{i,t}}{z_i} \tag{1.12}$$

where $w_{i,t}$ is the wage of fishery worker in exporter i.

Given equation (1.8), a representative firm in the outside good sector chooses its labor inputs, thus its output, to maximize the profit. The outside good is freely traded and serves as numeraire. I assume that the outside good sector is large enough and the fishery sector is relatively small such that the outside good is produced in all countries.

1.4.2.3 Labor Mobility

I assume a perfect mobility of workers across sectors. Since the outside good serves as numeraire, the wage that applies to all workers is exogenously determined as the productivity shifter of outside good such that

$$w_i^o = w_i = z_i^o \tag{1.13}$$

where w_i is the wage of outside good worker in exporter i.

1.4.2.4 Market Clearing

Goods market clearing on fishery sector requires that the revenue equals the expenditure for each variety of fishery:

$$Y_{ijk,st} = \pi_{ijk,st}\pi_{ij,st}\pi_{j,st}X_{j,t} \tag{1.14}$$

where $Y_{ijk,st}$ is the fishery revenue and $X_{j,t}$ is the total expenditure on fishery in importer j

Goods market clearing on outside good sector requires that the sum of revenue across all exporters equal the sum of expenditure across all importers:

$$\sum_{i \in I} Y_{i,t}^o = \sum_{j \in I} X_{j,t}^o \tag{1.15}$$

where $Y_{i,t}^o$ is the outside good revenue in exporter i and $X_{j,t}^o$ is the outside good expenditure in importer j.

Labor market clearing requires that payments to labor equal revenue for each sector:

$$w_{i,t}L_{ijk,st} = Y_{ijk,st}, \quad w^o_{i,t}L^o_{i,t} = Y^o_{i,t} \tag{1.16}$$

Lastly, the balance of household budget holds that the sum of factor rewards equals the sum of expenditures:

$$\sum_{j\in I}\sum_{s\in S}\sum_{k\in K} w_{i,t}L_{ijk,st} + w^o_{i,t}L^o_{i,t} = X_{i,t} + X^o_{i,t} \tag{1.17}$$

1.4.2.5 Equilibrium

Definition. ***[Competitive equilibrium]*** *Given taste and geography, initial vector of fish stock* $\{x_{k,s0}\}$ *and labor endowment* $\{\bar{L}_i\}$*, a* ***competitive equilibrium*** *is a path of consumption* $\{C_{ijk,st}, C^o_{i,t}\}$*, output* $\{Q_{ijk,st}, Q^o_{i,t}\}$*, labor allocation* $\{L_{ijk,st}, L^o_{i,t}\}$*, prices* $\{p_{ijk,st}\}$*, wages* $\{w_{i,t}, w^o_{i,t}\}$*, and fish stock* $\{x_{k,st}\}$*, such that household maximizes its utility according to (1.3), firms maximize their profits according to (1.7) and (1.8), stock of fish evolves according to (1.9), markets clear according to (1.14) and (1.15) and (1.16), and the balance of budget holds according to (2.23)*

Definition. ***[Steady-state equilibrium]*** *A* ***steady state equilibrium*** *is the allocation that satisfies the conditions of competitive equilibrium in addition to the condition where the regrowth of fishery equals with total harvest such that*

$$\gamma_{k,s}x_{k,st}(1 - \frac{x_{k,st}}{M_{k,s}}) = \sum_{i\in I}\sum_{j\in I} d_{ij,s}\tau_{ik,s}Q_{ijk,st} \quad \forall k, s \tag{1.18}$$

1.4.2.6 Fishery Consumption in the Decentralized Equilibrium

Rearranging the first-order conditions from households and firms, I can characterize the fishery consumption in the decentralized equilibrium as:

$$\underbrace{\frac{\partial U_{j,t}}{\partial C_{ijk,st}}}_{\text{MU of fishery consumption}} = \underbrace{\frac{\partial U_{j,t}}{\partial C^o_{j,t}}\left(\frac{\partial Q^o_{i,t}}{\partial L^o_{i,t}} / \frac{\partial Q_{ijk,st}}{\partial L_{ijk,st}}\right)}_{\text{MC of fishery consumption}} \tag{1.19}$$

Equation (1.19) implies that the fishery consumption for each variety is determined where the marginal utility equals the marginal cost of fishery consumption. Importantly, the decentralized equilibrium fails to internalize the impact of harvest today on future stock. As a result, the marginal cost of fishery consumption is purely static, representing the static opportunity cost of inputs that

could have been used to produce outside good if the fishery were not produced. This expression will be useful when comparing the outcomes with the planner allocation in Section 1.4.3, where the planner internalizes the dynamic impact of harvest.

1.4.3 Planner's Problem

This subsection characterizes the planner's problem, where the planner who owns exclusive property rights over global fishery stock maximizes the discounted present value of global welfare. I analytically provide the expression comparing the outcomes from the socially optimal allocation with the decentralized equilibrium.

1.4.3.1 Planner's FOC

Given the GE equations (1.3)$\sim$(1.11), define the global welfare W_t as

$$W_t = \sum_{i \in I} \phi_i U_{i,t} \tag{1.20}$$

where $\phi_i \geq 0$ is the Pareto weights.[22]

The planner allocates the labor, consumption, and fishery stock to maximize the net present value of global welfare such that

$$\begin{aligned} \max_{C_{ijk,st}, C^o_{j,t}, L_{ijk,st}, L^o_{i,t}, x_{k,st}} \sum_t \beta^t W_t \quad \text{s.t.} \quad & [\lambda_{k,st}] \quad x_{k,st-1} + G_{k,st} = H_{k,st} + x_{k,st} \\ & [\mu_{i,t}] \quad \bar{L}_i = \sum_{j \in I} \sum_{s \in S} \sum_{k \in K} L_{ijk,st} + L^o_{i,t} \\ & [\theta_{ijk,st}] \quad Q_{ijk,st} = C_{ijk,st} \\ & [\alpha_t] \quad \sum_i Q^o_{i,t} = \sum_j C^o_{j,t} \end{aligned} \tag{1.21}$$

where $\lambda_{k,st}, \mu_{i,t}, \theta_{ijk,st}, \alpha_t$ denote the Lagrangian multipliers for stock constraint, labor constraint, and technology constraint for fishery and outside good, respectively.

1.4.3.2 Fishery Consumption in the Planner Allocation

In this subsection, I compare the first-order conditions of the planner allocation and the decentralized equilibrium. Provided that the interior solution exists, rearranging the first-order conditions

[22] Without loss of generality, I assume that $\phi_i = 1$ is symmetric across countries to focus on the interior solution. The implication of symmetric ϕ_i is that the allocation of outside good is undetermined under the planner allocation. When ϕ_i is asymmetric, all of the outside good is allocated to the country with the largest ϕ_i, generating the corner solution.

of the planner at the steady state yields:

$$\underbrace{\frac{\partial U_{j,t}}{\partial C_{ijk,st}}}_{\text{MU of fishery consumption}} = \underbrace{\underbrace{\frac{\partial U_{j,t}}{\partial C^o_{j,t}}\left(\frac{\partial Q^o_{i,t}}{\partial L^o_{i,t}}/\frac{\partial Q_{ijk,st}}{\partial L_{ijk,st}}\right)}_{\text{static MC}} + \underbrace{\frac{\beta\Omega_{k,st}}{1-\beta\Theta_{k,st}}\frac{\partial H_{k,st}}{\partial Q_{ijk,st}}}_{\text{dynamic MC}}}_{\text{MC of fishery consumption}} \tag{1.22}$$

where $\Omega_{k,st} \coloneqq \partial W_{t+1}/\partial x_{k,st}$ and $\Theta_{k,st} \coloneqq \partial x_{k,st+1}/\partial x_{k,st}$. The allocation of outside good is undetermined with the symmetric Pareto weights where $\phi_i = 1$. The derivation details are provided in Appendix A.3.2.

For each variety of fishery $C_{ijk,st}$, the planner allocates the fishery consumption until the marginal utility equalizes with the marginal cost of the fishery consumption. The marginal cost of the fishery consumption consists of two terms: the static marginal cost and the dynamic marginal cost.

In equation (1.22), the first term on the right-hand side represents the static marginal cost, which is the opportunity cost of inputs that could have been used to produce the outside good instead of the fishery. While both the planner and decentralized equilibrium account for this static cost, the key difference lies in the second term: the dynamic marginal cost. This term captures the welfare loss from reduced future productivity as harvest today depletes fishery stocks.

The planner internalizes the dynamic marginal cost by explicitly accounting for the effect of harvest today on future fishery stocks. In contrast, the decentralized equilibrium disregards these future impacts, failing to internalize the dynamic marginal cost. The market failure to internalize the dynamic marginal cost becomes the source of externalities in global fisheries. Given that this dynamic marginal cost is positive and the fishery consumption exhibits diminishing marginal utility, the planner allocates fewer inputs to the fishery and maintains larger fishery stocks compared to the decentralized equilibrium.

The size of the dynamic marginal cost at the steady state depends on three terms: (i) the welfare loss per unit of stock decrease and (ii) the amount of stock decrease given one unit of fishery consumption.

First, the welfare loss per unit of stock decrease, $\Omega_{k,st} = \partial W_{t+1}/\partial x_{k,st}$, captures how much of the welfare decreases through the lower productivity given one unit decrease in stock. Given the fishery technology in equation (1.7), the fishery sector becomes less productive as the fishery stock decreases and the stock elasticity of output ξ governs the size of the effect. The lower productivity decreases the welfare from all countries in the economy. If there were no productivity gains from fishery stock ($\xi = 0$), there would be no externalities, implying that the planner allocation would coincide with the decentralized equilibrium.

Second, the total size of welfare loss depends also on the amount of stock decrease given one

unit of fishery consumption. Given equation (1.11), one unit of fishery consumption requires to decrease the stock by $\partial H_{k,st}/\partial Q_{ijk,st} = d_{ij,s}\tau_{ik,s}$ due to the iceberg trade and commuting frictions. Since regrowth and harvest of fish depend on the stock level from equation (1.9), the change in stock at the next period, given one unit change of stock today, is not necessarily one. However, it is endogenously determined by $\Theta_{k,st} = \partial x_{k,st+1}/\partial x_{k,st}$, which captures the change in the number of stocks next period, given one unit change in fishery stock today. Given a unit decrease in fishery stock today, the number of stock in the next period decreases by $\Theta_{k,st}$, and the effect is accumulated over periods. At the steady state, the total number of affected stock becomes $1/\left(1-\beta\Theta_{k,st}\right)$ units in the formulation of infinite sum up to the discount rate.

Finally, I point out the sufficient condition for $\Theta_{k,st}$ to converge.

Lemma. *At the steady state, sufficient conditions for $\theta_{k,st}$ to converge are i) $\xi \geq 1$ or ii) $0 < \xi < 1$ and $\gamma_{k,s} < \frac{1}{1-\xi}\left(\frac{1}{\beta} - 1\right)$*

Proof. See Appendix A.3.4. □

The intuition is as follows. When ξ is large enough, given a unit increase in stock, the harvest increases enough to suppress $\Theta_{k,st}$. When ξ is small, since the harvest does not suppress $\Theta_{k,st}$ as much as in the previous case, smaller $\gamma_{k,s}$ is required so that the regrowth does not respond too rapidly given a unit increase in stock. As ξ approaches zero, the required $\gamma_{k,s}$ decreases and gets closer to $1/\beta - 1$.

1.4.4 Optimal Policy

The First and Second Welfare Theorem guarantee that the following two approaches yield identical outcomes: the primal approach, where the planner directly chooses optimal allocation, and the dual approach, where the planner sets the optimal tax and the lump-sum international transfers [Ljungqvist and Sargent, 2018]. In this subsection, I extend the decentralized equilibrium with the tax and derive the expression for the optimal policy.

The tax $t_{ijk,st}$ additively increases the marginal cost of production so that the price after the tax $\tilde{p}_{ijk,st}$ becomes

$$\tilde{p}_{ijk,st} = p_{ijk,st} + t_{ijk,st} \tag{1.23}$$

where $p_{ijk,st}$ is the price from the decentralized equilibrium without the tax as described in equation (1.12). Since the tax $t_{ijk,st}$ is specific to the destination, this tax could be interpreted as the combination of domestic production tax and export tax.

The collected taxes are redistributed to the households as a lump-sum transfer. In turn, the balance of budget condition for households in equation (2.23) now becomes

$$\sum_{j\in I}\sum_{s\in S}\sum_{k\in K} w_{i,t}L_{ijk,st} + w^o_{i,t}L^o_{i,t} + \sum_{j}\sum_{s}\sum_{k} t_{ijk,st}Q_{ijk,st} = X_{i,t} + X^o_{i,t} \tag{1.24}$$

Following the dual approach, the planner can choose the optimal tax $t^*_{ijk,st}$ that achieves the socially optimal allocation from Section 1.4.3.1. There is no need to impose the lump-sum international transfers. Under the quasi-linear preferences, there is no income effect in the fishery consumption, and the lump-sum international transfer only affects the consumption of outside good across countries. However, in the planner allocation with the symmetric Pareto weights $\phi_i = 1$, the allocation of outside good is undetermined since the planner is indifferent to the consumption of outside good across countries. Therefore, any set of international transfers, including zero transfers across all countries, is consistent with the socially optimal allocation.[23]

Respecting the first-order conditions from the decentralized equilibrium, the optimal tax $t^*_{ijk,st}$ equals the dynamic marginal cost from equation (1.22).

$$t^*_{ijk,st} = \frac{\beta\Omega_{k,st}}{1-\beta\Theta_{k,st}}\frac{\partial H_{k,st}}{\partial Q_{ijk,st}}$$

where the details are explained in Appendix A.3.3.

1.5 Taking the Model to Data

This section provides the calibration of the quantitative model. As described in Section 1.2, I aggregate the world into 30 countries, the global oceans into 46 fishing locations, and the fishery species into 10 species. I take the model to data in 2018 to calibrate the model. I begin by describing the calibration of elasticities of substitutions, and proceed to the calibration of remaining parameters.

1.5.1 Calibration of Elasticities of Substitutions

In this subsection, I calibrate the parameters governing the elasticities of substitutions. In the spirit of Costinot et al. [2016], I use a supply-side instrument for productivity to identify the demand relationship in the gravity equation. I start by estimating the elasticity of substitution across countries η, then estimate the elasticity of substitution across species ν. Lastly, I estimate the elasticity

[23] If the Pareto weights were not symmetric, the lump-sum international transfer is necessary so that the outcome is consistent with the corner solution by the planner where a country with the largest weight consumes all of the outside good.

of substitution across fishing locations κ using the indirect inference disciplined by equation (1.2) about the relationship between the subsidies and the location of fishing.

1.5.1.1 Elasticity of Substitution across Exporters (η)

I estimate the elasticity of substitution across exporters η from the following gravity equation.

$$\log\left(\frac{X_{ij,s}}{X_{j,s}}\right) = (1-\eta)\log p_{i,s} + \phi_{j,s} + \phi_{ij} + \varepsilon_{ij,s} \tag{1.25}$$

where $X_{ij,s}/X_{j,s}$ is the expenditure share for exporter i in all expenditure by importer j for species s, $p_{i,s}$ is the producer prices at the border of exporter i for species s, $\phi_{j,s}$ is the importer-species fixed effect, ϕ_{ij} is the exporter-importer fixed effect, and $\varepsilon_{ij,s}$ is the residual term. I observe the expenditure share $X_{ij,s}/X_{j,s}$ from the trade dataset, and the producer prices at the border $p_{i,s}$ from the ex-vessel prices dataset, which is invariant cross fishing locations. In particular, the producer prices at the border $p_{i,s}$ is:

$$p_{i,s} = \left[\sum_{k\in K} b_{k,s}\left(p_{ik,s}\right)^{1-\kappa}\right]^{\frac{1}{1-\kappa}} \tag{1.26}$$

where $p_{ik,s}$ equals to the marginal cost of production by exporter i at fishing location k for species s. From the exporter-importer fixed effect $\phi_{j,s}$ and the residual term $\varepsilon_{ij,s}$, I recover the exporter-importer specific preference shifter b_{ij} and the trade cost $d_{ij,s}$ such that $b_{ij} = \exp\left(\phi_{ij}\right)$ and $d_{ij,s} = \exp\left(\frac{1}{1-\eta}\varepsilon_{ij,s}\right)$.

A concern about endogeneity arises because prices can be correlated with unobserved demand shifters. To mitigate this concern, I adopt a supply-side IV, which is correlated with the producer prices at the border but uncorrelated with an unobserved demand shifter. Specifically, I instrument the producer prices at the border $p_{i,s}$ with the proximity to suitable habitats $Z_{i,s}$ by exporter i for species s.

I construct the instrument, the proximity to suitable habitats $Z_{i,s}$, using the grid level data on habitat suitability and the linear distance between each grid and the closest port of countries. The grid level data on habitat suitability $Z_{g,s}$ measures how suitable habitat a grid g is for species s, using the geographic conditions including ocean depth, temperature, and climate. I construct the country level measure for proximity to habitat suitability $Z_{i,s}$:

$$Z_{i,s} = \sum_{g\in G} \frac{Z_{g,s}}{\log dist_{ig}}$$

where $dist_{ig}$ is the linear distance to each grid g from the closest port at country i. To construct the

Table 1.2: Estimation of η

	(1) PPML	(2) OLS	(3) IV	(4) IV	(5) IV
$\log P_{is}$	-0.386***	-0.808***	-4.025***	-3.905***	-5.917***
	(0.057)	(0.078)	(0.461)	(0.628)	(1.309)
Implied η	1.386	1.808	5.025	4.905	6.917
Importer-species FE	Y	Y	Y	Y	Y
Exporter-importer FE	Y	Y	Y	Y	Y
Sample	Full	Full	Full	HHI High	HHI Low
N	8,760	6,223	6,223	2,988	3,153
First stage			-1.903***	-1.771***	-1.262***
			(0.129)	(0.182)	(0.205)
CD-F			220.22	94.22	35.21

Notes: The Herfindahl–Hirschman Index is constructed to measure the concentration of exporters across species, such that $HHI_s = \sum_{i \in I} EXP_{i,s}^2$ where $EXP_{i,s}$ is the output share of country i from total output for species s. "HHI High" restricts the sample to the species of which the Herfindahl–Hirschman Index is aobve the median, while "HHI Low" restricts the sample to the species of which the Herfindahl–Hirschman Index is below the median.

country level measure for proximity to habitat suitability, I take the weighted average of the habitat suitability $Z_{g,s}$ across grids, where the inverse of weights is the log of $dist_{ig}$.

The argument for the valid instrument is as follows. The relevance condition requires that the producer prices at the border for species s in exporter i are lower than that in the other countries if exporter i is located closer to the suitable habitat for species s than other countries are. The exclusion restriction holds as long as the distance to the suitable habitat is not correlated with the unobserved demand shifter.

Table 1.2 shows the estimates of η. Columns (1) and (2) show the estimation results from PPML and OLS, respectively. Column (3) shows the result from IV regression, where I obtain the elasticity of substitution across exporters $\eta = 5.025$. The first stage is negative, confirming the relevance condition that the proximity to suitable habit is associated with lower fishery prices. The large difference in the coefficient between OLS and IV indicates that the endogeneity concern from OLS could be severe.

A concern for exclusion restriction is that tastes toward the importer could reflect the proximity to suitable habitats. For example, consumers might have built up a particular taste for Norwegian Salmon since Norway is known to have a better habitat for salmon. If such concern is valid, the coefficient might have an upward bias since the preference shifter would be positively correlated with the proximity to suitable habitats. To investigate the validity of the concern, I estimate the parameter restricting the sample by whether the species are produced by multiple countries. In particular, I construct the relevant Herfindahl–Hirschman Index to measure the concentration of

exporters across species such that

$$HHI_s = \sum_{i \in I} EXP_{i,s}^2$$

where $EXP_{i,s}$ is the output share of country i in total output of species s.

Column (4) restricts the sample to the species of which the production is concentrated in particular countries such that the HHI is above the median across all species. While the point estimate of column (4) is larger than that of column (3), I do not find a statistical significance that the coefficients are different across samples. Column (5) restricts the sample to the species of which the production is dispersed across countries such that the HHI is below the median across all species. While the point estimate of column (5) is smaller than that of column (3), I again do not find a statistical significance that the coefficients are different across samples.

1.5.1.2 Elasticity of Substitution across Species (ν)

Next, I estimate the elasticity of substitution across species ν from the gravity equation, in the similar step from the previous subsection.

$$\log\left(\frac{X_{j,s}}{X_j}\right) = (1-\nu)\log P_{j,s} + \phi_j + \varepsilon_{j,s}$$

where $X_{j,s}/X_j$ is the expenditure share for species s in all expenditure by importer j, $P_{j,s}$ is the consumer prices for fishery bundle of importer j for species s, ϕ_j is the importer fixed effect, and $\varepsilon_{j,s}$ is the residual term.

To construct the consumer prices for fishery bundle $P_{j,s}$, I use the observed producer prices at the border $p_{i,s}$ and the estimates of the preference shifter b_{ij}, the trade cost $d_{ij,s}$, and the elasticity of substitution across exporters η from the previous subsection such that

$$P_{j,s} = \left(\sum_i b_{ij} d_{ij,s}^{1-\eta} p_{i,s}^{1-\eta}\right)^{\frac{1}{1-\eta}}$$

Similarly, a concern about endogeneity arises because prices can be correlated with unobserved demand shifters. To alleviate this concern, I instrument the consumer prices $P_{j,s}$ with the proximity to suitable habitats $Z_{j,s}$ by importer j for species s. The relevance condition requires that the consumer prices in importer j for species s are lower than that for the other species if importer j is located closer to the suitable habitat of species s than to the other species. The exclusion restriction assumes that geography is uncorrelated with unobserved demand shifters across species.

Table 1.3 shows the estimates for ν . Columns (1) and (2) show the estimation results from

Table 1.3: Estimation of ν

	(1) PPML	(2) OLS	(3) IV	(4) IV	(5) IV
$\log P_{js}$	-0.695***	-0.938***	-6.562***	-7.889***	-6.872***
	(0.268)	(0.277)	(2.507)	(3.429)	(3.095)
Implied ν	1.695	1.938	7.562	8.889	7.872
Importer FE	Y	Y	Y	Y	Y
Sample	Full	Full	Full	HHI High	HHI Low
N	300	300	300	150	150
First stage			-1.155***	-1.289***	-0.798***
			(0.394)	(0.543)	(0.215)
CD-F			11.14	4.49	11.30

Notes: The Herfindahl–Hirschman Index is constructed to measure the concentration of importers across species, such that $HHI_s = \sum_{j \in I} IMP_{j,s}^2$ where $IMP_{j,s}$ is the expenditure share of country j from total expenditure of species s. "HHI High" restricts the sample to the species of which the Herfindahl–Hirschman Index is aobve the median, while "HHI Low" restricts the sample to the species of which the Herfindahl–Hirschman Index is below the median.

PPML and OLS. Column (3) shows the result from IV regression, where I obtain $\nu = 7.562$. The first stage is negative, as expected, confirming that the relevance condition holds. The large difference in the coefficient between OLS and IV justifies the need for the instrument.

Again, a concern for exclusion restriction is that tastes toward the species could reflect the proximity to suitable habitats. For instance, Norwegian consumers might have built up a particular taste for salmon if they were disproportinately exposed to salmon and lacked exposure to other species whose habitat is distant from Norway. The coefficient would be upward-biased if such concern is valid since the preference shifter is positively associated with the proximity to suitable habitats. To study the validity of the concern, I again estimate the parameter restricting the sample by whether the species are consumed by multiple countries. I construct the relevant Herfindahl–Hirschman Index to measure the concentration of importers across species such that:

$$HHI_s = \sum_{j \in I} IMP_{j,s}^2$$

where $IMP_{j,s}$ is the expenditure share of country j in total expenditure of species s.

Column (4) restricts the sample to the species of which the consumption is concentrated in particular countries such that the HHI is above the median across all species. Column (5) restricts the sample to the species of which the consumption is dispersed across countries such that the HHI is below the median across all species. I do not find a statistical significance that the coefficients are different across samples.

1.5.1.3 Elasticity of Substitution across Locations (κ)

Lastly, I estimate the elasticity of substitution across locations κ from the indirect inference. The idea is that equation (1.2) about the relationship between the fuel subsidies and the location of fishing is informative about the elasticity of substitution across locations κ. The impact of fuel subsidies on the outputs at high sea relative to EEZ depends on how substitutable the varieties across regions are.

To estimate the elasticity of substitution across locations κ, I start by simulating the extended version of the model in Section 1.4.4 with the policy instruments. For a given κ, I shock the model with exogenous changes in the fuel subsidies over time that are calibrated to match the changes in fuel subsidies from actual data, where the fuel subsidies are modeled to target the high sea to generate a disproportionate effect on fishing location. Then, for each κ, I run equation (1.2) using the simulated data. Finally, I pick κ that generates the coefficient β_1, which best matches the coefficient from Table 1.1 using the actual data. The detailed step is described in Appendix A.4.1.

Appendix Figure A.1 shows the relationship between the elasticity of substitution parameter across locations κ and the estimated coefficient β_1, confirming that the effect of fuel subsidies on the outputs at high sea relative to EEZ is larger when the elasticity of substitution across locations is larger. From the indirect inference, I obtain the elasticity of substitution $\kappa = 8.08$.

1.5.2 Calibration of Remaining Parameters

This subsection calibrates the remaining parameters along with fundamentals. I set the stock elasticity of output $\xi = 0.79$, following Zhang [2011]. The discount rate is set to $\beta = 0.97$, following Nordhaus [2007]. As discussed in Section 1.4.3, the Pareto weights are calibrated to have equal weights across countries such that $\phi_i = 1$.

Taking the model to data in 2018, I use the standard model inversion methods to recover the fundamentals. For the demand shifter toward the fishery bundle b_i, I directly match the fishery expenditure for each country i by leveraging the property of quasi-linear preference. For the demand shifter toward the species b_s, I match the expenditure share of species s in total fishery expenditure. For the demand shifter toward the exporter b_{ij}, I match the expenditure share of exporter i in total expenditure by importer j. Lastly, for the demand shifter toward the fishing location $b_{k,s}$, I match the expenditure share of fishing location k in all fishing locations for species s.

I then proceed to calibrate the productivity shifters. For the outside good productivity shifter z_i^o, I match the GDP per capita for each country i. For the fishery productivity shifter z_i, I match the levels of fishery output of country i. I recover the commuting costs $\tau_{ik,s}$ by matching the output share of fishing location k in all fishing locations by country i for species s. I use the gravity

Table 1.4: Parameter Calibration

Parameter	Value	Source
a. Preferences		
Demand shifter	$b_i, b_s, b_{ij}, b_{k,s}$	Model inversion
Elasticity of substitution	$\nu = 7.56$, $\eta = 5.03$	IV regression
	$\kappa = 8.08$	Subsidy regression
b. Technology and geography		
Productivity shifter	z_i^o, z_i	Model inversion
Stock elasticity	$\xi = 0.79$	Zhang [2011]
Commuting costs	$\tau_{ik,s}$	Model inversion
Trade costs	$d_{ij,s}$	Gravity residuals
c. Planner-related parameter		
Growth rate	$\gamma_{k,s}$	CMSY++ Package
Discount rate	$\beta = 0.97$	Nordhaus [2007]
Pareto weights	$\phi_i = 1$	

equation to recover the trade costs $d_{ij,s}$. Table 2.2 provides the summary of parameter calibration.

1.5.3 Model Fit

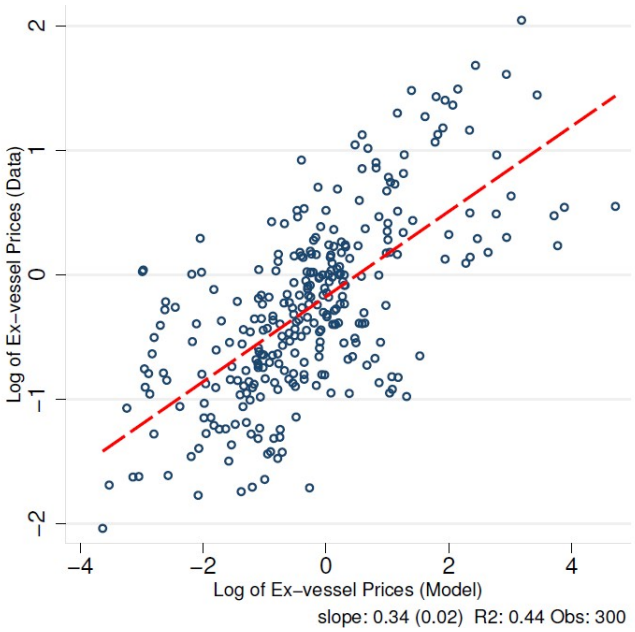
Before I present the quantitative results, I assess the model fit using non-targeted moments. While the calibration process targets the fishery outputs and expenditures, one of the non-targeted moments is the ex-vessel prices, which are the fishery prices when landed at the domestic port. As described in Subsection 1.5.1, these prices are directly observed in the data. In the model, I construct these prices by aggregating producer prices across fishing locations for each species and country following equation (1.26).

Figure 1.3 compares the ex-vessel prices implied by the model against the observed data. The observed data is normalized so that the mean of the observed ex-vessel prices equal to the mean of the ex-vessel prices implied by the model. The ex-vessel prices implied by the model fit well with the ex-vessel prices from the data, confirming the validity of the model.

1.6 Quantitative Results

In this section, I examine the quantitative results from three scenarios: the decentralized equilibrium, the planner allocation, and a policy counterfactual. Using the model calibrated to data in 2018, I first project the economy forward under a Business As Usual (BAU) scenario to assess the trajectory of the decentralized equilibrium. I then contrast the BAU outcomes with those from the planner allocation to quantitatively illustrate the externalities from open access to global fishery.

Figure 1.4: Model Fit



Notes: The figure shows the relationship between the ex-vessel prices implied by the model (x-axis) and the observed data (y-axis), where the ex-vessel prices refer to the prices of fish when landed at the domestic port. The units of observation are at the country-species level. The model-implied ex-vessel prices are constructed by aggregating producer prices across fishing locations for each species and country, following equation (1.26). The ex-vessel prices from the data are normalized so that the average of ex-vessel prices from the data matches the average of ex-vessel prices from the model.

Finally, I simulate a policy counterfactual that permanently eliminates fuel subsidies across all countries. The difference in outcomes between the BAU and the counterfactual demonstrates the impact of fuel subsidies.

1.6.1 Decentralized Equilibrium (Business As Usual) and Planner

Table 1.5 summarizes the comparison of the outcomes between the BAU and the planner allocation. Under the BAU, the average stock to capacity ratio exhibits a substantial decline from 42.2% in the initial year to 28.6% at the steady state. When the planner internalizes the externalities of the fishery production, the average stock to capacity ratio increases to 53.8% at the steady state, representing an 88% increase relative to the BAU steady state.

The socially optimum allocation by the planner involves initially relocating 35% of fishery labor to the outside good sector. This reallocation generates two immediate effects: a reduction in fishery output and an increase in outside good output. Given the quasi-linear utility preferences, I can decompose the welfare effects into fishery consumption and outside good consumption components. In the initial period, the welfare from fishery consumption decreases by 7.8%, while the welfare from outside good consumption increases by 0.13%.

The reallocation of fishery labor to the outside good sector facilitates stock accumulation over

Table 1.5: Quantitative Results: BAU and Planner

	BAU		Planner		% Difference	
	t=0	steady state	t=0	steady state	t=0	steady state
Average stock to capacity ratio	0.422	0.286	0.422	0.538	-	88.1%
Share of fishery labor					-35.1%	-39.0%
Share of outside good labor					0.28%	0.35%
Welfare from fishery					-7.8%	15.3%
Welfare from outside good					0.13%	0.12%
Welfare					-0.02%	0.39%
Net present value of welfare					0.11%	

Notes: This table compares the outcomes from the BAU and the planner allocation for the initial period and the steady state. "% Difference" refers to the percentage difference between the BAU to the planner allocation for the corresponding period. Welfare from fishery refers to the welfare portion of fishery consumption in the quasi-linear preferences, while welfare from outside good refers to the welfare portion of outside good consumption in the quasi-linear preferences.

time. As stocks accumulate, the productivity of the fishery sector increases, allowing for larger outputs despite lower labor inputs. At the steady state, the welfare from fishery consumption increases by 15.3% in the planner allocation relative to the BAU. Additionally, the larger labor allocation to the outside good sector generates a 0.12% increase in the welfare from outside good consumption. These welfare gains from the two sectors result in a 0.39% increase in total global welfare at the steady state.

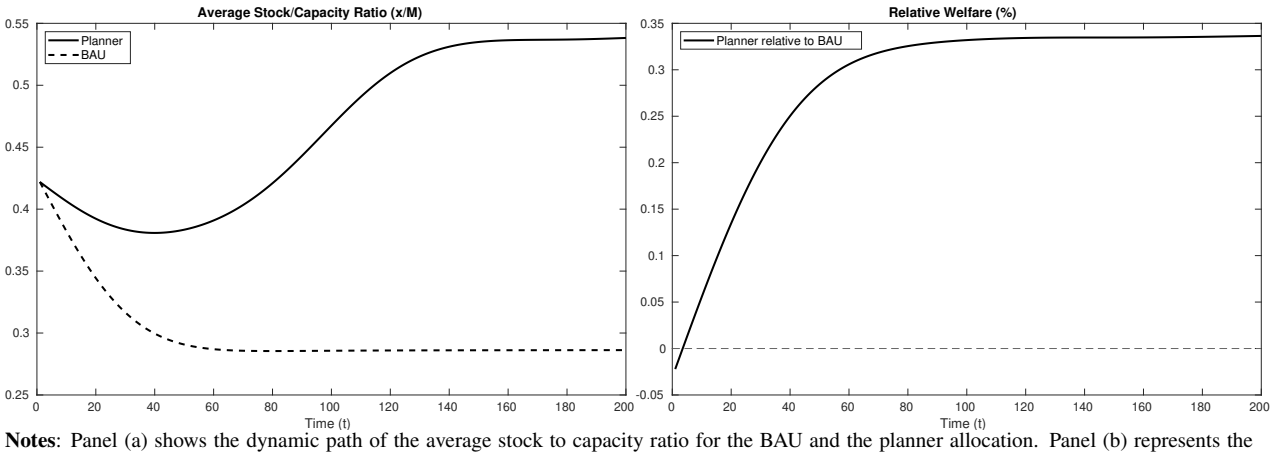
Figure 1.5 illustrates the dynamic transition paths under both scenarios. Panel (a) shows that even under the planner allocation, the average stock to capacity ratio initially decreases. This is because the planner, who discounts the future, prioritizes present consumption over future consumption. Panel (b) reveals the evolution of relative global welfare under the planner allocation compared to the BAU. While the trajectory shows a modest initial decline due to reduced fishery consumption, the increased fishery productivity from accumulated stocks generates a larger relative welfare at the steady state.

To evaluate the overall welfare implications, I construct the measure of the net present value of global welfare in the decentralized equilibrium following equations (1.20) and (1.21), which is comparable to the planner allocation. Accounting for the entire dynamic transition path, Table 1.5 shows that the net present value of global welfare under the planner allocation increases by 0.11% relative to BAU.

We now turn to the spatial heterogeneity across fishing locations. Figure 1.6 shows the difference in the average stock to capacity ratio between the initial year and the steady states of the BAU and the planner allocation. Panel (a) illustrates the average stock to capacity ratio at the BAU steady state relative to the initial year. Compared to the the initial year, most fishing locations experience substantial declines in their average stock to capacity ratio at the BAU steady state, with

Figure 1.5: Dynamic Path of Outcomes: BAU and Planner

(a) Average Stock to Capacity Ratio (b) Relative Welfare (Planner relative to BAU)



Notes: Panel (a) shows the dynamic path of the average stock to capacity ratio for the BAU and the planner allocation. Panel (b) represents the welfare of the planner allocation relative to the BAU in percentage change.

the exception of a few fishing locations such as the EEZs of Chile and Bangladesh. The decline is more pronounced in the high seas compared to the EEZs, with the Central Pacific Ocean showing the most severe reduction in the average stock to capacity ratio.[24]

Panel (b) depicts the average stock to capacity ratio at the steady state of planner allocation relative to the initial year. In contrast to the BAU scenario, as the planner internalizes the externalities of fishery production, many fishing locations show improved average stock to capacity ratios compared to their 2018 levels. The most evident contrast is that high seas show increases in their stock while most EEZs continue to experience declines.[25]

Panel (c) shows the average stock to capacity ratio at the steady state of planner allocation relative to the BAU steady state, providing the most direct comparison. Most fishing locations show a higher stock to capacity ratio except the EEZs in the African countries. The most drastic increases occur in the high seas of the Pacific and the Indian Oceans, where the difference in average stock to capacity ratio is almost one, implying that fishery stocks recover from near depletion to approach the carrying capacity.

1.6.2 Policy Counterfactual: Eliminating Fuel Subsidies

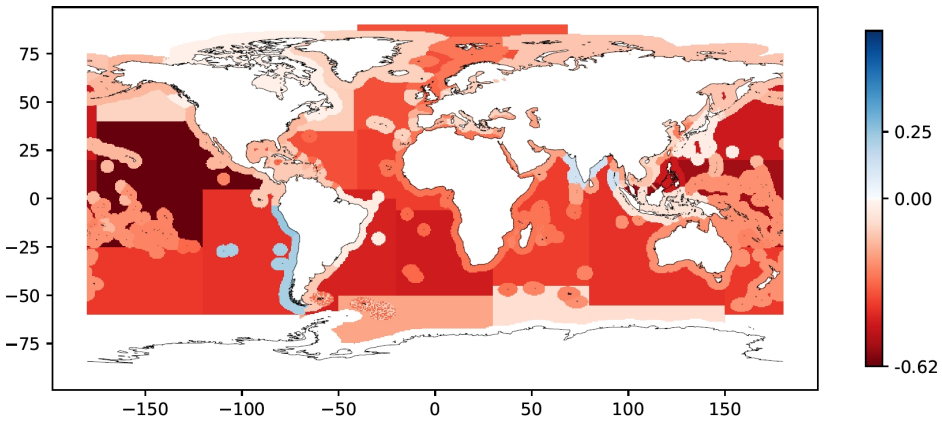
Next, I conduct a counterfactual analysis to examine the impact of fuel subsidies. Fuel subsidies have emerged as a major regulatory concern since they enable fishing fleets to exploit resources in

[24] Appendix Figure A.3 panel (a) and (b) show the average stock to capacity ratio in the initial year and at the steady state under the BAU.

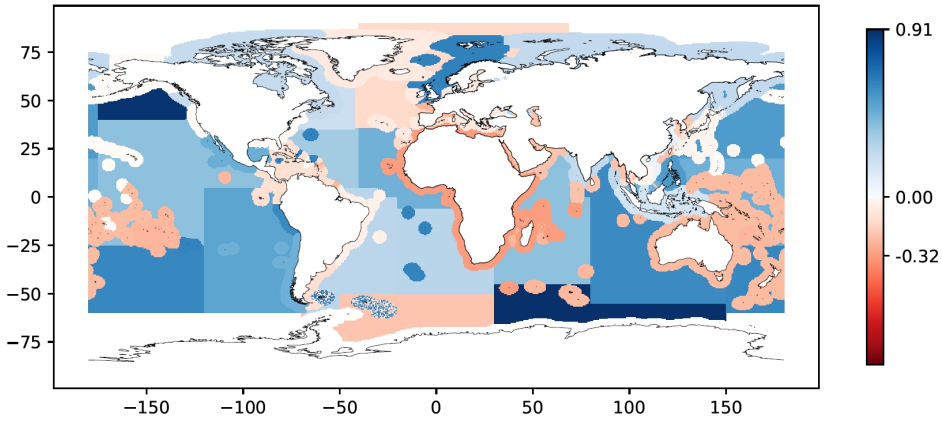
[25] Appendix Figure A.3 panel (c) displays the average stock to capacity ratio at the steady state of the planner allocation.

Figure 1.6: Average Stock to Capacity Ratio (BAU and Planner)

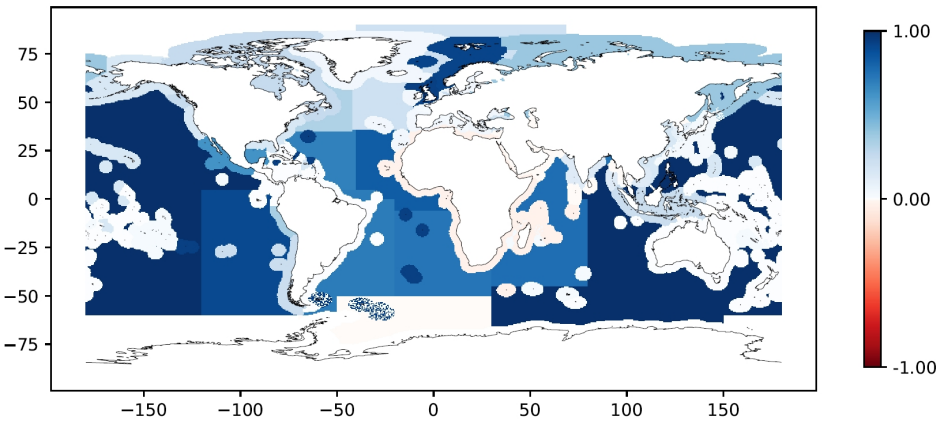
(a) BAU Steady State relative to Initial Year



(b) Planner Steady State relative to Initial Year



(c) Planner Steady State relative to BAU Steady State



Notes: The maps display the difference in average stock to capacity ratio across species in each fishing location from the quantitative exercises. Panel (a) shows the difference in average stock to capacity ratio between the initial year and the steady state under the BAU. Panel (b) depicts the difference in average stock to capacity ratio between the initial year and the steady state under the planner allocation. Panel (c) represents the difference in average stock to capacity ratio between the steady states under the BAU and the planner allocation.

Table 1.6: Quantitative Results: BAU and Counterfactual

	BAU		Counterfactual		% Difference	
	t=0	steady state	t=0	steady state	t=0	steady state
Average stock to capacity ratio	0.422	0.286	0.422	0.295	-	3.22%
high sea	0.379	0.090	0.379	0.099	-	10.3%
EEZ	0.431	0.326	0.431	0.335	-	2.76%
Welfare from fishery					-0.17%	1.42%
Welfare from outside good					0.001%	0.001%
Welfare					0.000%	0.01%
Net present value of welfare					0.004%	

Notes: This table compares the outcomes from the BAU and the counterfactual for the initial period and the steady state. "% Difference" refers to the percentage difference between the BAU to the counterfactual for the corresponding period. Welfare from fishery refers to the welfare portion of fishery consumption in the quasi-linear preferences, while welfare from outside good refers to the welfare portion of outside good consumption in the quasi-linear preferences.

remote high seas that would otherwise be economically inaccessible [Sumaila et al., 2019]. Building on Pattern 3 in Section 2.3, which demonstrates the disproportionate effect of fuel subsidies on high seas output, I assume that fuel subsidies are exclusively targeted to high seas.

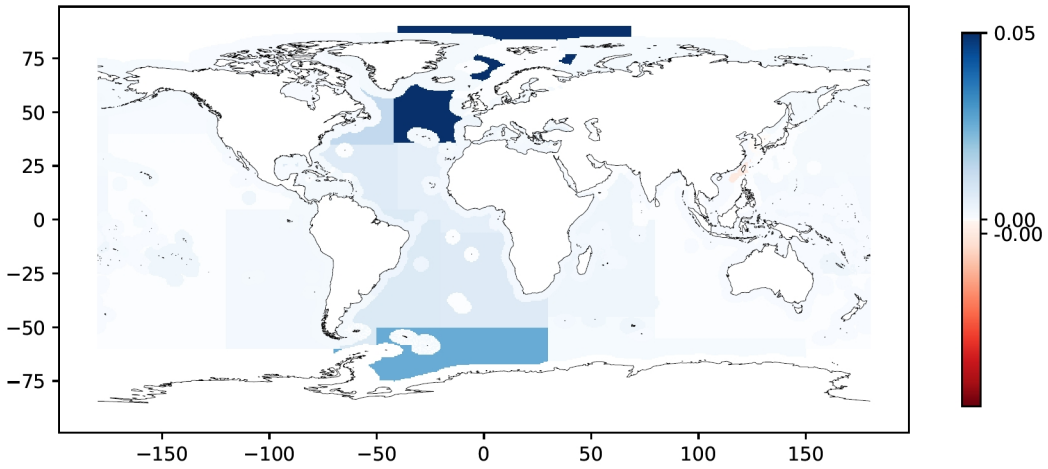
To counteract the fuel subsidies that are present in the BAU, I impose a production tax particularly on the high seas. From the extended model with policy instruments presented in Section 1.4.4, I calibrate country-specific tax to match the tax revenues in the counterfactual with the observed fuel subsidies in the data.

Table 1.6 compares the outcomes between the BAU and the counterfactual where the fuel subsidies are eliminated. While the average stock to capacity ratio falls to 28.6% at the steady state under the BAU, the ratio decreases only to 29.5% in the counterfactual. This indicates that the fuel subsidies reduce the average stock to capacity ratio by 3.22% at the steady state.

Given that fuel subsidies exclusively target fishing at the high seas, their impact exhibits significant heterogeneity between the high seas and the EEZs. In the BAU scenario, the high seas experience a dramatic decline in the average stock to capacity ratio from 37.9% initially to 9.0% at steady state. In contrast, the EEZs show a more moderate decline from 43.1% to 32.6%, suggesting that resource depletion predominantly occurs in the high seas. Eliminating fuel subsidies increases the average stock to capacity ratio to 9.9% in high seas and 33.5% in EEZs, representing increases of 10.3% and 2.76%, respectively, confirming the disproportionate impact on high seas.

The elimination of fuel subsidies initially raises the price of the fisheries and decreases the demand for the fishery, reallocating labor to the outside good, which is a pattern consistent with the planner allocation. While this reallocation of labor reduces the welfare from fishery consumption initially, fishing productivity increases in the long run as fishery stock accumulates. At the steady state, despite lower labor inputs, welfare from fishery consumption exceeds the BAU level.

Figure 1.7: Average Stock to Capacity Ratio (Counterfactual SS relative to BAU SS)



Notes: The map shows the difference in the average stock to capacity ratio between BAU steady state and counterfactual steady state.

Accounting for the entire dynamic path, the net present of welfare increases by 0.004% in the counterfactual relative to the BAU, indicating that fuel subsidies generate negative welfare impacts globally.[26]

Figure 1.7 illustrates the spatial distribution of changes in the average stock to capacity ratio between the counterfactual and BAU steady state across fishing locations. The results reveal substantial spatial heterogeneity in the impact of eliminating fuel subsidies. Most EEZs demonstrate minimal increase in stock or even experience lower stock as in Taiwan's EEZ. In contrast, high seas exhibit substantial gains, particularly throughout the Atlantic Ocean, with the Northeast Atlantic experiencing the most drastic increase.

1.7 Conclusion

This paper develops a dynamic spatial model of global fisheries to quantify the externalities arising from open access and evaluate the impact of fishery policies on global welfare. I calibrate the model and estimate key elasticities by leveraging novel geospatial data on fishery catch and stocks, providing a comprehensive framework for understanding global fishery.

The results reveal substantial inefficiencies under the Business As Usual scenario of the decentralized equilibrium. Under open access to the fishery, the atomistic firms fail to account for the externalities from fishery production, leading to the overexploitation of fishery stocks. In contrast, the social planner fully internalizes the externalities and reallocates the labor from the fishery sector to the outside good sector. While reducing the short-term fishery output, this reallocation leads

[26] Appendix Figure A.2 presents the dynamic path of the outcomes for the counterfactual and the BAU.

to long-term gains through larger stock and increased productivity. The stark difference between the BAU and the planner allocation underscores the magnitude of externalities in global fisheries and the potential gains from policy interventions.

The counterfactual analysis of eliminating fuel subsidies yields two policy insights. First, these subsidies generate negative welfare effects at the global level, with their elimination leading to both higher stock levels and increased welfare. This highlights the importance of multilateral coordination in global fishery policy. Second, while eliminating fuel subsidies is helpful, the resulting stock levels and welfare outcomes remain substantially below the social optimum. This indicates that more comprehensive policy instruments may be necessary to fully internalize the externalities from open access to global fishery.

It is crucial to acknowledge the feasibility of implementing the socially optimal allocation. To implement the socially optimal allocation, the corresponding optimal policy should vary across exporters, importers, fishing locations, species, and time. In practice, the policy tools are more constrained. For instance, production policies often lack the dimension of importers, while trade policies may not account for the dimension of fishing locations.

The contingent trade policies described in Harstad [2024] could offer a feasible approach. Such policies could mandate the specification of fishery fishing locations in trade agreements, with tariff rates contingent on the gap between current and optimal stock. For example, tariffs could be imposed when stocks fall below optimal levels, while subsidies could be offered when stocks exceed optimal levels. This paper provides theoretical foundations and quantitative evidence to support the design and implementation of such policies.

CHAPTER 2

Deforestation: A Global and Dynamic Perspective

Abstract

We study deforestation in a dynamic world trade system. We first document that between 1990-2020: (i) global forest area has decreased by 7.1 percent, with large heterogeneity across countries, (ii) deforestation is associated with expansions of agricultural land use, (iii) deforestation is larger in countries with a comparative advantage in agriculture, and (iv) larger population growth leads to deforestation. We build a model in which structural change and comparative advantage determine the extent, location, and timing of deforestation. We show analytically and quantitatively that, if agriculture is complementary in demand to other sectors, global reductions in trade costs reduce global deforestation, even if such shocks increase deforestation when experienced only by an individual economy. In our calibrated model, a 30 percent reduction in global agricultural trade costs increases steady-state forest share for world area by 0.5 percentage points, taking decades to occur. In the cross-section, countries with a comparative advantage in agriculture expand production at the expense of more deforestation there.[1]

2.1 Introduction

Deforestation has gathered speed in recent decades, bringing the adverse impacts of human action on the world's climate and biodiversity to the forefront of public debate.[2] Across countries, the experiences of individual countries have varied greatly and ranged from substantial deforestation in Brazil to reforestation in China. Seeking to understand these experiences, an important literature has identified several drivers of deforestation, such as international crop prices, infrastructure projects, institutional quality, and trade and environmental policies. World population, moreover,

[1] This chapter is co-authored with Farid Farrokhi, Heitor S. Pellegrina, and Sebastian Sotelo.

[2] For instance, global net emissions from deforestation and land-use change accounted for 11 percent of total human-caused CO_2 emissions between 2000 and 2010 [IPCC, 2014].

is expected to grow by 25% until 2050, which has renewed concerns about food production and pressures on global land use.[3]

In line with these considerations, and against a backdrop of increasing globalization, trade policy is emerging as a potential, feasible tool to curb climate change generally and deforestation in particular—e.g, the EU is working on legislation to ban imports of agricultural products that are linked to deforestation. Unlike in the case of manufacturing, however, agricultural tariffs remain high and have been a recurrent component in trade negotiations. This situation calls for evaluating the role of global policies to deepen integration in agricultural markets, an evaluation that is all the most important because previous work, which has thoroughly studied individual countries and industries, is less informative about the incidence of deforestation across countries and over time when government policies and global market conditions change.

We offer an approach that complements previous work by embracing a global and dynamic view of deforestation. The global dimension is crucial because international trade connects the demand for land across countries. For example, an increase in food demand in China can be met with an expansion in Brazil's agricultural frontier, instead of that of China itself. A global perspective makes such spatial linkages explicit and acknowledges that changes to policy or market conditions in one location will have repercussions elsewhere. In turn, dynamics are important for understanding the timing of deforestation and its impact on climate change. The design of policies to curb the trajectory of carbon emissions, in particular, requires an understanding of how the pace of deforestation responds to shifts in the supply and demand for food over time. An approach that is both global and dynamic is therefore important to design policies that have a bearing on deforestation, especially if they are to be applied simultaneously by many countries.

We start by collecting data on land use, sectoral production, international trade, and population growth. Using these data, we document four empirical patterns that describe the geography of forests and how it relates to international agricultural markets and population growth. First, since 1990 global forest area declined by 7.1 percent—an area the size of Argentina—, with substantial heterogeneity across countries. South America, South East Asia, and Sub-Saharan Africa experienced large rates of deforestation. Put together, these regions account for about 90 percent of the world's forest loss in this period. At the same time, forest area expanded in other regions, such as Europe and China. Second, during this period deforestation across countries was strongly and positively associated with expansions in the agricultural land. This observation suggests that understanding the incentives to use land for agricultural production is crucial to studying deforestation. Third, countries that had a revealed comparative advantage in agriculture in 1990 experienced both a larger increase in agricultural land and in deforestation between 1990 and 2020. This pattern

[3]For instance, see DeFries et al. [2010] that document a positive association between urban population growth and deforestation in the tropics.

suggests that international trade distributes the global pressure on land across countries. Fourth, population growth has led to deforestation—a relation that is important on its own in the face of expected future population growth, and one that is informative for model calibration.

Next, we develop a dynamic, general-equilibrium model to evaluate the quantitative response of deforestation to trade policy and population growth across the world and over time. The model incorporates many countries, three broad sectors—agriculture, manufacturing, and services—and disaggregated activities within agriculture. There is also a market and, therefore, a price for new land. New land is supplied by a firm that employs labor to transform open-access forests into land. Landowners incorporate new land to their existing stock to rent it to other sectors in the economy. Lastly, we introduce frictions to the reallocation of labor between sectors.

The equilibrium allocation of land in our model is shaped by three mechanisms: (i) structural change determines the size of the agricultural sector and the aggregate demand for land; (ii) comparative advantage distributes pressures on agricultural land use and forests across countries, and together with absolute advantage, determines whether trade further alleviates pressures on forests; and (iii) forward-looking land accumulation decisions control the pace of forest adjustments to shocks.

To guide our quantitative analysis, we produce a set of analytical results in stripped-down versions of our model's steady state. First, reducing agricultural export costs *unilaterally* for a small open economy leads to deforestation there. The key to this result is that the world import-demand elasticity is positive and equal to the trade elasticity. Second, and in contrast to the first result, we show that when countries are symmetric—which shuts down the channel of comparative advantage—a *multilateral* trade-cost reduction in agriculture increases global forest area. This is because, when agriculture becomes relatively cheap and agriculture is complementary in consumption with non-agricultural sectors (as in the data), relative demand for agriculture shrinks. A worldwide reduction in land demand follows, which leads to larger forest area. This result extends Borlaug's hypothesis—that agricultural productivity growth is land-saving in a closed economy Borlaug [2000]—to the domain of trade barriers in open economies. Third, we study the role of comparative advantage in a setting with unitary elasticity of substitution between agriculture and non-agriculture, but where productivity differs across countries. We show that the *correlation* between comparative and absolute advantage in agriculture determines whether trade leads to a gain or loss in global forest area. When this correlation is positive, countries with an absolute advantage in agriculture specialize in agriculture, making the move from autarky to free trade globally land-saving.

We next bring our model to data. We begin by calibrating the parameters that govern the initial, static equilibrium using production, trade, and forest data from 2010. To do so, we disaggregate the world into 33 countries and 7 regions, and we divide the economy into agriculture, manufacturing,

and services, further dividing agriculture into main staple crops, pasture-related products, and a bundle of other agricultural products. We choose the parameters governing the conversion of forest into land so that our model replicates the reduced-form impact of population growth on forest area, at different time horizons. Lastly, we develop a method for separately calibrating policy and non-policy driven trade costs.[4]

We then deploy our calibrated model to study several counterfactual scenarios. We compare two polar cases of trade liberalization that echo our first two analytical results: A 30 percent reduction in the policy component of export costs for Brazil only versus a global export cost reduction of the same size. In each case, we study the evolution of global forest area and its distribution across countries compared to a business-as-usual (BAU) scenario in which the economy evolves under no change in fundamentals, starting in 2010.

The first scenario is close to the small open economy case that has been prominent in the study of the impact of trade on the environment.[5] In this scenario, global forest share declines by about 0.1 percentage points in the steady state, most of it in Brazil, whose forest share declines by 3 percentage points, relative to BAU. In the global trade-cost reduction scenario, in contrast, global forest share increases by 0.5 percentage points. Structural change reduces the global demand for land, while comparative advantage in agriculture determines the cross-section of deforestation. Our data, moreover, exhibits a positive correlation between absolute and comparative advantage in agriculture, which in light of our third analytical result, suggests that moving toward free trade alleviates the global pressure on forests.

Having established the quantitative importance of the mechanisms in our model, we create a new BAU scenario in which each country's population grows according to the UN projection in coming decades. In this BAU, many African countries experience large rates of deforestation since their growing population increases the demand for food. We find that a multilateral trade cost reduction would substantially mitigate deforestation in Africa by reallocating land use to other regions that are relatively more efficient in agricultural production.

We conclude by evaluating the CO_2 emissions costs brought about by deforestation.[6] We do so under a broad range of assumptions, so as to highlight the role of different economic mechanisms and measurement approaches that allow for reforestation, carbon heterogeneity or carbon sequestration. In our simplest exercise, the climate costs of export costs reductions in the global versus Brazil-only scenario are roughly the same, despite the large difference in their global welfare impact. In turn, including the sequestration benefits of new forests in our calculation or considering

[4]Our quantitative model features, in addition, a fallow land sector. We introduce this block to capture the fact that in the data fallow land is a sizable share of total land and an important source of expansion in agricultural land.

[5]For example, see Brander and Taylor [1997] and Taylor [2003] and Copeland and Taylor [2004].

[6]This evaluation adheres to the guidelines routinely used by the International Panel on Climate Change. While we acknowledge the negative impacts of deforestation on biodiversity and amenities, we do not intend to examine them.

a BAU that includes population growth turns the climate costs of global trade cost reductions into gains.

We contribute to research at the intersection of trade, spatial economics, and the environment. Costinot et al. [2016] and Gouel and Laborde [2021] study the extent to which trade mitigates the impacts of climate change. Other recent studies have formulated dynamic trade and migration models to evaluate the consequences of climate change (e.g. Desmet et al., 2018, Conte et al., 2021, Balboni, 2019). Kortum and Weisbach [2021] and Farrokhi and Lashkaripour [2024] study instead the design of optimal trade and carbon policy on global carbon emissions. Shapiro [2016] evaluates the impact of international shipping on CO_2 emissions. A few recent papers study quantitatively the relations between trade and natural resources. For example, Farrokhi [2020] studies the impact of trade-related policies in global oil markets, and Carleton et al. [2024] examine the relation between agricultural trade and the allocation of water use across the world. Focusing on deforestation, Dominguez-Iino [2023] examines the effects of environmental policies along supply chains in South America, and Hsiao [2024] studies international cooperation and commitment in the market for palm oil. See Copeland and Taylor [2004] and Copeland et al. [2021] for a review of previous work. Closer to our research is Hertel [2012], who points out that the impact of agricultural technological innovations on land use and emissions depends on the elasticity of demand faced by farmers. Relative to this literature, we are the first to incorporate deforestation dynamics into a quantitative general equilibrium framework to study how economic forces and international trade policy shape land use around the world. Our multi-country equilibrium approach demonstrates the role of structural change and comparative advantage in shaping the deforestation impact of trade openness.

Second, we contribute to research examining the welfare impacts of agricultural trade (Donaldson, 2018, Sotelo, 2020, Pellegrina, 2022) and how agriculture relates to structural change and development (Tombe, 2015, Fajgelbaum and Redding, 2014, Farrokhi and Pellegrina, 2022, Gollin et al., 2018). Our work gives deforestation a central role in the analysis of agricultural trade, focusing on how structural change determines worldwide pressures on land use and how the resulting impact on deforestation evolves over time. We also relate to a long-standing and rich tradition, reviewed in Hertel [2002], that formulates computational general equilibrium (CGE) models to study global agricultural markets. Relative to the latter, we introduce dynamics in land development and we provide an analytical characterization of the mechanisms driving global deforestation.

Lastly, we complement a large literature that uses detailed micro-data to study different drivers of deforestation and forest management, including the role of national institutions [Burgess et al., 2019], land use taxes and payment programs for forest conservation [Jayachandran et al., 2017, Assunção et al., 2020, Souza-Rodrigues, 2019, Araujo et al., 2022], roads and access to markets [Pfaff, 1999, Asher et al., 2020], demand for wood and forest products [Foster and Rosenzweig,

2003], and externalities generated by forest fires [Balboni et al., 2020]. We build on these studies, which focus on individual country experiences, to examine how incentives to deforest transmit across countries through international trade, emphasizing that government policies and market conditions in one country have the potential to drive or curb deforestation elsewhere.

2.2 Data sources

We combine data on global deforestation and carbon content of forests with other, more standard country-level information on trade, production, and factor employment required in global trade models. After merging these data sets, we have 150 countries in five periods (1990, 2000, 2010, 2015 and 2020). Later, we group countries into 40 countries and regional aggregates to quantify our model. Below we summarize our data. Appendix B.1 provides additional details about each data source.

Forests and Forest Carbon Stock Since 1948, FAO has published a periodic report called Forest Resource Assessment (FAO-FRA), which reflects the FAO's efforts to measure country-level forest area from national forest inventories. We focus on these data for two reasons. First they are publicly available and they offer ample coverage in time and space. The data that we use come from the last edition of FRA, FAO [2020], which covers a 30-year period between 1990 and 2020. Second, they are the key reference for policy debate on global deforestation and for assessments of the impact of deforestation on climate change [Brown and Zarin, 2013]. They are used, for example, for the estimation of CO_2 emissions from deforestation by the Intergovernmental Panel on Climate Change (IPCC). Since the 1990s, the methodology used by FAO has been improved to ensure that the measurement of forest areas are comparable over years. This is the earliest year for which we can build consistent time series.

We also employ FAO-FRA information on the carbon content of living biomass above ground—which includes all living biomass above the soil—as well as below ground—which incorporates all biomass of living roots.

Other Country-level Data. We use data on agricultural production, land use, and international trade, disaggregated by agricultural commodity, from FAO-STAT. For agriculture, manufacturing and services, we take data on employment from UN-ILO and value added, final and intermediate-input expenditures, and international trade from the GTAP database.

2.3 Empirical Patterns about Global Deforestation

This section documents four empirical patterns about global deforestation that motivate our modeling approach. We first document the evolution of deforestation between 1990 and 2020. Second, we show that deforestation has been strongly associated with expansions in agricultural land use. Third, deforestation was larger in countries with a comparative advantage in agriculture. Fourth, we estimate the impact of population growth on deforestation, which will later discipline the calibration of our model.

Pattern 1. Between 1990 and 2020, global forest area dropped by 7.1%. While in the tropics, forest area dropped substantially, in several non-tropical regions there was forest regrowth.

We use "country area" as a shorthand for total area of a country net of deserts, glaciers and lakes. Panel (a) in Figure 2.1 shows the share of country area covered by forest. Countries with higher forest concentration tend to be in regions close to the North Pole, including the large boreal forests of Canada, Russia, and the Nordic countries or areas near the equator, including the tropical forests of the Amazon, Congo Basin, and Southeast Asia. Panel (b) depicts global deforestation in 2020 relative to 1990 (as percentage points of the each country's area). The 7.1% loss of global forest area—from 4.07 billion hectares in 1990 to 3.78 billions in 2020—amounts to the size of a country between Argentina and India. Deforestation was relatively mild in the northern countries while it was substantial in the tropics, such as in Brazil, Congo, and Indonesia where their forest area fell respectively by 17%, 16%, and 26% during 1990-2020.[7] Other countries, primarily China and several European countries, reforested over this period. The correlation between a country's forest share in 1990 and its deforestation between 1990-2020 is sizable, equal to 0.61, and statistically significant, suggesting a land-clearing technology that depends on the current share of forest.

Appendix Table B.2 provides an accounting of global deforestation disaggregated by the 33 countries plus 7 aggregate regions we bring to data for quantitative analysis.[8] The table shows for each country the forest share in country area in 1990, percentage point change in forest share and percentage change in forest area during 1990-2020. It also shows each country's contribution to the global deforestation during 1990-2020. Brazil alone accounts for one-third of global deforestation, followed by Central African countries and Indonesia together accounting for one-fourth of global deforestation. Our model aims at capturing economic mechanisms driving these different

[7] The figure shows these numbers in terms of the percentage point (p.p.) change in each country's forest share rather than percentage change since the latter gives uninformatively large magnitudes in countries where forest share is tiny. The p.p. change in forest share (multiplied by 100) was -2.2 at the global level and -12.0, -10.8, and -16.4 respectively in Brazil, Congo, and Indonesia.

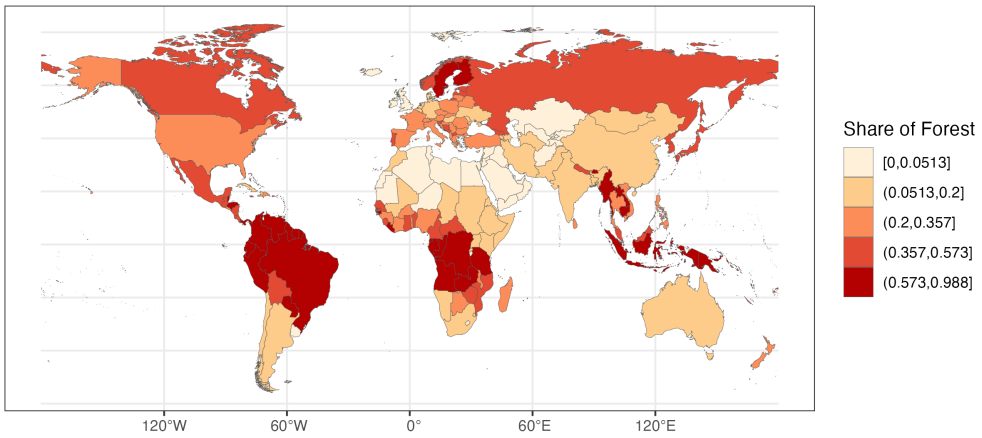
[8] Appendix Table B.4 reports these deforestation-related variables at the individual country level and Appendix Table B.1 lists the individual countries that constitute each of our regional aggregates.

deforestation.

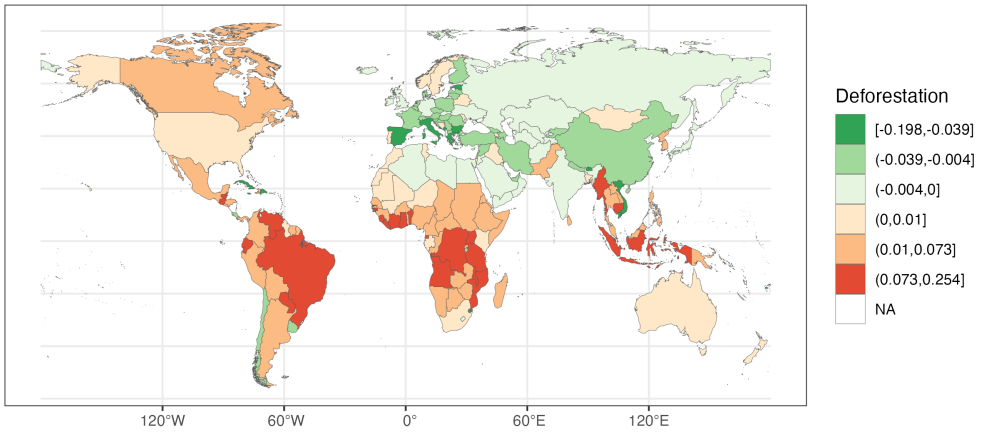
Before moving on, we note that forests are heterogeneous in their carbon content. Figure B.1 in the appendix depicts each country's forest carbon intensity (tons of carbon stock per hectare of forest), suggesting that the carbon emission implications of deforestation depend on where it occurs. We incorporate this heterogeneity into our analysis of the climate costs of different trade integration scenarios, following the IPCC and FAO guidelines [Tubiello et al., 2020].

Figure 2.1: Forest and Deforestation across the World (1990-2020)

(a) Forest share in Country Area (1990)



(b) Deforestation (2020 relative to 1990)



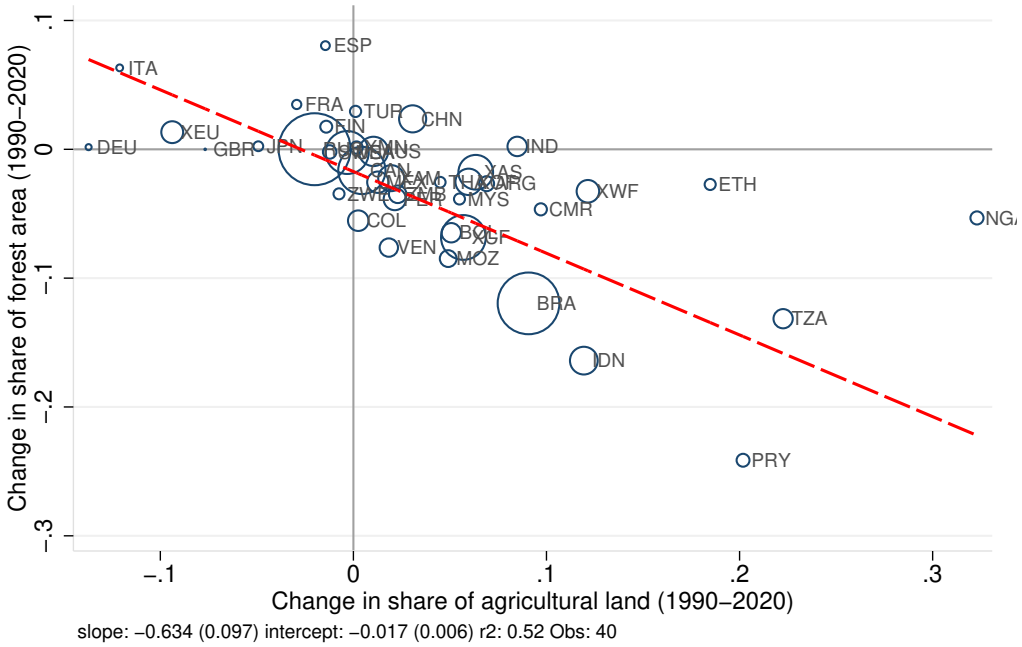
Notes: Panel (a) shows "forest share" for each country—as the share of a country's area covered by forest in 1990. Panel (b) shows the percentage point change in forest share for each country between 1990 and 2020.

Pattern 2. Changes in forest area are negatively correlated with changes in agricultural land use.

Figure 2.2 plots the change in forest area against the change in agricultural land use across countries, both measured as a share of their corresponding country area. The two variables are strongly and negatively correlated, with the share of forest area decreasing at a slope of -0.63 with respect to the share of agricultural land.

This empirical regularity motivates us to design a land-use model in which expansions in land use, particularly from agriculture, may come at the cost of deforestation. We next turn to two mechanisms driving the demand for agricultural land in a country, namely, agricultural trade and population growth.

Figure 2.2: Change in Share of Land in Forest versus Share of Land in Agriculture (1990-2020)



Notes: This figure shows the relationship between changes from 1990 to 2020 in agricultural land use and changes forest area across countries, each as a share of country area, in percentage changes from 1990 to 2020. The size of circles represents the share of forest area in each country. The red dashed line shows the linear fit weighting the observations by each country's forest area in 1990.

Pattern 3. Between 1990 and 2020, countries with a comparative advantage in agriculture experienced a larger expansion in their agricultural land use and a larger reduction in their forest area.

We next examine countries' change in agricultural and forest area in relation to their international position in agricultural specialization. To this end, we employ the index of *revealed comparative advantage* for each country i, defined as:

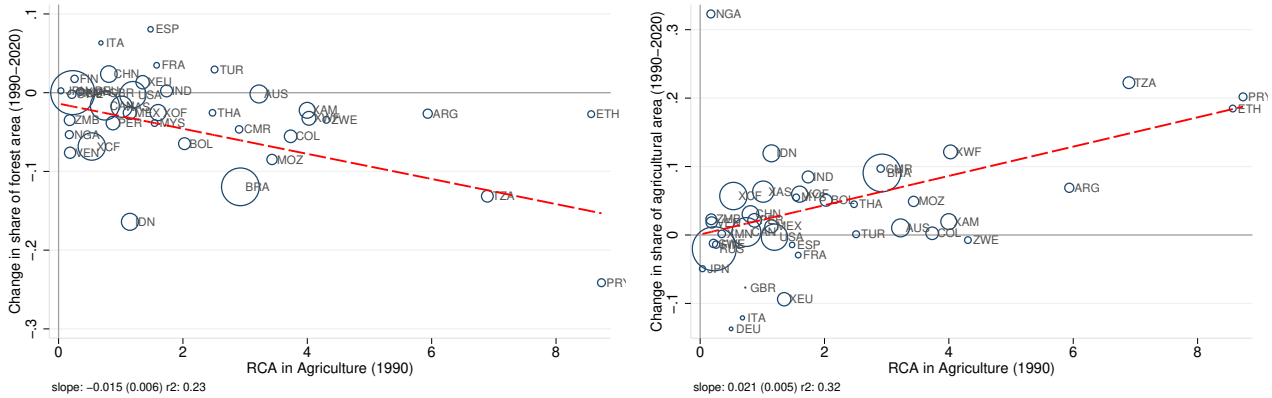
$$\text{RCA}_i^{(\text{Agr})} = \frac{(\text{Agr Exports})_i/(\text{Total Exports})_i}{(\text{World Agr Exports})/(\text{World Total Exports})}$$

Panels (a) and (b) of Figure 2.3 show that in countries with a higher RCA (measured in 1990) the expansion agricultural land and the reduction of forest area has been larger during 1990-2020. This pattern motivates a model in which comparative advantage governs the relative demand for land, and therefore the pressure on forests, across countries.

Figure 2.3: Change in Agricultural Land and Forest Area against Comparative Advantage in Agriculture

(a) Forest area

(b) Agricultural area



Notes: This figure shows the 1990-2020 change in agricultural land share in country area (Panel a) and forest share in country area (Panel b) against the index of revealed comparative advantage (measured in 1990) across countries.

Pattern 4. Population growth leads to agricultural land expansion and deforestation.

We examine the impact of population growth on agricultural land use and forest area across countries. Figure 2.4 shows that between 1990 and 2020 countries with higher rates of population growth experienced a larger reduction in their forest area and a larger expansion in their agricultural land use. To explore this relationship more systematically, we consider the following

equation:

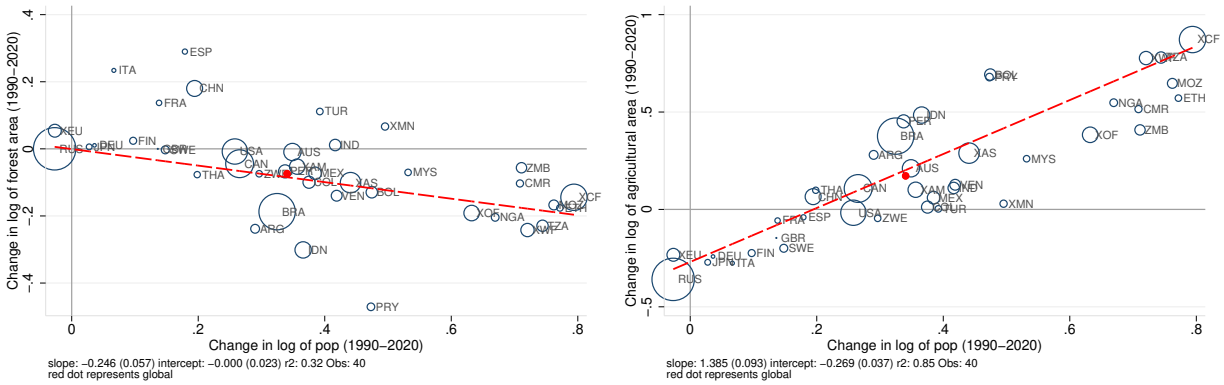
$$\Delta \ln y_{i,t} = \beta_0 + \beta_1 \Delta \ln \text{Population}_{i,t} + \beta_X \mathbf{X}_{i,t} + \epsilon_{i,t} \tag{2.1}$$

where $y_{i,t}$ represents either agricultural land or forest area, and $\text{Population}_{i,t}$ $\mathbf{X}_{i,t}$, and $\epsilon_{i,t}$ denote population, control variables—see description in the table—, and the error term for country i at time t. The Δ operator denotes 30-year time differences. The coefficient of interest, β_1, captures the impact of population growth on net forest or agricultural land growth.

Figure 2.4: Change in Forest and Agricultural Area on Population Growth

(a) Forest Area

(b) Agricultural Area



Notes: This figure shows the 1990-2020 change in log agricultural land area (Panel a) and log forest area (Panel b) against the 1990-2020 change in log population across countries.

An OLS estimation of equation (2.1) may suffer from endogeneity bias. For example, shocks to agricultural productivity can lead to a rise of both population and deforestation, creating a correlation between population growth and the error term. We therefore instrument $\Delta \ln \text{Population}_{i,t}$ with the median age in country i at time period $t-1$. Our identifying assumption is that countries with a higher fraction of population in that range will tend to have more births, for purely biological reasons, and that past demographic structure is uncorrelated with future productivity shocks.

Table 2.1 shows the OLS and IV estimates of equation (2.1). Panel (a) reports a negative and statistically significant elasticity of forest area to population, for both OLS and IV, with and without controls for institutions and environmental regulations. In particular, the IV estimate under Column (4) implies that a 10 percent increase in a country's population reduces its forest area by 4.6 percent. Turning to Panel (b), it shows a positive and statistically significant response of agricultural land to population growth, which is again similar across specifications. Here, the IV estimate in Column (4) indicates that a 10 percent increase in population leads to 10.8 percent increase in agricultural land use.

These results are important in their own right, especially considering that the world population

is expected to grow by 35% between 2020 and 2100. In addition, through the lens of our model, changes in population map transparently into land use pressures, both by raising the demand for food and increasing the supply of labor. We will therefore target these reduced-form results to calibrate the parameters of our land-producing sector, which governs the response of deforestation to shocks to fundamentals (including trade costs).

Table 2.1: The Relationship between Population Growth and Forest Area (30 Years Interval)

	OLS	OLS	IV	IV
	(1)	(2)	(3)	(4)
a. DV is the log of Forest Area				
Δ Log(Pop)	-0.362***	-0.242**	-0.409***	-0.329*
	(0.082)	(0.123)	(0.076)	(0.189)
R2 or K-P	0.337	0.384	58.419	35.763
Obs	40	40	40	40
b. DV is the log of Agricultural Area				
Δ Log(Pop)	1.220***	1.128***	1.211***	0.933***
	(0.111)	(0.198)	(0.096)	(0.268)
R2 or K-P	0.761	0.778	58.419	35.763
Obs	40	40	40	40
Controls				
- Institutions	-	Y	-	Y
- Environmental tax	-	Y	-	Y
- GDP pc	-	Y	-	Y

Notes: Observations are weighted by forest share in 1990. Robust standard errors clustered at country level are reported in parenthesis. Columns 2 and 4 control for log of GDP per capita (linear and square), regulatory quality, government corruption, and environmental tax in the initial year. Columns 3 and 4 employ the media age (linear, square and cubic) as instruments for population growth.

2.4 Theory

We develop a dynamic, multi-country, multi-sector general equilibrium model of global deforestation and international trade. The main forces allocating pressures on land use are sectoral comparative advantage and structural change. To study how deforestation responds to changes in fundamentals, we introduce a forward-looking land-producing sector that converts forest area into cleared land.

2.4.1 Environment

Time, Commodities, and Markets. The economy consists of multiple countries, indexed by i or $j \in \mathcal{I}$. Time is continuous and indexed by t. There are three broad sectors producing tradable goods for final consumption: Agriculture, A, Manufacturing, M, and Services, S. An additional sector, which we call the land-producing sector, T, clears the forest and produces land that can be used in the production of consumption goods. We index sectors by $s \in \mathcal{S} = \{A, M, S, T\}$. The agricultural sector is disaggregated into K industries, whereas the manufacturing and service sectors consist of one industry each. Accordingly, we define each good g as a pair of industry-sector, $g \equiv (k, s) \in \mathcal{G}$, where the set $\mathcal{G}$ of goods is defined as

$$\mathcal{G} \equiv \{ \underbrace{1, ..., K}_{\text{agriculture}} , \underbrace{M}_{\text{manufacturing}} , \underbrace{S}_{\text{service}} \}$$

Shipping good g from i to j entails an iceberg cost $d_{ij,g} \geq 1$, with $d_{ii,g} = 1$. Markets are perfectly competitive. We drop the time index whenever it does not create confusion. Hereafter, we let $\dot{y} = dy/dt$ for any variable y.

Endowments and Preferences. At any point in time, each country is endowed with a working population, N_i, and total land area, H_i, which is divided between land for production, L_i, and forest available for conversion, F_i, so that $H_i = F_i + L_i$.[9]

Varieties of every good $g \in \mathcal{G}$ are differentiated by their origin. Consumers combine varieties of every good g according to CES preferences with elasticity of substitution $\eta_g > 0$ and demand shifters $b_{ij,g}$. Country j's expenditure in good g produced by country i equals

$$\pi_{ij,g} = \frac{b_{ij,g} \left(c_{i,g} d_{ij,g}\right)^{1-\eta_g}}{p_{j,g}^{1-\eta_g}}, \tag{2.2}$$

where $c_{i,g}$ is the marginal cost of production, and $p_{j,g}$ is the price index of good g in destination market j, given by:

$$p_{j,g} = \left[\sum_{i \in \mathcal{I}} b_{ij,g} \left(d_{ij,g} c_{i,g}\right)^{1-\eta_g} \right]^{\frac{1}{1-\eta_g}} \tag{2.3}$$

The bundle of agricultural consumption, in turn, is a CES aggregator across goods $k = 1, ..., K$ in the agriculture sector $s = A$, with elasticity of substitution κ and demand shifters $b_{i,k}$. The

[9] Our second empirical pattern shows that, although agricultural land use and deforestation are strongly associated, the relation is not one-to-one. Agricultural land expands from other sources as well, such as previously land left to fallow. We allow for this possibility in our quantitative analysis and discuss this extension in Appendix B.3.1..

resulting within-agriculture expenditure shares equal:

$$\beta_{i,k} = b_{i,k} \left(\frac{p_{i,k}}{P_{i,A}} \right)^{1-\kappa}. \tag{2.4}$$

The sector-level price index of agriculture, $P_{i,A}$, follows from the CES specification between agricultural goods, and those of manufacturing and service are trivially given by their corresponding good-level price indices:

$$P_{i,A} = \left[\sum_{k=1}^{K} b_{i,k} p_{i,k}^{1-\kappa} \right]^{\frac{1}{1-\kappa}}, \qquad P_{i,M} = p_{i,M}, \qquad P_{i,S} = p_{i,S} \tag{2.5}$$

Lastly, the upper-tier CES aggregator combines the bundles of agriculture, manufacturing, and services with substitution elasticity σ and demand shifters $b_{i,s}$. The expenditure share on sector $s \in \{A, M, S\}$ equals:

$$\beta_{i,s} = \frac{b_{i,s} P_{i,s}^{1-\sigma}}{P_i^{1-\sigma}}, \tag{2.6}$$

where the final consumer price is given by,

$$P_i = \left[\sum_{s \in \{A,M,S\}} b_{i,s} P_{i,s}^{1-\sigma} \right]^{\frac{1}{1-\sigma}}, \tag{2.7}$$

In the empirically relevant case of $\sigma < 1$, agriculture and other sectors are gross complements if $\sigma \in (0, 1)$, so expenditure shares shift away from agriculture when the price index of agriculture falls relative to that of the other sectors.

Land-Producing Sector. At any point in time, the frontier of cleared land in country i is denoted by $z_i \in [0, 1]$, which defines the fraction of the total land available for productive uses. Therefore, the cleared land area is $L_i = z_i H_i$, and forest area is $F_i = (1 - z_i) H_i$.

Given the frontier, z_i, a firm in the land-producing sector employs labor, $N_{i,T}$, and produces a flow of new land, $Q_{i,T}$, according to

$$Q_{i,T} = J_i (z_i) N_{i,T}^{\gamma_T}, \tag{2.8}$$

where $J_i (z_i)$ is a decreasing function of z_i, capturing the notion that it becomes more costly to deforest—be it due to policy action, terrain variation, or distance to markets—as the share of forest decreases. Moreover, $J(1) = 0$ since there can be no production of new land if the entire forest is

gone. Lastly, γ_T measures the decreasing returns to labor.[10]

The firm behaves competitively and therefore the price of new land, q_i, equals its marginal cost[11]:

$$q_i = \frac{w_{i,T}}{\gamma_T J_i(z_i)} N_{i,T}^{1-\gamma_T}, \tag{2.9}$$

where $w_{i,T}$ denotes the wage in the land-producing sector . The land frontier evolves according to:

$$\dot{z}_i H_i = x_i - \delta_L L_i, \tag{2.10}$$

where δ_L is the natural rate of reforestation and x_i is the gross inflow of new land.

Landowners. There is a continuum of landowners who are risk-neutral and have perfect foresight. Each of them owns one unit of land which she rents out at a rate r_i. Landowners discount the future at a rate of ρ and, with an arrival rate of δ_L, each unit of land "depreciates", turning back into forest. Land productivity is homogeneous across different uses.

Under these assumptions, the value function v_i^L of a landowner can be expressed as:

$$(\rho + \delta_L) v_i^L = r_i + \dot{v}_i^L. \tag{2.11}$$

There is also a mass of potential entrants who buy new land if its value is at least as large as its cost, $v_i^L \geq q_i$. In an equilibrium with a finite flow of new land per instant, we must have equality, which we impose from now on. This corresponds to the following free entry condition:

$$v_i^L = q_i. \tag{2.12}$$

Using this result, we obtain the following asset pricing equation for land,

$$(\rho + \delta_L) q_i = r_i + \dot{q}_i, \tag{2.13}$$

which can be solved to show that the price of new land equals the present value of land rents, discounted by $(\rho + \delta_L)$, a rate that accounts for both time preference and the rate of forest regrowth, $q_i(t) = \int_t^\infty e^{-(\rho+\delta_L)(s-t)} r_i(s)\, ds$.

[10] Our specification is rooted in the literature on renewables, e.g., Brander and Taylor, 1997, that assumes $Q_{i,T} \propto (1 - z_i) N_{i,T}$. This corresponds to a special case of our specification where $J_i(z_i) = 1 - z_i$ and $\gamma_T = 1$. Moreover, we implicitly assume open access to land, since we can reinterpret equation (2.8) as $\min\left\{J_i(z_i) N_{i,T}^{\gamma_T}, F_i\right\}$, where sector T uses the forest without paying for it. Note that one unit of forest is then always converted to one unit of land.

[11] This equation can be alternatively expressed as an (inverse) supply schedule, $q_i = \bar{q}_i w_{i,T} Q_{i,T}^{\tilde{\gamma}_T}$ where $\bar{q}_i \equiv J_i(z_i)^{-\frac{1}{\gamma_T}} / \gamma_T$ and $\tilde{\gamma}_T \equiv \frac{1-\gamma_T}{\gamma_T}$ is the inverse supply elasticity. A reduction in the stock of forest shifts the supply curve upward via raising z_i. Insofar as $\gamma_T \in (0, 1)$, the price on the supply schedule remains finite unless the stock of forest is completely depleted, i.e., $z_i \to 1$.

Workers and Sectoral Choices. Following Artuç et al. [2010] and Caliendo et al. [2019], we assume workers are forward looking and have perfect foresight. They are endowed with one unit of labor, which they supply inelastically. Workers receive opportunities to move out of their current sector with an arrival rate of ψ. When an opportunity arrives, a worker draws a vector of preference shocks, $\epsilon_{i,s}^N$, from a Type-I extreme value distribution with dispersion parameter ν, and can choose to reallocate from its current sector s to another sector s', subject to moving cost $f_{i,ss'}^N$. Accordingly, the expected present value of the stream of a worker's utility who is currently in sector s, $v_{i,s}^N$, is the solution to:

$$(\rho + \psi)\, v_{i,s}^N = u\left(\frac{w_{i,s}}{P_i}\right) + \psi W_{i,s} + \dot{v}_{i,s}^N, \tag{2.14}$$

where $W_{i,s}$ is the expected continuation value for a worker employed in sector s who receives a moving opportunity,

$$W_{i,s} \equiv \mathbb{E}\left[\max_{s'}\left\{v_{i,s'}^N - f_{i,ss'}^N + \varepsilon_{i,s'}^N\right\}\right] = \nu \log \sum_{s' \in S} \exp\left(\frac{1}{\nu}\left(v_{i,s'}^N - f_{i,ss'}^N\right)\right). \tag{2.15}$$

Conditional on the arrival of the option to move, the probability of moving from sector s to s' equals:

$$\mu_{i,ss'} = \frac{\exp\left(\left(v_{i,s'}^N - f_{i,ss'}^N\right)/\nu\right)}{\sum_{l \in S} \exp\left(\left(v_{i,l}^N - f_{i,sl}^N\right)/\nu\right)}. \tag{2.16}$$

Technology for producing Agriculture, Manufacturing, and Services. The production technology of each good aggregates labor, land, and intermediate inputs in a Cobb-Douglas fashion. Accordingly, the marginal cost of producing good g in country i is given by:

$$c_{i,g} = \frac{1}{Z_{i,g}}\left(w_{i,g}^{\gamma_{i,g}} r_i^{1-\gamma_{i,g}}\right)^{\alpha_{i,g}} \left(p_{i,g}^I\right)^{1-\alpha_{i,g}}, \tag{2.17}$$

where $\alpha_{i,g}$ is the value added share divided between land and labor with shares $\gamma_{i,g}$ and $(1-\gamma_{i,g})$. Assuming perfect labor mobility within the agriculture sector, agricultural industries pay the same wage $w_{i,A} = w_{i,1} = ... = w_{i,K}$. However, wage rates are different only between broadly-defined sectors. Moreover, $Z_{i,g}$ is total factor productivity, r_i is the rental rate of land, and $p_{i,g}^I$ is the price index of intermediate bundle used in the production of good g which is a CES aggregator of prices of all goods $g' \in \mathcal{G}$ with elasticity parameter σ^I:

$$p_{i,g}^I = \left(\sum_{g' \in \mathcal{G}} b_{i,g'g}^I p_{i,g'}^{1-\sigma^I}\right)^{\frac{1}{1-\sigma^I}} \tag{2.18}$$

Recall that the price $p_{i,g'}$ is determined by Equation 2.3. We denote the associated expenditure shares of industry g on goods produced by industry g' in country i by $\beta^I_{i,g'g}$, which equals $b^I_{i,g'g}\left(p_{i,g'}/p^I_{i,g}\right)^{1-\sigma^I}$.

2.4.2 Expenditures and Market Clearing Conditions.

Country $i's$ total sales of good g equal

$$Y_{i,g} = \sum_j \pi_{ij,g} X_{j,g}, \tag{2.19}$$

where $X_{j,g}$ is the total expenditure on good g in destination j, comprised of final and intermediate demand:

$$X_{i,g} = \underbrace{\beta^F_{i,g} E_i}_{\text{final expenditure}} + \underbrace{\sum_{g' \in G} \beta^I_{i,g'g} \left(1 - \alpha_{i,g'}\right) Y_{i,g'}}_{\text{intermediate expenditure}}. \tag{2.20}$$

Here, $\beta^F_{i,g}$ is the final expenditure share on each good g.[12] Labor market clearing requires the wage bill to equal payments to labor in each sector s, that is:

$$w_{i,A} N_{i,A} = \sum_{k=1}^{K} \alpha_{i,k} \gamma_{i,k} Y_{i,k}, \quad w_{i,M} N_{i,M} = \alpha_{i,M} \gamma_{i,M} Y_{i,M}, \quad w_{i,S} N_{i,S} = \alpha_{i,S} \gamma_{i,S} Y_{i,S} \tag{2.21}$$

Land market clearing requires total land rents to equal payments to land:

$$r_i L_i = \sum_{g \in \mathcal{G}} \alpha_{i,g} \left(1 - \gamma_{i,g}\right) Y_{i,g} \tag{2.22}$$

The profits in the land-producing sector are given by: $\Pi_{i,T} = (1 - \gamma_{i,T}) q_i Q_{i,T}$. In turn, the market clearing in the production of new land entails $Q_{i,T} = x_i$ in every country i.

Lastly, under balance of trade, final expenditure equals the sum of factor rewards,[13]

$$E_i = r_i L_i + \sum_{s=\{A,M,S\}} w_{i,s} N_{i,s}. \tag{2.23}$$

[12] For manufacturing and services $g = s \in \{M, S\}$, $\beta^F_{i,g} = \beta_{i,s}$; for agricultural products $g \in (k = 1, ..., K \mid A)$, $\beta^F_{i,g} = \beta_{i,A}\beta_{i,k}$.

[13] Since the net payment to land is $(r_i L_i - w_{i,T} N_{i,T})$, the balance of budget could be equivalently expressed as $E_i = (r_i L_i - w_{i,T} N_{i,T}) + \sum_{s=\{A,M,S,T\}} w_{i,s} N_{i,s}$. Moreover, market clearing conditions ensure that final expenditure also equals aggregate value added, $E_i = \Sigma_g \alpha_{i,g} Y_{i,g}$.

2.4.3 Evolution of Labor, Land and Forest Area

To keep track of worker reallocation across sectors, we define the matrix, $\mathbf{M}_i$, with elements $\mathbf{M}_i[s,s'] = \psi\mu_{i,ss'}$ if $s \neq s'$, and $\mathbf{M}_i[s,s'] = -\psi(1-\mu_{i,ss})$ if $s = s'$.[14] In country i, the mass of workers in each sector evolves according to:

$$\dot{\mathbf{N}}_i = \mathbf{M}_i^T \mathbf{N}_i, \tag{2.24}$$

where $\mathbf{N}_i$ is the vector of employments across sectors in country i. The above equation together with the initial labor allocation, $\mathbf{N}_i(0)$, characterize the evolution of labor.

The evolution of land across uses, in turn, follows from the definition of the land frontier, $L_i = z_i H_i$. Thus,

$$\dot{L}_i = \dot{z}_i H_i = x_i - \delta_L L_i, \tag{2.25}$$

and hence, the evolution of forest area is given by:

$$\dot{F}_i = -\dot{L}_i = \delta_L \left(\sum_{g \in \mathcal{G}} L_{i,g} \right) - x_i \tag{2.26}$$

Coupled with initial stocks of productive land and forests, $L_i(0)$ and $F_i(0)$, Equations 2.25 and 2.26 characterize the evolution of land. Deforestation is the decrease in forest cover, $\dot{D}_i \equiv -\dot{F}_i$.

2.4.4 Equilibrium

The fundamentals of the economy are land endowments, $\{H_i\}_i$, technology and preference parameters $\mathbf{Z}(t) = \{Z_{i,g}(t)\}_{i,g}$ $\bar{\mathbf{a}} \equiv \left\{ \left\{ b^I_{i,g'g} \right\}_{g,g'}, \{\alpha_{i,g}, \gamma_{i,g}\}_g, \{b_{i,k}\}_k, \{b^s_i\}_s \right\}_i$, trade costs $\mathbf{d} = \{d_{ij,g}(t)\}_{ij,g,t}$, reallocation costs for workers $\mathbf{f} = \left\{ \left\{ f^N_{i,ss'} \right\}_{s,s'} \right\}_i$, and constants $\mathbf{\Theta} = \left\{ \{\eta_g\}_g, \kappa, \sigma, \sigma^I, \psi, \theta, \xi, \nu, \delta_L \right\}$. At any time, the state of the economy is given by labor endowments, $\mathbf{N}(t) = \{N_i(t)\}_t$ and allocations $\mathbf{S}(t) = \left\{ F_i(t), L_i(t), \{N_{i,s}(t)\}_s \right\}_i$, satisfying resource constraints on the endowments: $\sum_{g \in \mathcal{G}} L_{i,g}(t) = L_i(t)$, $F_i(t) + L_i(t) = H_i$, and $\sum_{s \in \mathcal{S}} N_{i,s}(t) = N_i(t)$.

Definition. [Instantaneous equilibrium] Given $\{\bar{\mathbf{a}}, \mathbf{d}, \mathbf{f}, \mathbf{\Theta}\}$, the current state of the economy, $\{\mathbf{S}(t), \mathbf{Z}(t), \mathbf{N}(t)\}$, and the price of new land $\{q_i\}_i$, an instantaneous equilibrium consists of wages in each sector $\{w_{i,s}\}$, rental rates $\{r_i\}$, and new land production$\{x_i\}$, such that labor and land markets clear according to equations (2.21) and (2.22).

[14] When population growth is nonzero, we alter the on-diagonal elements to $\mathbf{M}_i[s,s'] = -\psi(1-\mu_{i,ss}) + \delta^N_i$, where δ^N_i is country i's population growth at a point in time. This is equivalent to assuming that workers who enter the workforce do so in each sector with equal probability.

Definition. [Dynamic equilibrium] Given $\{\bar{\mathbf{a}}, \mathbf{d}, \mathbf{f}, \mathbf{\Theta}\}$, paths for $\mathbf{Z}$, and an initial condition $\mathbf{S}(0)$, a dynamic equilibrium consists of paths for cleared land $\{L_i\}$, labor allocations $\{N_{i,s}\}$, value functions for workers $\left\{v_{i,s}^N\right\}_{i,s}$ and for the landowners $\left\{v_i^L\right\}$, such that labor evolves according to (2.24), land evolves according to (2.25)–(2.26), land price $\{q_i\}$ satisfies the entry condition 2.12, value functions evolve according to (2.14), (2.11) and (2.12) with corresponding continuation values $\{W_{i,s}\}_{i,s}$ for labor by (2.15) and wages and rental rates satisfy the instantaneous equilibrium.

Definition. [Steady-state equilibrium] The allocation that satisfies the conditions of dynamic equilibrium in addition to: $\dot{N}_{i,s} = \dot{L}_i = \dot{v}_{i,s}^N = \dot{v}_i^L = 0$.

2.5 Analytical Results

This section uses a stripped-down version of our model to provide sharp characterizations of the impact of trade on deforestation. First, we show that when a small open economy experiences reductions in its export costs, it loses forests. Second, and in contrast to our first result, in a world consisting of symmetric countries, a multilateral reduction in agricultural trade costs results in global forest gain. Third, in a world consisting of asymmetric economies and where the elasticity of substitution between agriculture and other sectors equals one, trade leads to a global forest gain if comparative and absolute advantage in agriculture align across countries.

In the rest of this section, we suppose that *(i)* in addition to the land-producing sector *T*, there are only two sectors: agriculture *A* and manufacturing *M*, *(ii)* workers are perfectly mobile across industries and incur no switching costs, and *(iii)* *A* uses only land, and *M* and *T* use only labor:

$$Q_{i,A} = Z_{i,A} L_i; \qquad Q_{i,M} = Z_{i,M} N_{i,M}; \qquad Q_{i,T} = Z_{i,T} N_{i,T}.$$

We focus on the model's steady state. Appendix B.2 collects the proofs of the propositions in this section.

Our first proposition clarifies the context in which the conventional intuition—that trade leads to deforestation—can be most clearly understood. To this end, we consider country i as a small open economy a la Alvarez and Lucas [2007] and drop the country indicator i.

Proposition 1. *A unilateral reduction in export costs of a small open economy leads to an increase in its stock of land,*

$$\frac{d \log L}{-d \log \tau_A} = \frac{N_M}{N} (\eta - 1) > 0 \quad \textit{for} \quad \eta > 1.$$

The relevant demand elasticity for a small open economy is the elasticity of substitution between domestic and foreign varieties, η, which is empirically larger than unity. When a small open economy experiences a reduction in its agricultural export costs, the extent to which its agricultural

exports expand is governed by the trade elasticity, $(\eta - 1)$, which is positive. The derived demand for land also expands, causing deforestation.

In contrast, multilateral trade cost reductions can have markedly different impact on deforestation. Suppose that all countries in the world are symmetric, in the sense that they have the same endowments, geography and productivity. Under symmetry, we can drop country the indicator i.The next proposition shows that, in contrast to Proposition 1, if trade liberalization is implemented multilaterally, the global forest area expands.

Proposition 2. *A worldwide reduction in agricultural trade costs in a system of symmetric economies leads to a decrease in the global stock of land,*

$$\frac{d\log L}{-d\log \tau_A} = \frac{N_M}{N}(\sigma - 1)\left(1 - \pi_A^D\right) < 0 \quad \textit{for} \quad \sigma < 1.$$

where π_A^D is the domestic expenditure share within the agriculture sector.

Here, the demand elasticity that controls the response in the amount of land is governed by the elasticity of substitution between agriculture and non-agriculture sectors, σ. In the empirically relevant case, agriculture and non-agriculture are complements, i.e. $\sigma \in (0, 1)$, and a trade cost reduction results in a reduction in agricultural land and hence an expansion of forest area. The reason is that, in response to the change in prices, structural change reallocates resources away from agriculture and deforestation. In other words, at the global level, demand for land is sufficiently inelastic for global trade to be a land-saving technology. This result is reminiscent of Borlaug's hypothesis, which posits that in a closed economy, agricultural productivity growth is land-saving when σ lies within the range of zero to one.[15] . Proposition 2 extends Borlaug's hypothesis to an open economy setting in which trade can be thought of as an export-biased productivity shock. Accordingly, trade openness can become land-saving when it is implemented by all countries multilaterally rather than toward a single country unilaterally.

While the above results are stark and provide guidance to unpack our quantitative results, they are subject to two important considerations. First, the above results assume iceberg trade costs wherein payments to agricultural trade costs are made to land. Therefore, reducing iceberg-type agricultural trade costs can further decrease land use beyond the effect on the land content of agricultural products. Proposition 5 in Appendix B.2.1.4 presents an analysis analogous to Proposition 2 but under tariff reductions. It demonstrates that the impact of a global tariff reduction in symmetric economies is land-expanding at high levels of trade openness and land-saving at low levels of trade openness. The latter case hinges on the presence of love-of-variety in the agriculture sector, represented by a finite η. Under this empirically-relevant case, tariff reductions can redistribute

[15] See Proposition 4 in Appendix B.2.

land use between countries in a way that reduces overall global land use, yet preserves or even increases the consumption of agricultural products. This effect is dominant when agricultural trade is sufficiently protected, that is when there is significant disparity between the imported versus domestic land content of agricultural consumption.

The insight we draw from Proposition 2 and its tariff-based counterpart is that a multilateral trade integration has a substantially lower impact on global land use than the simple sum of the impacts from unilateral trade integrations. Under iceberg trade costs or tariffs at high levels of trade protection, this effect is sufficiently strong to flip the direction of the impact. However, even when tariff reductions increase global land use, the effect is significantly tempered by the low elasticity of sectoral demand for agriculture.[16]

Second, our above result assumes symmetric countries. In an asymmetric world, countries specialize according to their comparative advantage. Trade integration, therefore, can lead these countries to expand their agricultural frontier and reinforce or mitigate the results in Proposition 2. To shed light on this matter, we next illustrate the role of comparative advantage.

To state our next result in the clearest way, we consider a continuum of countries $i \in [0, 1]$ that have heterogenous productivities in agriculture and manufacturing, but identical otherwise. In addition, we shut down the mechanism behind Proposition 2 by assuming that the elasticity of substitution between agriculture and manufacturing is unity ($\sigma = 1$) and the additional mechanism behind its tariff-based counterpart by assuming that goods within each sector are homogenous ($\eta \to \infty$). Without loss of generality, we order countries in decreasing order of comparative advantage in agriculture, i.e. $Z_{i,A}/Z_{i,M}$ decreases with i.

Proposition 3. *(Comparative and absolute advantage). Suppose goods within each sector are homogeneous and preferences are Cobb-Douglas (i.e., $\eta \to \infty$ and $\sigma = 1$). For a move from autarky to free trade:*

(i) Comparative advantage drives international specialization: There is a cutoff country i^* such that all countries $i < i^*$ specialize in agriculture, and the rest specialize in manufacturing.

(ii) Global forest area expands if comparative and absolute advantage in agriculture align across countries: (a) if $Z_{i,M}$ increases in i, global forest area expands, and (b) if $Z_{i,A}$ decreases in i, global forest area shrinks.

Proposition 3 carries two main messages. The first message, in line with standard results from trade theory, is that comparative advantage is a key determinant of cross-country patterns of specialization.

[16] In our quantitative analysis we acknowledge that a fraction of trade costs are not of iceberg type and can generate revenues in the form of tariffs. We also present robustness checks to our quantitative results based on various specifications of trade costs.

Table 2.2: Parameter Calibration

Parameter	Value	Source
a. Technology and Preferences		
Cost share of VA and labor, $\alpha_{i,g}, \gamma_{i,g}$	–	GTAP, FAOSTAT
Discount rate, ρ	0.05	
Elast. of substitution	$\sigma = 0.5$, $\kappa = 3$, $\eta = 5$	Comin et al. (2021), Sotelo (2020) Simonovska and Waugh (2014)
Trade costs and productivity	$d_{ni,g}, Z_{i,g}$	Model inversion in 2010
b. Technology for the production of new-land		
Forest regrowth rate, δ_f	0.5%	Brazil's data (Mapbiomas)
Fallow land regrowth rate, δ_o	0.5%	Brazil's data (Mapbiomas)
$x_i = \underbrace{\zeta_i \left(1 - z_i\right)^{\lambda}}_{J_i(z_i)} N_{i,T}^{\gamma_T}$	ζ_i	L_i in 2010 to be at steady state
	$\lambda = 2.0$	Population and deforestation reg.
	$\gamma_T = 0.9$	Population and deforestation reg.
c. Dynamics of Labor and Land		
Transition costs for labor, $f_{i,ss'}^N$	$5 \cdot (\text{annual income}_{US})$	Artuc et al. (2010) in SS
T1EV dispersion for labor	$\nu = 0.5$	Artuc et al. (2010) in SS
Arrival rates	$\psi = 1$	–

The second message, to the best of our knowledge, is novel. It states that the correlation between absolute and comparative advantage determines whether trade increases the globally-aggregate land use. When $Z_{i,M}$ increases in i, (which implies that $Z_{i,A}$ does as well), countries with comparative advantage in agriculture have also an absolute advantage in agriculture. In this case, agricultural production is undertaken by the most efficient agricultural producers in the free-trade equilibrium. Relative to autarky, the global amount of resources used in agriculture, i.e., land, decreases. If instead $Z_{i,A}$ decreases in i, trade reallocates land use toward least efficient countries in agricultural production.

2.6 Taking the Model to Data

This section presents our model calibration and explains how we enrich the model in Section 2.4 before taking it to the data. We divide agriculture into main staple crops, pasture-related products, and the rest. We disaggregate the world into the 40 countries and regional aggregates described in Section 2.3. We calibrate our model parameters in three steps. First, we calibrate the parameters related to the static equilibrium using data from the year 2010 (the exception are the observations taken from GTAP, which are for 2014). Second, we calibrate the labor-dynamics parameters based on previous literature. Third, we calibrate the technology in the land-producing sector so that the model matches reduced-form relationships between population growth and growth in agricultural land and forest area (some of which we presented as motivation in Section 2.3). We next explain each step. Table 2.2 summarizes our calibrated parameters.

2.6.1 Calibration of the Baseline Static Equilibrium

In this step we exploit the property that, in each time t, our model behaves like a static trade model with fixed employment of labor and land. We set the elasticity of substitution between agriculture, manufacturing and services, both in production and consumption, at $\sigma = \sigma^I = 0.5$, following Comin et al. [2021]; the trade elasticity in each of the sectors, $\eta - 1 = 4$, following Simonovska and Waugh [2014], and the elasticity of substitution between crops at $\kappa = 3$, following Sotelo [2020]. For the cost share parameters, we use GTAP dataset to directly calibrate the share of value added in gross output $(\alpha_{i,g})$ for all sectors and the labor share in value added $(\gamma_{i,g})$ for agriculture. For non-agricultural sectors, the GTAP dataset does not provide information on the land share in value added. We, therefore, set the land share in value added $(1 - \gamma_{i,g})$ to match the global share of urban areas.

Then, taking GTAP data from 2014 on international trade flows, gross output by industry and input-output matrices, we apply standard inversion methods to back out productivity shifters $(Z_{i,g})$, trade costs $(d_{ij,g})$, and demand shifters ($b_{ij,g}$, $b_{i,s}$, $b^I_{i,g'g}$ and $b_{i,k}$).

2.6.2 Calibration of Dynamics-related Parameters

For the dynamic components of the labor market, we set the sectoral labor supply elasticity at $1/\nu = 2$ and the labor mobility costs, f^N, in line with previous work on labor mobility.[17] We also set arrival rates of move opportunities ψ to 1.

2.6.3 Calibration of the Land-producing Technology

We extend our model to incorporate a margin for fallow land, as detailed in Appendix B.3.1. Let the cleared land L_i be divided into *usable* land $L_{i,u}$ and *fallow* land $L_{i,o}$, with country area specified as $H = F + L_{i,u} + L_{i,o}$.[18] We begin by parametrizing $J_i(z_i) = \zeta_{i,f} \times (1 - z_i)^{\lambda_f}$ in equation (2.8), the production of usable land from forest can be rewritten as:

$$Q_{i,Tf} = \zeta_{i,f} \times (1 - z_i)^{\lambda_f} \times N^{\gamma_f}_{i,Tf} \tag{2.27}$$

where $\zeta_{i,f}$ is a country-specific productivity shifter, λ_f denotes the elasticity of J_i with respect to country i's land share of forest $F_i/H_i \equiv (1 - z_i)$, and γ_f is the output elasticity of labor. Next, we

[17] Caliendo et al. [2019] report that the yearly equivalent of their labor elasticity equals our choice of $1/\nu = 2$. For labor mobility cost, f^N, we follow McLaren [2017] who reports estimates of about five times yearly real income, which we target for US service workers in the steady state.

[18] Our goal is to provide accurate quantitative responses of deforestation in several trade-cost scenarios. The fallow land module we introduce here provides us with a simple way to capture a first-order feature of the data, which is the existence of other sources, besides forests, that feed the expansion of land in production, including fallow land.

define $u_i \equiv L_{i,u}/L_i$ as the share of usable land in cleared land. With this definition, we introduce a production function of usable land from fallow land, in a manner symmetric to 2.27:

$$Q_{i,To} = \zeta_{i,o} \times \left(z_i \left(1 - u_i\right)\right)^{\lambda_o} \times N_{i,To}^{\gamma_o} \tag{2.28}$$

where $\zeta_{i,o}$ is a productivity shifter, λ_o controls the extent to which the productivity falls with increases in country i's land share of fallow land $L_{i,o}/H_i \equiv u_i \left(1 - z_i\right)$, and γ_f is the output elasticity of labor. Total employment and total production in the land-producing sector are given by $N_{i,T} = N_{i,Tf} + N_{i,To}$ and $Q_{i,T} = Q_{i,Tf} + Q_{i,To}$.

Our calibration of the parameters in the land-producing sector follows two steps. First, we recover the productivity shifters $(\zeta_{i,o}, \zeta_{i,f})$ such that the model prediction of agricultural land, fallow land, and forest area in the steady state match their observed values in the initial year of our sample.

Second, in the spirit of indirect inference, we choose values of the elasticities $(\lambda_f, \gamma_f, \lambda_o, \gamma_o)$ so that our model mimics the reduced-form responses of deforestation and land use to population shocks. Specifically, (i) we simulate the model under the UN population growth projection until 2100, and (ii) using these simulated data, we run a set of regressions along the lines of equation (2.1). We search for the elasticity parameters that minimize the distance between the regression coefficients of the simulated data versus those of the actual data.[19] Appendix Figure B.2 shows our model fit.

Our procedure can separately pin down the four above elasticity parameters. First, in the data fallow land accounts for a sizable share of a country area and, as suggested by Empirical Pattern 2, it is a source of expansion of agricultural land. Therefore, a population shock can lead to an expansion of agricultural land not fully accounted for by a reduction in forest area. This distinction separately identifies the parameters that govern the expansion from forest, (λ_f, γ_f), from those that control the expansion from fallow land, (λ_o, γ_o). Second, our regressions reveal that agricultural land responds differently at various time horizons to a 30-year change in population, with a longer time horizon associated with a larger response. This variation helps us pin down the labor elasticity

[19] Specifically, we target the coefficients of the following regression:

$$\underbrace{\log\left(\text{Forest}_{i,t}\right) - \log\left(\text{Forest}_{i,s}\right)}_{\text{different time lags}} = \beta_0 + \beta_{t,s} \underbrace{\left[\log\left(\text{Pop}_{i,2020}\right) - \log\left(\text{Pop}_{i,1990}\right)\right]}_{\text{30 years lag}} + \epsilon_i,$$

where we chose t and $s > t$ among $\{1990, 2000, 2010, 2020\}$, so as to construct intervals of different lengths. Writing β as the vector containing $\beta_{t,s}$, we pick $(\lambda_f, \gamma_f, \lambda_o, \gamma_o)$ to minimize

$$M = \left(\beta^{\text{(data)}} - \beta^{\text{(model)}}\right) W \left(\beta^{\text{(data)}} - \beta^{\text{(model)}}\right)'$$

where W is a weighting matrix, $\beta^{\text{(data)}}$ is the vector of parameters estimated using the actual data, and $\beta^{\text{(model)}}$ is the vector of parameters estimated using model-generated data. We pick the diagonal elements of the inverse of the variance-covariance matrix of $\beta^{\text{(model)}}$ as W.

separately from the area elasticity, i.e., γ_f versus λ_f and γ_o versus λ_o. Higher labor elasticities scale up the overall deforestation responses, whereas higher area elasticities, λ_f and λ_o, reduce future land-clearing productivity, and makes short-run responses relatively larger.

Lastly, pick the regrowth rate of forest δ_f and δ_o from MAPBIOMAS for Brazil, which separates gross losses and gains in forest.[20]

2.6.4 Components of Trade Costs

Our calibration of trade costs distinguishes the components of trade costs that are associated with policy barriers. To do so, we adopt the following parametrization of $d_{ij,g}$,

$$d_{ij,g} = (1 + \kappa_{ij,g}) \left(1 + t^{ice}_{ij,g}\right) \left(1 + t^{rev}_{ij,g}\right),$$

where $\kappa_{ij,g}$ is an iceberg trade cost unrelated to policy, $t^{ice}_{ij,g}$ is an iceberg trade cost generated by policy, and $t^{rev}_{ij,g}$ is a revenue-generating non-iceberg trade cost. We provide here a brief description of the method that we employ to recover each of these terms, relegating details to Appendix B.4.1.

Our procedure consists of three steps. First, following common practices in the trade literature, we recover $d_{ij,g}$ from the residuals generated by the estimation of gravity equations. Second, similar to Nath [2020], we regress $d_{ij,g}$ on observables related to policy barriers, including the number of days to import, tariffs, and import fees in destination j, and an indicator for trade agreements between i and j. This second step allows us to separate $\kappa_{ij,g}$ from $t^{ice}_{ij,g}$ and $t^{rev}_{ij,g}$. Third, we calibrate the relative magnitude of $t^{ice}_{ij,g}$ with respect to $t^{rev}_{ij,g}$ so that the model-implied tariff revenues per agricultural GDP in each country matches this same statistic in the data.

2.7 Counterfactual Analysis

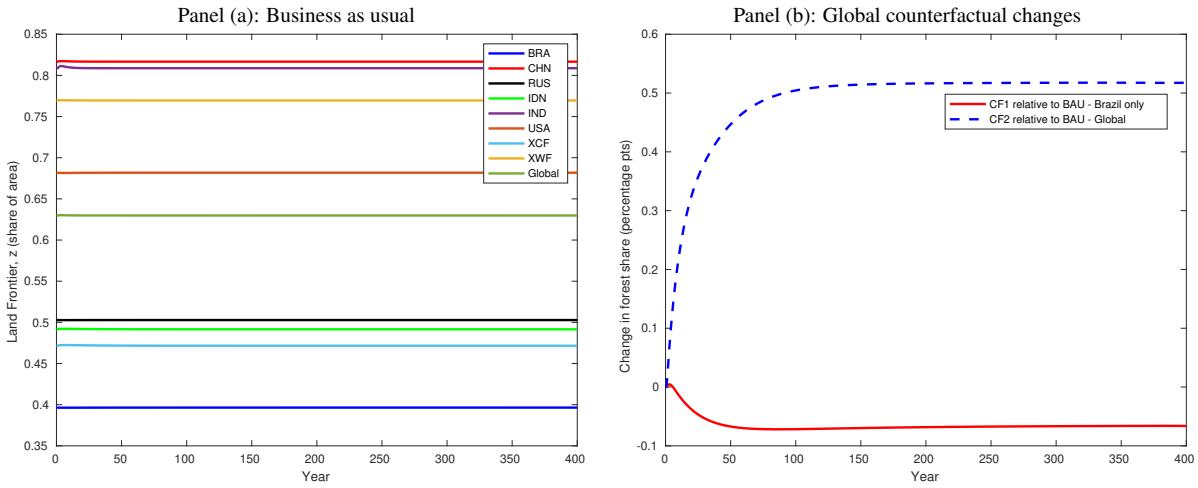
In this section, we examine the implications of agricultural trade cost reductions for deforestation and welfare around the world. We specifically study the impacts of a global trade cost reduction, which we contrast with a scenario in which countries open up to trade only toward Brazil.

2.7.1 The Path of Forests

Business as usual. We begin by reporting the frontier of cleared land in the business as usual (BAU) scenario—which is the baseline outcome of our model where no policy or shock is in-

[20] MAPBIOMAS provides information on the full transition of land between uses—pasture, forest, fallow and cropland—across years in municipalities in Brazil. We pick the average share of cleared land that transitions to forest area. See Araujo et al. [2022] for a detailed description of the MAPBIOMAs data.

Figure 2.5: Multilateral versus Unilateral Trade Cost Reduction: Change in Global Forest Area relative to Baseline



troduced. Panel (a) in Figure 2.5 shows this path for select countries, as well as for the global economy. As a consequence of our approach to calibration, the land frontier remains almost constant across countries and globally.

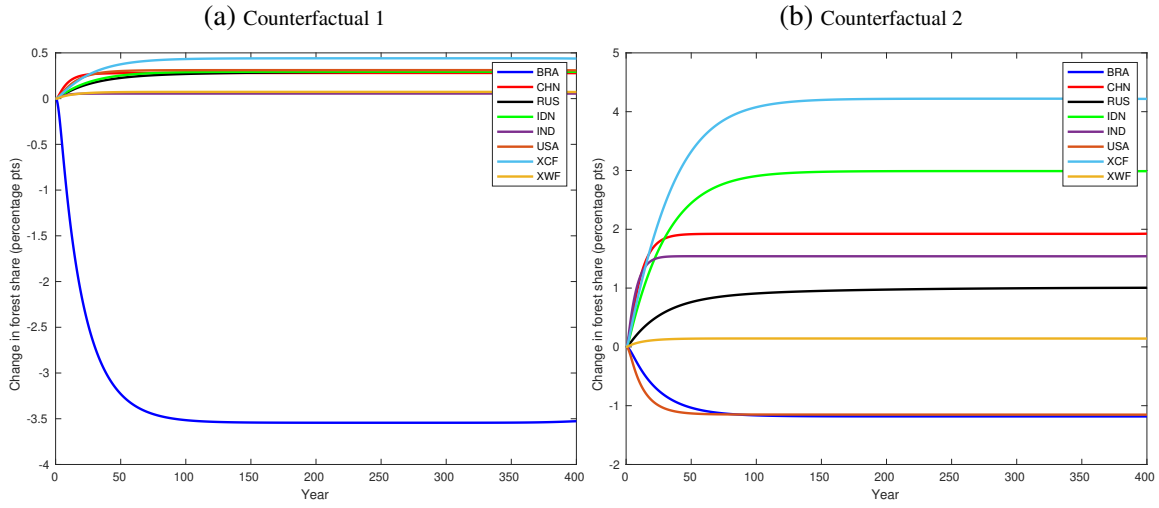
We emphasize that this baseline is not a forecast based on our model. In our baseline scenario, productivity, population, and land remain constant over time, while one would need to know their future paths to forecast the future of forests. In subsection 2.7.3, we incorporate population growth into an alternative BAU scenario and evaluate how it affects our quantitative conclusions.

Counterfactual #1: Reduction in Brazil's Export Costs. We begin by considering a 30 percent reduction in policy-related trade costs of agricultural goods produced in Brazil.[21] As shown in Figure 2.5, Panel (b) global forest area monotonically decreases over time. Figure 2.6, Panel (a) disaggregates this global trend into the experiences of individual countries, and Appendix Table B.3 presents the details. The reason global forest area falls is that Brazil's forest (as share of country area) drops by 3 percentage points; regrowth in the rest of the world, while attenuating the aggregate impact of Brazil's response, does not offset it completely.

Counterfactual #2: Multilateral trade cost reductions. We now turn to a policy scenario in which countries agree to liberalize trade in agriculture multilaterally. We implement this policy in a simple way by considering a 30% reduction in trade costs of agricultural goods across all countries. This shock has starkly different implications compared to the previous one.

[21] Specifically, we adjust the reductions in $\left(1 - t_{ij,g}^{ice}\right)$ and $\left(1 - t_{ij,g}^{rev}\right)$ by $(0.70)^{1/2}$ so that each term accounts for half of the 30% reduction in trade costs.

Figure 2.6: Multilateral versus Unilateral Trade Cost Reduction: Select Countries



Worldwide, the forest share would grow by 0.7 percentage points in the steady state following the multilateral trade cost reduction. Turning to individual countries, forest area would grow in Central Africa, as well as China and Indonesia; whereas North America and Brazil would experience a decline in their forest area (Figure 2.6, Panel (b) and Appendix Table B.3). This cross-country variation highlights a key mechanism in our model. As we explain below, although structural change leads to aggregate reforestation, countries that have a comparative advantage in agriculture or that are geographically well-positioned to serve economies that specialize in non-agriculture, as the shock ensues, take advantage of the trade cost reduction by expanding their agricultural sector and deforesting more.

Figure 2.6, Panel (b) shows that half of the effects unfold in the first 50 years, although it takes substantially more to approach the steady state. Moreover, the figure highlights another key feature: Since (i) some countries tend to reforest and forest regrowth takes time, and (ii) the land use across countries are linked through international trade, deforestation cannot be too quick, resulting in a slow convergence to the steady state.

2.7.2 The Roles of Structural Change and Comparative Advantage

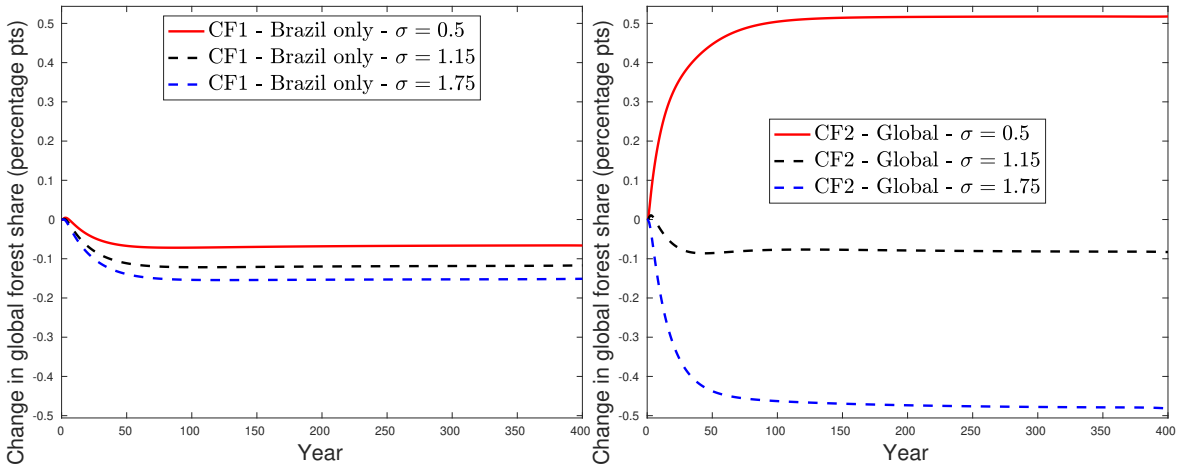
We next examine the quantitative importance of structural change and comparative advantage as adjustment mechanisms.

2.7.2.1 Structural Change

To illustrate the contribution of structural change, in Figure 2.7 we display the counterfactual path of forests under larger values of the elasticity of substitution, $\sigma \in \{0.5, 1.1, 1.75\}$. Doing so limits the scope of structural change for reducing land demand, by muting the complementarity between agriculture and non-agriculture sectors. The figure demonstrates that, a larger value of σ reverts the path of forests in Counterfactual #2 but does not change that of Counterfactual #1. These quantitative results—which are in line with Propositions 1 and 2—show that the relevant elasticity of demand for agricultural goods depends on the geographic scope of trade-cost shock. For a small open economy, demand is elastic, due to trade; globally it is inelastic, due to structural change.

Figure 2.7: The Role of the Elasticity of Substitution, σ

(a) Counterfactual 1 (b) Counterfactual 2



2.7.2.2 Comparative Advantage

To explore quantitatively the role of comparative advantage, Figure 2.8a relates Balassa's revealed comparative advantage (RCA) index in Agriculture in 2010, the initial year of our calibration (on the x-axis) and the counterfactual change in the forest share in the steady state (on the y-axis) for our main specification at $\sigma = 0.5$. Comparative advantage governs the cross-sectional responses: Upon a reduction in trade costs, countries with a comparative advantage in agriculture take advantage of the new trade opportunities and, to expand their agricultural sector, they cut into their forests.

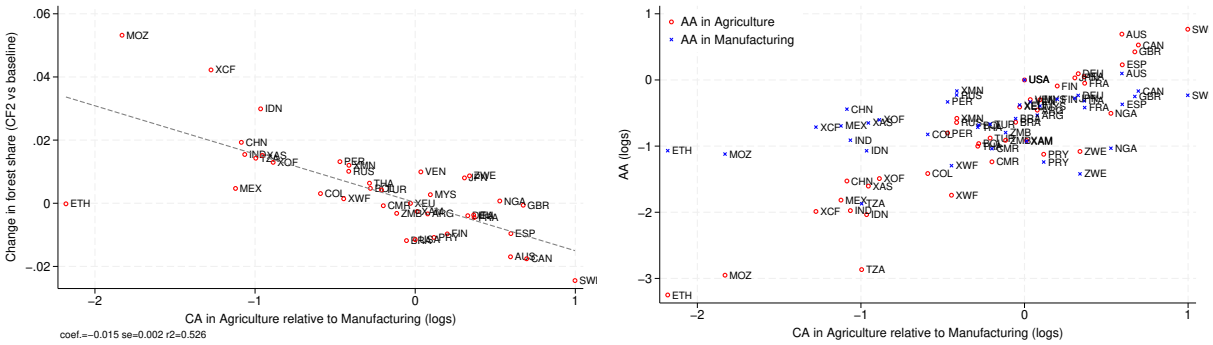
In addition, Proposition 3 suggests trade is land-saving. Figure 2.8b shows that across countries relative productivity in agriculture, $Z_{i,A}/Z_{i,M}$, is positively correlated with absolute agricultural productivity, $Z_{i,A}$ (recovered via model inversion), which means that trade reallocates agricultural

production to the most efficient agricultural producers.

Figure 2.8: The Role of Comparative Advantage

(a) Deforestation in the cross-section

(b) Absolute and Comparative Advantage in Agriculture



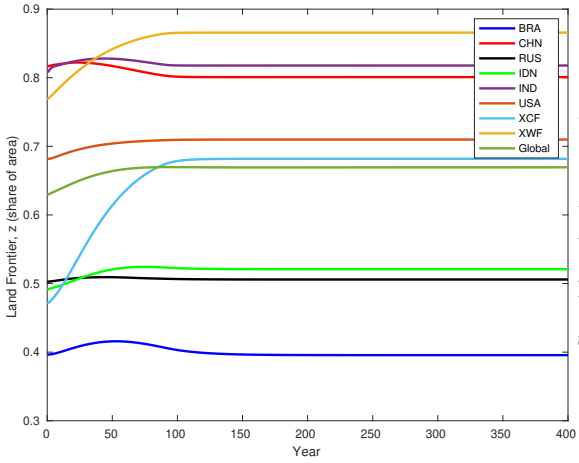
2.7.3 Incorporating Population Growth

This section examines Counterfactuals #1 and #2 under an alternative business-as-usual scenario that incorporates population growth according to the UN projections between until 2100. There are two main reasons to study this new scenario. First, population size is a key determinant of the equilibrium amount of cleared land and forest, as it fuels both demand for agricultural goods and the availability of labor needed to sustain cleared land. This is all the more relevant since population is expected to grow substantially over the course of the following decades, and unevenly so across countries. Average population growth until the end of this century will be 35%, and it will range from population reductions in Japan to more than 300 percent increases in parts of Africa, where large forests areas remain untouched. As we show next, these heterogenous rates of population growth will alter the allocation of land use across countries. Second, as we show next, population growth is expected to be larger in countries with a comparative *disadvantage* in agriculture, which means that global trade cost reductions will have additional leverage to reduce deforestation.

Panel (a) of Figure 2.9 displays our new BAU scenario. We see large increases in the amount of cleared land (and hence, reductions in forest) in countries in which population growth is projected to be largest. Countries such as Brazil and Indonesia, where population growth is smaller, experience early but moderate expansion in their cleared land, which are then partially reverted as countries with higher population growth develop new land to serve their growing domestic demand for agricultural goods. Figure 2.10 shows, for our whole sample, that countries with larger population growth experience larger deforestation (steady-state relative to 2010) in the new BAU.

Figure 2.9: The Role of Population Growth

(a) Baseline with Population Growth



(b) Global Counterfactual Changes

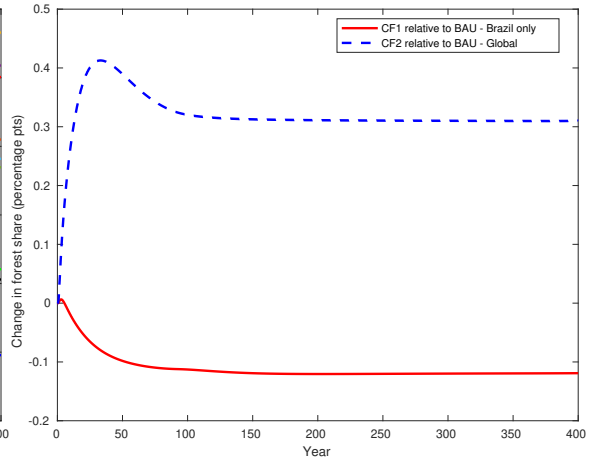
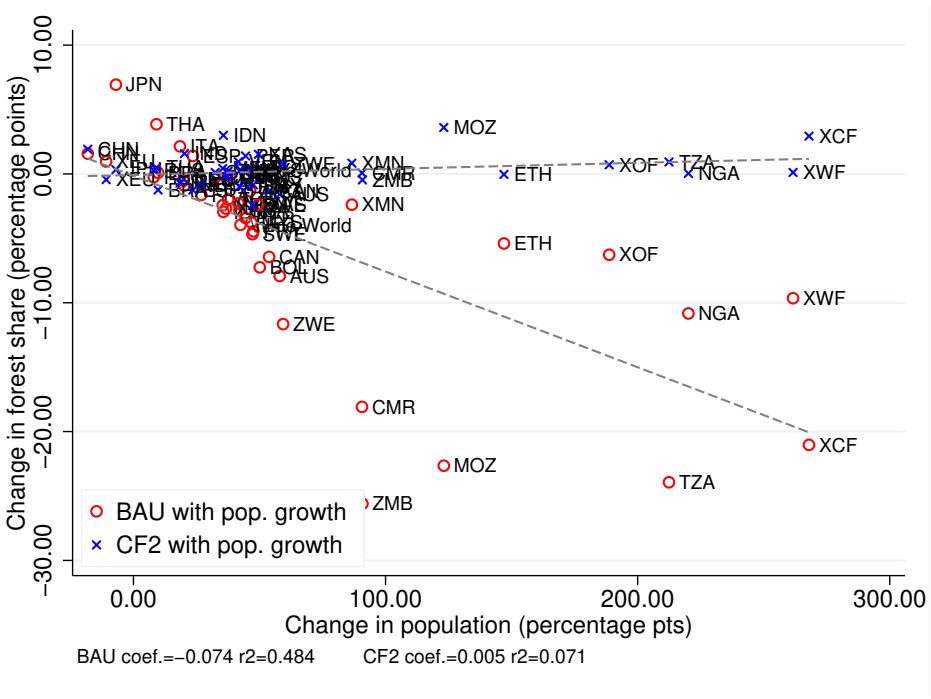


Table B.3 in the Appendix reports the corresponding values.

Panel (b) of Figure 2.9 shows that, relative to this new BAU, our counterfactual scenarios remain qualitatively similar to those without population growth: A global trade cost reduction mitigates pressures on land and economizes on forests at the global scale, whereas the global forest area shrinks in the Brazil-only scenario. Figure 2.10, however, shows an important difference. Global trade cost reductions (Counterfactual #2) mitigate deforestation that would otherwise occur in the business-as-usual, especially in African countries, since trade reallocates land use toward regions of the world that produce agriculture more efficiently (recall Figure 2.8b).

Figure 2.10: Change in Forest Share versus Population



2.7.4 The Deforestation Impact of Raising Trade Costs

To complement our previous analysis, we consider two additional counterfactual scenarios wherein instead of reducing trade costs, we increase them. In Counterfactual #3, countries raise their agricultural trade costs when they import from Brazil by 30%, as trade penalties on a country whose agricultural exports are linked to deforestation. In Counterfactual #4, agricultural trade costs are raised by 30% globally, representing a move away from globalization in agriculture. Appendix Figure B.3 shows the results.

In Counterfactual #3, global forest area rises by 0.4% and 0.6% relative to the BAU scenarios without and with population growth. These aggregate results come from a sizable reforestation in Brazil, which is partially offset by deforestation elsewhere. In Counterfactual #4, global forest area decreases by 0.3% in the no population growth scenario and it increases by less than 0.6% in the case with population growth. Therefore, unilateral trade penalties imposed on Brazil's agricultural exports save a larger amount of global forest area than a worldwide increase in agricultural trade costs. The key to understanding this results is the relevant elasticities of substitution. When trade costs increase globally (Counterfactual #4), the low elasticity of substitution between agriculture and non-agriculture increases the relative demand for agriculture putting additional pressure on forests. These results reinforce our previous findings by highlighting that multilateral coordination on agricultural trade policy matters for reductions in deforestation.

2.7.5 Carbon Heterogeneity, Dynamics, and Reforestation.

We evaluate the impact of changes in trade costs on the implied CO_2 emissions from deforestation. [22] In our simplest exercise, we follow the guidelines used by the IPCC to calculate the climate costs from deforestation-related CO_2 emissions. Each hectare of forest loss per country and year corresponds to an implied CO_2 emission released to the climate.[23] We put a cost on the global level of CO_2 emissions at any point in time using a social cost of CO_2 set at 51 \$/tC, based on the 2021 report by the United States Interagency Working Group on Social Cost of Greenhouse Gases, and compute the discounted present value of the stream of these costs. To benchmark the results, we present them relative to the total cost of CO_2 emissions from agriculture in 2010.

Table 2.3 compares these costs across multiple parameterizations and assumptions on carbon content of forests. Panel (a) focuses on our main parameterization with $\sigma = 0.5$. Column (1) presents the results that emerge from the above method. In this case, the emissions costs of global trade cost reductions are slightly lower than those of trade cost reductions only for Brazil, despite the large difference in the scale of the shocks. Panel (b), which assumes instead that goods are substitutes, with $\sigma = 1.75$, shows much larger costs of global trade cost reductions. This result is expected as the demand elasticity for agriculture is set at a substantially larger value. Column (2) shows that ignoring Brazil's rich carbon intensity would lead to substantial underestimation of lowering its export costs. We next acknowledge that the carbon content of forests is not limited to their above- and under-ground biomass, which are the basis of our calculation in Columns (1) and (2). Accordingly, Column (3) shows the emission costs associated with carbon contained in the forest biomass plus its soil and litter.

A feature of the IPCC guidelines we have used so far is that it does not take into account the possibility of carbon sequestration from forest regrowth. Columns (4) and (5) show that this assumption can have important consequences, as under full and partial sequestration scenarios, the balance of gains and losses in forests across countries turn to a positive net gain in the global trade cost scenario (Counterfactual #2).[24] In fact, in Column (5), a global trade cost reduction

[22] Our evaluation does not incorporate other costs associated with deforestation. These other costs stem from the loss of wildlife endemic to each forest, the change in landscape that increases the likelihood of flooding, the amenity value of forests, and desertification. Additionally, we abstract away from the costs associated with reforestation such as the adverse health effects of pollen.

[23] Specifically, following the guidelines described in Tubiello et al. [2020], we use the following equation to compute CO_2 emissions from deforestation: $NFC_{i,t} = -\frac{B_{i,t-1}}{A_{i,t-1}} \min\left[A_{i,t} - A_{t,t-1}, 0\right] \frac{44}{12}$,where $NFC_{i,t}$ is the net deforestation, expressed in tonnes of CO_2. The term $\frac{44}{12}$ converts C to CO_2—it is the ratio of the molecular weight of carbon dioxide, which equals 44, to that of carbon, which equals 12. Note that this is a somewhat pessimistic approach since (i) it assumes when a hectare of forest is lost, all the carbon previously stored in that hectare is immediately released, and (ii) it does not account for reforestation.

[24] In the full sequestration scenario, net reforestation absorbs from the atmosphere all the CO2 that would be released by the same amount of net deforestation. In the no sequestration scenario, net reforestation does not absorb any

entails the minimal cost among all four counterfactual scenarios, which was not the case in the no-sequestration scenarios, which do not value reforestation and therefore make trade cost increases look more desirable.

Columns (6)-(8) shift attention to the scenarios that include population growth, retaining the assumption of partial carbon sequestration. Column (6) shows that, when we consider population growth, losses in Counterfactual #2 decrease. The reason is that with population growth deforestation occurs in the baseline, and trade cost reductions avoid deforestation, which the IPCC guidelines value more than reforestation. Column (7) increases the social cost of carbon to $200/ton, while Column (8) shows that ignoring dynamics would lead us to overestimate the costs of reducing Brazil's export costs, but underestimate the gains of global trade cost reductions.

CO2 from the atmosphere. In the partial sequestration scenario, we use the simple rule that net reforestation absorbs from the atmosphere 30% of all the CO2 emissions that would be released by the same amount of net deforestation.

Table 2.3: Social Costs of Deforestation under Different Trade Integration Scenarios

	Cost as % of Ag Emissions in 2010							
	(1)	(2)	(3)	(4)	(5)	(6)	(7)	(8)
Panel A: Complements ($\sigma = 0.5$)								
CF - Brazil only reduction	39.79	61.59	87.42	37.86	14.59	32.76	128.47	382.56
CF - Worldwide reduction	51.07	51.43	149.58	-0.27	-88.81	-63.29	-248.19	-189.32
CF - Brazil only increase	9.97	8.45	22.45	-16.89	-43.91	-13.66	-53.57	33.44
CF - Worldwide increase	82.19	72.12	134.46	38.19	-8.90	-34.97	-137.14	-567.32
Panel B: Substitutes ($\sigma = 1.75$)								
CF - Brazil only reduction	38.91	59.49	85.03	27.80	8.88	62.08	243.44	578.07
CF - Worldwide reduction	119.29	117.36	322.00	78.49	42.82	304.65	1194.72	1996.03
CF - Brazil only increase	4.28	3.49	9.62	-31.05	-56.62	-20.16	-79.07	-48.34
CF - Worldwide increase	23.63	23.08	38.49	-24.51	-80.54	-150.78	-591.28	-1215.63
Carbon Density Assumptions								
- Above-below ground biomass	Y	Y	Y	Y	Y	Y	Y	Y
- Carbon in soil and litter	-	-	Y	Y	Y	Y	Y	Y
- Homogenous density	-	Y	-	-	-	-	-	-
Carbon Sequestration Assumptions								
- None	Y	Y	Y	-	-	-	-	-
- Partial	-	-	-	-	Y	Y	Y	Y
- Full	-	-	-	Y	-	-	-	-
Economic Assumptions								
- Population Growth	-	-	-	-	-	Y	Y	Y
- SSC = 51	Y	Y	Y	Y	Y	Y	-	-
- SSC = 200	-	-	-	-	-	-	Y	Y
- Ignore dynamics	-	-	-	-	-	-	-	Y

Notes: This table shows the gains in terms of real gdp and the costs in terms of carbon emissions of different policy counterfactuals using different parametrizations of the model. For column 1, we compute the present value of all the future flows of real GDP and compare that value with the present value of all the future flows in the BAU. For column 2 to 4, we present the total gains and costs measured relative to the cost of total agricultural emissions in 2010. We compute the climate costs of deforestation using the methodology of IPCC described in Section 2.2.

2.8 Conclusion

Global deforestation drives carbon emissions and reduces biodiversity, which poses an important challenge for policy. Meanwhile, the potential for agricultural trade liberalizations raises the concern over the impact on deforestation. We have developed a framework to study, analytically and quantitatively, the deforestation impact of trade policy. The key insight of our paper is that in a

trading world, structural change and comparative advantage interact to determine aggregate land use and how it is distributed across countries. Our results provide a new rationale for international cooperation in trade policy, by showing that multilateral trade liberalization can help circumvent trade offs between the gains from trade and preservation of the forests.

CHAPTER 3

Playing with Blocs: Quantifying Decoupling

Abstract

We adopt a data-driven approach to measure trade fragmentation over the period 2015-2023. We assign countries to the US bloc, the China bloc, or to an unaligned group based on whether their trade costs with the US and China increased or decreased over this period. We find that the US bloc and the China bloc each contain roughly a quarter of the countries in the world, with about half the countries remaining unaligned. However, we also find that as cross-bloc trade costs increased, within-bloc trade costs fell. We use a quantitative model to compute the real income effects of this reconfiguration of the global trade costs. The median country in the world, and the median country within each bloc, has 0.4-0.6% *higher* real income as a result of the observed decoupling, contrary to the widespread belief that fragmentation has been welfare-reducing. Finally, we find a modest amount of bloc misalignment: the median country in the US bloc would actually be better off in the China bloc, and vice versa. These results suggest that trade decoupling does not always follow trade-driven economic interests.[1]

3.1 Introduction

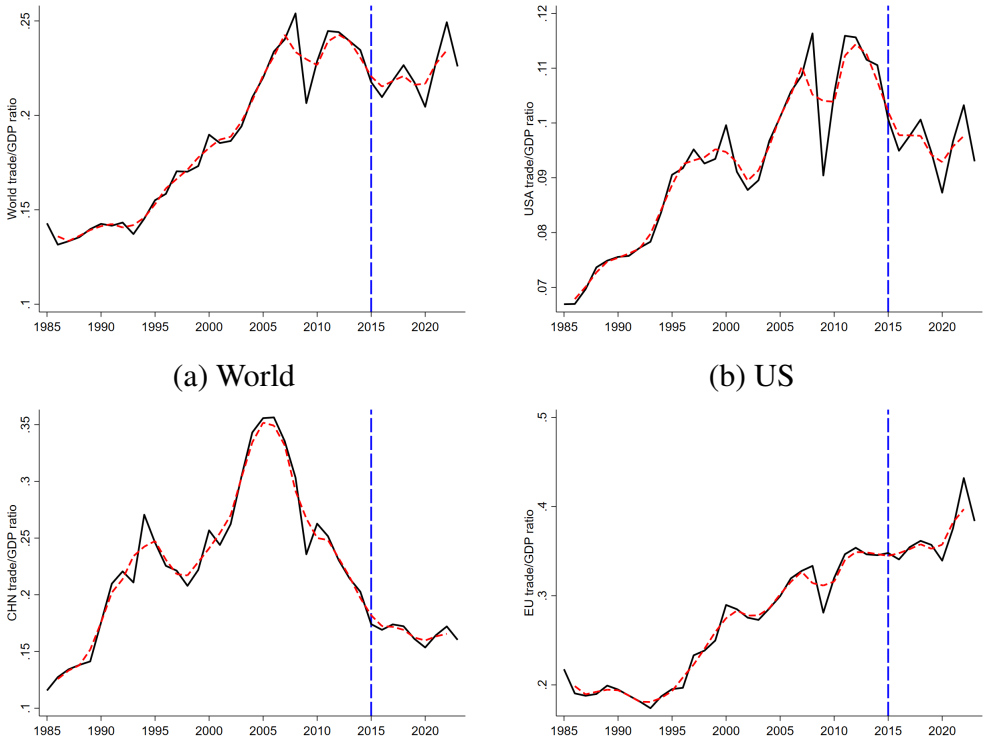
After a long era of ever-increasing globalization, in the past decade the world entered a period of substantial headwinds to economic integration, punctuated by Brexit, the US-China trade war, and the rupture of economic relations between the West and Russia. It is now common to wonder whether these events mark the onset of "deglobalization."

However, world trade relative to economic activity has not in fact fallen since the onset of these shocks. Figure 3.1(a) plots the evolution of world goods trade to GDP from 1985 to 2023, with the vertical line at 2015, the year prior to the Brexit vote in the UK and the Trump victory in the

[1]This chapter is co-authored with Barthélémy Bonadio, Zhen Huo, Andrei A. Levchenko, Nitya Pandalai-Nayar, Hiroshi Toma, and Petia Topalova.

US. Since that year, world trade has remained resilient; in fact it partly reversed the downward trend that started in 2009. Even more strikingly, the trade-GDP ratio did not fall even for the large economies at the center of the policy-induced trade disruptions: the US, China, and the EU, as displayed in panels (b)-(d) of Figure 3.1. Even the main parties to the trade conflicts did not experience a discernible fall in total trade.

Figure 3.1: Trade/GDP Ratios



(a) World (b) US

(c) China (d) European Union

Notes: Solid line denotes the trade-GDP ratio, defined as $\frac{0.5\times(\text{exports+imports})}{\text{GDP}}$. Dashed line denotes the 3-year moving average of the trade-GDP ratio. Vertical line denotes the beginning of the US-China trade war.
Sources: DOTS, WEO.

The proximate explanation is that even as countries in trade conflicts disengaged from each other, they increased trade with other countries. Table 3.1 confirms this. It reports the changes in bilateral trade in these major economies. Even as trade between the US and China fell, trade between those economies and the rest of the world increased. The world economy is experiencing decoupling or fragmentation, rather than deglobalization.

This paper measures decoupling and quantifies its impact on real GDP and income in a large sample of countries.[2] First, we use an entirely data-driven approach to detect fragmentation fault

[2]In the paper, we use decoupling and fragmentation interchangeably to denote policy-induced changes in the sources and destinations of cross-border trade flows, which could be guided by strategic considerations, such as na-

Table 3.1: Change in Trade (2015-2023)

↓ Exporter | Importer →	USA	China	EU	ROW
USA		-0.275	0.262	0.015
China	-0.401		0.237	0.137
EU	0.050	-0.066	0.148	-0.014
ROW	0.012	0.047	0.035	0.105
Change in total imports-to-GDP	-0.070	0.005	0.128	0.076

Notes: Table presents the percentage change in the imports-to-GDP ratio from the source economy to the destination economy between 2015 and 2023. Rows represent exporters and columns represent importers. "ROW" denotes rest-of-the-world.

lines in international trade flows and classify countries into trade blocs. Relying on the gravity tradition of measuring trade costs, we project the log changes in bilateral goods trade over the period 2015-2023 on multilateral resistance (as captured by importer and exporter fixed effects). The residual from this estimation can be interpreted as the relative change in the bilateral component of trade costs between pairs of countries. Based on these, we classify countries into 3 groups: the US bloc, the China bloc, and unaligned. Countries in the US bloc are those that experienced a relative fall in trade costs with the US, and a relative rise in trade costs with China. The opposite is true for the countries in the China bloc. We classify countries whose trade costs with the US and China changed in the same direction as unaligned. In the full sample of 187 countries for which bilateral trade data are available, 43 are in the US bloc, 46 in the China bloc, and the remaining 98 are unaligned.

Next, we assess the aggregate consequences of decoupling in a quantitative multi-country, multi-sector international trade model following Huo et al. [2025], Bonadio et al. [2021], and Bonadio et al. [2023a]. Starting from the 2015 world economy, we apply the matrix of bilateral trade cost changes that occurred between 2015 and 2023, and compute the resulting changes in real GDP and real incomes. This exercise isolates the changes in trade costs occurring over this period from other shocks experienced by the world economy, and individual countries, such as productivity or structural change.

An important challenge we face is that we cannot use the usual model inversion techniques to recover the changes in trade costs that explain the trade data, because we do not have domestic absorption data for 2023. We also cannot compute the absolute changes in trade costs from the gravity regressions, because they only yield changes in trade costs relative to an omitted im/exporter in the regression. To overcome this challenge, we scale the gravity regression-implied bilateral trade cost changes by a common factor so that the model matches the 2015-23 change in the world trade/GDP

tional and economic security, sovereignty, and autonomy.

ratio depicted in Figure 3.1(a). This approach allows us to preserve the full heterogeneity in trade cost changes at the country pair level, while matching the world trade trend.

We find that the median country experienced a 0.6% real GDP and real income *increase* from the trade cost changes occurring from 2015 to 2023. Thus, contrary to conventional wisdom, the decoupling process has not reduced world GDP as a whole thus far. Predictably, the income changes are larger for nonaligned countries (0.8%) than the countries in the US or the China blocs, since those countries do not systematically increase their trade costs with either bloc. But even the countries in the US and China blocs on average experience real income gains from these trade cost changes. The positive impacts of these trade cost changes are in fact quite broad-based: 51 out of 66 countries in the sample experienced real income increases from the observed trade cost changes. The ultimate source of this finding is that global trade has remained quite stable relative to global activity between 2015-23, with the decline in trade flows between some countries (e.g. the US and China) more than offset by increasing trade flows between others. Prima facie, this points to no major increases in average trade costs, with consequent lack of adverse impact on real GDP on average.

We then explore the consequences of bloc alignment. In particular, for each country we compute the counterfactual changes in real GDP and income that would have occurred had it belonged to a different bloc. We find that the bloc alignment uncovered in the data corresponds poorly to trade-related economic interests. On average, countries in the US bloc would gain from moving to the China bloc, while the China bloc countries would gain from moving to the US bloc. Unaligned countries would on average lose from joining either bloc. These results suggest that other motives (presumably geopolitically driven) are likely at play in the rewiring of trade flows in recent years. Behind these averages is complete heterogeneity across countries within each bloc: one can find both potential winners and losers from inter-bloc moves.

Related Literature This paper contributes to several fast-growing strands of literature. A number of studies have examined the causes and consequences of recent policies that have heralded greater inward orientation by major advanced economies, such as the US increase in tariffs of Chinese imports [e.g. Fajgelbaum et al., 2024]; Amiti et al. [2019] or Brexit [e.g. Sampson, 2017, Dhingra and Sampson, 2022]. These papers document the negative consequences of these policies on individual countries, but do not provide a quantitative analysis of the GDP impacts worldwide, which is one of our contributions. While the focus of this literature is primarily on large adverse shocks to trade costs, fostering the narrative of rising barriers to globalization, Bown et al. [2019] document that trade costs did not uniformly increase in all episodes. In fact, during the US-China trade war, China lowered its most favored nation (MFN) tariffs, effectively decreasing the trade barriers it imposes on the rest of the world, while raising them against the US. Our analysis cor-

roborates the highly heterogeneous patterns of changes in bilateral trade costs across country pairs thus far.

The slowdown in the pace of globalization following the Global Financial Crisis in 2008 has generated debate about whether we are in an era of deglobalization. Recent studies have argued that there is no evidence supporting a deglobalization narrative based on trends in aggregate trade to GDP ratios [Antràs, 2020, Goldberg and Reed, 2023]. Gopinath et al. [2024] also find no evidence of a large decrease in trade flows overall, and patterns more suggestive of fragmentation, with trade between geopolitically distant blocs significantly lower than trade within blocs since Russia's invasion of Ukraine. However, that paper documents that the barriers to trade and FDI have continued to increase in recent years. The reallocation of trade and FDI flows and the lengthening of supply chains is documented by an ever growing number of studies [e.g. Aiyar et al., 2023a, Freund et al., 2023b,a, Alfaro and Chor, 2023, Blanga-Gubbay and Rubínová, 2023]. The existing work on fragmentation and reallocation has focused either on the decoupling between the US and China, or fragmentation of trade between pre-defined blocs of countries. We complement these studies by examining the reallocation of trade flows across all country pairs within the gravity framework to deduce the relative changes in bilateral trade costs from the data and quantify their impact. Our methodology also allows us to identify the set of "unaligned" countries based on observed trade patterns, and examine the correlates of being a "connector" in a systematic manner.

Our paper is also related to the fast-growing literature studying geoeconomics including Clayton et al. [2023], Aiyar et al. [2023b], Attinasi et al. [2023], Bolhuis et al. [2023], Cerdeiro et al. [2021], Javorcik et al. [2024], and Hakobyan et al. [2023]. A subset of these papers use quantitative models to study the economic implications of fragmentation. We contribute to this literature by assigning countries to blocs using revealed trade cost changes, and studying whether countries have optimally selected their blocs, given the choices of the rest of the world.

Finally, our approach to bloc assignment uses revealed trade barriers in a simple gravity equation setting. Several recent papers have alternatively used UN votes to assign countries to blocs [Góes and Bekkers, 2022, Bolhuis et al., 2023]. We find that UN votes are correlated with our revealed blocs, albeit not perfectly. Other approaches to bloc assignment include treating the US-EU as a bloc, and China-Russia as a bloc [e.g. Fernández-Villaverde et al., 2024].[3]

The rest of the paper is organized as follows. Section 3.2 describes the data and the classification of countries into blocs. Section 3.3 lays out the quantitative model and results. Section 3.4 concludes. Further details on bloc classification, model solution, and alternative exercises are collected in the appendix.

[3]Yang and Liu [2024] study the evolution of international power arising through trade relationships and find countries build up power in anticipation of future disputes. However they do not relate their measures of power to eventual formation of geopolitical blocs.

3.2 Data, Basic Facts, and Bloc Classification

3.2.1 Data

The analysis uses data from two main sources. Bilateral trade flows up to 2023 come from the IMF's Direction of Trade Statistics (DOTS). This dataset has the advantage of being quite up to date, with 2023 already available. This is important as some of the most significant fragmentation events, such as the 2022 invasion of Ukraine, are quite recent. In addition, it covers 187 countries. We supplement the bilateral data with nominal GDP data from the IMF World Economic Outlook. Model quantification requires more detailed data on production and input use. The quantitative model and the counterfactual exercises use the OECD's Inter-Country Input-Output (ICIO) tables to calibrate input shares. The sample is thus reduced to 66 countries, listed in Appendix Table C.1. Our model implementation employs an aggregation to 22 sectors, listed in Appendix Table C.2. We use the 2015 as the initial (pre-shock) period when applying the estimated trade cost changes to the world economy.

3.2.2 Bloc Classification

To classify countries into blocs, we start from the standard gravity equation, log-differenced between 2015 and 2023:

$$\Delta \ln X_{mn} = \delta_m + \delta_n + w_{mn}, \tag{3.1}$$

where $\Delta \ln X_{mn}$ is the log change in exports from country m to country n, δ_m and δ_n are importer and exporter fixed effects, and w_{mn} is the residual. The fixed effects δ_m and δ_n capture the changes in exporter and importer multilateral resistance terms. These absorb all the country-specific demand and supply shocks, changes in price indices, and any changes in trade barriers that occur at the importer or exporter (rather than bilateral pair) level. The residual then reflects the change in all bilateral trade barriers – observed and unobserved – between country m and country n, up to the trade elasticity. See, among many others, Anderson and van Wincoop [2003], Head and Ries [2001], Anderson and van Wincoop [2004], or Head and Mayer [2015] for this type of structural interpretation of the gravity estimates, which is standard in the literature. We choose 2015 as the initial year, as the Brexit vote and the election of Donald Trump in 2016 were the first major events of the decoupling era. We end in 2023 as the Russian invasion of Ukraine happened in 2022. The appendix reports results for 2016-2023, since the first US-China trade war tariffs went into force in 2017.

Having recovered the estimated residual $\hat{w}_{mn}$ from estimating (3.1), we transform it into the change in bilateral trade costs by applying the trade elasticity $1-\gamma$: $\Delta \ln \tau_{mn} = \hat{w}_{mn}/(1-\gamma)$. This step is also standard, see e.g. Head and Mayer [2015]. As these data do not include domestic

Table 3.2: Log Change in Average Trade Cost between Blocs (187 countries, 2015-2023)

↓ Exporter | Importer →	Bloc USA	Bloc CHN	Unaligned	Overall
Bloc USA	-0.020	0.076	0.006	0.001
Bloc CHN	0.105	-0.043	0.085	0.075
Unaligned	0.013	0.009	0.045	0.025
Overall	0.034	0.031	0.038	0.035

Notes: We classify countries into 3 groups, Bloc USA, Bloc CHN, and Unaligned. Then, all country pairs are classified into 9 group pairs. We report the average $\Delta \ln \tau_{mn}$ for country pairs belonging to each group pair, weighted by bilateral trade flows in 2015. The Overall column is the average $\Delta \ln \tau_{mn}$ of all trade flows from(to) each exporter(importer) group.

trade flows, the residual is interpreted as the change in bilateral trade costs relative to a reference (omitted) country pair, rather than in absolute terms.

Our bloc classification scheme is simple. A country is in the US bloc if its average import and export costs with respect to the US fell, and the trade costs with respect to China rose. A country is in the China bloc if the opposite is true. Formally:

$$n \in l \text{ bloc} \;\text{ if } \frac{1}{2}(\tau_{n,l} + \tau_{l,n}) < 0 \text{ and } \frac{1}{2}(\tau_{n,m} + \tau_{m,n}) > 0; \{l, m\} \in \{\text{USA, China}\}, l \neq m.$$

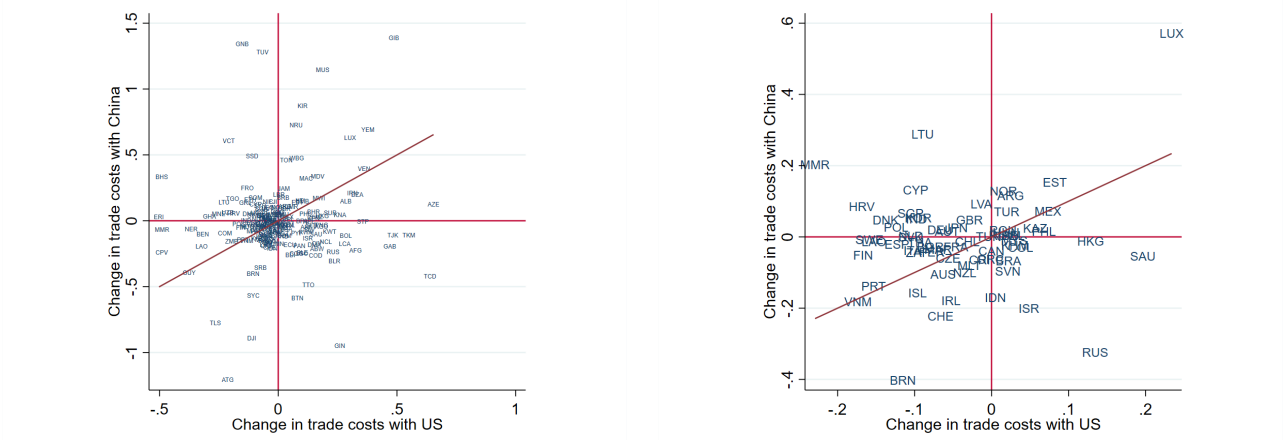
All other countries are unaligned.

Figure 3.2 illustrates this classification scheme. It displays the changes in trade costs with the US on the horizontal axis and with China on the vertical axis. The left panel displays all countries available in the IMF DOTS dataset, and the right panel retains only countries included in the quantitative model implemented below. The countries in the upper left quadrant are the US bloc, and the countries in the lower right quadrant are the China bloc. The countries in the other quadrants either increased their trade costs with both China and the US, or decreased their trade costs with both. Appendix Table C.3 displays the full list of countries in all blocs.

Out of 187 countries, 43 align with the US and 46 with China. The majority of countries (98) remain non-aligned by our metric. Table 3.2 displays the average trade cost changes across blocs. Focusing on countries included in our quantitative model, Russia, Saudi Arabia, Israel and Hong Kong are clearly aligned with China. Countries in the US bloc are predominantly European, but also include India, Korea, Japan, and Singapore.

We next turn to the quantitative assessment of the global real impact of this cross section of trade cost changes. Since the regression above can only identify relative trade cost changes, an important use of the quantitative model will be to discipline the mean level of trade cost changes.

Figure 3.2: Change in Trade Costs with the US and China (2015-2023)



All countries Countries in the quantitative model

Notes: The x-axis refers to the change in trade costs with the US, measured as $d\ln\tau_n^{USA} = \frac{1}{2}\left(\frac{1}{1-\gamma}\hat{w}_{n,USA} + \frac{1}{1-\gamma}\hat{w}_{USA,n}\right)$, which is recovered from equation (3.1). Similarly, the y-axis refers to the change in trade costs with China, measured as $d\ln\tau_n^{CHN} = \frac{1}{2}\left(\frac{1}{1-\gamma}\hat{w}_{n,CHN} + \frac{1}{1-\gamma}\hat{w}_{CHN,n}\right)$. The left panel displays all countries for which trade data is available until 2023. The right panel displays the countries included in our quantitative model.

3.3 Quantitative Framework

We implement the multi-country multi-sector global production network model of Huo et al. [2025], Bonadio et al. [2021], and Bonadio et al. [2023a]. This framework enables us to quantify changes in GDP and real income resulting from the observed changes in trade costs for all countries in general equilibrium.

3.3.1 Setup

Preliminaries Let there be N countries indexed by n, m, and ℓ, and J sectors indexed by j, i, and k. Each country n is populated by households that consume the final good available in country n and supply labor to firms.

Households There is a continuum of households indexed by ω, that maximize

$$\max_{\mathcal{F}_n(\omega), H_n(\omega)} \left(\mathcal{F}_n(\omega) - \chi_n \frac{H_n(\omega)^{1+1/\psi}}{1+1/\psi} \right) \tag{3.2}$$

subject to

$$P_n \mathcal{F}_n = W_n(\omega) H_n(\omega)$$

where $\mathcal{F}_n(\omega)$ is consumption of final goods, P_n is its price index, and $H_n(\omega)$ is the supply of hours worked, receiving a wage $W_n(\omega)$. Each household can supply labor to any sector j with household-specific productivity $b_{nj}(\omega)$. If household ω decides to work in sector j, it supplies $b_{nj}(\omega) H_n(\omega)$ effective units of labor and collects the labor income of $W_n(\omega) H_n(\omega) = W_{nj} b_{nj}(\omega) H_n(\omega)$, where W_{nj} is the equilibrium price of one efficiency unit of labor in that country-sector. The household idiosyncratic labor productivity in sector j is distributed $b_{nj}(\omega) \sim$ Fréchet(ξ_{nj}, μ), with dispersion parameter μ and central tendency parameter ξ_{nj} that can potentially vary by country and sector. With some manipulation [see Bonadio et al., 2023b], labor supply to sector j can be written as:

$$H_{nj} = \xi_{nj} \left(\frac{1}{\chi_n} \frac{W_n}{P_n} \right)^{\psi} \left(\frac{W_{nj}}{W_n} \right)^{\mu - 1}, \tag{3.3}$$

up to a normalization constant and under the regularity condition that $\mu > \psi + 1$, and where $W_n \equiv (\sum_i \xi_{ni} W_{ni}^{\mu})^{\frac{1}{\mu}}$ is an economy-wide wage index. Aggregate labor supply is:

$$H_n = \left(\frac{W_n}{P_n \chi_n} \right)^{\psi} \tag{3.4}$$

up to a normalization constant. Aggregate labor supply thus coincides with the GHH utility formulation [Greenwood et al., 1988], and is governed by the Frisch elasticity ψ. At the same time, conditional on the aggregate labor supply, labor supply to an individual sector is isoelastic with elasticity $\mu - 1$ in that sector's relative wage, as in the "Roy-Fréchet" formulation [e.g. Lagakos and Waugh, 2013, Hsieh et al., 2019, Galle et al., 2023].

Final consumption $\mathcal{F}_{nt}$ is a CES aggregate of sectoral consumption bundles:

$$\mathcal{F}_n = \left[\sum_j \zeta_{nj}^{\frac{1}{\rho}} \mathcal{F}_{nj}^{\frac{\rho - 1}{\rho}} \right]^{\frac{\rho}{\rho - 1}}, \qquad P_n = \left[\sum_j \zeta_{nj} \left(P_{nj}^f \right)^{1 - \rho} \right]^{\frac{1}{1 - \rho}},$$

where $\mathcal{F}_{nj}$ is the sector j quantity consumed, and P_{nj}^f is its price. Trade is subject to iceberg costs τ_{mnj}^f to ship final good j from country m to country n (throughout, we adopt the convention that the first subscript denotes source, and the second destination). Sector j bundle is an Armington

aggregate of goods coming from different countries:

$$\mathcal{F}_{nj} = \left[\sum_m \mu_{mnj}^{\frac{1}{\gamma}} \mathcal{F}_{mnj}^{\frac{\gamma-1}{\gamma}}\right]^{\frac{\gamma}{\gamma-1}}, \qquad P_{nj}^f = \left[\sum_m \mu_{mnj} (\tau_{mnj}^f P_{mj})^{1-\gamma}\right]^{\frac{1}{1-\gamma}},$$

where $\mathcal{F}_{mnj}$ is the final consumption by country n of sector j goods imported from country m, and γ controls the substitution elasticity between different origin-sector goods within a category. The P_{mj}'s are the prices of sector j country m's product "at the factory gate" in the origin country. No arbitrage in shipping implies that the price faced by the consumer in n is P_{mj} times the iceberg cost τ_{mnj}^f.

The share of sector j composite in total final expenditure π_{nj}^f, and the share of the good from country m in total sector j final expenditure π_{mnj}^f are given by

$$\pi_{nj}^f = \frac{\zeta_{nj}\left(P_{nj}^f\right)^{1-\rho}}{\sum_k \zeta_{nk}\left(P_{nk}^f\right)^{1-\rho}} \qquad \pi_{mnj}^f = \frac{\mu_{mnj}\left(\tau_{mnj}^f P_{mj}\right)^{1-\gamma}}{\sum_\ell \mu_{\ell nj}\left(\tau_{\ell nj}^f P_{\ell jt}\right)^{1-\gamma}}.$$

Firms A representative firm in sector j in country n operates a CRS production function

$$Y_{nj} = Z_{nj} H_{nj}^{\eta_j} X_{nj}^{1-\eta_j}, \tag{3.5}$$

where the total factor productivity is denoted by Z_{nj}, and the intermediate input usage X_{nj} is an aggregate of sectoral inputs:

$$X_{nj} \equiv \left(\sum_i \vartheta_{i,nj}^{\frac{1}{\varepsilon}} X_{i,nj}^{\frac{\varepsilon-1}{\varepsilon}}\right)^{\frac{\varepsilon}{\varepsilon-1}}.$$

Because it is the only primary factor of production, H_{nj} should be interpreted as "equipped labor" that encompasses all primary factor services [Alvarez and Lucas, 2007]. The total use of sector i inputs in sector j in country n is an Armington aggregate across different source countries:

$$X_{i,nj} \equiv \left(\sum_m \mu_{mi,nj}^{\frac{1}{\nu}} X_{mi,nj}^{\frac{\nu-1}{\nu}}\right)^{\frac{\nu}{\nu-1}} \qquad P_{i,nj}^X = \left(\sum_m \mu_{mi,nj}\left(\tau_{mi,nj}^x P_{mi}\right)^{1-\nu}\right)^{\frac{1}{1-\nu}},$$

where $X_{mi,nj}$ is the usage of inputs coming from sector i in country m in production of sector j in country n, $\mu_{mi,nj}$ is a taste shifter, and $P_{i,njt}^X$ is the price index of sector i inputs in production of sector j in country n. We allow the iceberg trade cost for intermediate inputs $\tau_{mi,nj}^x$ to generically differ from the iceberg trade cost for final goods τ_{mni}^f.

Let $\pi_{i,nj}^x$ be the share of sector i in total intermediate expenditure by (n,j), and $\pi_{mi,nj}^x$ be the

share of intermediates from country m in total intermediate spending on sector i by (n, j):

$$\pi^x_{i,nj} = \frac{\vartheta_{i,nj}\left(P^X_{i,nj}\right)^{1-\varepsilon}}{\sum_k \vartheta_{k,nj}\left(P^X_{k,nj}\right)^{1-\varepsilon}} \qquad \pi^x_{mi,nj} = \frac{\mu_{mi,nj}\left(\tau^x_{mi,nj}P_{mi}\right)^{1-\nu}}{\sum_\ell \mu_{\ell i,nj}\left(\tau^x_{\ell i,nj}P_{\ell it}\right)^{1-\nu}}.$$

To summarize, both final use and intermediate input bundles have two nests, governed by different elasticities. The upper nest combines broad sectors, such as textiles and apparel, machinery, or retail trade. The lower nest is an Armington aggregate of items coming from different source countries.

Firms are competitive and price at marginal cost. Cost minimization implies that the payments to primary factors and intermediate inputs are:

$$W_{nj}H_{nj} = \eta_j P_{nj}Y_{nj} \tag{3.6}$$

$$P_{mi,nj}X_{mi,nj} = \pi^x_{i,nj}\pi^x_{mi,nj}\left(1-\eta_j\right)P_{nj}Y_{nj}. \tag{3.7}$$

Equilibrium An equilibrium in this economy is a set of goods and factor prices $\{P_{nj}, W_{nj}\}$, factor allocations $\{H_{nj}\}$, and goods allocations $\{Y_{nj}\}$, $\{\mathcal{F}_{mnj}, X_{mi,nj}\}$ for all countries and sectors such that (i) households maximize utility; (ii) firms maximize profits; and (iii) all markets clear.

At the sectoral level, the following market clearing condition has to hold for each country n sector j:

$$P_{nj}Y_{nj} = \sum_m P_m\mathcal{F}_m\pi^f_{mj}\pi^f_{nmj} + \sum_m\sum_i (1-\eta_i)P_{mi}Y_{mi}\pi^x_{j,mi}\pi^x_{nj,mi}. \tag{3.8}$$

Meanwhile, trade balance implies that each country's final expenditure equals the sum of value added across domestic sectors:

$$P_m\mathcal{F}_m = \sum_i \eta_i P_{mi}Y_{mi}. \tag{3.9}$$

Our simulations shock the world economy with changes in iceberg trade costs and compute changes relative to the pre-shock equilibrium. We report results for two aggregate outcomes: real GDP and real income. The real GDP change in any country n following a vector of trade cost shocks is to first order given by

$$d\ln G_n = \sum_{j=1}^{J} \eta_j \frac{P_{nj,0}Y_{nj,0}}{G_{n,0}} d\ln H_{nj}, \tag{3.10}$$

where the items subscripted by a "0" denote the steady state/pre-shock values. This expression for the real GDP follows from the systems of national accounts definition of real GDP as output

Table 3.3: Parameter Values

Param.	Value	Source	Related to
ρ	1		final cross-sector substitution elasticity
ε	1		intermediate cross-sector subst. elasticity
γ	4	Broda and Weinstein [2006]	trade elasticity in final consumption
ν	4	Broda and Weinstein [2006]	trade elasticity in intermediate inputs
ψ	1	Chetty et al. [2011]	Frisch elasticity of labor supply
μ	1.5	Galle et al. [2023]	Sectoral labor supply elasticity
η_j		ICIO	value added share in gross output
π^f_{njt},$\pi^x_{i,njt}$		ICIO	sectoral consumption and intermediate shares
π^f_{mnjt},$\pi^x_{mi,njt}$		ICIO	final and intermediate trade shares

Notes: This table summarizes the parameters and data targets used in the quantitative model and their sources.

evaluated at base prices minus inputs evaluated at base prices [Bonadio et al., 2023b, Huo et al., 2025]. The advantage of real GDP is that it is a familiar object that is tracked by national accounts. The disadvantage is that because it keeps prices at their pre-shock values, it does not take into account the fact that changes in trade costs affect import prices, which are in the consumption price index. Thus, we will also report results for the real income, defined as W_n/P_n (and also referred to as real wage).

Equilibrium in changes We use exact-hat algebra to solve the model in changes. We denote gross proportional changes from an initial equilibrium using "hat" variables: $\hat{X} = \frac{X'}{X}$, where X is the initial equilibrium value and X' is the new equilibrium value. For a given change in trade costs $\hat{\tau}^x_{mi,nj}$ and $\hat{\tau}^f_{mnj}$, we can solve for the change in all endogenous variables according to the formulas derived in Appendix C.2.

3.3.2 Calibration

Table 3.3 summarizes the parameters we use. We set the substitution elasticities between sectors in final consumption (ρ) and intermediate use (ε) to 1. For the Armington elasticities of substitution between goods coming from different source countries in the final (γ) and intermediate (ν) bundles, we adopt a conventional value of 4 [e.g. Broda and Weinstein, 2006]. The Frisch labor supply elasticity is set to 1 following the business cycle literature [Chetty et al., 2011], and the parameter μ which governs the sectoral labor supply elasticity μ is set to 1.5 following Galle et al. [2023]. Production function parameters and final/input shares are taken directly from the data.

3.3.3 Baseline Trade Cost Change Scenario

As mentioned above, the gravity estimation only identifies the relative trade cost changes. To pin down the absolute changes, we use the model to target the data on the world trade to GDP ratio. Specifically, we start from the 2015 equilibrium and shock it with the following trade cost changes for all exporting manufacturing sectors i:

$$\hat{\tau}^x_{mi,nj} = \hat{\tau}^f_{mni} = \exp\left(\Delta \ln \tau_{mn} + \Delta \ln \tau^{base}\right) \qquad \forall m \neq n, \tag{3.11}$$

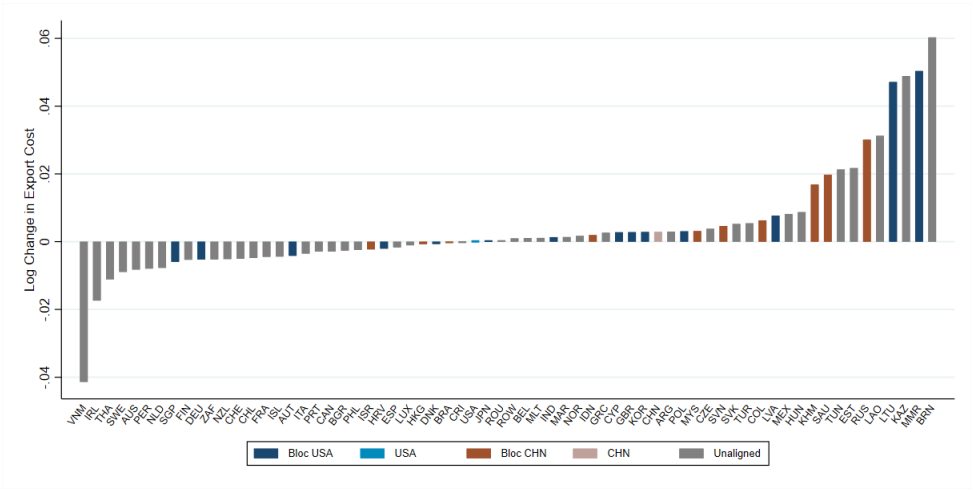
where $\Delta \ln \tau_{mn}$ are the bilateral (relative) trade costs backed out in Section 3.2.2, and $\Delta \ln \tau^{base}$ is a trade cost shifter common to all country pairs. We search for a $\Delta \ln \tau^{base}$ such that the change in the world trade to GDP ratio in the model matches the change in the data from 21.8% in 2015 to 22.6% in 2023, a 0.8 percentage point increase.

We find a $\Delta \ln \tau^{base} = -0.003$, implying that if anything, on average trade costs decreased by 0.3%.[4] Figure 3.3 displays the trade-weighted import and export trade cost changes for each country. Table 3.4 shows the average trade cost changes across blocs, inclusive of the calibrated $\Delta \ln \tau^{base}$, as well as the overall trade cost changes for each bloc pair. As expected, trade costs between the US and China bloc have increased. Trade costs from the China bloc to the US bloc increased by 11.7%, and in the opposite direction they rose by 4.3%. However, these increases are counteracted by reductions in within-bloc trade costs, as well as in import trade costs from the unaligned countries. Only the China bloc experiences an overall increase in export costs, and none of the blocs see significant increases in overall import costs. Hence, the more structural approach confirms the picture emerging from the raw data in Table 3.1 in the Introduction: while fragmentation has happened, overall trade costs have not increased. Appendix Table C.4 presents the classification of the countries in the model into blocs. This classification is done based on the calibrated absolute changes in trade costs $\hat{\tau}^f_{mni}/\hat{\tau}^x_{mi,nj}$ in (3.11), rather than the relative ones in Section 3.2. According to the classification, 14 countries are in the US bloc and 10 in the China bloc (beyond the US and China themselves).

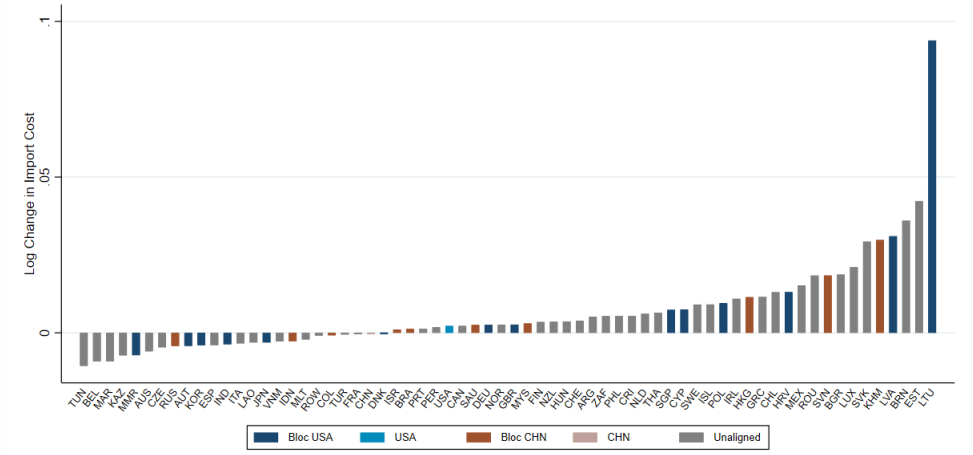
Figure 3.4 illustrates the changes in real GDP and real incomes for each country in the model factual. Table 3.5 displays summary statistics of the changes in real GDP and incomes. While there is quite a bit of heterogeneity, the median country actually sees a 0.6% gain, and three-quarters of the countries experience an increase in both real GDP and real incomes, with the median changes positive in all blocs. The US and China themselves see changes close to zero. Neither countries

[4] While the model can accommodate standard shocks such as productivity or demand, we abstract from shocks that are not changes to trade costs in this exercise. Additional shocks would help match the evolution of GDP in each country. We discipline the average ("base") trade cost change using the differential change in trade relative to GDP worldwide. World GDP growth and its level are not pinned down by this exercise. While we refer to the base change as a change in average trade costs, these incorporate average changes in preferences for foreign goods as well.

Figure 3.3: Baseline Change in Trade Costs (2015-2023)



(a) Export costs



(b) Import costs

Notes: The top and bottom panels show the log change in export and import costs implied by the model factual, respectively. The changes in trade costs are measured as the trade-weighted mean change in trade cost across all sectors.

in the US bloc nor countries in the China bloc see uniform gains or losses. Even at the 25th percentiles, only in the China bloc the changes are negative. Recall that this scenario mutes any productivity or demand shocks. The equilibrium changes in GDP predicted here are entirely due to the observed trade cost changes in the data during the decoupling period. The factual suggests that, given the observed pattern of trade cost changes and taking into account the general equilibrium effects such as substitution towards partners facing lower trade costs, most countries' output and real incomes increased during this period.

The modest positive average effects are accompanied by large heterogeneity in GDP and income

Table 3.4: Log Change in Average Trade Costs between Blocs (2015-2023)

↓ Exporter | Importer →	Bloc USA	Bloc CHN	Unaligned	Overall
Bloc USA	-0.043	0.043	0.007	0.000
Bloc CHN	0.117	-0.069	0.027	0.053
Unaligned	-0.030	-0.032	-0.005	-0.021
Overall	0.005	-0.009	0.007	0.003

Notes: We classify countries into 3 groups, Bloc USA, Bloc CHN, and Unaligned. Then, all country pairs are classified into 9 group pairs. We report the average $\Delta \ln \tau_{mn} + \Delta \ln \tau^{base}$ for country pairs belonging to each group pair, weighted by bilateral trade flows in 2015. The Overall column/row is the average $\Delta \ln \tau_{mn} + \Delta \ln \tau^{base}$ of all trade flows from(to) each exporter(importer) group.

Table 3.5: Baseline Change in Real GDP and Real Income, Percentage Points (2015-2023)

Bloc	Real GDP			Real Income		
	Median	p25	p75	Median	p25	p75
Overall	0.588	0.061	1.297	0.619	0.059	1.322
Bloc USA	0.532	0.125	0.712	0.536	0.147	0.699
Bloc CHN	0.299	-0.263	0.773	0.372	-0.261	0.780
Unaligned	0.787	0.034	1.397	0.755	0.066	1.432

Notes: Baseline change in GDP and real income are reported in percentage points.

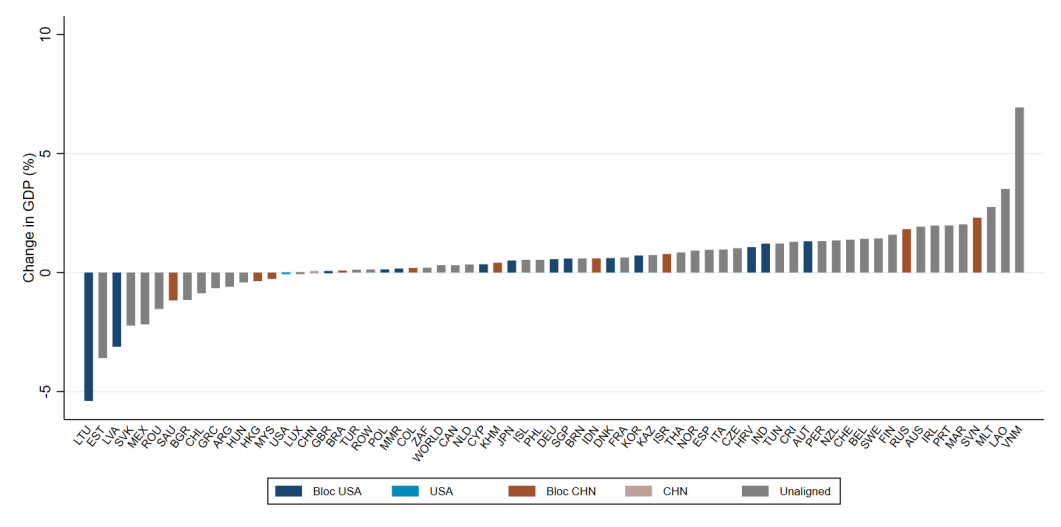
impacts across countries. At the top, Vietnam and Laos strongly benefit, gaining 6.9% and 3.5%, respectively. Vietnam and Laos experienced trade cost declines with both the US and China. While our classification considers Vietnam and Laos unaligned, the quantification shows large increases in bilateral trade with these countries, and increases in their GDP and real incomes. This is consistent with the anecdotal accounts of supply chains shifting away from China and towards countries like Vietnam.[5] At the opposite extreme are the Baltic countries, whose close trade links with Russia unraveled, without a compensating decrease in trade costs elsewhere. As a result, these countries experienced losses of 3-5%.

3.3.4 Counterfactuals

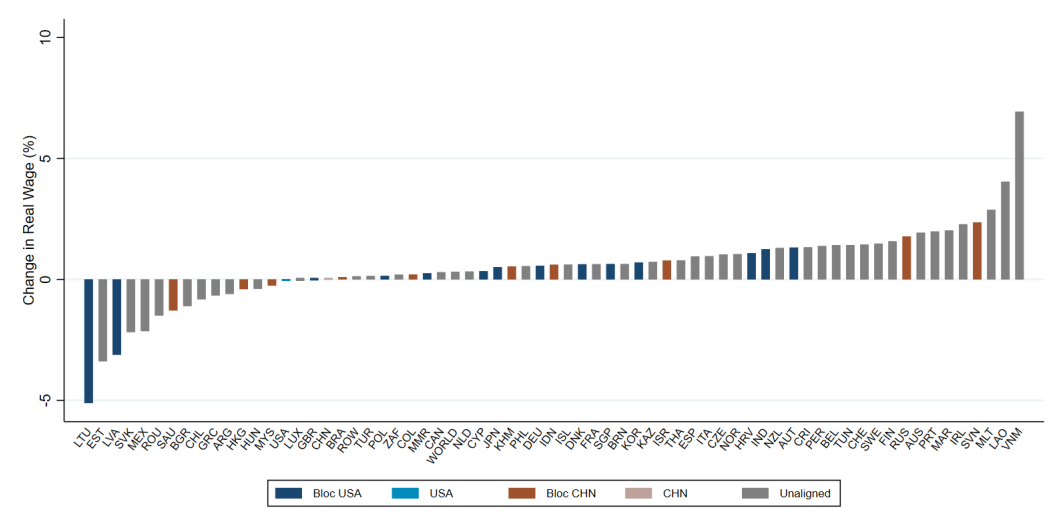
According to the factual simulation above, most countries are actually better off in the fragmented world, as trade costs decreases within blocs more than offset trade cost increases across blocs. A natural question is whether countries sort into blocs according to benefits arising from international

[5]See for example "Vietnam is emerging as a winner from the era of deglobalisation", The Economist, Sept. 22, 2022.

Figure 3.4: Baseline Change in Real GDP and Real Income (2015-2023)



(a) Real GDP



(b) Real Income

Notes: The top panel shows the change in GDP, in percentage points, implied by the model baseline change in trade costs. The bottom panel shows the change in real income implied by the model baseline change in trade costs.

trade. To answer this question, we perform counterfactual exercises in which we move countries to different blocs and compare their real outcomes to the baseline.

Specifically, we first construct the average import and export trade cost change between each country and a given bloc. For each country m and bloc l, we compute the average export cost

change from the bloc to country m:

$$d\ln\tau_{l,m} = \frac{1}{N_l}\sum_{n\in l} d\ln\tau_{n,m}$$

and the average import cost change from m to the bloc:

$$d\ln\tau_{m,l} = \frac{1}{N_l}\sum_{n\in l} d\ln\tau_{m,n}.$$

Thus, $d\ln\tau_{l,m}$ and $d\ln\tau_{m,l}$ are the average export and import trade cost changes for countries in bloc $= l$ with respect to country m.

Then, we move each country n to a particular bloc by replacing its factual trade cost changes with the averages for that bloc for every potential partner m. However, country n's factual average change in trade costs might differ from the bloc-level average. To avoid this type of mechanical level effect, we renormalize the country's counterfactual trade cost changes such that their trade-weighted average change is equal to the factual. Specifically, for each country n moving to bloc l, we compute an adjustment factors $d\ln\tau^{adj,l}_{n,imports}$ and $d\ln\tau^{adj,l}_{n,exports}$ such that:

$$\underbrace{\sum_{m,i,j,u=\{f,x\}}\frac{IM^u_{mi,nj}}{IM_n}d\ln\tau_{mi,nj}}_{\text{actual}} = \underbrace{d\ln\tau^{adj,l}_{n,imports}}_{\text{adjustment factor}} + \underbrace{\sum_{m,i,j,u=\{f,x\}}\frac{IM^u_{mi,nj}}{IM_n}d\ln\tau_{m,l}}_{\text{counterfactual: moving to bloc}},$$

and

$$\underbrace{\sum_{m,i,j,u=\{f,x\}}\frac{EX^u_{nj,mi}}{EX_n}d\ln\tau_{nj,mi}}_{\text{actual}} = \underbrace{d\ln\tau^{adj,l}_{n,exports}}_{\text{adjustment factor}} + \underbrace{\sum_{m,i,j,u=\{f,x\}}\frac{EX^u_{nj,mi}}{EX_n}d\ln\tau_{l,m}}_{\text{counterfactual: moving to bloc}},$$

where $IM^u_{mi,nj}$ is imports of category $u\in\{f,x\}$ from country sector mi to sector j in n, IM_n are n's total imports, and similarly for exports $EX^u_{mi,nj}$ and EX_n. We then construct the counterfactual trade cost changes when putting country n into bloc l as:

$$d\ln\tau^{CF:l}_{m,n} = d\ln\tau_{m,l} + d\ln\tau^{adj,l}_{n,imports}$$

$$d\ln\tau^{CF:l}_{n,m} = d\ln\tau_{l,m} + d\ln\tau^{adj,l}_{n,exports}.$$

This counterfactual answers the question, what is the effect of rearranging the country's trade costs such that it looks like bloc l, while keeping its average trade cost change the same? While there are many permutations of groups of countries that could be subjected to this counterfactual, we perform it one country at a time, keeping the trade cost changes for all other countries at their

factual values.

Since each country is in exactly one bloc in the factual, for each country there are 2 possible moves, into one of the other 2 blocs. Thus, for each unaligned country the counterfactuals put it into the US and China blocs. For countries already in the US or China bloc, the counterfactuals put it into the other bloc or into the unaligned group.

Figure 3.5 displays the results for real GDP, while Appendix Figure C.1 displays the results for real income. Table 3.6 reports the summary statistics of the counterfactuals by bloc. The top panel of the figure and the table shows the change compared to the factual when moving countries to the US bloc. Countries in the China bloc are marked in brown. Six out of ten China bloc countries would actually benefit from switching to the US bloc, with the median real income benefit of 0.66%. The unaligned countries would on average lose from moving to the US bloc, through there is wide heterogeneity of effects ranging from positive to negative.

The middle panel shows the results of moving countries not aligned with China to the China bloc. Countries in the US bloc would on average benefit from moving to the China bloc, with eight out of fourteen of the US bloc countries gaining from moving to the China bloc, with the median US bloc country gaining 0.2% from the move. Once again in both the US bloc and unaligned groups, the benefits range from positive to negative. The bottom panel shows the results of moving the aligned countries to the non-aligned bloc. While on average moving countries from the US and China blocs to unaligned reduces real GDP and income, a few countries such as Saudi Arabia, Latvia, and Lithuania would see GDP increases of over 2% by becoming unaligned. Figure C.1 in the Appendix displays the counterfactual changes in real incomes with similar results.

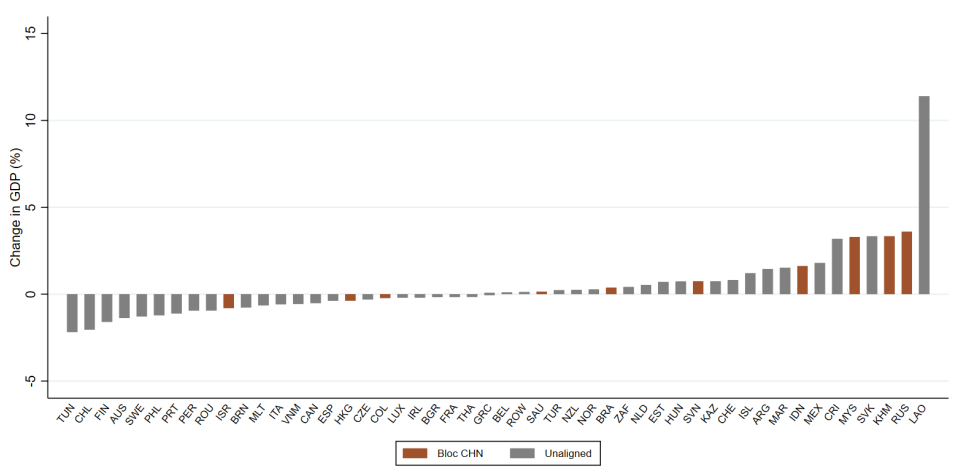
Overall, it appears that on average countries in the US and China blocs are in the "wrong" bloc. At the same time, countries in these blocs would also on average lose from becoming unaligned. The averages hide complete variation from negative to positive within each possible category of move.

3.3.5 Robustness and Sensitivity

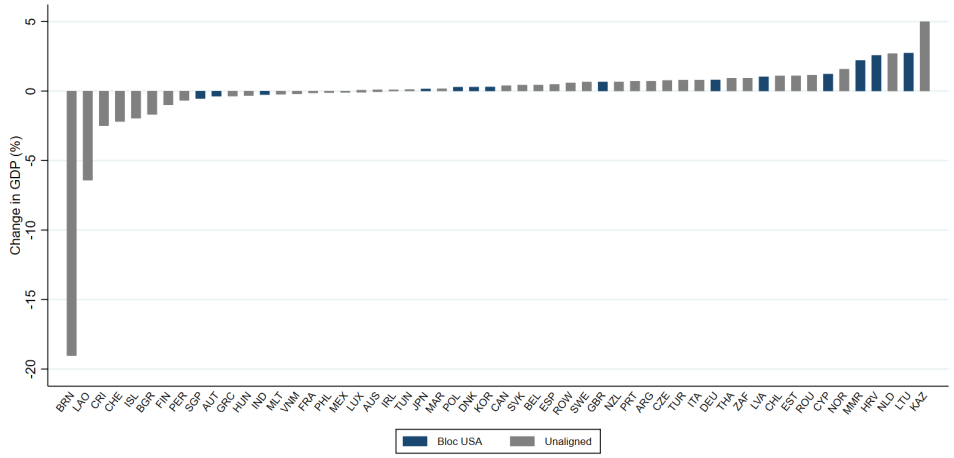
We now perform several sensitivity checks on the bloc assignment and the inferred trade cost changes.

Observable trade costs: tariffs Since the absolute level of trade cost changes is pinned down by our model matching the overall trade to GDP ratio change, one might worry that the outcome is model-dependent. Appendix Figure C.2 provides support for our finding that some trade costs rose and some fell by using the component of trade costs directly observable in the data: tariffs. The most recent tariff data are for 2021, so we document the tariff changes between 2015 and 2021.

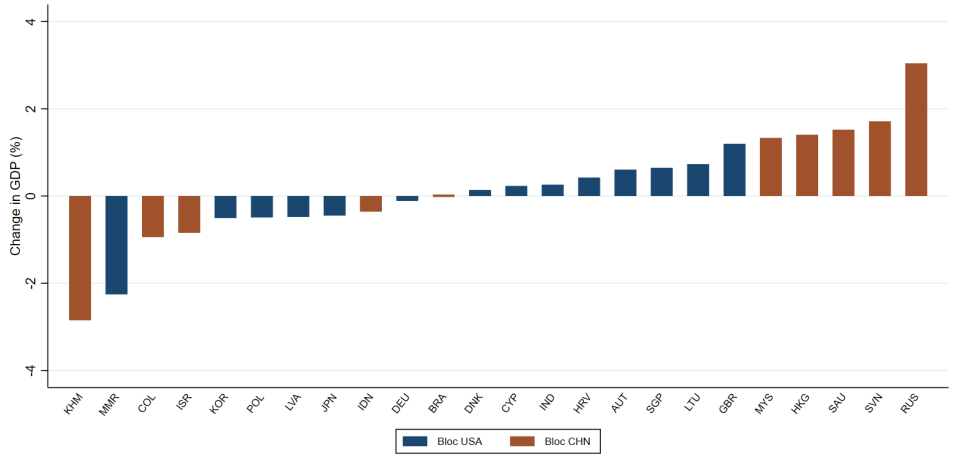
Figure 3.5: Counterfactual Real GDP Changes (2015-2023)



(a) Moving to USA bloc



(b) Moving to China bloc



(c) Moving to unaligned bloc

Notes: Each bar in each plot shows the percentage change in GDP for each country, relative to factual, when the country is moved to different bloc.

Table 3.6: Counterfactual GDP and Real Income, Percentage Points (2015-2023)

Counterfactual	Bloc	Real GDP			Real Income		
		Median	p25	p75	Median	p25	p75
Moving to Bloc USA	Overall	-0.445	-1.534	0.969	-0.448	-1.512	0.945
	Bloc USA	-	-	-	-	-	-
	Bloc CHN	0.658	-0.411	1.796	0.661	-0.410	1.906
	Unaligned	-0.710	-1.638	0.618	-0.762	-1.636	0.589
Moving to Bloc CHN	Overall	-0.269	-1.465	0.740	-0.289	-1.430	0.717
	Bloc USA	0.211	-0.405	1.527	0.238	-0.369	1.612
	Bloc CHN	-	-	-	-	-	-
	Unaligned	-0.501	-1.856	0.676	-0.476	-1.951	0.606
Moving to Unaligned	Overall	-0.593	-0.944	1.203	-0.589	-0.967	1.253
	Bloc USA	-0.622	-0.943	0.065	-0.629	-0.940	0.020
	Bloc CHN	-0.324	-1.131	1.589	-0.328	-1.138	1.581
	Unaligned	-	-	-	-	-	-

Notes: Counterfactual change in GDP and real income, relative to baseline, are reported in percentage points.

The source of the tariff data is UN-TRAINS. The left panel plots the histogram of the applied tariff changes. Because MFN tariff changes are measured with less error [Teti, 2024], the right panel also reports the histogram of MFN tariff changes only. While there is large dispersion in the effectively applied tariff changes, the average change is close to 0, and 39.5% of bilateral pairs experience tariff decreases.

Bloc assignments We next use an alternative methodology to assign countries to blocs, based on the Leiden algorithm [Traag et al., 2019]. The Leiden algorithm is a machine learning method designed to detect non-overlapping communities in large networks. We feed in the same residualized trade growth between 2015 and 2023 as in our baseline classification, but use the Leiden algorithm to classify the countries in blocs. The algorithm contains a random component, so we perform many draws and assign countries to blocs based on the percentage of times they are classified in the same community as the US or China. Appendix C.3.1 presents the details of the procedure. Table C.5 summarizes the overlap between our baseline and the Leiden algorithm approach. Overall, our baseline procedure is more conservative in that it classifies more countries as unaligned. However, the two methods agree more than 70% of the time when both assign the country to either the US or China bloc.

Alternative start year Our baseline uses 2015 as the pre-period, since it is the year before the Brexit referendum and the Donald Trump election. In the Appendix, we instead use 2016 as a

start date, since the tariffs in US-China trade war first increased in 2017. Tables C.6 and C.7 show that the bloc assignment in that case is similar to our baseline. While some countries move to being unaligned, no country in our quantitative model sample is classified in the opposite bloc to the baseline results. Tables C.8 and C.9 display summary statistics of the changes in trade costs and GDP respectively. The results are qualitatively the same as our baseline scenario: while trade costs across blocs are increasing, they are compensated by decreases within bloc and to/from the unaligned bloc.

Placebo period We conduct a placebo exercise, where we repeat our procedure with data from before the US-China trade tensions, between 2002 and 2007. In that case, we find no evidence of fragmentation. Table C.10 displays the bloc assignment compared to our baseline 2015-23 classification. Only 3 countries are assigned to the China bloc, including China. More countries are unaligned than in our baseline (70% instead of 60% in our baseline). Table C.11 displays the change in trade costs across bloc pairs between 2002 and 2007. Most bloc pairs, including China bloc to US bloc, experience trade cost declines.

We also compute the changes in trade costs between 2002 and 2007, for the blocs identified in our baseline using 2015-23 trade data. Table C.12 reports the average 2002-2007 trade cost changes across the 2015-23 bloc pairs. Contrary to the 2015-23 trade cost changes, we find no evidence of fragmentation: all cross-bloc pairs experience trade cost decreases, in the same order of magnitude as the within bloc pairs.

Fit of trade costs Our procedure matches the global trade to GDP ratio to pin down the level of trade cost changes. The reason is that domestic absorption data are not available for 2023, which prevents us from identifying trade costs levels following the Head and Ries [2001, henceforth HR] method. To provide evidence that our trade/GDP-targeting procedure is reliable, we implement our procedure on years where domestic absorption data are available, which allows us to compare our method to HR. We use 8-year windows starting from 2000 until 2010. On average, our procedure and the HR method produce similar trade cost changes: the difference between our approach and the HR method is -0.9% at the mean (-0.03% at the median), and the correlation is 0.79. Appendix C.3.4 details the exercise.

3.3.6 Determinants of Trade Changes

The counterfactual results from Section 3.3.4 imply that some countries do not necessarily sort into their economically optimal bloc. In this section, we investigate potential drivers of changes in trade patterns after 2015.

Table 3.7: Explanatory Variables for Trade Flow Changes

	2015 to 2023	Placebo 2010 to 2015
UN vote agreement	0.672***	0.184
	(0.197)	(0.186)
Log initial flows	-0.423***	-0.354***
	(0.0294)	(0.0435)
Log 2000 flows	0.148***	0.0957***
	(0.0212)	(0.0313)
Log distance	-0.288***	-0.291***
	(0.0563)	(0.0428)
Observations	3674	3674
Importer FE	✓	✓
Exporter FE	✓	✓

Notes: Vote agreement measures the likelihood of agreement between country pairs in the UN voting at the initial year (2015 in the first column, 2010 in the second column). Log initial trade flows is the log of bilateral trade flow between country pairs at the initial year. Distance comes from CEPII gravity database. The sample includes all country pairs in our quantitative model sample. Standard errors are clustered twoway at the exporter and importer level.

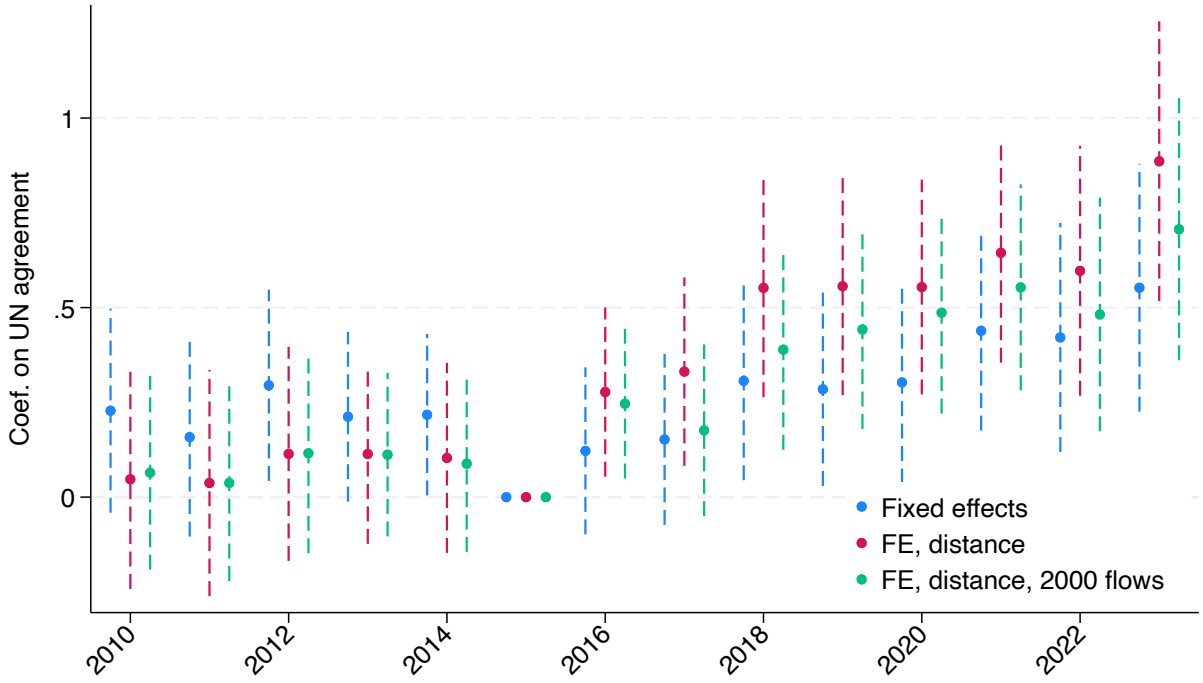
We start by regressing the change in bilateral trade flows between 2015 and 2023 on the United Nations general assembly vote agreement in 2015 [Bailey et al., 2017]. We control for trade flows in 2015, historical trade flows from 2000, and distance. The first column of Table 3.7 displays the results. Country pairs who voted together at the UN assembly in 2015 witnessed a relative increase in bilateral trade flows after 2015. Large flows in 2015 tend to decrease subsequent trade growth, while trade flows from 2000 are positively correlated with the growth of trade post-2015. This indicates that trade grew more for geopolitically close pairs, and patterns moved away from 2015 partners back towards historical 2000 partners. The second column of Table 3.7 reports results of a placebo regression that uses instead the change in trade flows between 2010 and 2015. There, there is no correlation with UN agreement.

To probe this further, we perform an event-study type regression:

$$\ln X_{mn,t} = \eta_{mt} + \gamma_{nt} + \delta_{mn} + \sum_t \beta_t^{UN} UNagree_{mn} + \sum_t X'_{mn}\beta_t^x + \varepsilon_{mnt}. \tag{3.12}$$

We include importer-year and exporter-year fixed effects, as well as bilateral pair fixed effects that

Figure 3.6: Bilateral Trade Flows and Political Alignment: Coefficient on UN Agreement (β_t^{UN})



Notes: The figure displays the estimates of β_t^{UN} from regression 3.12. Each dot color corresponds to different controls. The blue coefficients only include the fixed effects. The red coefficients include time-varying coefficients on distance, and the green coefficients include time-varying coefficients on 2000 bilateral trade flows. The sample covers countries in our quantitative model. Appendix Figure **??** replicates the findings with all available country pairs.

capture any time-invariant trade costs. We then add a year-specific coefficient β_t^{UN} on UN vote agreement, as well as year-specific coefficients on a vector of other controls potentially correlated with vote agreement X_{mn}, such as 2000 trade flows and bilateral distance. The UN vote agreement is measured as the average voting similarity over the UN voting sessions between 2000 and 2022, as computed by Bailey et al. [2017].

Figure 3.6 displays the results of estimating specification (3.12), with the coefficient for 2015 normalized to 0. All specifications indicate that prior to 2015, there is no impact of the UN agreement on trade, relative to the reference year. After 2015, the correlation between UN vote and trade flow starts to increase, getting progressively stronger over time.

Overall, the results suggest that 2015-2017 marked the start of an increase in the role of geopolitical forces in international trade. After 2015, countries increased trade with their pre-2015 allies, at the expense of trade with non-allies.

3.4 Conclusion

The year 2016 ushered an era of significant changes in policies that are weighing on international trade: the Brexit vote, the US-China trade war, the Russian invasion of Ukraine and the resulting severing of trade links between Russia and the West, and the Biden administration's semiconductor export bans, to name a few of the most important ones. A reasonable expectation is that world trade would have decreased over this period. However, at least as of 2023, this has not been the case. Instead, these policies have triggered a reallocation of trade flows across sources and destinations as also argued by a number of recent studies.

To understand how this rewiring of international trade is occurring, this paper adopts a data-driven approach to measure trade cost changes in a large sample of countries and detect which countries are in which blocs. We do find evidence of decoupling: about half the countries in the world appear to have aligned themselves with either the US or China, at the expense of higher trade costs with the other bloc. However, we find that as cross-bloc trade costs went up, within-bloc trade costs fell. On net, the median country in the world, and the median country within each bloc, has slightly *higher* real income as a result of this reconfiguration of the global trade costs. At the same time, we find a modest level of bloc misalignment: the median country in the US bloc would actually be better off in the China bloc, and vice versa. This suggests that considerations other than international trade are dominating bloc alignment, at least so far.

APPENDIX A

Appendix to Chapter 1

A.1 Data Details

Table A.1: List of Fishing Location

EEZ				High Sea	
BGD	FRA	MEX	TWN	Atlantic, Northwest	Indian, Eastern
BRA	GBR	MYS	USA	Atlantic, Northeast	Indian, Antarctic
CAN	IDN	NOR	VNM	Atlantic, Western Central	Pacific, Northwest
CHL	IND	PER	XAF	Atlantic, Eastern Central	Pacific, Northeast
CHN	ITA	PHL	XAM	Atlantic, Southwest	Pacific, Western Central
DEU	JPN	RUS	XAS	Atlantic, Southeast	Pacific, Eastern Central
ESP	KOR	THA	XEU	Atlantic, Antarctic	Pacific, Southwest
		TUR	XOC	Indian, Western	Pacific, Southeast

Notes: This table provides the list of 46 fishing locations in the quantitative model, which consist of 30 EEZs and 16 high seas.

Table A.2: List of Fishery Species

Cods, hakes, haddocks	Shrimps, prawns	Other Demersal and Pelagic fish
Crustaceans and mollusks	Squids, cuttlefishes, octopuses	Other Diadromous fish
Herrings, sardines, anchovies	Tunas, bonitos, billfishes	Other fish not identified
Salmons, trouts, smelts		

Notes: This table provides the list of 10 fishery species in the quantitative model. While the original ISSCAAP classifies the fishery into 51 species, but I aggregate them into 10 larger categories to harmonize with the fishery trade dataset.

Table A.3: List of Countries

Name	Region	Name	Region	Name	Region	Name	Region
Bangladesh	BGD	Comoros	XAF	Puerto Rico	XAM	Estonia	XEU
Brazil	BRA	Lesotho	XAF	Jamaica	XAM	Slovenia	XEU
Canada	CAN	Tanzania	XAF	Nicaragua	XAM	Croatia	XEU
Chile	CHL	Sudan	XAF	Greenland	XAM	Faroe Islands	XEU
China	CHN	Namibia	XAF	Guatemala	XAM	Greece	XEU
Germany	DEU	Madagascar	XAF	Venezuela	XAM	Iceland	XEU
Spain	ESP	Sudan	XAF	Uruguay	XAM	Montenegro	XEU
France	FRA	Gabon	XAF	Bahamas, The	XAM	San Marino	XEU
United Kingdom	GBR	Botswana	XAF	Ecuador	XAM	Romania	XEU
Indonesia	IDN	Benin	XAF	Cuba	XAM	Netherlands	XEU
India	IND	Seychelles	XAF	Costa Rica	XAM	Luxembourg	XEU
Italy	ITA	Angola	XAF	Turks and Caicos Islands	XAM	Slovak Republic	XEU
Japan	JPN	Sierra Leone	XAF	Yemen, Rep.	XAS	Andorra	XEU
Korea, Rep.	KOR	Ethiopia	XAF	West Bank and Gaza	XAS	Austria	XEU
Mexico	MEX	Togo	XAF	Qatar	XAS	Switzerland	XEU
Malaysia	MYS	Djibouti	XAF	Hong Kong	XAS	Ireland	XEU
Norway	NOR	Algeria	XAF	Iran, Islamic Rep.	XAS	Isle of Man	XEU
Peru	PER	Liberia	XAF	Cyprus	XAS	Ukraine	XEU
Philippines	PHL	Mali	XAF	Macao	XAS	Monaco	XEU
Russian Federation	RUS	Mauritius	XAF	Lebanon	XAS	Malta	XEU
Thailand	THA	Zimbabwe	XAF	Georgia	XAS	Lithuania	XEU
Turkey	TUR	Senegal	XAF	Mongolia	XAS	Czech Republic	XEU
Taiwan	TWN	Mauritania	XAF	Maldives	XAS	Poland	XEU
United States	USA	Guinea	XAF	Turkmenistan	XAS	Finland	XEU
Vietnam	VNM	South Africa	XAF	Nepal	XAS	Albania	XEU
Mozambique	XAF	Burkina Faso	XAF	Pakistan	XAS	North Macedonia	XEU
Tunisia	XAF	Guyana	XAM	Oman	XAS	Serbia	XEU
Cabo Verde	XAF	Virgin Islands	XAM	Tajikistan	XAS	Bulgaria	XEU
Chad	XAF	Suriname	XAM	Lao PDR	XAS	Hungary	XEU
Burundi	XAF	Aruba	XAM	Myanmar	XAS	Belgium	XEU
Congo, Dem. Rep.	XAF	Sint Maarten	XAM	Bahrain	XAS	Liechtenstein	XEU
Zambia	XAF	St. Vincent and the Grenadines	XAM	Israel	XAS	Portugal	XEU
Somalia	XAF	Barbados	XAM	Uzbekistan	XAS	Denmark	XEU
Sao Tome and Principe	XAF	Dominican Republic	XAM	Azerbaijan	XAS	Latvia	XEU
Egypt, Arab Rep.	XAF	Honduras	XAM	Kuwait	XAS	Moldova	XEU
Kenya	XAF	Bermuda	XAM	Cambodia	XAS	Marshall Islands	XOC
Rwanda	XAF	Trinidad and Tobago	XAM	Iraq	XAS	American Samoa	XOC
Ghana	XAF	Haiti	XAM	Kyrgyz Republic	XAS	Fiji	XOC
Nigeria	XAF	Bolivia	XAM	United Arab Emirates	XAS	Vanuatu	XOC
Gambia	XAF	Paraguay	XAM	Jordan	XAS	Nauru	XOC
Morocco	XAF	Argentina	XAM	Saudi Arabia	XAS	Northern Mariana Islands	XOC
Cameroon	XAF	Antigua and Barbuda	XAM	Singapore	XAS	Micronesia, Fed. Sts.	XOC
Libya	XAF	Cayman Islands	XAM	Afghanistan	XAS	Palau	XOC
Niger	XAF	Panama	XAM	Sri Lanka	XAS	Kiribati	XOC
Guinea-Bissau	XAF	Dominica	XAM	Armenia	XAS	Papua New Guinea	XOC
Equatorial Guinea	XAF	Grenada	XAM	Kazakhstan	XAS	Tuvalu	XOC
Central African Republic	XAF	Curacao	XAM	Timor-Leste	XAS	Samoa	XOC
South Sudan	XAF	Colombia	XAM	Bhutan	XAS	New Zealand	XOC
Congo, Rep.	XAF	Belize	XAM	Brunei Darussalam	XAS	Guam	XOC
Cote d'Ivoire	XAF	St. Lucia	XAM	Belarus	XEU	Solomon Islands	XOC
Uganda	XAF	El Salvador	XAM	Bosnia and Herzegovina	XEU	Australia	XOC
Eswatini	XAF	St. Kitts and Nevis	XAM	Sweden	XEU	Tonga	XOC
Malawi	XAF						

Notes: This table provides the mapping of individual country ISO (column ISO) to 30 regions (column region) in the quantitative model, which are 25 individual countries and 5 continental aggregates. The regions beginning with "X" refer to the continental aggregates. "XAF" stands for "Rest of Africa", "XAM" stands for "Rest of America", "XAS" stands for "Rest of Asia", "XEU" stands for "Rest of Europe", and "XOC" stands for "Rest of Oceania".

A.2 Additional Tables and Figures

Table A.4: Summary Statistics of Fishery Stock

	Carrying Cap. (mil. tonnes)	Stock (mil. tonnes)		Stock/Cap. (%)		Stock (% chg.)	Stock/Cap. (p.p chg.)
		1980	2018	1980	2018		
Species	(1)	(2)	(3)	(4)	(5)	(6)	(7)
Cods, hakes, haddocks	220.6	111.9	98.0	50.7	44.4	-6.3	-12.4
Crustaceans and mollusks	38.3	28.4	17.8	74.2	46.5	-27.6	-37.3
Herrings, sardines, anchovies	454.3	289.6	179.2	63.8	39.4	-24.3	-38.1
Salmons, trouts, smelts	80.7	59.9	40.1	74.3	49.7	-24.6	-33.1
Shrimps, prawns	18.7	14.3	9.5	76.1	50.5	-25.7	-33.7
Squids, cuttlefishes, octopuses	27.6	22.9	11.1	83.0	40.1	-43.0	-51.7
Tunas, bonitos, billfishes	112.3	83.1	57.7	74.0	51.3	-22.6	-30.6
Other Demersal and Pelagic fish	551.0	301.3	272.0	54.7	49.4	-5.3	-9.7
Other Diadromous fish	91.7	38.4	37.8	41.9	41.2	-0.7	-1.6
Other fish not identified	218.4	118.8	115.9	54.4	53.0	-1.3	-2.5

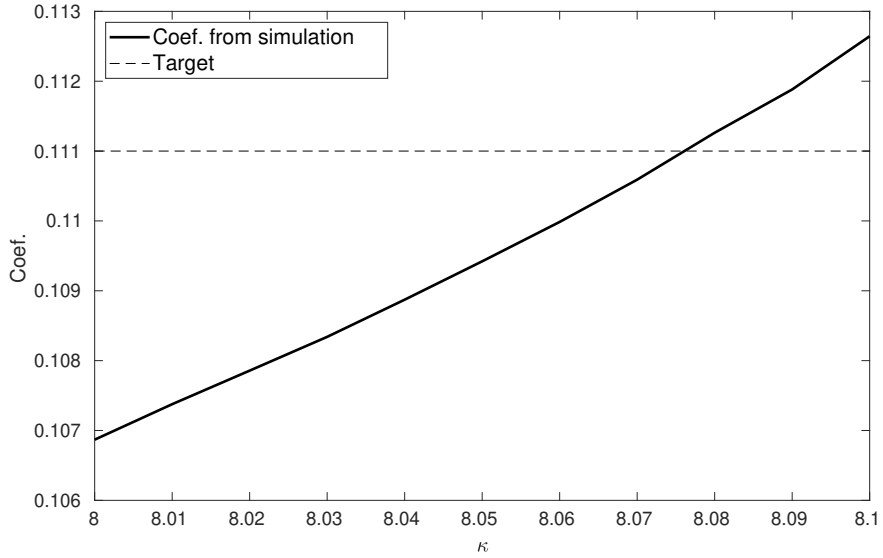
Notes: This table reports summary statistics of changes in global stock between 1980 and 2018 by fishery species used in quantitative model. Column 1 shows the global carrying capacity of species, where the global carrying capacity is calculated by summing the carrying capacity over all regions. Column 2 and 3 report the global stock of species in 1980 and 2018, where the global stock is calculated by summing the stock over all regions. Column 4 and 5 show the stock to capacity ratio in 1980 and 2018. Column 6 and 7 display the percentage change in stock and the percentage points change in stock to capacity ratio, respectively.

Table A.5: Summary Statistics of Fuel Subsidies

ISO	Fuel Subsidies in 2003 (MM) (1)	Fuel Subsidies in 2018 (MM) (2)	Country Share in 2003 (%) (3)	Country Share in 2018 (%) (4)
CHN	1,814	3,433	28.85	44.44
JPN	1,115	632	17.73	8.18
KOR	331	604	5.26	7.82
TWN	120	593	1.91	7.67
XEU	147	479	2.34	6.21
THA	241	251	3.83	3.25
XAF	129	246	2.06	3.19
USA	243	201	3.86	2.60
IDN	171	141	2.72	1.83
XAS	116	121	1.84	1.56
XAM	129	113	2.05	1.47
ITA	0	104	0.00	1.35
IND	222	90	3.53	1.17
FRA	85	87	1.36	1.13
PHL	166	87	2.63	1.12
ESP	120	86	1.91	1.11
MYS	116	75	1.84	0.97
CAN	93	69	1.48	0.89
GBR	0	64	0.00	0.83
NOR	110	58	1.75	0.75
XOC	69	53	1.10	0.69
TUR	17	53	0.27	0.68
BGD	8	35	0.13	0.45
MEX	175	24	2.78	0.31
DEU	0	18	0.00	0.23
BRA	60	6	0.96	0.08
RUS	491	2	7.81	0.02
CHL	0	0	0.00	0.00
PER	0	0	0.00	0.00
VNM	0	0	0.00	0.00
World	6,288	7,727	100.00	100.00

Notes: This table shows the summary statistics of fuel subsidies for our model regions. Column 1 and 2 report the fuel subsidies measured in million USD for 2003 and 2018, respectively. Column 3 and 4 report the country share of fuel subsides among all regions in 2003 and 2018, respectively. The regions beginning with "X" refer to the continental aggregates. "XAF" stands for "Rest of Africa", "XAM" stands for "Rest of America", "XAS" stands for "Rest of Asia", "XEU" stands for "Rest of Europe", and "XOC" stands for "Rest of Oceania".

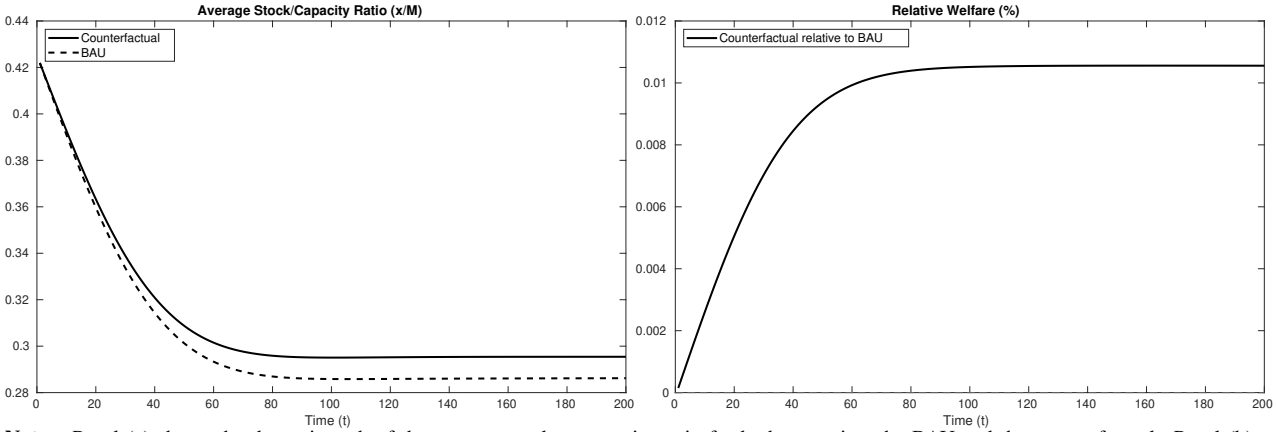
Figure A.1: Relationship between κ and β_1



Notes: The figure shows the relationship between the parameter value of κ and the regression coefficient β_1 from equation (1.2).

Figure A.2: Dynamic Path of Outcomes: BAU and Counterfactual

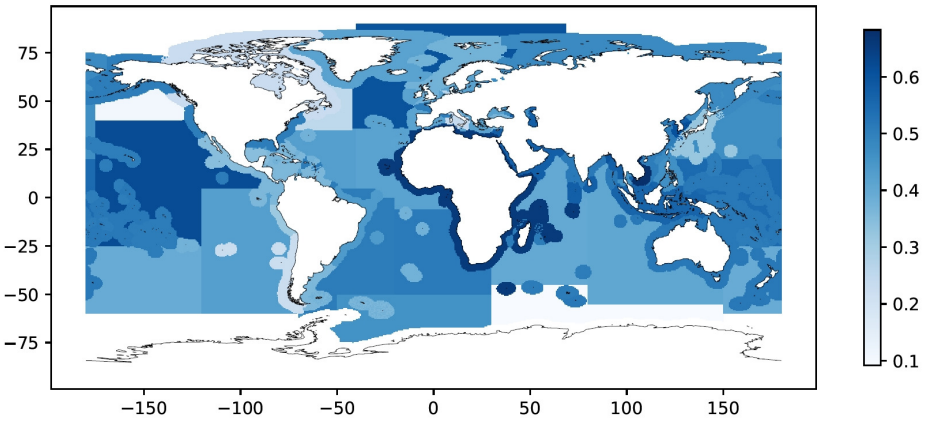
(a) Average Stock to Capacity Ratio (b) Relative Welfare (Counterfactual relative to BAU)



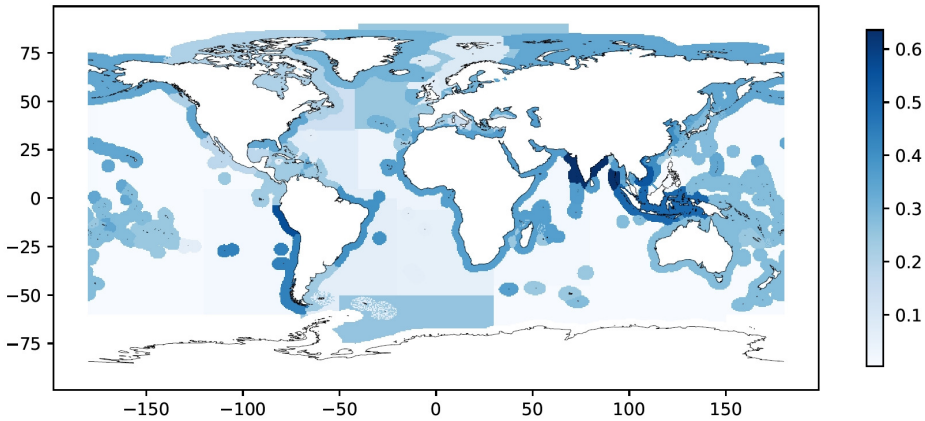
Notes: Panel (a) shows the dynamic path of the average stock to capacity ratio for both scenarios, the BAU and the counterfactual. Panel (b) represents the welfare from the counterfactual relative to the BAU, in percentage change.

Figure A.3: Average Stock to Capacity Ratio

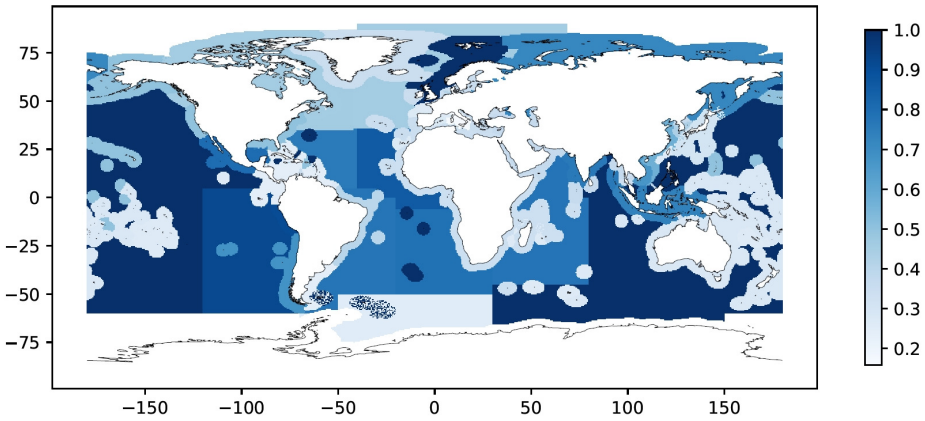
(a) Initial Year



(b) BAU Steady State



(c) Planner Steady State



Notes: The map shows the average stock to capacity ratio across species in each fishing location from the quantitative model. Panel (a) shows the average stock to capacity ratio in the initial year. Panel (b) and (c) represent the average stock to capacity ratio in the BAU steady state and the planner steady state, respectively.

A.3 Derivations

A.3.1 Decentralized Equilibrium

- FOC of households

$$\max_{C_{ijk,st},C^o_{j,t}} U_{j,t} \quad \text{s.t.} \quad \sum_{i\in I}\sum_{k\in K}\sum_{s\in S} p_{ijk,st}C_{ijk,st} + p^o_{j,t}C^o_{j,t} = E_{j,t} \quad \forall t$$

$$\begin{aligned}
\mathcal{L} &= U_{j,t} + \lambda_{j,t}\left(E_{j,t} - p^o_{j,t}C^o_{j,t} - \sum p_{ijk,st}C_{ijk,st}\right) \\
\left[C^o_{j,t}\right]: &\qquad \frac{\partial U_{j,t}}{\partial C^o_{j,t}} = \lambda_{j,t}p^o_{j,t} \\
\left[C_{ijk,st}\right]: &\qquad \frac{\partial U_{j,t}}{\partial C_{ijk,st}} = \lambda_{j,t}p_{ijk,st}
\end{aligned}$$

- Rearranging,

$$\frac{\partial U_{j,t}}{\partial C_{ijk,st}} = \frac{\partial U_{j,t}}{\partial C^o_{j,t}}\frac{p_{ijk,st}}{p^o_{j,t}} \tag{A.1}$$

- FOC of atomistic fishery firms

$$\max_{L_{ijk,st}} \sum_t \left(p_{ijk,st}Q_{ijk,st} - w_{i,t}L_{ijk,st}\right) \quad \text{where} \quad Q_{ijk,st} = \frac{z_i\left(x_{k,st-1}/M_{k,s}\right)^{\xi}}{d_{ij,s}\tau_{ik,s}}L_{ijk,st}$$

$$\begin{aligned}
\mathcal{L} &= p_{ijk,st}Q_{ijk,st} - w_{i,t}L_{ijk,st} \\
\left[L_{ijk,st}\right]: &\qquad p_{ijk,st}\frac{\partial Q_{ijk,st}}{\partial L_{ijk,st}} = w_{i,t}
\end{aligned} \tag{A.2}$$

- Price

$$p_{ijk,st} = \frac{d_{ij,s}\tau_{ik,s}}{\left(x_{k,st-1}/M_{k,s}\right)^{\xi}}\frac{w_{i,t}}{z_i} \tag{A.3}$$

- FOC of outside good firms

$$\begin{aligned}
\mathcal{L} &= p^o_{i,t}Q^o_{i,t} - w^o_{i,t}L^o_{i,t} \\
\left[L^o_{i,t}\right]: &\qquad p^o_{i,t}\frac{\partial Q^o_{i,t}}{\partial L^o_{i,t}} = w^o_{i,t}
\end{aligned} \tag{A.4}$$

- Note that outside good is freely traded $p^o_{i,t} = p^o_{j,t}$ and labor is perfectly mobile $w_{i,t} = w^o_{i,t}$

- Putting (A.2) and (A.4) into (A.1), we get (1.19)

$$\frac{\partial U_{j,t}}{\partial C_{ijk,st}} = \frac{\partial U_{j,t}}{\partial C^o_{j,t}} \left(\frac{\partial Q^o_{i,t}}{\partial L^o_{i,t}} / \frac{\partial Q_{ijk,st}}{\partial L_{ijk,st}} \right)$$

- From (A.2), we get (1.12)

$$p_{ijk,st} = \frac{d_{ij,s}\tau_{ik,s}}{z_i \left(x_{k,st-1}/M_{k,s} \right)^{\xi}} w_{i,t}$$

A.3.2 Planner

$$\mathcal{L} = \sum_t \beta^t \Bigg[W_t + \sum_{k\in K}\sum_{s\in S} \lambda_{k,st} \left(x_{k,st-1} + G_{k,st} - H_{k,st} - x_{k,st} \right) + \sum_{i\in I} \mu_{i,t} \left(\bar{L}_i - \sum_{s\in S}\sum_{k\in K}\sum_{j\in I} L_{ijk,st} - L^o_{i,t} \right)$$
$$+ \sum_{i\in I}\sum_{s\in S}\sum_{k\in K}\sum_{j\in I} \theta_{ijk,st} \left(Q_{ijk,st} - C_{ijk,st} \right) + \alpha_t \left(\sum_{i\in I} Q^o_{i,t} - \sum_{j\in I} C^o_{j,t} \right) \Bigg]$$

- FOCs

$$[C_{ijk,st}]: \quad \theta_{ijk,st} = \frac{\partial W_t}{\partial C_{ijk,st}} \tag{A.5}$$

$$\left[C^o_{j,t}\right]: \quad \alpha_t = \frac{\partial W_t}{\partial C^o_{j,t}} \tag{A.6}$$

$$[L_{ijk,st}]: \quad \theta_{ijk,st} = \left(\mu_{i,t} + \lambda_{k,st} \frac{\partial H_{k,st}}{\partial L_{ijk,st}} \right) / \left(\frac{\partial Q_{ijk,st}}{\partial L_{ijk,st}} \right) \tag{A.7}$$

$$\left[L^o_{i,t}\right]: \quad \alpha_t = \mu_{i,t} / \left(\frac{\partial Q^o_{i,t}}{\partial L^o_{i,t}} \right) \tag{A.8}$$

$$[x_{k,st}]: \quad \lambda_{k,st} = \beta \left[\lambda_{k,st+1} \left(1 + \frac{\partial G_{k,st+1}}{\partial x_{k,st}} - \frac{\partial H_{k,st+1}}{\partial x_{k,st}} \right) + \sum_{i\in I}\sum_{j\in J} \theta_{ijk,st+1} \frac{\partial Q_{ijk,st+1}}{\partial x_{k,st}} \right] \tag{A.9}$$

$$[\mu_{i,t}]: \quad \bar{L}_i = \sum_{s\in S}\sum_{k\in K}\sum_{j\in I} L_{ijk,st} + L^o_{i,t} \tag{A.10}$$

$$[\theta_{i,st}]: \quad Q_{ijk,st} = C_{ijk,st} \tag{A.11}$$

$$[\alpha_t]: \quad \sum_{i\in I} Q^o_{i,t} = \sum_{j\in I} C^o_{j,t} \tag{A.12}$$

$$[\lambda_{k,st}]: \quad x_{k,st-1} + G_{k,st} = H_{k,st} + x_{k,st} \tag{A.13}$$

- From (A.6) and (A.8),

$$\mu_{i,t} = \frac{\partial W_t}{\partial C^o_{j,t}} \frac{\partial Q^o_{i,t}}{\partial L^o_{i,t}} \tag{A.14}$$

- Putting (A.5) and (A.14) into (A.7),

$$\frac{\partial W_t}{\partial C_{ijk,st}} \frac{\partial Q_{ijk,st}}{\partial L_{ijk,st}} = \frac{\partial W_t}{\partial C^o_{j,t}} \frac{\partial Q^o_{ij,t}}{\partial L^o_{i,t}} + \lambda_{k,st} \frac{\partial H_{k,st}}{\partial L_{ijk,st}} \tag{A.15}$$

- From (A.9) and (A.13),

$$\lambda_{k,st} = \beta \left[\lambda_{k,st+1} \left(1 + \frac{\partial G_{k,st+1}}{\partial x_{k,st}} - \frac{\partial H_{k,st+1}}{\partial x_{k,st}} \right) + \frac{\partial W_{t+1}}{\partial C_{ijk,st+1}} \frac{\partial Q_{ijk,st+1}}{\partial x_{k,st}} \right] \tag{A.16}$$

- Let $\Omega_{k,st} = \partial W_{t+1} / \partial x_{k,st}$ and $\Theta_{k,st} = \partial x_{k,st+1} / \partial x_{k,st}$

$$\lambda_{k,st} = \beta \left[\lambda_{k,st+1} \Theta_{k,st} + \Omega_{k,st} \right]$$

- At any point of time t,

$$\frac{\partial W_t}{\partial C_{ijk,st}} = \frac{\partial W_t}{\partial C^o_{j,t}} \left(\frac{\partial Q^o_{i,t}}{\partial L^o_{i,t}} / \frac{\partial Q_{ijk,st}}{\partial L_{ijk,st}} \right) + \lambda_{k,st} \frac{\partial H_{k,st}}{\partial Q_{ijk,st}} \tag{A.17}$$

- At the steady state, $\lambda_{k,st} = \lambda_{k,st+1} = \lambda_{k,st+2} ...$

$$\lambda_{k,st} = \frac{\beta \Omega_{k,st}}{1 - \beta \Theta_{k,st}} \tag{A.18}$$

- Putting (A.18) into (A.15), and rearranging, we get (1.22)

$$\frac{\partial W_t}{\partial C_{ijk,st}} = \frac{\partial W_t}{\partial C^o_{j,t}} \left(\frac{\partial Q^o_{i,t}}{\partial L^o_{i,t}} / \frac{\partial Q_{ijk,st}}{\partial L_{ijk,st}} \right) + \frac{\beta \Omega_{k,st}}{1 - \beta \Theta_{k,st}} \frac{\partial H_{k,st}}{\partial Q_{ijk,st}} \tag{A.19}$$

  where t is at the steady state

A.3.3 Dual Approach

- Now the government imposes per unit tax $t_{ijk,st}$ where $\tilde{p}_{ijk,st} = p_{ijk,st} + t_{ijk,st}$

- FOC of households

$$\begin{aligned}\mathcal{L} &= U_{j,t} + \lambda_{j,t}\left(E_{j,t} - p^o_{j,t}C^o_{j,t} - \sum \tilde{p}_{ijk,st}C_{ijk,st}\right)\\ \left[C^o_{j,t}\right]: &\quad \frac{\partial U_{j,t}}{\partial C^o_{j,t}} = \lambda_{j,t}p^o_{j,t}\\ \left[C_{ijk,st}\right]: &\quad \frac{\partial U_{j,t}}{\partial C_{ijk,st}} = \lambda_{j,t}\tilde{p}_{ijk,st}\end{aligned}$$

- Rearranging,

$$\frac{\partial U_{j,t}}{\partial C_{ijk,st}} = \frac{\partial U_{j,t}}{\partial C^o_{j,t}}\frac{\tilde{p}_{ijk,st}}{p^o_{j,t}} \tag{A.20}$$

- FOC of fishery firms

$$\begin{aligned}\mathcal{L} &= \left(\tilde{p}_{ijk,st} - t_{ijk,st}\right)Q_{ijk,st} - w_{i,t}L_{ijk,st}\\ \left[L_{ijk,st}\right]: &\quad \left(\tilde{p}_{ijk,st} - t_{ijk,st}\right)\frac{\partial Q_{ijk,st}}{\partial L_{ijk,st}} = w_{i,t}\\ \tilde{p}_{ijk,st} &= w_{i,t}\left(\frac{\partial Q_{ijk,st}}{\partial L_{ijk,st}}\right)^{-1} + t_{ijk,st}\\ &= p_{ijk,st} + t_{ijk,st}\end{aligned} \tag{A.21}$$

- FOC of outside good firms

$$\begin{aligned}\mathcal{L} &= p^o_{i,t}Q^o_{i,t} - w^o_{i,t}L^o_{i,t}\\ \left[L^o_{i,t}\right]: &\quad p^o_{i,t}\frac{\partial Q^o_{i,t}}{\partial L^o_{i,t}} = w^o_{i,t}\end{aligned} \tag{A.22}$$

- Balance of Budget

$$w^o_{i,t}L^o_{i,t} + w_{i,t}L_{i,t} + t_{ijk,st}Q_{ijk,st} = X^o_{i,t} + X_{i,t}$$

- Claim: the following optimal policy $t^*_{ijk,st}$ realizes the optimal allocation from equation (A.19)

$$t^*_{ijk,st} = \frac{\beta\Omega_{k,st}}{1 - \beta\Theta_{k,st}}\frac{\partial H_{k,st}}{\partial Q_{ijk,st}}$$

- With $\phi_j = 1$, note that

$$\frac{\partial W_t}{\partial C_{ijk,st}} = \frac{\partial U_{j,t}}{\partial C_{ijk,st}}, \quad \frac{\partial W_t}{\partial C^o_{j,t}} = \frac{\partial W_t}{\partial C^o_{j,t}}$$

- Then, (A.19) becomes

$$\frac{\partial U_{j,t}}{\partial C_{ijk,st}} = \frac{\partial U_{j,t}}{\partial C^o_{j,t}} \left(\frac{\partial Q^o_{i,t}}{\partial L^o_{i,t}} / \frac{\partial Q_{ijk,st}}{\partial L_{ijk,st}} \right) + \frac{\beta \Omega_{k,st}}{1 - \beta \Theta_{k,st}} \frac{\partial H_{k,st}}{\partial Q_{ijk,st}}$$

- Plugging in (A.20), (A.21), and (A.22) into (A.19)

$$\frac{\partial U_{j,t}}{\partial C^o_{j,t}} \frac{\tilde{p}_{ijk,st}}{p^o_{j,t}} = \frac{\partial U_{j,t}}{\partial C^o_{j,t}} \frac{\left(\tilde{p}_{ijk,st} - t^*_{ijk,st} \right)}{w_{i,t}} + \frac{\beta \Omega_{k,st}}{1 - \beta \Theta_{k,st}} \frac{\partial H_{k,st}}{\partial Q_{ijk,st}}$$

- With the quasi-linear preferences, free labor mobility, and choice of numeraire where $\partial U_{j,t} / \partial C^o_{j,t} = 1$, $w_{i,t} = z^o_i$, and $p^o_{j,t} = 1$, the optimal policy $t^*_{ijk,st}$ is indeed

$$\begin{aligned} \tilde{p}_{ijk,st} &= \left(\tilde{p}_{ijk,st} - t^*_{ijk,st} \right) + \frac{\beta \Omega_{k,st}}{1 - \beta \Theta_{k,st}} \frac{\partial H_{k,st}}{\partial Q_{ijk,st}} \\ \Leftrightarrow t^*_{ijk,st} &= \frac{\beta \Omega_{k,st}}{1 - \beta \Theta_{k,st}} \frac{\partial H_{k,st}}{\partial Q_{ijk,st}} \end{aligned}$$

A.3.4 Proof for Lemma

Want to show: the sufficient conditions i) $\xi \geq 1$ or ii) $0 < \xi < 1$ and $\gamma_{k,s} < \frac{1}{1-\xi} \left(\frac{1}{\beta} - 1 \right)$ guarantee $\theta_{k,st} < 1/\beta$ for all ranges of $\frac{x_{k,st}}{M_{k,s}} \in [0, 1]$ at the steady state.

Taking partial derivative of equation (1.9) with respect to $x_{k,st}$,

$$\theta_{k,st} = \frac{\partial x_{k,st+1}}{\partial x_{k,st}} = \frac{\partial G_{k,st+1}}{\partial x_{k,st}} - \frac{\partial H_{k,st+1}}{\partial x_{k,st}} = (1 + \gamma_{k,s}) - 2\gamma_{k,s} \frac{x_{k,st}}{M_{k,s}} - \frac{\xi}{x_{k,s}} \sum_i \sum_j d_{ij,s} \tau_{ik,s} Q_{ijk,st} \tag{A.23}$$

From equation (1.18), at the steady state,

$$\gamma_{k,s} x_{k,st} (1 - \frac{x_{k,st}}{M_{k,s}}) = \sum_{i \in I} \sum_{j \in I} d_{ij,s} \tau_{ik,s} Q_{ijk,st} \tag{A.24}$$

Combining (A.23) and (A.24), at the steady state,

$$\begin{aligned} \theta_{k,st} &= (1 + \gamma_{k,s}) - 2\gamma_{k,s} \frac{x_{k,st}}{M_{k,s}} - \xi \gamma_{k,s} (1 - \frac{x_{k,st}}{M_{k,s}}) \\ &= 1 + \gamma_{k,s} \left(1 - 2 \frac{x_{k,st}}{M_{k,s}} - \xi (1 - \frac{x_{k,st}}{M_{k,s}}) \right) \end{aligned}$$

1) $\xi \geq 1$

For all ranges of $\frac{x_{k,st}}{M_{k,s}} \in [0,1]$, I have

$$1 - 2\frac{x_{k,st}}{M_{k,s}} - \xi(1 - \frac{x_{k,st}}{M_{k,s}}) < 1$$

Thus,

$$\Theta_{k,st} < 1 < 1/\beta$$

2) $0 < \xi < 1$ and $\gamma_{k,s} < \frac{1}{1-\xi}\left(\frac{1}{\beta} - 1\right)$

$$\begin{aligned} &\gamma_{k,s} < \frac{1}{1-\xi}\left(\frac{1}{\beta} - 1\right) \\ \Leftrightarrow &\left(1 - \frac{1}{2-\xi}\right) - \frac{1}{(2-\xi)\,\gamma_{k,s}}\left(\frac{1}{\beta} - 1\right) < 0 \end{aligned} \tag{A.25}$$

At the steady state,

$$\begin{aligned} \Theta_{k,st} =& 1 + \gamma_{k,s}\left(1 - 2\frac{x_{k,st}}{M_{k,s}} - \xi(1 - \frac{x_{k,st}}{M_{k,s}})\right) < 1/\beta \\ \Leftrightarrow &\frac{x_{k,st}}{M_{k,s}} > \left(1 - \frac{1}{2-\xi}\right) - \frac{1}{(2-\xi)\,\gamma_{k,s}}\left(\frac{1}{\beta} - 1\right) \end{aligned} \tag{A.26}$$

Combining (A.25) and (A.26),

$$\Theta_{k,st} < 1/\beta \quad \text{for all ranges of } \frac{x_{k,st}}{M_{k,s}} \in [0,1]$$

A.4 Calibration Details

A.4.1 Steps for Calibration of κ

1. Under the environment described in 1.4.4, the government imposes the policy instruments $t_{ijk,st} = s_{i,t}$

2. For each κ, calibrate subsidy rate $s_{i,16}$ to match the change in amount of fuel subsidy assuming $s_{i,0} = 0$. That is, $\Delta_{0\to16} S_{i,t}^{model} = \Delta_{2002\to2018} S_{i,t}^{Data}$

3. Run regression using simulated data and obtain κ that matches β_1 from equation (1.2)

A.5 Numerical Algorithm

A.5.1 Business As Usual

A.5.1.1 Static Equilibrium

For every period, given the geography, fundamentals, and endowment including fishery stock $x_{k,st}$, solve for the allocation of labor $L_{ijk,st}$

1. Initial guess for the allocation of labor $L_{ijk,st}$
2. Compute quantity and output
3. Compute prices and wages and expenditure
4. Compute $L^{new}_{ijk,st} = \frac{Y_{ijk,st}}{w_{i,t}}$
5. Update $L_{ijk,st} = \alpha L^{new}_{ijk,st} + (1-\alpha) L_{ijk,st}$ and go back to Step 1, where $0 < \alpha < 1$ is the dampening parameter
6. Iterate until convergence

A.5.1.2 Steady State Equilibrium

1. Initial guess for steady state stock $x_{k,st}$
2. Given the guess of stock $x_{k,st}$, solve for static equilibrium as described in A.5.1.1
3. Compute the growth $G(x_{k,st})$ and harvest $H(x_{k,st})$ as
   $G(x_{k,st}) = \gamma_{k,s} x_{k,st}(1 - \frac{x_{k,st}}{M_{k,s}})$ and $H(x_{k,st}) = \sum_{i \in I} \sum_{j \in I} d_{ij,s} \tau_{ik,s} Q_{ijk,st}$
4. Update $x_{k,st} = x_{k,st} \times \left(\frac{G(x_{k,st})}{H(x_{k,st})} \right)^{\alpha}$ and go back to Step 1, where α is the dampening parameter
5. Iterate until convergence

A.5.1.3 Dynamic Equilibrium

1. Given the stock endowment at the initial period, $x_{k,s0}$, solve for static equilibrium as described in A.5.1.1
2. Obtain $x_{k,s1}$ using the law of motion for fish

$$x_{k,st} - x_{k,st-1} = \gamma_{k,s} x_{k,st-1}(1 - \frac{x_{k,st-1}}{M_{k,s}}) - \sum_{i \in I} \sum_{j \in I} d_{ij,s} \tau_{ik,s} Q_{ijk,st}$$

3. Solve for static equilibrium as described in A.5.1.1
4. Solve for $t = 2, ..., T$

A.5.2 Planner's Problem

A.5.2.1 Steady State Equilibrium

1. Initial guess for steady state stock $x_{k,st}$
2. Given $x_{k,st}$, solve for $L_{ijk,st}$ that satisfies

$$\frac{\partial W_t}{\partial C_{ijk,st}} = \frac{\partial W_t}{\partial C^o_{i,t}} \left(\frac{\partial Q^o_{i,t}}{\partial L^o_{i,t}} / \frac{\partial Q_{ijk,st}}{\partial L_{ijk,st}} \right) + \frac{\beta \Omega_{k,st}}{1 - \beta \Theta_{k,st}} \frac{\partial H_{k,st}}{\partial Q_{ijk,st}}$$

   where $\Omega_{k,st} = \frac{\partial W_t}{\partial x_{k,st}}$ and $\Theta_{k,st} = \frac{\partial x_{k,st+1}}{\partial x_{k,st}}$
3. Compute the growth $G(x_{k,st})$ and harvest $H(x_{k,st})$
   where $G(x_{k,st}) = \gamma_{k,s} x_{k,st}(1 - \frac{x_{k,st}}{M_{k,s}})$ and $H(x_{k,st}) = \sum_{i \in I} \sum_{j \in I} d_{ij,s} \tau_{ik,s} Q_{ijk,st}$
4. Update $x_{k,st} = x_{k,st} \times \left(\frac{G(x_{k,st})}{H(x_{k,st})} \right)^{\alpha}$ and go back to step 1, where α is the dampening parameter
5. Iterate until convergence
6. Obtain the steady state $x_{k,st}, L_{ijk,st}, \lambda_{k,st}, \Omega_{k,st}, \Theta_{k,st}$ where $\lambda_{k,st} = \frac{\beta \Omega_{k,st}}{1 - \beta \Theta_{k,st}}$

A.5.2.2 Dynamic Equilibrium

Given the initial stock $x_{k,s0}$ and steady state $x_{k,st}, L_{ijk,st}, \lambda_{k,st}, \Omega_{k,st}, \Theta_{k,st}$ from A.5.2.1, I assume that the last period converges to steady state such that $x_{k,sT} = x_{k,st}$, $L_{ijk,sT} = L_{ijk,st}$, and $\lambda_{k,sT} = \lambda_{k,st}$.

1. Initial guess for $\{x_{k,st}\}_{t=1}^{T-1}$ by interpolating $x_{k,st} = \frac{(T-t)x_{k,s0} + (t)x_{k,sT}}{T}$
2. Given $\{x_{k,st}\}_{t=0}^{T}$, roll backward from $t = T$
   (a) solve backward for $\lambda_{k,st-1}$ using

$$\lambda_{k,st-1} = \beta \left[\lambda_{k,st} \Theta_{k,st} + \Omega_{k,st} \right]$$

   (b) solve for $L_{ijsk,t-1}$, $\Theta_{k,st-1}$, $\Omega_{k,st-1}$ using

$$\frac{\partial W_{t-1}}{\partial C_{ijk,st-1}} = \frac{\partial W_{t-1}}{\partial C^o_{i,t-1}} \left(\frac{\partial Q^o_{i,t-1}}{\partial L^o_{i,t-1}} / \frac{\partial Q_{ijk,st-1}}{\partial L_{ijk,st-1}} \right) + \lambda_{k,st-1} \frac{\partial H_{k,st-1}}{\partial Q_{ijk,st-1}}$$

(c) solve for $t = T-2, T-3, ..., 1$ and obtain $\{L_{ijk,st}, \lambda_{k,st}, \Omega_{k,st}, \Theta_{k,st}\}_{t=1}^{T}$

3. Given $x_{k,s0}$ and $\{L_{ijk,st}, \lambda_{k,st}, \Omega_{k,st}, \Theta_{k,st}\}_{t=1}^{T}$, roll forward from $t = 1$

   (a) solve for $x_{k,st}^{new}$ using the law of motion for fish

$$x_{k,st}^{new} - x_{k,st-1} = \gamma_{k,s} x_{k,st-1}(1 - \frac{x_{k,st-1}}{M_{k,s}}) - \sum_{i \in I} \sum_{j \in I} d_{ij,s} \tau_{ik,s} Q_{ijk,st}$$

4. Update $x_{k,st} = \alpha x_{k,st}^{new} + (1-\alpha) x_{k,st}$ and go back to Step 1, where $0 < \alpha < 1$ is the dampening parameter

5. Iterate until convergence

A.5.3 Partial Derivatives

$$\frac{\partial W_t}{\partial C_{ijk,st}} = b_j b_s b_{ij} b_{k,s} C_{j,t}^{-1+\frac{1}{\nu}} C_{j,st}^{\frac{1}{\eta}-\frac{1}{\nu}} C_{ij,st}^{\frac{1}{\kappa}-\frac{1}{\eta}} C_{ijk,st}^{-\frac{1}{\kappa}}$$

$$\frac{\partial W_t}{\partial C_{j,t}^o} = 1$$

$$\frac{\partial Q_{ijk,kt}}{\partial L_{ijk,st}} = \frac{z_i}{d_{ij,s}\tau_{ik,s}} \left(\frac{x_{k,st-1}}{M_{k,s}}\right)^{\xi}$$

$$\frac{\partial Q_{i,t}^o}{\partial L_{i,t}^o} = z_i^o$$

$$\frac{\partial Q_{ijk,st}}{\partial x_{k,st-1}} = \frac{\xi}{x_{k,st-1}} z_i \left(\frac{x_{k,st-1}}{M_{k,s}}\right)^{\xi} L_{ijk,st}$$

$$\frac{\partial G_{k,st}}{\partial x_{k.st-1}} = (1+\gamma_{k,s}) - 2\gamma_{k,s}\frac{x_{k,st-1}}{M_{k,s}}$$

$$\frac{\partial H_{k,st}}{\partial x_{k,st-1}} = \sum_i \sum_j d_{ij,s}\tau_{ik,s}\frac{\partial Q_{ijk,st}}{\partial x_{k,st-1}} = \sum_i \sum_j \frac{\xi}{x_{k,st-1}} z_i \left(\frac{x_{k,st-1}}{M_{k,s}}\right)^{\xi} L_{ijk,st} = \frac{\xi}{x_{k,st-1}} \sum_i \sum_j Q_{ijk,st}$$

$$\frac{\partial H_{k,st}}{\partial L_{ijk,st}} = d_{ij,s}\tau_{ik,s}\frac{\partial Q_{ijk,kt}}{\partial L_{ijk,st}}$$

APPENDIX B

Appendix to Chapter 2

B.1 Details on Data

Forest Area. Our main source of information on forest area comes from FAO-FRA (FAO Global Forest Resources Assessment), which is based on questionnaires that are submitted to the agricultural agencies of every country. Since the 1990s, these data have been compared with measures of forest cover identified from satellite imagery such as Landsat [MacDicken, 2015]. Nowadays, about 70% of national forest inventories utilize remote sensing to validate at least some portion of the inventory.

The FRA data are available for the years of 1990, 2000, 2005, 2010, 2015 and 2020 and they provide different measures of forest area.[1] When available, we use information on the naturally regenerating forest, which excludes forest area related to industrial forests planted for the production of, for example, paper. Our statistics sometimes diverge slightly from the ones reported by FAO-FRA since they report net deforestation, which incorporates both forest regeneration and forest plantation and we exclude the second from our measure. For our empirical analysis in Section 2.3, we grouped islands (e.g., Virgin Islands and Gibraltar), small regions (e.g., as Monaco and the Vatican), and countries with negligible forest areas (e.g., Kuwait and Bahrain) into larger regions. Appendix Table B.4 documents summary statistics for all countries in our final data.

In addition to FRA, another increasingly used source of data comes from Hansen et al. [2013], who measures global deforestation using satellite imagery at a high spatial resolution (30 meters). Different from the data from FAO-FRA, which is designed to measure forest area based on land use classifications, the data from Hansen et al. [2013] measures forest area based on forest cover. As such, Hansen et al. [2013] tends to capture transitory changes in forest area such as the ones related to fires and insect outbreaks, even when

[1]The main definition of forest is any land spanning more than 0.5 hectares with trees higher than 5 meters and a canopy cover of more than 10 percent, or trees able to reach these thresholds on site—it does not include land that is predominantly under agricultural or urban land use. The data, however, also provides information on planted trees and naturally regenerating forest.

there are no changes in land use, which is the concept that we use in the formulation of our model.[2][3]

Agricultural Area and Fallow Land. We construct the total area in cropland using data from FAO-STAT on total harvested area. These data do not provide, however, information on the total area dedicated to cattle grazing. To recover that information, we multiply data on the total cattle stock by a simple conversion rate of 0.75 hectares per cattle, which we define as the pasture land.[4] Based on that information, we then compute the fallow land as the residual land, that is, the total land in the country minus the artificial surface, the watersurface, the forest area, the cropland, and the pasture land.

To compute the share of forest in a country, we use the total area of the country, as reported by FRA, which already excludes the water surface in a country. In addition, using data from FAOSTAT on land cover, we remove from the total area of the country the snow cover and the barren land—which includes desert areas. We refer to this resulting variable as "country area".

Trade Costs. To calibrate the trade costs generated by policy, we use data on (i) tariffs from the World Bank World Development Indicators—specifically, we use the simple unweighted average of the effectively applied rates for all products subject to tariffs—, (ii) import fees and days to import from the World Bank Doing Business, and (iii) trade agreements from CEPII Gravity Database—we take the country-destination specific free trade agreement indicator for year 2010, which is the dummy variable that takes the value of 1 if the country pair is engaged in a regional trade agreement. For the trade costs generated by geography, we use data from CEPII, which includes data on contiguity, distance, common language, and colonial relationships.

Carbon Stock. Our main data source for the carbon stock of forests is FAO-FRA. FRA contains data on six carbon pools: above- and below-ground carbon stock, dead wood, litter, soil, organic carbon, and harvested wood products. In our simplest exercise, we use the information on above- below-ground carbon stock, which is the typical approach when measuring the CO2 emissions from deforestation [IPCC, 2006]. The definition of carbon in above-ground biomass is all carbon in living biomass above the soil, including stems, stumps, branches, bark, seeds, and foliage, whereas the definition of carbon in below-ground biomass is all carbon in all biomass of live roots (fine roots of less than 2 mm diameter are excluded, because these often cannot be distinguished empirically from soil organic matter or litter).

[2] As identified by Curtis et al. [2018], about 23% of global forest disturbances between 2001 and 2015 can be attributed to wildfires. This driver of forest loss has been the dominant one in Russia, Australia and New Zealand. In contrast, agricultural-related activities have been the main source of deforestation in South America, Africa and South-east Asia. Urbanization accounts for a minimal share of the changes in forest area. In addition, as discussed in Keenan et al. [2015], since Hansen et al. [2013] use difference methodologies to measure deforestation and reforestation, one must interpret net changes in forest area coming from Hansen et al. [2013] with caution.

[3] Moreover,Coulston et al. [2014] found that measures of forest land and forest land cover in the southeastern USA are poorly correlated and suggest that these measures are better correlated in tropical areas. Recent papers that exploit the high-resolution data from Hansen et al. [2013] to identify the reduced-form impact of different policies on deforestation are unlikely to be affected by these considerations about the limitations of satellite based data sets, since they focus on deforestation in tropical countries.

[4] According to the agricultural census of Brazil, the total cattle stock per pasture area in hectares equals approximately 0.30, whereas technical reports give 0.6 units per hectare in the UK and almost 1 in the US.

For a more thorough analysis, in addition to the carbon in above and below ground, we incorporate the following into our measurement: The carbon in litter, which is all the carbon in all non-living biomass with a diameter less than the minimum diameter for dead wood (e.g. 10 cm), lying dead in various states of decomposition above the mineral or organic soil, as well as measures of carbon in mineral and organic soils (including peat) and measures of carbon in woody biomass not contained in the litter, either standing, lying on the ground, or in the soil.

Our calculation of the climate cost of deforestation is limited to its implied carbon emissions. We do not incorporate other types of greenhouse emissions, such as methane and oxides of nitrogen which may matter where forest fires play a significant role in forest degradation. We also highlight that the emissions coming from these other gases are typically an order of magnitude smaller than the ones associated with CO_2 [Federici et al., 2015].

B.2 Proofs

B.2.1 Section 2.4

B.2.1.1 Proof of Proposition 1

Our definition of a small open economy, "SOE", follows that of Alvarez and Lucas [2007]. Specifically, country i is considered as a SOE in a limiting case where *(i)* $N_i, Z_{i,A}, Z_{i,M} \to 0$, *(ii)* $Z_{i,M}^{\eta-1}/N_i \to \kappa_{i,M} > 0$, $Z_{i,A}^{\eta-1}/N_i \to \kappa_{i,A} > 0$. Additionally, recall that, labor is perfectly mobile across sectors and production technologies are given by:

$$Q_{i,A} = Z_{i,A}L_i; \qquad Q_{i,M} = Z_{i,M}N_{i,M}; \qquad Q_{i,T} = Z_{i,T}N_{i,T}.$$

For relevance, suppose $L_i < H_i$, *i.e.,* the land frontier has room to expand.

In the steady state, the stock of land is pinned down by $g_L L_i = Z_{i,T}N_{i,T}$, and the rental rate of land equals $r_i = (\rho + g_L)\, q_i = (\rho + g_L)\, w_i/Z_{i,T}$. These two equations imply the following relationship between payments to labor in the land-producing sector and payments to land:

$$r_i L_i = \frac{\rho + g_L}{g_L} w_i N_{i,T}$$

Replacing the above equation into the land market clearing condition, $r_i L_i = \Sigma_j \left(w_i d_{ij,A}\right)^{1-\eta} Z_{i,A}^{\eta-1} P_{j,A}^{\eta-1} X_{j,A}$, yields:

$$w_i N_{i,T} = \frac{g_L}{\rho + g_L} \sum_j \left(w_i d_{ij,A}\right)^{1-\eta} Z_{i,A}^{\eta-1} P_{j,A}^{\eta-1} X_{j,A} \tag{B.1}$$

In turn, the market clearing for the manufacturing sector pins down the payments to labor there:

$$w_i N_{i,M} = \sum_j \left(w_i d_{ij,M}\right)^{1-\eta} Z_{i,M}^{\eta-1} P_{j,M}^{\eta-1} X_{j,M} \tag{B.2}$$

where in the above two equations, recall, $P_{j,s}$ and $X_{j,s}$ for $s \in \{A, M\}$ denote the CES price indices and industry-level expenditures.

First, let us show that the wage rate in the SOE, w_i, converges to a positive number. From our SOE assumptions, it follows that country i is infinitesimal as a source of expenditure in its own sectoral demand, *i.e,* $\pi_{ii,A}, \pi_{ii,M} \to 0$. Noting this point and the fact that $N_{i,T} + N_{i,M} = N_i$, we can combine equations (B.1) and (B.2) to express w_i as:

$$w_i^{\eta} = \sum_{j \neq i} \frac{\left(d_{ij,M}\right)^{1-\eta}}{P_{j,M}^{1-\eta}} \frac{Z_{i,M}^{\eta-1}}{N_i} X_{j,M} + \frac{g_L}{\rho + g_L} \sum_{j \neq i} \frac{\left(d_{ij,A}\right)^{1-\eta}}{P_{j,A}^{1-\eta}} \frac{Z_{i,A}^{\eta-1}}{N_i} X_{j,A}$$

Since $Z_{i,M}^{\eta-1}/N_i \to \kappa_{i,M} > 0, Z_{i,A}^{\eta-1}/N_i \to \kappa_{i,A} > 0$, and $P_{j,s}^{\eta-1} X_{j,s}$ is a positive, finite number for each foreign country $j \neq i$ in each sector $s \in \{A, M\}$, the SOE's wage rate, w_i, must converge to a positive, finite number.

Having established that $w_i \in (0, \infty)$, we can now divide equation (B.1) by (B.2), where the wages are canceled out to deliver:

$$N_{i,T} = N_{i,M} \frac{g_L}{\rho + g_L} \frac{d_{i,A}^{1-\eta}}{d_{i,M}^{1-\eta}} \frac{\bar{X}_{-i,A}}{\bar{X}_{-i,M}}, \qquad \text{where} \qquad \bar{X}_{-i,s} \equiv \sum_{j \neq i} Z_{i,s}^{\eta-1} P_{j,s}^{\eta-1} X_{j,s};$$

Note that, here, for a clearer exposition, we let country i's exports costs be common across all destinations, $d_{ij,s} \equiv d_{i,s}$ for all $j \neq i$. Using the above expression, we obtain the effect of a uniform increase in country i's export costs on the employment in the land-producing sector:

$$\frac{\mathrm{d} \ln N_{i,T}}{\mathrm{d} \ln d_{i,A}} = \frac{N_{i,M}}{N_i} (1 - \eta); \tag{B.3}$$

Using equation (B.3) and the steady-state stock of land, $L_i = \frac{1}{g_L} Z_{i,T} N_{i,T}$, the impact on the stock of land can be similarly expressed as:

$$\frac{\mathrm{d} \ln L_i}{\mathrm{d} \ln d_{i,A}} = \frac{N_{i,M}}{N_i} (1 - \eta). \tag{B.4}$$

B.2.1.2 Borlaug's Hypothesis

Consider the stripped-down version of our model presented in Section 2.5. Borlaug's hypothesis can be articulated as follows:

Proposition 4. *An agricultural productivity growth in a closed economy is land-saving when the elasticity*

of substitution between agriculture and manufacturing is below one, namely:

$$\frac{d\log L}{d\log Z_A} = \frac{N_M}{N}(\sigma - 1) < 0 \quad \textit{for} \quad \sigma < 1.$$

Since the proof involves similar, and more straightforward, steps to those in the next section, we have deferred it to that section for clarity.

B.2.1.3 Proof of Proposition 2

We proceed in three steps. First we derive the sectoral labor supply elasticity in the steady state. Second, we show that relative payments to land and labor are determined by sectoral relative productivities and trade openness. Third, we connect these relative payments to land supply and, consequently, to deforestation.

Labor supply in the steady state. Under the assumptions we made in Section 2.5, in the steady state equations 2.14 and 2.15 become

$$(\rho + \psi)\, v_{i,s}^N = \underbrace{\log\left(\frac{w_{i,s}}{P_i}\right)}_{u_{i,s}} + \psi W_{i,s} \tag{B.5}$$

$$W_{i,s} = \nu \log \sum_{s'} \exp\left(\frac{1}{\nu} v_{i,s'}^N\right). \tag{B.6}$$

Here, $u_{i,s}$ is the instantaneous utility for a worker in sector s, and the last equation implies that $W_{i,s} = W_i$, $\forall s$. Substituting B.5 into B.6, we can solve for W_i:

$$W_i = \log\left\{\sum_{s'} c_{i,s}^{\chi}\right\}^{\frac{1}{\rho\chi}},$$

where $\chi = [\nu(\rho + \psi)]^{-1}$ and $c_{i,s} = w_{i,s}/P_i$. Considering that W_i does not vary across sectors, the moving shares in equation 2.16 collapse to:

$$\mu_{i,ss'} \equiv \mu_{i,s'} = \frac{w_{i,s'}^{\chi}}{\sum_l w_{i,l}^{\chi}}, \tag{B.7}$$

which are not anymore a function of the origin sector s.

Finally, the value function of working in sector s reflects the flow value of working in the current sector and the option value of drawing an opportunity to move, where the discount rate reflects the arrival rate of

such opportunities. Rewriting equation B.5, we obtain

$$\begin{aligned} v_{i,s}^{N} &= \frac{1}{\rho+\psi}u_{i,s} + \frac{\psi}{\rho+\psi}W_i \\ &= \frac{1}{\rho+\nu}u_{i,s} + \frac{\psi}{\rho+\nu}\log\left\{\sum_{s'} c_{i,s}^{\chi}\right\}^{\frac{1}{\rho\chi}}. \end{aligned}$$

In turn, equation B.7 gives the steady-state values of labor supply. To see this, note that in the steady state $\dot{N}_{i,s} = 0, \forall i, s$, and therefore equation 2.24 implies

$$0 = \psi\left(-\sum_{l\neq s}\mu_{i,sl}\right)N_{i,s} + \psi\sum_{l\neq s}\mu_{i,ls}N_{i,l}, \qquad \forall s, i.$$

Since $\mu_{i,sl} = \mu_{i,l}$, after a little manipulation, we can obtain that:

$$N_{i,s} = \mu_{i,s}N_i.$$

Relative payments to land and labor. Before proceeding, note that without intermediate input use and under perfect competition, total payments to each factor equal the sum of value added in the sectors that employ it. Furthermore, with symmetric countries, the market clearing conditions for manufacturing and agricultural goods can be expressed in relative terms as:

$$\frac{w_M N_M}{rL} = \frac{b_M}{b_A}\left(\frac{P_M}{P_A}\right)^{1-\sigma}, \tag{B.8}$$

where we have dropped country indexes due to symmetry. Since we have assumed that land is only used in agriculture, the above equation already imposes that $r_A = r$. However, since labor is employed in both manufacturing and land-producing sectors, we carry sector-specific wages. In addition, we can express the sectoral price index, P_s, as a function of the domestic expenditure share, π_s^D, the trade elasticity, $(\eta - 1)$, and the marginal costs, that are w_M/Z_M in manufacturing and r/Z_A in agriculture. Thus, the price indexes of manufacturing and agriculture are given by:

$$P_M = \frac{w_M}{Z_M}\left(\pi_M^D\right)^{\frac{1}{\eta-1}}, \qquad P_A = \frac{r}{Z_A}\left(\pi_A^D\right)^{\frac{1}{\eta-1}}, \tag{B.9}$$

where the domestic expenditure share can be expressed as (due to symmetry),

$$\pi_s^D = \left[(I-1)\,\tau_s^{1-\eta} + 1\right]^{-1}, \qquad s \in \{A.M\}$$

Finally, substituting B.9 into B.8, and solving for relative factor payments, we obtain the manufacturing wage-to-rent ratio:

$$\frac{w_M}{r} = \left(\frac{b_M}{b_A}\frac{L}{N_M}\right)^{\frac{1}{\sigma}}\left(\frac{Z_A}{Z_M}\right)^{\frac{1-\sigma}{\sigma}}\left(\frac{\pi_M^D}{\pi_A^D}\right)^{\frac{1}{\eta-1}\frac{1-\sigma}{\sigma}} \tag{B.10}$$

Connecting factor supplies to factor rewards. In the steady state, the law of motion equation 2.10 implies

$$L = \frac{Z_T N_T}{\delta_L}.$$

where we have used our simplifying assumption that $J_i(z) = Z_{i,T}$ and $\gamma_T = 1$. Using the steady-state labor supply equation B.7, we obtain the steady state supply of land:

$$L = N \frac{w_T^{\chi}}{\sum_l w_l^{\chi}} \frac{Z_T}{\delta_L}. \tag{B.11}$$

Combining this equation with equation B.7, we obtain the ratio of land to manufacturing labor,

$$\frac{L}{N_M} = \left(\frac{w_T}{w_M}\right)^{\chi} \frac{Z_T}{\delta_L}. \tag{B.12}$$

At this point, recall the steady state relationship between the price of new land and the rental rate per unit of agricultural land,

$$q = \frac{r}{\rho + \delta_L}. \tag{B.13}$$

Using the equilibrium pricing in the land-producing sector, 2.9, the rental rate of land can be expressed as a function of the wage rate in the land-producing sector:

$$r = (\rho + \delta_L) w_T / Z_T.$$

Finally, substituting the above equation and B.12 into B.10, the relative wage of manufacturing to that of land-producing sector equals:

$$\frac{w_M}{w_T} = \left[\frac{(\rho + \delta_L)}{Z_T} \left(\frac{Z_T}{\delta_L}\right)^{\frac{1}{\sigma}} \left(\frac{b_M}{b_A}\right)^{\frac{1}{\sigma}} \left(\frac{Z_A}{Z_M}\right)^{\frac{1-\sigma}{\sigma}} \left(\frac{\pi_M^D}{\pi_A^D}\right)^{\frac{1}{\eta-1}\frac{1-\sigma}{\sigma}} \right]^{\frac{\sigma}{\sigma+\chi}} \tag{B.14}$$

Equations B.11 and B.14 deliver the general equilibrium elasticities presented by Proposition 2.

B.2.1.4 Impact of Agricultural Tariff Reductions on Global Land Use

This section characterizes the land use impact of a uniform reduction in agricultural tariffs. Following the previous section, we consider a system of symmetric large open economies, using a two-country model for clearer exposition. In contrast to the previous section, this section assumes that trade barriers in the agriculture sector are represented by tariffs, $\tau_A = (1+t_A)$. The market clearing conditions for manufacturing and agriculture are as follows:

$$wN_M = \beta_M E, \qquad rL = \Lambda_A \beta_A E;$$

where E is the national expenditure:

$$E = rL + wN_M + \underbrace{(1 - \Lambda_A)\,\beta_A E}_{\text{Tariff Rev.}}$$

and, Λ_A denotes the fraction of each dollar spent on agriculture that is received by land,

$$\Lambda_A \equiv 1 - \frac{t_A}{1 + t_A}\left(1 - \pi_A^D\right)$$

The equations that describe the model are otherwise the same as the previous section.

The effect of a multilateral reduction in agricultural tariffs on land demand can be decomposed into two components. First, lowering agricultural tariffs, represented by $\tau_A = (1 + t_A)$, has an effect similar to that of iceberg trade costs. Second, lowering agricultural tariffs modifies land demand by altering the fraction Λ_A of each dollar of spending on agriculture that is received by land in supplying countries.[5] Incorporating this tariff-driven effect into the general equilibrium (GE) elasticity of land, the impact on land use from a uniform global reduction in agricultural tariffs can be expressed as:

$$\frac{\mathrm{d}\ln L}{-\mathrm{d}\ln\left(1 + t_A\right)} = \frac{N_M}{N}\left[\overbrace{(\sigma - 1)\left(1 - \pi_A\right)}^{\text{iceberg-type impact}} + \overbrace{\frac{\mathrm{d}\ln\Lambda_A}{-\mathrm{d}\ln(1 + t_A)}}^{\text{tariff adjustment}}\right] \tag{B.15}$$

The "tariff adjustment" itself consists of two opposing forces: (a) When the imported expenditure share, $(1 - \pi_A)$, is held constant, reducing the agricultural tariff increases the fraction of spending on agriculture that is received by land, thereby boosting land demand. *(b)* When $\frac{t_A}{1+t_A}$ is held constant, lowering the agricultural tariff shifts demand from domestic transactions to imports, where land receives a smaller fraction of agricultural spending, thus decreasing land demand.

Key to this second force is that tariff reductions increase the imported share of agricultural expenditure. Our model allows for this possibility via the presence of love-of-variety in the agriculture sector. Specifically, when the elasticity of substitution between home and foreign agricultural goods is finite (i.e., $\eta > 0$), tariff reductions can reallocate land use between countries in a way that lowers the global land use while maintaining or increasing the consumption quantity of agriculture. As we demonstrate below, channel (a) dominates at high levels of trade openness whereas channel (b) dominates at low levels of trade openness. That is, the love-of-variety effect, that is operative through channel (b), is dominant only when there is sufficient difference between the imported versus domestic land content of agricultural consumption.

[5]Note that the fraction $1-\Lambda_A = \frac{t_A}{1+t_A}(1-\pi_A)$ is received by households as a lump sum transfer. Since preferences are homothetic, the increase in households' income does not change demand for agriculture *relative* to manufacturing, and so, it does not change demand for land relative to labor, or the land rent relative to wage. Consequently, this income effect does not have a direct effect on the sectoral expenditure share on agriculture.

Let us now unpack the above two channels:

$$\frac{\mathrm{d}\Lambda_A}{-\mathrm{d}\ln(1+t_A)} = \underbrace{\left(1-\pi_A^D\right)\frac{\mathrm{d}\left(\frac{t_A}{1+t_A}\right)}{\mathrm{d}\ln(1+t_A)}}_{\text{Channel (a)}} + \underbrace{\frac{t_A}{1+t_A}\frac{\mathrm{d}\pi_A^D}{\mathrm{d}\ln(1+t_A)}}_{\text{Channel (b)}}.$$

After some algebra, the combined effect of channels (a) and (b) can be expressed as:

$$\frac{\mathrm{d}\ln\Lambda_A}{-\mathrm{d}\ln(1+t_A)} = \frac{(1-\pi_A)}{1+t_A\pi_A}\left[1-(\eta-1)\,t_A\pi_A\right] \tag{B.16}$$

By replacing Equation (B.16) into (B.15), we obtain the following expression for the land use impact of a global uniform reduction in agricultural tariffs:

$$\frac{\mathrm{d}\ln L}{-\mathrm{d}\ln(1+t_A)} = \frac{N_M}{N}(1-\pi_A)\times\left[\sigma-\frac{t_A\pi_A}{1+t_A\pi_A}\eta\right], \tag{B.17}$$

We now determine the sign of the above expression. Consider the critical tariff rate t_A^* (and its corresponding domestic expenditure share, π_A^*) as the solution to the following equation:

$$h(t_A^*) = t_A^*\times\pi_A^D(t_A^*) - \frac{\sigma}{\eta-\sigma} = 0, \qquad \text{with} \quad \pi_A^D(t_A^*) = \frac{1}{\left(1+t_A^*\right)^{1-\eta}+1} \tag{B.18}$$

Since $h(.)$ is continuous with $h(0)<0$ and $h(\infty)>0$ (provided that $\eta>\sigma$), the Intermediate Value Theorem implies that there exists some positive t_A^*, and since $h'>0$, this solution is unique. Therefore, provided that $\eta>\sigma$ as the empirically relevant case, the term $\left[\sigma-\frac{t_A\pi_A}{1+t_A\pi_A}\eta\right]$ in Equation B.17 is negative when $t<t_A^*$ and it becomes positive when $t>t_A^*$. We are now prepared to produce the tariff-based counterpart to Proposition 2.

Proposition 5. *(Multilateral reduction in agricultural tariffs)* Suppose $\eta>\sigma$. A worldwide uniform *decrease* in agricultural tariffs in a system of symmetric economies leads to an *increase* in the global stock of land at low level of trade openness (when $t<t_A^*$) and a *decrease* in the global stock of land at high levels of trade openness (when $t_A>t_A^*$) where $t_A^*>0$ is the solution to Equation (B.18).

B.2.1.5 Proof of Proposition 3

Under the assumptions of the proposition, countries only differ in their productivity to produce agriculture and manufacturing, $Z_{i,A}$ and $Z_{i,M}$. Note that, because we assume that $Z_{i,T}$ is the same across countries, the productivity of the land-producing sector is not a source of comparative or absolute advantage in agriculture. In steady state, country i's unit cost to produce agricultural goods boils down to

$$c_{i,A} = \frac{1}{Z_{i,A}Z_T/\delta}w_i.$$

We next characterize the autarky and free-trade equilibria.

Autarky. In autarky, the assumption that preferences are Cobb-Douglas with equal weights between agriculture and manufacturing implies that each country allocates half its labor to each sector.

Free trade. In the free trade equilibrium, the assumption that goods are homogeneous in each sector implies there is a single relative price of agriculture relative to manufacturing. We denote this price by p^*. All countries whose autarkic relative price of agriculture, Z is lower than p^* completely specialize in agriculture, while the rest completely specialize in manufacturing:

$$\begin{cases} \text{Country } i \text{ produces agriculture} & \text{if } \frac{Z_{i,A}}{Z_{i,M}} \leq p^* \\ \text{Country } i \text{ produces manufacturing} & \text{if } \frac{Z_{i,A}}{Z_{i,M}} > p^* \end{cases}$$

Let country i^* be the the marginal country for which the above holds with equality:

$$p^* = \frac{Z_{i^*,M}}{Z_{i^*,A}} \tag{B.19}$$

Next, note that with Cobb-Douglas preferences, global expenditure on agriculture is the same as that on manufacturing. Therefore, market clearing requires:

$$p^* = \frac{\int_0^{i^*} Z_{i,M} di}{\int_{i^*}^1 Z_{i,A} di}. \tag{B.20}$$

An equilibrium consists of a cutoff country i^* and an equilibrium relative price of agriculture p^*, such that these equations B.19 and B.20 jointly hold. The right-hand side of equation B.19 is decreasing in i^* by our choice of ordering. The right-hand side of equation B.20 is strictly increasing, and moreover, equals zero at $i^* = 0$ and tends to infinity as $i^* \to 1$. This means the equilibrium exists and is unique. This proves result (i) in Proposition 3.

To determine the total demand for factors under free trade, we rearrange equation B.20 as

$$\frac{1 - n_A}{n_A} = \frac{\mathbb{E}\left[Z_{i,A} | i \geq i^*\right] / Z_{i^*,A}}{\mathbb{E}\left[Z_{i,M} | i < i^*\right] / Z_{i^*,M}}. \tag{B.21}$$

where $n_A \equiv N_N/N$ is the labor share in agriculture. Since all countries have the same size, free trade increases the amount of labor in agriculture relative to autarky if $n_A > 1/2$. Therefore, we focus on sufficient conditions such that the right hand side of B.21 is greater or smaller than one. When there is positive selection into sector $g \in \{A, M\}$, the average country specializing in that sector is more productive than the marginal country, i.e.,

$$\mathbb{E}\left[Z_{i,g} | i \geq i^*\right] / Z_{i^*,g} > 1,$$

while the opposite is true with negative selection.

We distinguish two cases to obtain result (ii) in Proposition 3. First, suppose $Z_{i,M}$ is increasing in i. Given our ordering of countries this implies that $Z_{i,A}$ is also increasing in i at a larger rate than $Z_{i,M}$.

Since countries with $i > i^*$ fully specialize in agriculture, this ensures that both $\mathbb{E}\left[Z_{i,A}|i \geq i^*\right]/Z_{i^*,A} > 1$ and $\mathbb{E}\left[Z_{i,M}|i < i^*\right]/Z_{i^*,M} < 1$, which yields part (a). To obtain part (b), proceed analogously supposing instead that $Z_{i,A}$ is decreasing in i.

B.3 Extensions

B.3.1 Fallow Land

This section provides an extension to our model for incorporating *fallow* land. For a clearer exposition, we drop country subscript i. The country area, H, is the sum of forest area, F, and *cleared* land, L, which is itself classified into *usable* land L_u and *fallow* land L_o,

$$H = F + L, \qquad L = L_u + L_o.$$

As before, we denote the cleared land's frontier by z, and (new to this extension) the utilization rate in the cleared land by u. Namely:

$$z = \frac{L}{H}, \qquad u = \frac{L_u}{L}.$$

Land-producing sector. Land-producing firms seek to produce usable land for agricultural use by converting (1) forest or (2) fallow land. Production in each of these two sub-sectors requires the employment of labor under decreasing-returns-to-scale technologies. Labor is freely mobile between the two sub-sectors, and so, the marginal product of labor must equalize between them. Moreover, we assume that the flows of land-conversion from forest or fallow land provide homogeneous land, and so, at any point in time, there is a single market price q for purchases that add to the usable land.

Production of usable land via forest conversion. Land-producing firms can employ labor to convert forest into usable land:

$$x^{f\to u} = \phi_f \times N_f^{\gamma_f}; \qquad \textit{where} \quad \phi_f \equiv \bar{\phi}_f \times F^{\lambda_f}, \quad \gamma_f \in (0,1)$$

The production technology is decreasing-returns-to-scale implying an upward-sloping supply curve with an inverse supply elasticity of $(1-\gamma_f)/\gamma_f > 0$. The productivity parameter, ϕ_f, depends on the current stock of forest. Each land-producing firm, however, takes the stock of forest as given, and so, it does not internalize the deforestation effects of its production decision on its future productivity. The extent to which forest stock affects the productivity of the forest-to-land-conversion is governed by parameter $\lambda_f > 0$. The above equation can be equivalently expressed as:

$$x^{f\to u} = \zeta_f \times (1-z)^{\lambda_f} \times N_f^{\gamma_f}, \qquad \gamma_f \in (0,1) \tag{B.22}$$

where $\zeta_f \equiv \bar{\phi}_f H^{-\lambda_f}$ is a constant. Note, under $J(z) = \zeta_f \times (1-z)^{\lambda_f}$, the above resembles equation 2.8.

Production of usable land via fallow land. Land-producing firms can also employ labor to convert fallow land into usable land:

$$x^{o\to u} = \phi_o \times N_o^{\gamma_o}; \qquad \text{where} \quad \phi_o \equiv \bar{\phi}_o \times L_o^{\lambda_o}, \quad \gamma_o \in (0,1)$$

The functional form which we have adopted for the conversion of fallow land to usable land is similar to that of forest to usable land. The parameters, however, are different reflecting the differences in the quantitative behavior of the two activities. Similarly, we can express the above equation as:

$$x^{o\to u} = \zeta_o \times (z(1-u))^{\lambda_o} \times N_o^{\gamma_o}, \qquad \gamma_o \in (0,1) \tag{B.23}$$

where $\zeta_o \equiv \bar{\phi}_o H^{-\lambda_o}$ is a constant.

Wage and price in the land-producing sector. Since labor is freely mobile within the land-producing sector, the marginal product of labor equalizes between the two sub-sectors, which in turn pins down the wage rate w_T,

$$w_T \;=\; \gamma_o\zeta_o \times (z(1-u))^{\lambda_o} \times N_o^{\gamma_o-1} \;=\; \gamma_f\zeta_f \times (1-z)^{\lambda_f} \times N_f^{\gamma_f-1} \tag{B.24}$$

Moreover, since the two sub-sectors produce a homogenous usable land, they face the same price level q which intersects the supply curves of the two sub-sectors. This relationship can be expressed as:

$$q \;=\; \frac{w_T}{\gamma_f\zeta_f\,(1-z)^{\lambda_f}} N_f^{1-\gamma_f} \;=\; \frac{w_T}{\gamma_o\zeta_o\,(z(1-u))^{\lambda_o}} N_o^{1-\gamma_o} \tag{B.25}$$

Free entry condition & Value function. Let v_f and v_o denote the per-unit discounted present value of usable land when converted, respectively, from forest and fallow land. The no-arbitrage condition requires the return to land-conversion to be equal between the two sub-sectors, $v_f = v_o = v$, and the free entry condition requires:

$$v = q. \tag{B.26}$$

Similar to the model in Section 2.4, the value function is given by:

$$\rho v = r + \dot{v} - (\delta_o + \delta_f) \tag{B.27}$$

where r is (as before) the rental rate of usable land, and (new to this extension) δ_o and δ_f are respectively the regrowth rates of fallow land and forest.

Law of motion. The fallow land evolves according to:

$$\dot{L_o} = -x^{o\to u} - \delta_f \overbrace{(1-u)zH}^{L_o} + \delta_o \overbrace{uzH}^{L_u}, \tag{B.28}$$

where $(x^{o \to u})$ is the out-flow from fallow land to usable land, $\delta_f L_o$ is the outflow from fallow land to forest, and $(\delta_o L_u)$ is the in-flow from the usable land to fallow land. Similarly, the forest area evolves according to:

$$\dot{F} = -x^{f \to u} + \delta_f z H \tag{B.29}$$

where $\delta_f z H$ is the inflow to forest from usable and fallow land. The above two equations, in turn, pin down the law of motion for usable land:

$$\dot{L}_u = x^{f \to u} + x^{o \to u} - (\delta_o + \delta_f) u z H \tag{B.30}$$

Here, in contrast to the model presented in Section 2.4, generically $\dot{L}_u \neq -\dot{F}$. Under this extension, therefore, the expansion of agricultural land use can be different from the loss of forest area. For our quantitative analysis, this is an important consideration because our empirical findings suggest that in response to demand shocks the agricultural land use may expand at a different rate than the rate of deforestation.

B.4 Details of Calibration

B.4.1 Trade costs

Our calibration of trade costs follows a three step procedure. Recall that we parametrize trade costs as follows

$$d_{ij,g} = (1 + \kappa_{ij,g}) \left(1 + t^{ice}_{ij,g}\right) \left(1 + t^{rev}_{ij,g}\right)$$

where $\kappa_{ij,g}$ is an iceberg trade cost unrelated to policy, $t^{ice}_{ij,g}$ is an iceberg trade cost generated by policy, and $t^{rev}_{ij,g}$ is a non-iceberg trade cost that generates revenues.

Step 1 - Recover trade costs $d_{ij,g}$ from gravity equations.

In the first step, we follow common practices in the empirical gravity literature and estimate the following regression:

$$\log\left(X_{ij,g}\right) = \alpha_{i,g} + \beta_{j,g} + \epsilon_{ij,g}$$

where $\alpha_{i,g}$ is an origin fixed effect, $\beta_{j,g}$ is a destination fixed effect and $\epsilon_{ij,g}$ is the residual. Here, the residual equals $(1 - \sigma_g) \log\left(d_{ij,g}\right)$. Assuming that $d_{ii,g} = 1$, we recover $d_{ij,g} = exp\left(\widehat{\epsilon}_{ij,g} / \left(1 - \sigma_g\right)\right)$, where $\widehat{\epsilon}_{ij,g}$ are the estimates of the residual term.

Step 2 - Separate policy trade costs from non-policy trade costs.

In the second step, we run regressions of $d_{ij,g}$ against observables related to policy barriers. We start by defining

$$d_{ij,g} = \underbrace{\tilde{d}_{ij,g} \exp\left(\gamma X_{ij,g}^{geography}\right)}_{\equiv(1+\kappa_{ij,g})} \underbrace{\exp\left(\beta X_{ij,g}^{policy}\right)}_{\equiv\left(1+t_{ij,g}^{ice}\right)\left(1+t_{ij,g}^{rev}\right)},$$

where $X_{ij,g}^{policy}$ are observables related to policy barriers and $X_{ij,g}^{geography}$ are observables related to geography. For convenience, we re-define the policy variables $X_{ij,g}^{policy}$ so that $X_{ij,g}^{policy} = 0$ represents the "no-policy" barrier case.[6] Taking logs, we estimate

$$\log\left(d_{ij,g}\right) = \gamma X_{ij,g}^{geography} + \beta X_{ij,g}^{policy} + \log\left(\tilde{d}_{ij,g}\right)$$

which gives $\widehat{\gamma}$, $\widehat{\beta}$, and $\widehat{\log\left(\tilde{d}_{ij,g}\right)}$. Lastly, by setting $X_{ij,g}^{policy} = 0$, we can recover the trade barriers that are unrelated to policy

$$(1+\kappa_{ij,g}) = \exp\left(\widehat{\gamma} X_{ij,g}^{geography} + \log\left(\tilde{d}_{ij,g}\right)\right).$$

Using the above expression, we can recover the policy barriers as:

$$\left(1+t_{ij,g}^{ice}\right)\left(1+t_{ij,g}^{rev}\right) = \frac{d_{ij,g}}{(1+\kappa_{ij,g})}.$$

Step 3 - Separate iceberg trade costs from non-icerberg trade costs generated by policy.

In the third and final step, we make the assumption that $t_{ij,g}^{ice}$ is proportional to $t_{ij,g}^{rev}$

$$t_{ij,g}^{ice} = \omega_j t_{ij,g}^{rev}.$$

We calibrate ω_j so that the model matches, for each destination country, the tariff revenues per agricultural GDP observed in the data.

[6] For example, our "free trade agreement" dummy variable is defined as 1 if a country does not have a free-trade, and 0 otherwise.

B.5 Additional Tables and Figures

Table B.1: Mapping of Countries to Regions

ISO	Region	Individual Country
ARG	Argentina	ARG
AUS	Australia	AUS
BOL	Bolivia	BOL
BRA	Brazil	BRA
CAN	Canada	CAN
CHN	China	CHN
CMR	Cameroon	CMR
COL	Colombia	COL
DEU	Germany	DEU
ESP	Spain	ESP
ETH	Ethiopia	ETH
FIN	Finland	FIN
FRA	France	FRA
GBR	United Kingdom	GBR
IDN	Indonesia	IDN
IND	India	IND
ITA	Italy	ITA
JPN	Japan	JPN
MEX	Mexico	MEX
MOZ	Mozambique	MOZ
MYS	Malaysia	MYS
NGA	Nigeria	NGA
PER	Peru	PER
PRY	Paraguay	PRY
RUS	Russia	RUS
SWE	Sweden	SWE
THA	Thailand	THA
TUR	Turkey	TUR
TZA	Tanzania	TZA
USA	USA	USA
VEN	Venezuela	VEN
XAM	Rest of America	ABW, AIA, ATG, BES, BHS, BLM, BLZ, BMU, BRB, CHL, CRI, CUB, CUW, CYM, DMA, DOM ECU, FLK, GRD, GTM, GUF, GUY, HND, HTI, JAM, KNA, LCA, MAF, MSR, NIC, PAN, PRI SJM, SLV, SPM, SUR, SXM, TCA, TTO, URY, VCT, VGB, VIR
XAS	Rest of Asia	AFG, ASM, BGD, BRN, BTN, COK, FJI, FSM, GUM, HKG, KAZ, KGZ, KHM, KIR, KOR, LAO LKA, MDV, MHL, MMR, MNG, MNP, NCL, NIU, NPL, NRU, NZL, PAK, PCN, PHL, PLW, PNG PRK, PYF, SGP, SLB, TJK, TKL, TKM, TLS, TON, TUV, TWN, UZB, VNM, VUT, WLF, WSM
XCF	Central Africa	AGO, CAF, COD, COG, GAB, GNQ, RWA, STP, TCD
XEU	Rest of Europe	ALB, AND, AUT, BEL, BGR, BIH, BLR, CHE, CZE, DNK, EST, FRO, GGY, GIB, GRC, HRV HUN, IMN, IRL, ISL, JEY, LIE, LTU, LUX, LVA, MCO, MDA, MKD, MLT, MNE, NLD, NOR POL, PRT, ROU, SMR, SRB, SVK, SVN, UKR, VAT
XMN	Rest of Mena	ARE, ARM, AZE, BHR, CYP, DZA, EGY, ESH, GEO, IRN, IRQ, ISR, JOR, KWT, LBN, LBY MAR, OMN, PSE, QAT, SAU, SYR, TUN, YEM
XOF	Other Africa	BDI, BWA, COM, DJI, ERI, KEN, LSO, MDG, MUS, MWI, MYT, NAM, SDN, SOM, SSD, SWZ SYC, UGA, ZAF
XWF	Rest of West Africa	BEN, BFA, CIV, CPV, GHA, GIN, GMB, GNB, LBR, MLI, MRT, NER, SEN, SHN, SLE, TGO
ZMB	Zambia	ZMB
ZWE	Zimbabwe	ZWE

Table B.2: Summary Statistics by Regions (1990-2020)

	% of Global	% area in 1990		Change in Forest			% of Global
	Forest	Forest	Utilized	%	p.p.	Total	Deforestation
Country	(1)	(2)	(3)	(4)	(5).	(6)	(7)
Russia	19.50	51	61	0.02	0.01	0.13	-0.05
Brazil	14.33	68	99	-17.07	-11.68	-99.94	34.32
Canada	8.41	39	45	-4.33	-1.68	-14.89	5.11
Central Africa	7.54	60	70	-13.44	-8.01	-41.36	14.21
USA	6.97	41	73	-0.79	-0.32	-2.24	0.77
Rest of Asia	4.54	26	68	-9.58	-2.45	-17.76	6.10
Australia	3.25	29	62	-0.94	-0.27	-1.24	0.43
Indonesia	2.90	59	91	-26.01	-15.43	-30.79	10.58
China	2.77	13	69	19.73	2.52	22.29	-7.66
Other Africa	2.62	22	54	-17.41	-3.87	-18.61	6.39
Rest of America	2.55	47	72	-5.16	-2.45	-5.38	1.85
Rest of West Africa	1.91	18	41	-21.50	-3.86	-16.78	5.76
Peru	1.87	66	75	-6.49	-4.29	-4.94	1.70
Rest of Europe	1.79	25	77	5.56	1.41	4.07	-1.40
Mexico	1.73	47	87	-7.03	-3.33	-4.96	1.70
Colombia	1.59	69	99	-9.48	-6.58	-6.15	2.11
India	1.43	15	87	1.15	0.17	0.67	-0.23
Bolivia	1.41	68	82	-12.14	-8.31	-7.01	2.41
Tanzania	1.39	64	100	-20.49	-13.06	-11.65	4.00
Venezuela	1.26	63	82	-13.04	-8.27	-6.73	2.31
Zambia	1.16	82	89	-5.48	-4.51	-2.59	0.89
Mozambique	1.06	89	100	-15.39	-13.62	-6.67	2.29
Argentina	0.84	14	56	-21.20	-2.92	-7.30	2.51
Sweden	0.69	67	78	-0.30	-0.20	-0.08	0.03
Nigeria	0.64	26	97	-18.47	-4.76	-4.85	1.67
Paraguay	0.63	64	100	-37.55	-23.93	-9.59	3.29
Rest of Mena	0.57	3	11	6.88	0.18	1.60	-0.55
Cameroon	0.55	44	69	-9.80	-4.32	-2.20	0.76
Finland	0.54	69	80	2.44	1.69	0.53	-0.18
Turkey	0.47	26	76	11.78	3.07	2.27	-0.78
Ethiopia	0.46	15	74	-16.14	-2.40	-3.05	1.05
Malaysia	0.46	57	83	-6.78	-3.87	-1.27	0.44
Zimbabwe	0.46	58	79	-7.16	-4.13	-1.34	0.46
Thailand	0.43	30	82	-7.40	-2.25	-1.31	0.45
Japan	0.36	47	81	0.60	0.28	0.09	-0.03
France	0.32	22	83	14.69	3.26	1.92	-0.66
Spain	0.29	27	87	33.64	9.13	4.02	-1.38
Italy	0.17	22	85	26.34	5.75	1.86	-0.64
Germany	0.14	15	85	1.05	0.16	0.06	-0.02
United Kingdom	0.01	2	84	0.00	0.00	0.00	0.00
World	100.00	36	65	-7.13	-2.59	-291.17	100.00

Notes: This table reports summary statistics of changes in forest area between 1990 and 2020 based on the Forest Resource Assessment report of 2020 from FAO. Column 1 is based on forest area as of 1990. Column 2 shows percentage change in forest area between 1990 and 2020. Column 3 shows percentage change in agricultural land use area year. Column 4 shows the share of global forest coming from each region.

Table B.3: Counterfactual Changes in Forest Area

		Baseline			Baseline + Pop. growth			
ISO	Region	BAU(pp)	C1(pp)	C2(pp)	BAU(pp)	C1(pp)	C2(pp)	Pop. growth(%)
ARG	Argentina	-0.00	0.08	-0.33	-1.33	0.07	-0.26	39.3
AUS	Australia	-0.00	0.31	-1.65	-7.91	0.28	-1.58	94.6
BOL	Bolivia	-0.00	0.14	0.52	-7.25	0.13	0.56	73.1
BRA	Brazil	-0.00	-3.53	-1.12	0.08	-3.74	-1.20	-7.7
CAN	Canada	-0.00	0.37	-2.08	-6.44	0.28	-1.62	67.5
CHN	China	-0.00	0.28	1.96	1.57	0.26	1.99	-20.4
CMR	Cameroon	-0.00	0.10	-0.06	-18.08	0.05	0.08	343.6
COL	Colombia	-0.00	0.14	0.42	-0.31	0.14	0.22	-0.0
DEU	Germany	-0.00	0.15	-0.37	-0.55	0.14	-0.38	-8.6
ESP	Spain	-0.00	0.23	-0.92	1.33	0.27	-1.23	-28.7
ETH	Ethiopia	-0.00	0.02	-0.01	-5.40	0.01	-0.04	235.9
FIN	Finland	-0.00	0.32	-0.87	-0.18	0.30	-0.94	-2.0
FRA	France	-0.00	0.23	-0.41	-1.71	0.22	-0.83	3.0
GBR	United Kingdom	0.02	0.01	-0.06	-0.11	0.01	-0.06	24.4
IDN	Indonesia	-0.00	0.29	3.03	-2.95	0.25	3.05	32.6
IND	India	-0.00	0.05	1.57	-0.91	0.05	1.61	17.2
ITA	Italy	-0.00	0.19	-0.31	2.08	0.20	-0.65	-32.5
JPN	Japan	-0.00	0.19	1.19	6.89	0.26	0.98	-41.5
MEX	Mexico	-0.00	0.17	0.14	-2.43	0.15	0.14	24.0
MOZ	Mozambique	-0.00	0.84	5.33	-22.73	0.47	3.86	425.5
MYS	Malaysia	-0.00	0.20	0.32	-3.78	0.17	0.35	42.1
NGA	Nigeria	-0.00	0.00	0.07	-10.83	0.00	0.04	362.4
PER	Peru	-0.00	0.06	1.32	-3.43	0.06	1.39	34.9
PRY	Paraguay	-0.00	0.15	-1.05	-4.46	0.16	-0.82	39.8
RUS	Russia	-0.00	0.29	1.13	-0.32	0.30	0.44	-11.7
SWE	Sweden	-0.00	0.34	-2.43	-4.68	0.38	-2.54	38.9
THA	Thailand	-0.00	0.36	0.70	3.85	0.33	0.54	-31.5
TUR	Turkey	-0.00	0.21	0.56	-2.00	0.20	0.34	19.1
TZA	Tanzania	-0.00	0.04	1.45	-23.94	0.03	0.93	544.1
USA	USA	-0.00	0.31	-1.01	-2.82	0.23	-0.87	40.3
VEN	Venezuela	-0.00	0.26	1.02	-2.29	0.23	1.01	20.4
XAM	Rest of America	-0.00	0.21	-0.16	-2.69	0.18	-0.13	29.3
XAS	Rest of Asia	-0.00	0.16	1.63	-2.39	0.14	1.64	49.6
XCF	Central Africa	-0.00	0.43	4.25	-21.05	0.28	3.04	468.1
XEU	Rest of Europe	-0.00	0.16	0.05	0.94	0.18	-0.37	-26.0
XMN	Rest of Mena	-0.00	0.09	1.21	-2.39	0.07	0.91	98.7
XOF	Other Africa	-0.00	0.07	1.31	-6.29	0.04	0.76	249.8
XWF	Rest of West Africa	-0.00	0.07	0.17	-9.64	0.03	0.12	405.5
ZMB	Zambia	-0.00	0.05	-0.31	-25.61	0.04	-0.47	499.3
ZWE	Zimbabwe	-0.00	0.12	0.94	-11.67	0.12	0.81	143.9
World		-0.00	-0.07	0.55	-3.97	-0.12	0.35	40.0

Notes: Columns 1 to 3 report results from our first baseline scenario (in percentage points). Column "BAU" reports the change in steady state relative to time 0; Columns "C1" and "C2" report the steady state change in each counterfactual, relative to the steady state in BAU. Columns 4 to 6 repeat the same results, for the baseline scenario that includes population growth. The last column contains the changes in population we feed into the model, in percentage terms relative to time 0.

Table B.4: Summary Statistics by Country (1990-2020) - First Part

	% of Global	% area in 1990		Change in Forest			% of Global
	Forest	Forest	Utilized	%	p.p.	Total	Deforestation
Country	(1)	(2)	(3)	(4)	(5).	(6)	(7)
Russia	19.50	51	61	0.02	0.01	0.13	-0.05
Brazil	14.33	68	99	-17.07	-11.68	-99.94	34.32
Canada	8.41	39	45	-4.33	-1.68	-14.89	5.11
USA	6.97	41	73	-0.79	-0.32	-2.24	0.77
DRC	3.69	70	77	-16.26	-11.40	-24.48	8.41
Australia	3.25	29	62	-0.94	-0.27	-1.24	0.43
Indonesia	2.90	59	91	-26.01	-15.43	-30.79	10.58
China	2.77	13	69	19.73	2.52	22.29	-7.66
Angola	1.92	92	100	-15.97	-14.76	-12.50	4.29
Peru	1.87	66	75	-6.49	-4.29	-4.94	1.70
Mexico	1.73	47	87	-7.03	-3.33	-4.96	1.70
Colombia	1.59	69	99	-9.48	-6.58	-6.15	2.11
India	1.43	15	87	1.15	0.17	0.67	-0.23
Bolivia	1.41	68	82	-12.14	-8.31	-7.01	2.41
Tanzania	1.39	64	100	-20.49	-13.06	-11.65	4.00
Venezuela	1.26	63	82	-13.04	-8.27	-6.73	2.31
Zambia	1.16	82	89	-5.48	-4.51	-2.59	0.89
Mozambique	1.06	89	100	-15.39	-13.62	-6.67	2.29
Myanmar	0.96	47	81	-28.25	-13.17	-11.07	3.80
Papua New Guinea	0.89	79	83	-1.50	-1.19	-0.54	0.19
Argentina	0.84	14	56	-21.20	-2.92	-7.30	2.51
Central Africa	0.81	28	47	-3.71	-1.06	-1.22	0.42
Sweden	0.69	67	78	-0.30	-0.20	-0.08	0.03
Nigeria	0.64	26	97	-18.47	-4.76	-4.85	1.67
Paraguay	0.63	64	100	-37.55	-23.93	-9.59	3.29
Gabon	0.58	98	100	-0.97	-0.95	-0.23	0.08
Sudan	0.57	14	48	-22.26	-3.20	-5.22	1.79
Cameroon	0.55	44	69	-9.80	-4.32	-2.20	0.76
Republic of Congo	0.54	91	95	-1.66	-1.51	-0.37	0.13
Finland	0.54	69	80	2.44	1.69	0.53	-0.18
Turkey	0.47	26	76	11.78	3.07	2.27	-0.78
Ethiopia	0.46	15	74	-16.14	-2.40	-3.05	1.05
Botswana	0.46	57	64	-18.87	-10.69	-3.55	1.22
Malaysia	0.46	57	83	-6.78	-3.87	-1.27	0.44
Zimbabwe	0.46	58	79	-7.16	-4.13	-1.34	0.46
Guyana	0.46	97	100	-1.00	-0.97	-0.19	0.06
Thailand	0.43	30	82	-7.40	-2.25	-1.31	0.45
South Africa	0.40	7	17	-6.04	-0.40	-0.99	0.34
Laos	0.40	71	84	-8.70	-6.16	-1.41	0.49
Suriname	0.38	97	99	-1.19	-1.15	-0.18	0.06
Japan	0.36	47	81	0.60	0.28	0.09	-0.03
Ecuador	0.36	56	80	-15.09	-8.43	-2.20	0.76
Mongolia	0.35	30	69	-1.27	-0.38	-0.18	0.06
Chile	0.33	22	31	10.49	2.28	1.43	-0.49
Madagascar	0.33	42	75	-9.99	-4.16	-1.34	0.46
Mali	0.33	13	23	-4.24	-0.57	-0.56	0.19
France	0.32	22	83	14.80	3.27	1.91	-0.66
Norway	0.30	32	38	-0.49	-0.16	-0.06	0.02
Spain	0.29	27	87	33.64	9.13	4.02	-1.38
Mena	0.29	3	14	11.47	0.38	1.34	-0.46

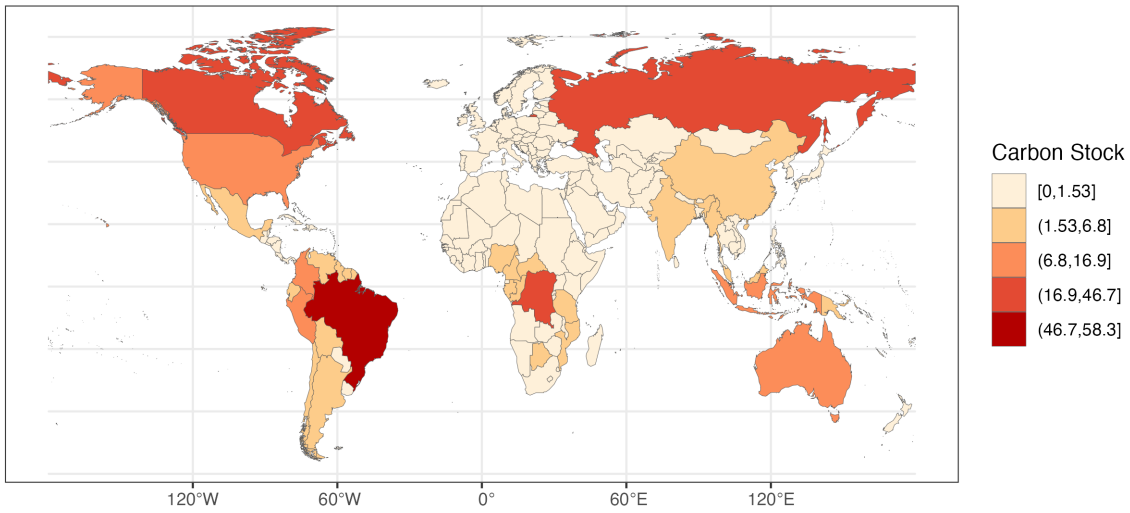
Table B.5: Summary Statistics by Country (1990-2020) - Second Part

	% of Global	% area in 1990		Change in Forest			% of Global
	Forest	Forest	Utilized	%	p.p.	Total	Deforestation
Country	(1)	(2)	(3)	(4)	(5).	(6)	(7)
Cambodia	0.27	58	88	-31.75	-18.57	-3.47	1.19
Ghana	0.24	49	99	-22.13	-10.94	-2.19	0.75
Senegal	0.23	53	94	-13.32	-7.06	-1.23	0.42
Poland	0.22	27	91	6.77	1.86	0.60	-0.21
Namibia	0.21	19	26	-24.29	-4.54	-2.13	0.73
Vietnam	0.21	21	60	19.27	4.05	1.66	-0.57
Liberia	0.21	95	100	-10.95	-10.42	-0.93	0.32
Somalia	0.20	34	56	-27.81	-9.51	-2.30	0.79
Other South America	0.20	96	98	-1.50	-1.44	-0.12	0.04
Cote Divoire	0.19	30	81	-64.01	-19.41	-5.02	1.72
New Zealand	0.19	35	97	-0.42	-0.15	-0.03	0.01
Burkina Faso	0.19	24	68	-21.59	-5.24	-1.66	0.57
Phillipines	0.18	22	68	-9.08	-2.00	-0.68	0.23
Guinea	0.18	33	86	-15.26	-4.98	-1.10	0.38
Italy	0.17	22	85	26.34	5.75	1.86	-0.64
Honduras	0.17	60	92	-8.99	-5.44	-0.63	0.22
Chad	0.16	6	32	-36.11	-2.31	-2.43	0.83
Belarus	0.16	36	84	-0.32	-0.11	-0.02	0.01
Nicaragua	0.16	50	87	-47.78	-23.90	-3.06	1.05
Romania	0.14	28	91	3.27	0.91	0.19	-0.07
North Korea	0.14	47	79	-12.79	-5.98	-0.74	0.25
Germany	0.14	15	85	1.05	0.16	0.06	-0.02
Nepal	0.14	27	78	2.82	0.76	0.16	-0.05
Morocco	0.13	20	67	-1.15	-0.22	-0.06	0.02
Oceania	0.13	61	74	1.35	0.83	0.07	-0.02
Benin	0.12	35	70	-35.47	-12.35	-1.71	0.59
Guatemala	0.12	38	87	-29.04	-10.97	-1.38	0.47
Pakistan	0.12	4	68	-26.64	-1.09	-1.26	0.43
Ukraine	0.12	9	87	2.87	0.27	0.13	-0.05
South Korea	0.11	44	91	-13.32	-5.85	-0.62	0.21
Panama	0.11	65	90	-9.75	-6.31	-0.45	0.15
Turkmenistan	0.10	24	57	0.00	0.00	0.00	0.00
Balkans	0.10	33	84	26.07	8.64	1.06	-0.36
Kenya	0.09	7	50	-6.68	-0.47	-0.25	0.08
Uganda	0.08	13	82	-45.01	-6.04	-1.53	0.53
Portugal	0.08	39	79	-2.56	-1.01	-0.09	0.03
Malawi	0.08	32	84	-35.59	-11.45	-1.20	0.41
Greece	0.08	30	97	18.30	5.48	0.58	-0.20
Sierra Leone	0.08	52	79	-19.44	-10.13	-0.61	0.21
Costa Rica	0.07	57	100	2.34	1.33	0.07	-0.02
Latvia	0.07	51	91	3.03	1.53	0.09	-0.03
Georgia	0.07	44	84	1.93	0.86	0.05	-0.02
Kazakhstan	0.06	3	49	14.69	0.43	0.39	-0.13
Czech Republic	0.06	26	87	1.81	0.48	0.05	-0.02
Bhutan	0.06	53	63	8.72	4.66	0.22	-0.07
Serbia	0.06	24	89	14.64	3.45	0.33	-0.11
Guinea-Bissau	0.05	69	100	-11.37	-7.89	-0.25	0.09
Bosnia	0.05	49	84	-1.00	-0.49	-0.02	0.01
Sri Lanka	0.05	29	78	-11.00	-3.21	-0.23	0.08
Austria	0.05	29	79	9.37	2.72	0.19	-0.07

Table B.6: Summary Statistics by Country (1990-2020) - Third Part

	% of Global	% area in 1990		Change in Forest			% of Global
	Forest	Forest	Utilized	%	p.p.	Total	Deforestation
Country	(1)	(2)	(3)	(4)	(5).	(6)	(7)
Estonia	0.05	47	85	10.54	4.92	0.21	-0.07
Niger	0.05	2	20	-49.54	-0.82	-0.94	0.32
Bangladesh	0.05	5	98	-6.49	-0.30	-0.12	0.04
Hungary	0.04	20	92	13.18	2.64	0.24	-0.08
Croatia	0.04	31	77	6.42	1.97	0.11	-0.04
Cuba	0.04	17	81	58.35	9.65	1.00	-0.34
Belize	0.04	68	76	-20.23	-13.80	-0.32	0.11
Dominican Republic	0.04	27	88	24.16	6.46	0.38	-0.13
Lithuania	0.04	26	84	3.65	0.95	0.06	-0.02
Uzbekistan	0.03	4	61	4.92	0.22	0.07	-0.02
Togo	0.03	27	82	-14.34	-3.86	-0.19	0.07
West Africa	0.03	2	6	-16.68	-0.30	-0.20	0.07
Afghanistan	0.03	3	34	0.00	0.00	0.00	0.00
Slovakia	0.03	29	88	1.17	0.34	0.01	-0.00
Eritrea	0.03	16	78	-11.25	-1.84	-0.13	0.04
West Europe	0.03	23	71	14.38	3.36	0.15	-0.05
Kyrgyzstan	0.02	9	29	11.12	0.97	0.11	-0.04
Timor Leste	0.02	63	86	-4.36	-2.76	-0.04	0.01
Caribbean	0.02	42	61	-1.89	-0.79	-0.02	0.01
Macedonia	0.02	41	86	9.81	4.05	0.09	-0.03
Albania	0.02	28	70	0.01	0.00	0.00	-0.00
El Salvador	0.02	25	100	-20.13	-5.08	-0.14	0.05
Azerbaijan	0.02	10	57	26.74	2.59	0.17	-0.06
Uruguay	0.01	4	87	42.21	1.81	0.25	-0.09
Denmark	0.01	10	87	18.25	1.89	0.10	-0.03
Jamaica	0.01	45	92	14.83	6.68	0.08	-0.03
Tunisia	0.01	4	49	-0.57	-0.03	-0.00	0.00
Gambia	0.01	31	99	-41.66	-13.02	-0.17	0.06
Brunei	0.01	76	81	-9.04	-6.90	-0.04	0.01
Haiti	0.01	10	80	-15.00	-1.44	-0.06	0.02
Netherlands	0.01	6	81	7.00	0.42	0.02	-0.01
United Kingdom	0.01	2	84	0.00	0.00	0.00	0.00
Armenia	0.01	13	44	-3.43	-0.46	-0.01	0.00
Puerto Rico	0.01	27	89	54.94	14.91	0.18	-0.06
Swaziland	0.01	27	98	33.06	9.06	0.10	-0.03
Tajikistan	0.01	3	22	3.77	0.10	0.01	-0.00
Belgium	0.01	5	77	8.70	0.44	0.02	-0.01
Libya	0.01	0	2	0.00	0.00	0.00	0.00
Rwanda	0.00	5	93	-38.24	-1.96	-0.08	0.03
East Africa	0.00	25	76	-4.87	-1.23	-0.01	0.00
Moldova	0.00	6	87	-6.31	-0.38	-0.01	0.00
Ireland	0.00	1	90	32.68	0.34	0.03	-0.01
Egypt	0.00	0	9	2.67	0.00	0.00	-0.00
Central America	0.00	36	76	-3.32	-1.19	-0.00	0.00
Lesotho	0.00	2	57	0.00	0.00	0.00	0.00
Singapore	0.00	15	48	5.01	0.77	0.00	-0.00
Iceland	0.00	0	4	12.18	0.02	0.00	-0.00
Djibouti	0.00	0	15	0.00	0.00	0.00	0.00
Maldives	0.00	3	30	0.00	0.00	0.00	0.00
World	100.00	36	65	-7.13	-2.58	-291.17	100.00

Figure B.1: Carbon Stock per Hectare across the World



Notes: This figure shows, for each country, the carbon content of forests, measured as tons of carbon per hectare of forest, which we use to compute the CO_2 emissions from deforestation. Data comes from FRA-FAO.

Figure B.2: Model Fit

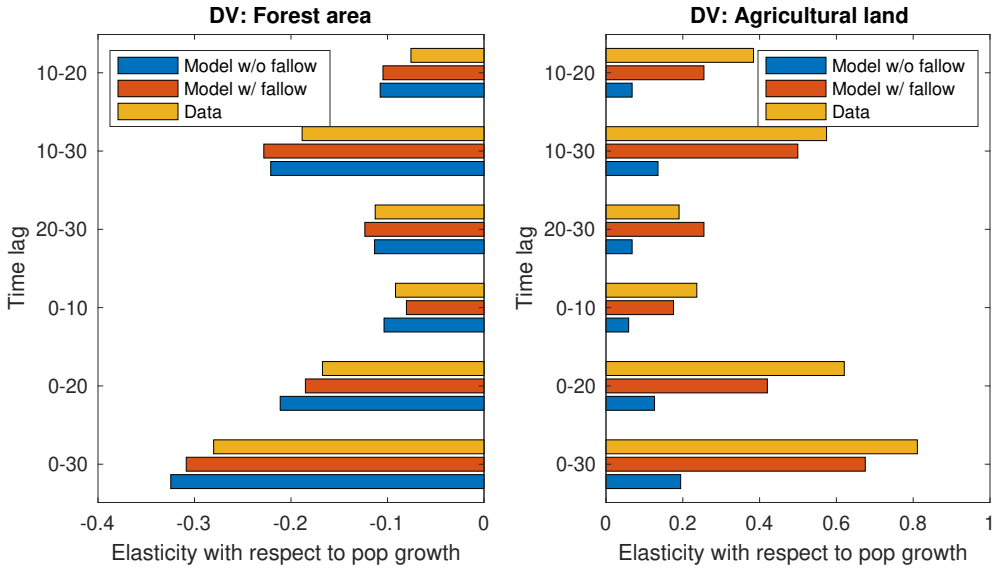
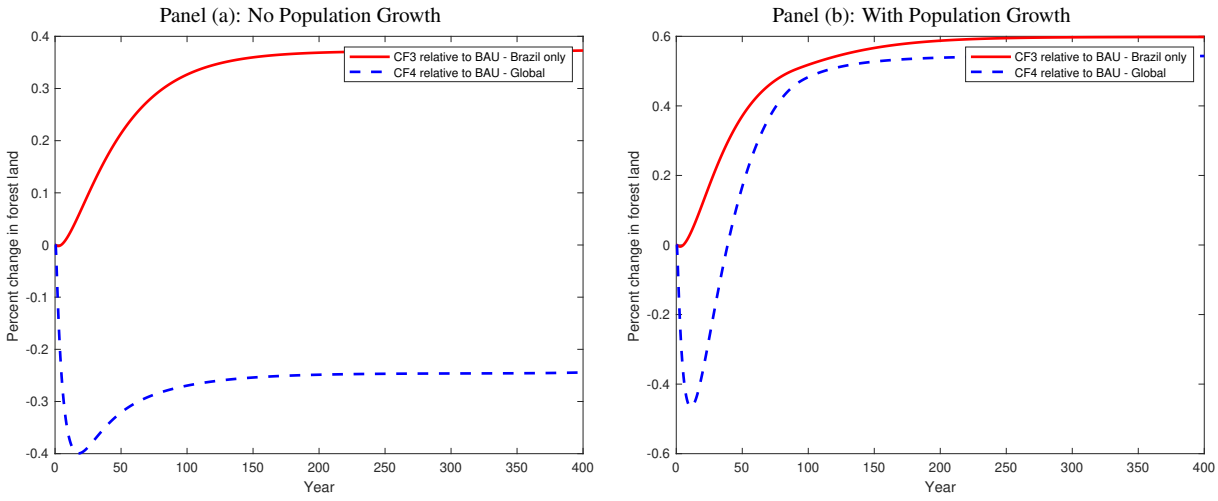


Figure B.3: Multilateral vs Unilateral Trade Cost Increase: Change in Global Forest Area



APPENDIX C

Appendix to Chapter 3

C.1 Data and Bloc Assignment

Table C.1: Country List

Country code	Country name	Country code	Country name
AUS	Australia	KAZ	Kazakhstan
ARG	Argentina	KHM	Cambodia
AUT	Austria	KOR	Korea
BEL	Belgium	LAO	Lao People's Democratic Republic
BGR	Bulgaria	LTU	Lithuania
BRA	Brazil	LUX	Luxembourg
BRN	Brunei Darussalam	LVA	Latvia
CAN	Canada	MAR	Morocco
CHE	Switzerland	MEX	Mexico
CHL	Chile	MLT	Malta
CHN	China	MMR	Myanmar
COL	Colombia	MYS	Malaysia
CRI	Costa Rica	NLD	Netherlands
CYP	Cyprus	NOR	Norway
CZE	Czech Republic	NZL	New Zealand
DEU	Germany	PER	Peru
DNK	Denmark	PHL	Philippines
ESP	Spain	POL	Poland
EST	Estonia	PRT	Portugal
FIN	Finland	ROU	Romania
FRA	France	ROW	Rest of the World
GBR	United Kingdom	RUS	Russian Federation
GRC	Greece	SAU	Saudi Arabia
HKG	Hong Kong	SGP	Singapore
HRV	Croatia	SVK	Slovak Republic
HUN	Hungary	SVN	Slovenia
IDN	Indonesia	SWE	Sweden
IND	India	THA	Thailand
IRL	Ireland	TUN	Tunisia
ISL	Iceland	TUR	Turkey
ISR	Israel	USA	United States
ITA	Italy	VNM	Viet Nam
JPN	Japan	ZAF	South Africa

Notes: This table displays the list of countries included in our quantitative model.

Table C.2: Sector Key

ICIO code	ICIO description	Sector code	Sector description
01T02	Agriculture, hunting, forestry	1	Agriculture, hunting, forestry and fishing
03	Fishing and aquaculture	1	Agriculture, hunting, forestry and fishing
05T06	Mining and quarrying, energy producing products	2	Mining and quarrying, energy producing products
07T08	Mining and quarrying, non-energy producing products	3	Other mining and quarrying
09	Mining support service activities	3	Other mining and quarrying
10T12	Food products, beverages and tobacco	4	Food products, beverages and tobacco
13T15	Textiles, textile products, leather and footwear	5	Textiles, textile products, leather and footwear
16	Wood and products of wood and cork	6	Wood products, paper products and printing
17T18	Paper products and printing	6	Wood products, paper products and printing
19	Coke and refined petroleum products	7	Coke and refined petroleum products
20	Chemical and chemical products	8	Chemical products
21	Pharmaceuticals	8	Chemical products
22	Rubber and plastics products	8	Chemical products
23	Other non-metallic mineral products	9	Other non-metallic mineral products
24	Basic metals	10	Metal products
25	Fabricates metal products	10	Metal products
26	Computer, electronic and optical equipment	11	Computer, electronic and optical equipment
27	Electrical equipment	12	Electrical equipment
28	Machinery and equipment nec	13	Machinery and equipment nec
29	Motor vehicles, trailers and semi-trailers	13	Machinery and equipment nec
30	Other transport equipment	13	Machinery and equipment nec
31T33	Manufacturing nec	14	Manufacturing nec
35	Electricity, gas, steam and air conditioning supply	15	Electricity, gas, steam and water supply
36T39	Water supply; sewage, waste management	15	Electricity, gas, steam and water supply
41T43	Construction	16	Construction
45T47	Wholesale and retail trade; repair of motor vehicles	17	Wholesale and retail trade; repair of motor vehicles
49	Land transport and transport via pipelines	18	Transportation and postal services
50	Water transport	18	Transportation and postal services
51	Air transport	18	Transportation and postal services
52	Warehousing and support activities for transportation	18	Transportation and postal services
53	Postal and courier activities	18	Transportation and postal services
55T56	Accommodation and food service activities	19	Accommodation and food service activities
58T60	Publishing, audiovisual and broadcasting activities	20	Broadcasting, telecommunications and IT services
61	Telecommunications	20	Broadcasting, telecommunications and IT services
62T63	IT and other information services	20	Broadcasting, telecommunications and IT services
64T66	Financial and insurance activities	21	Financial, real estate, professional and administrative services
68	Real estate activities	21	Financial, real estate, professional and administrative services
69T75	Professional, scientific and technical activities	21	Financial, real estate, professional and administrative services
77T82	Administrative and support services	21	Financial, real estate, professional and administrative services
84	Public administration and defense	22	Public administration, education and other services
85	Education	22	Public administration, education and other services
86T88	Human health and social work activities	22	Public administration, education and other services
90T93	Arts, entertainment and recreation	22	Public administration, education and other services
94T96	Other service activities	22	Public administration, education and other services
97T98	Activities of households as employers	22	Public administration, education and other services

Table C.3: Bloc Assignment, 187 Countries (2015-2023)

Country	Bloc	Country	Bloc	Country	Bloc	Country	Bloc
AUT	USA	BDI	CHN	AZE	Unaligned	LAO	Unaligned
BGD	USA	BFA	CHN	BEL	Unaligned	LBN	Unaligned
BHS	USA	BLR	CHN	BEN	Unaligned	LBR	Unaligned
CYP	USA	BOL	CHN	BGR	Unaligned	LUX	Unaligned
DEU	USA	BRA	CHN	BHR	Unaligned	MAC	Unaligned
DNK	USA	BTN	CHN	BIH	Unaligned	MAR	Unaligned
EGY	USA	CAN	CHN	BLZ	Unaligned	MDA	Unaligned
ERI	USA	CIV	CHN	BMU	Unaligned	MDG	Unaligned
ETH	USA	COD	CHN	BRB	Unaligned	MDV	Unaligned
FJI	USA	COG	CHN	BRN	Unaligned	MEX	Unaligned
FRO	USA	COL	CHN	BWA	Unaligned	MKD	Unaligned
GHA	USA	DMA	CHN	CAF	Unaligned	MMR	Unaligned
GNB	USA	DOM	CHN	CHE	Unaligned	MNG	Unaligned
GNQ	USA	ECU	CHN	CHL	Unaligned	MOZ	Unaligned
GRL	USA	GAB	CHN	CMR	Unaligned	MUS	Unaligned
HRV	USA	GIN	CHN	COM	Unaligned	MWI	Unaligned
IND	USA	GTM	CHN	CPV	Unaligned	NAM	Unaligned
JPN	USA	HND	CHN	CRI	Unaligned	NER	Unaligned
KOR	USA	ISR	CHN	CZE	Unaligned	NGA	Unaligned
LTU	USA	KGZ	CHN	DJI	Unaligned	NRU	Unaligned
LVA	USA	KWT	CHN	DZA	Unaligned	OMN	Unaligned
MLI	USA	LCA	CHN	ESP	Unaligned	PAK	Unaligned
MNE	USA	LSO	CHN	EST	Unaligned	PER	Unaligned
MRT	USA	MLT	CHN	FIN	Unaligned	PHL	Unaligned
NIC	USA	MYS	CHN	FRA	Unaligned	POL	Unaligned
NLD	USA	NCL	CHN	GBR	Unaligned	PRT	Unaligned
NOR	USA	NPL	CHN	GEO	Unaligned	PRY	Unaligned
SGP	USA	NZL	CHN	GIB	Unaligned	QAT	Unaligned
SOM	USA	PAN	CHN	GMB	Unaligned	ROU	Unaligned
SSD	USA	PNG	CHN	GRC	Unaligned	SEN	Unaligned
SWE	USA	PYF	CHN	GUY	Unaligned	SRB	Unaligned
SYR	USA	RUS	CHN	HKG	Unaligned	SUR	Unaligned
TGO	USA	RWA	CHN	HTI	Unaligned	SVK	Unaligned
THA	USA	SAU	CHN	HUN	Unaligned	SVN	Unaligned
TUR	USA	SLB	CHN	IDN	Unaligned	SWZ	Unaligned
TUV	USA	SLE	CHN	IRL	Unaligned	SYC	Unaligned
UGA	USA	SLV	CHN	IRN	Unaligned	TLS	Unaligned
UKR	USA	STP	CHN	IRQ	Unaligned	TON	Unaligned
URY	USA	TCD	CHN	ISL	Unaligned	TUN	Unaligned
UZB	USA	TJK	CHN	ITA	Unaligned	TZA	Unaligned
VCT	USA	TKM	CHN	JAM	Unaligned	VEN	Unaligned
VUT	USA	TTO	CHN	JOR	Unaligned	VNM	Unaligned
WSM	USA	ALB	Unaligned	KAZ	Unaligned	WBG	Unaligned
ABW	CHN	ARG	Unaligned	KEN	Unaligned	YEM	Unaligned
AFG	CHN	ARM	Unaligned	KHM	Unaligned	ZAF	Unaligned
AGO	CHN	ATG	Unaligned	KIR	Unaligned	ZMB	Unaligned
ARE	CHN	AUS	Unaligned	KNA	Unaligned	ZWE	Unaligned

Notes: A country is assigned to the USA bloc if $d\ln\tau_i^{USA} < 0$ and $d\ln\tau_i^{CHN} > 0$. Similarly, a country is assigned to the CHN bloc if $d\ln\tau_i^{CHN} < 0$ and $d\ln\tau_i^{USA} > 0$. All other countries are assigned to the Unaligned bloc.

C.2 Quantification

This section presents how to solve for the equilibrium change following a change in exogenous trade costs $\hat{\tau}^f_{mnj}$ and $\hat{\tau}^x_{mi,nj}$ and potential exogenous change in trade deficit $\hat{D}_n$. The following system of equations determines output $\hat{Y}_{nj}$, prices $\hat{P}_{nj}$, consumption sectoral shares $\hat{\pi}^f_{mj}$, final trade shares $\hat{\pi}^f_{nmj}$, intermediate sectoral shares $\hat{\pi}^x_{j,mi}$, intermediate trade shares $\hat{\pi}^x_{nj,mi}$, and sectoral wages $\hat{W}_{nj}$:

$$\left(\hat{P}_{nj}\hat{Y}_{nj}\right)\left(P_{nj}Y_{nj}\right) = \sum_m \left(\sum_i \eta_i \left(\hat{P}_{mi}\hat{Y}_{mi}\right)\left(P_{mi}Y_{mi}\right) + \hat{D}_m D_m\right)\pi^f_{mj}\hat{\pi}^f_{mj}\pi^f_{nmj}\hat{\pi}^f_{nmj} + \sum_m \sum_i \left(1-\eta_i\right)\left(\hat{P}_{mi}\hat{Y}_{mi}\right)\left(P_{mi}Y_{mi}\right)\pi^x_{j,mi}\hat{\pi}^x_{j,mi}\hat{\pi}^x_{nj,mi}\pi^x_{nj,mi}$$

$$\hat{\pi}^f_{nj} = \frac{\left(\hat{P}^F_{nj}\right)^{1-\rho}}{\sum_k \pi^f_{nk,t}\left(\hat{P}^F_{nk}\right)^{1-\rho}}$$

where $\hat{P}^F_{nj} = \left[\sum_m \pi^f_{mnj,t}(\widehat{\tilde{\tau}^f_{mnj}}\hat{P}_{mj})^{1-\gamma}\right]$

$$\hat{\pi}^f_{mnj,t+1} = \frac{\left(\widehat{\tau^f_{mnj}}\hat{P}_{mj}\right)^{1-\gamma}}{\sum_k \pi^f_{knj,t}\left(\widehat{\tau^f_{knj}}\hat{P}_{kj}\right)^{1-\gamma}}$$

$$\hat{\pi}^x_{i,nj,t+1} = \frac{\left(\hat{P}^X_{i,nj}\right)^{1-\varepsilon}}{\sum_k \pi^x_{k,nj,t}\left(\hat{P}^X_{k,nj}\right)^{1-\varepsilon}}$$

where $\hat{P}^X_{i,nj} = \left[\sum_i \pi^x_{mi,nj,t}\left(\widehat{\tau^x_{mi,nj}}\hat{P}_{mi}\right)^{1-\nu}\right]^{\frac{1}{1-\nu}}$

$$\hat{\pi}^x_{mi,nj,t+1} = \frac{\left(\widehat{\tilde{\tau}^x_{mi,nj}}\hat{P}_{mj}\right)^{1-\nu}}{\sum_k \pi^x_{ki,nj,t}\left(\widehat{\tilde{\tau}^x_{ki,nj}}\hat{P}_{kj}\right)^{1-\nu}}$$

$$\hat{P}_{nj} = \left(\hat{Z}_{nj}\right)^{-1}\hat{W}_{nj}^{(1-\alpha_j)\eta_j}\left(\hat{P}_{nj}\hat{Y}_{nj}\right)^{\alpha_j\eta_j}\left(\hat{K}_{nj}\right)^{-\alpha_j\eta_j}\left(\hat{P}^X_{nj}\right)^{1-\eta_j}$$

where $\hat{P}^X_{nj} = \left[\sum_i \pi^x_{i,nj,t}\left(\hat{P}^X_{i,nj}\right)^{1-\varepsilon}\right]^{\frac{1}{1-\varepsilon}}$

$$\hat{W}_{nj}\left(\frac{\hat{W}_n}{\hat{P}_n}\right)^{\psi}\left(\frac{\hat{W}_{nj}}{\hat{W}_n}\right)^{\mu-1} = \hat{P}_{nj}\hat{Y}_{nj}$$

where $\hat{W}_n = \left(\sum \pi^H_{nj} \left(\hat{W}_{nj}\right)^{\mu}\right)^{\frac{1}{\mu}}$, $\hat{P}_n = \left[\sum_j \pi^f_{nj,t} (\hat{P}^F_{nj})^{1-\rho}\right]$

The following algorithm provides a numerical solution to the above system of equations:

1. Guess $\hat{P}_{nj}$

2. Solve for $\hat{\pi}^f_{nj}$, $\hat{\pi}^f_{mnj}$, $\hat{\pi}^x_{i,nj}$, $\hat{\pi}^x_{mi,nj}$ using:

$$\hat{\pi}^f_{nj} = \frac{\left(\hat{P}^F_{nj}\right)^{1-\rho}}{\sum_k \pi^f_{nk,t} \left(\hat{P}^F_{nk}\right)^{1-\rho}}$$

where $\hat{P}^F_{nj} = \left[\sum_m \pi^f_{mnj,t} (\widehat{\tau^f_{mnj}} \hat{P}_{mj})^{1-\gamma}\right]$

$$\hat{\pi}^f_{mnj} = \frac{\left(\widehat{\tau^f_{mnj}} \hat{P}_{mj}\right)^{1-\gamma}}{\sum_k \pi^f_{knj,t} \left(\widehat{\tau^f_{knj}} \hat{P}_{kj}\right)^{1-\gamma}}$$

$$\hat{\pi}^x_{i,nj} = \frac{\left(\hat{P}^X_{i,nj}\right)^{1-\varepsilon}}{\sum_k \pi^x_{k,nj,t} \left(\hat{P}^X_{k,nj}\right)^{1-\varepsilon}}$$

where $\hat{P}^X_{i,nj} = \left[\sum_i \pi^x_{mi,nj,t} \left(\widehat{\tilde{\tau}^x_{mi,nj}} \hat{P}_{mi}\right)^{1-\nu}\right]^{\frac{1}{1-\nu}}$

$$\hat{\pi}^x_{mi,nj} = \frac{\left(\widehat{\tilde{\tau}^x_{mi,nj}} \hat{P}_{mj}\right)^{1-\nu}}{\sum_k \pi^x_{ki,nj,t} \left(\widehat{\tilde{\tau}^x_{ki,nj}} \hat{P}_{kj}\right)^{1-\nu}}$$

3. Solve for $\hat{P}_{nj}\hat{Y}_{nj}$ using the new trade shares

$$\begin{aligned}\left(\hat{P}_{nj}\hat{Y}_{nj}\right)(P_{nj}Y_{nj}) = &\sum_m \left(\sum_i \eta_i \left(\hat{P}_{mi}\hat{Y}_{mi}\right)(P_{mi}Y_{mi}) + \hat{D}_m D_m\right) \pi^f_{mj}\hat{\pi}^f_{mj}\pi^f_{nmj}\hat{\pi}^f_{nmj} \\ &+ \sum_m \sum_i (1-\eta_i)\left(\hat{P}_{mi}\hat{Y}_{mi}\right)(P_{mi}Y_{mi})\,\pi^x_{j,mi}\hat{\pi}^x_{j,mi}\hat{\pi}^x_{nj,mi}\pi^x_{nj,mi}\end{aligned}$$

4. Solve for wages $\hat{W}_{nj}$ using

$$\hat{W}_{nj}\left(\frac{\hat{W}_n}{\hat{P}_n}\right)^{\psi}\left(\frac{\hat{W}_{nj}}{\hat{W}_n}\right)^{\mu-1} = \hat{P}_{nj}\hat{Y}_{nj}$$

5. Solve for prices $\hat{P}_{nj}$

$$\hat{P}_{nj} = \left(\hat{Z}_{nj}\right)^{-1} \hat{W}_{nj}^{(1-\alpha_j)\eta_j} \left(\hat{P}_{nj}\hat{Y}_{nj}\right)^{\alpha_j\eta_j} \left(\hat{K}_{nj}\right)^{-\alpha_j\eta_j} \left(\hat{P}_{nj}^{X}\right)^{1-\eta_j}$$

where $\hat{P}_{nj}^{X} = \left[\sum_i \pi_{i,nj,t}^{x} \left(\hat{P}_{i,nj}^{X}\right)^{1-\varepsilon}\right]^{\frac{1}{1-\varepsilon}}$

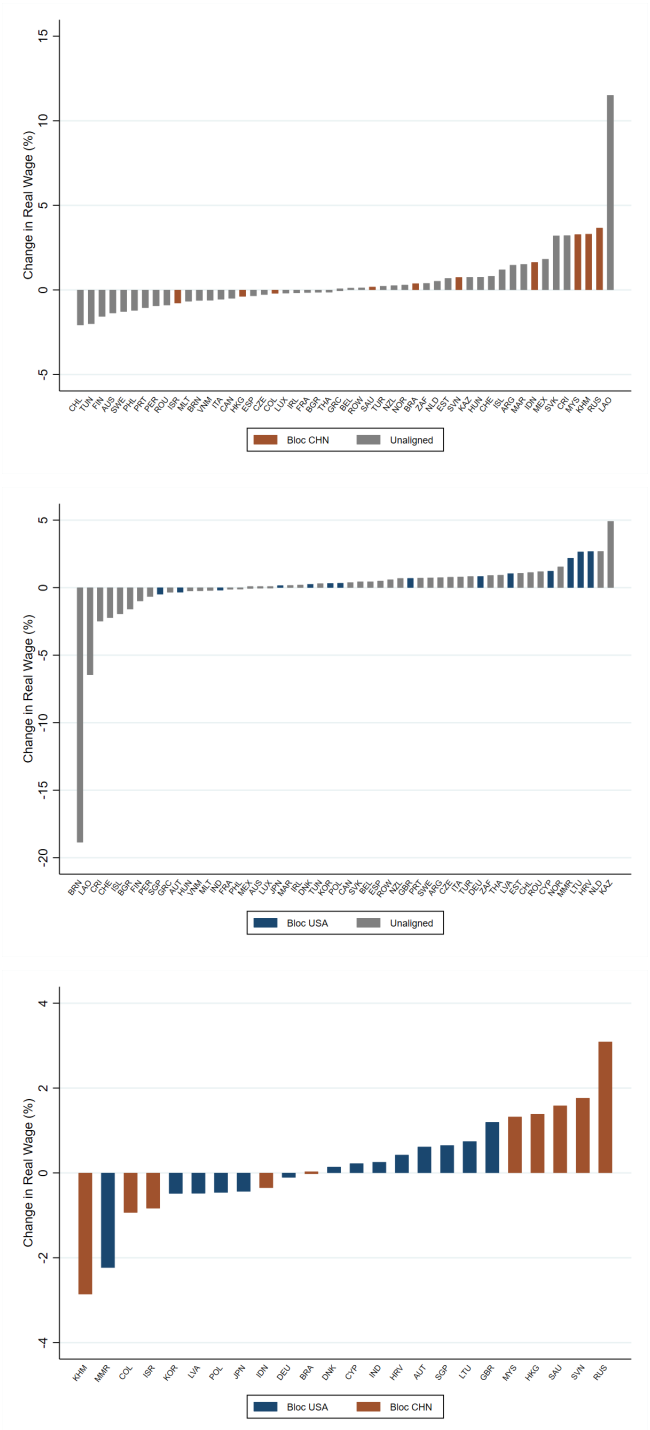
6. Go back to 1

Table C.4: Bloc Assignment, 66 Model Countries (2015-2023)

Country	Bloc	Country	Bloc	Country	Bloc
AUT	USA	MYS	CHN	ITA	Unaligned
CYP	USA	RUS	CHN	KAZ	Unaligned
DEU	USA	SAU	CHN	LAO	Unaligned
DNK	USA	SVN	CHN	LUX	Unaligned
GBR	USA	ARG	Unaligned	MAR	Unaligned
HRV	USA	AUS	Unaligned	MEX	Unaligned
IND	USA	BEL	Unaligned	MLT	Unaligned
JPN	USA	BGR	Unaligned	NLD	Unaligned
KOR	USA	BRN	Unaligned	NOR	Unaligned
LTU	USA	CAN	Unaligned	NZL	Unaligned
LVA	USA	CHE	Unaligned	PER	Unaligned
MMR	USA	CHL	Unaligned	PHL	Unaligned
POL	USA	CRI	Unaligned	PRT	Unaligned
SGP	USA	CZE	Unaligned	ROU	Unaligned
USA	USA	ESP	Unaligned	ROW	Unaligned
BRA	CHN	EST	Unaligned	SVK	Unaligned
CHN	CHN	FIN	Unaligned	SWE	Unaligned
COL	CHN	FRA	Unaligned	THA	Unaligned
HKG	CHN	GRC	Unaligned	TUN	Unaligned
IDN	CHN	HUN	Unaligned	TUR	Unaligned
ISR	CHN	IRL	Unaligned	VNM	Unaligned
KHM	CHN	ISL	Unaligned	ZAF	Unaligned

Notes: The x-axis refers to the change in trade costs with the US, measured as $d\ln\tau_i^{USA} = \frac{1}{2}\left[\left(\frac{1}{1-\gamma}\hat{w}_{i,USA} + d\ln\tau^{base}\right) + \left(\frac{1}{1-\gamma}\hat{w}_{USA,i} + d\ln\tau^{base}\right)\right]$, where $\hat{w}_{ij}$ is recovered from equation (3.1) and $d\ln\tau^{base}$ is calibrated to match the change in trade/GDP ratio. Similarly, the y-axis refers to the change in trade costs with China, measured as $d\ln\tau_i^{CHN} = \frac{1}{2}\left[\left(\frac{1}{1-\gamma}\hat{w}_{i,CHN} + d\ln\tau^{base}\right) + \left(\frac{1}{1-\gamma}\hat{w}_{CHN,i} + d\ln\tau^{base}\right)\right]$

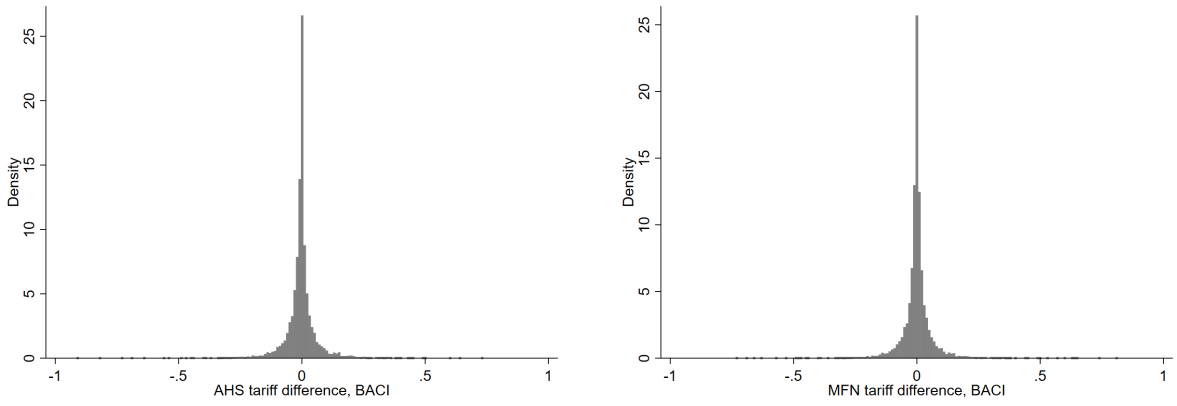
Figure C.1: Counterfactual Real Income Changes (2015-2023)



Notes: Each bar in each plot shows the percentage change in real income for each country, relative to factual, when the country is moved to a different bloc.

C.3 Additional exercises and robustness

Figure C.2: Bilateral Tariff Changes, 2021-2015



(a) Effectively applied tariff (AHS) (b) Most favored nation tariff (MFN)

Notes: Figure shows histogram of the non-zero changes in bilateral average tariffs between 2021-2015.
Sources: BACI, TRAINS.

C.3.1 Community detection algorithm

In this section we perform an alternative exercise where we classify countries into blocs using a community detection algorithm. More specifically, we use the Leiden algorithm (Traag et al. 2019), which is designed to find non-overlapping communities in large networks.

In the first step, we run the regression

$$\Delta \ln x_{mn}^{2023-2015} = \alpha_m + \alpha_n + \varepsilon_{mn},$$

where $\Delta \ln x_{mn}^{2023-2015}$ is the log-change in aggregate trade flows from source m to destination n between 2015 and 2023, while α_m and α_n are source and destination fixed effects, respectively. As in the main text, the trade data we use comes from the Direction of Trade Statistics (DOTS) dataset and has an annual frequency.

Then, we recover the predicted residual $\widehat{\varepsilon_{mn}}$ and calculate the undirected trade weight w_{mn} as

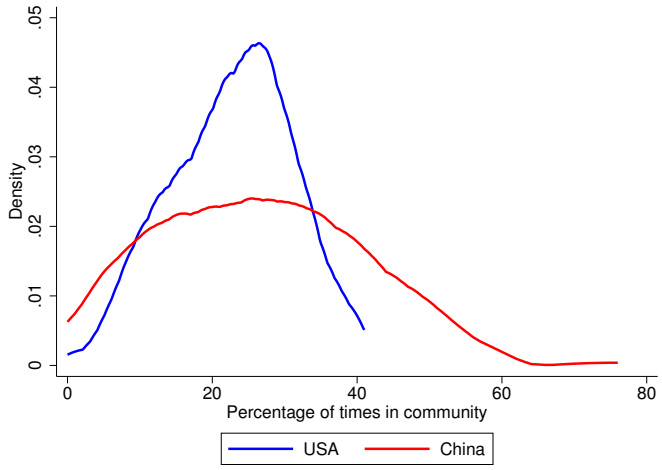
$$w_{mn} = \frac{\widehat{\varepsilon_{mn}} + \widehat{\varepsilon_{mn}}}{2}.$$

The undirected trade weight w_{mn} captures the average effect of the trade occurring between countries m and n that is not due to source-specific or destination-specific characteristics. With this measure, we rule out the effect of countries that increased or decreased trade with all their partners between 2015 and 2023, focusing only on the bilateral effects. Because $w_{mn} = w_{nm}$, we drop any repeated pair from our dataset.

In the next step, we run the Leiden algorithm using the undirected trade weights w_{mn} as inputs. In terms of the country trade-based network, the larger the weight between two countries, the stronger their link and vice versa. We perform 100 draws of the Leiden algorithm, where each draw returns a list of communities to which each country belongs.[1] Intuitively, a community is a group of countries with particularly strong links between them with respect to the other countries. Moreover, because communities are non-overlapping, a country may not belong to more than one community.

As we run the algorithm 100 times, we can calculate the percentage of times each country belongs to the same community as the US or China out of the total draws. Let p_{USA} be the percentage of times a country belongs to the same community as the US and p_{CHN} be the percentage of times a country belongs to the same community as China. We present the density of these percentages in Figure C.3.

Figure C.3: Density of Percentages, Leiden Algorithm



Notes: Figure shows the density of the percentage of times a country belongs to the same community as the US and the same community as China. Each observation is a country.

We now introduce a frequency-based classification of countries into blocs. First, we classify a country as belonging to the US bloc if $p_{USA} > 0.2$ and $p_{USA} > p_{CHN}$. Second, we classify a country as belonging to the China bloc if $p_{CHN} > 0.2$ and $p_{CHN} > p_{USA}$. Finally, we classify a country as unaligned if $p_{USA} < 0.2$ and $p_{CHN} < 0.2$.

[1] We perform 100 draws because the Leiden algorithm contains a random component. We only count draws where (i) USA and China belong in different communities and (ii) there are 5 communities or less.

Table C.5: Bloc Comparison, Community Detection Algorithm and Baseline Classification

		Baseline		
		USA bloc	China bloc	Unaligned
Community detection, Leiden alg.	USA bloc	24	10	32
	China bloc	11	28	57
	Unaligned	7	7	10

Notes: Table shows number of countries in each bloc according to each classification.

Table C.5 presents the comparison between the blocs resulting from the community detection algorithm and the baseline classification. We see that after using a different method to classify countries into blocs, we get similar results to the baseline ones. The baseline procedure is more conservative in classifying more countries as unaligned. However, for the 73 countries assigned by both procedures to either the USA or China bloc, 52 (or 71%) are assigned to the same bloc.

C.3.2 Start year: 2016

Table C.6: Bloc Comparison, Baseline 2015 versus Baseline 2016 (All Countries)

		Baseline 2015		
		USA bloc	China bloc	Unaligned
Baseline 2016	USA bloc	31	2	18
	China bloc	2	38	10
	Unaligned	11	7	71

Notes: Table shows number of countries in each bloc according to each classification. USA(CHN) bloc includes USA(CHN) itself.

Table C.7: Bloc Comparison, Baseline 2015 versus Baseline 2016 (Model Countries)

		Baseline 2015		
		USA bloc	China bloc	Unaligned
Baseline 2016	USA bloc	12	0	5
	China bloc	0	6	2
	Unaligned	3	5	33

Notes: Table shows the number of countries in each bloc according to each classification. USA(CHN) bloc includes USA(CHN) itself.

Table C.8: Log Change in Average Trade Cost between Blocs (Model Countries, 2016-2023)

$\downarrow$ Exporter | Importer $\rightarrow$	Bloc USA	Bloc CHN	Unaligned	Overall
Bloc USA	-0.051	0.040	-0.034	-0.027
Bloc CHN	0.081	-0.150	-0.020	0.019
Unaligned	-0.053	-0.059	-0.050	-0.053
Overall	-0.020	-0.027	-0.037	-0.010

Notes: We classify countries into 3 groups, Bloc USA, Bloc CHN, and Unaligned. Then, all country pairs are classified into 9 group pairs. We report the average $\Delta \ln \tau_{mn} + \Delta \ln \tau^{base}$ for country pairs belonging to each group pair, weighted by bilateral trade flows in 2016. The Overall column is the average $\Delta \ln \tau_{mn} + \Delta \ln \tau^{base}$ of all trade flows from(to) each exporter(importer) group.

Table C.9: Baseline Change in GDP and Real Income (2016-2023)

Bloc	GDP			Real Income		
	Median	p25	p75	Median	p25	p75
Overall	1.262	0.720	1.868	1.257	0.748	1.919
Bloc USA	0.774	0.210	1.135	0.815	0.203	1.137
Bloc CHN	1.672	0.903	2.554	1.855	0.895	2.562
Unaligned	1.581	0.839	2.521	1.607	0.846	2.519

Notes: Baseline change in GDP and real income are reported in percentage changes.

C.3.3 Placebo: 2002-2007

Table C.10: Bloc Comparison, Baseline 2015 versus Baseline 2002 (Model Countries)

		Baseline 2015		
		USA bloc	China bloc	Unaligned
Baseline 2002	USA bloc	5	3	9
	China bloc	1	2	0
	Unaligned	9	6	31

Notes: Table shows the number of countries in each bloc according to each classification. USA(CHN) bloc includes USA(CHN) itself.

Table C.11: Log Change in Average Trade Cost between Blocs (Model Countries, 2002-2007)

$\downarrow$ Exporter | Importer $\rightarrow$	Bloc USA	Bloc CHN	Unaligned	Overall
Bloc USA	-0.081	0.081	-0.140	-0.102
Bloc CHN	-0.032	-0.063	-0.135	-0.075
Unaligned	-0.159	-0.085	-0.196	-0.176
Overall	-0.122	-0.009	-0.174	-0.145

Notes: We classify countries into 3 groups, Bloc USA, Bloc CHN, and Unaligned. Then, all country pairs are classified into 9 group pairs. We report the average $\Delta \ln \tau_{mn} + \Delta \ln \tau^{base}$ for country pairs belonging to each group pair, weighted by bilateral trade flows in 2002. The Overall column is the average $\Delta \ln \tau_{mn} + \Delta \ln \tau^{base}$ of all trade flows from(to) each exporter(importer) group.

Table C.12: Log Change in Average Trade Costs between 2015 Blocs (Model Countries, 2002-2007)

↓ Exporter | Importer →	Bloc USA	Bloc CHN	Unaligned	Overall
Bloc USA	-0.145	-0.004	-0.139	-0.124
Bloc CHN	-0.118	-0.015	-0.172	-0.127
Unaligned	-0.165	-0.124	-0.180	-0.167
Overall	-0.152	-0.055	-0.160	-0.145

Notes: Using 2015 blocs, we classify countries into 3 groups, Bloc USA, Bloc CHN, and Unaligned. Then, all country pairs are classified into 9 group pairs. We report the average $\Delta \ln \tau_{mn} + \Delta \ln \tau^{base}$ for country pairs belonging to each group pair, weighted by bilateral trade flows in 2002. The Overall column is the average $\Delta \ln \tau_{mn} + \Delta \ln \tau^{base}$ of all trade flows from(to) each exporter(importer) group.

C.3.4 Validation of the trade cost estimates

For each 8-year period since 2000 for which the ICIO dataset is available, we compute the Head and Ries ratio to back out estimates of trade cost changes implied by trade data including own-trade data. Starting from the gravity equation in changes:

$$d \ln X_{mn} = \eta_m + \gamma_n + (1-\gamma)\, d \ln \tau_{mn}, \tag{C.1}$$

we can recover the change in bilateral trade cost from:

$$\tilde{\tau}_{mn}^{HR} = \Delta_{t,t-8} \left(\ln \tau_{mn} + \ln \tau_{nm} \right) = \frac{1}{(1-\gamma)} \Delta_{t,t-8} \ln \left(\frac{X_{mn}}{X_{nn}} * \frac{X_{nm}}{X_{mm}} \right). \tag{C.2}$$

For every 8-year period from 2000-2008 to 2010-2018, we compute $\tilde{\tau}_{mn}^{HR}$ from trade data, and we also compute an estimate of $\Delta_{t,t-8} \left(\ln \tau_{mn} + \ln \tau_{mn} \right)$ from our procedure using residuals of the gravity regression, and then targeting the change in world trade to GDP ratio to pin down the level.

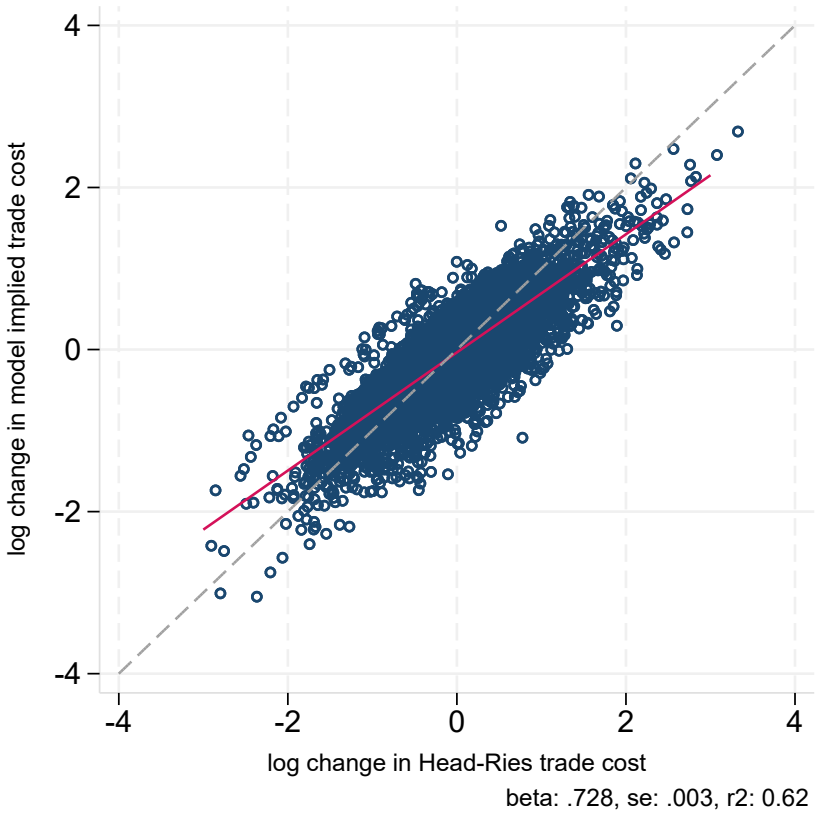
Table C.13 shows summary statistics of the difference between $\tilde{\tau}_{mn}^{HR}$ and our estimates. Figure C.4 shows a scatter plot.

Table C.13: Model implied Trade Cost and Head-Ries Trade Cost

	Average	Median	p25	p75
Log Change in Model implied Trade Cost	-0.105	-0.097	-0.308	0.106
Log Change in Head-Ries Trade Cost	-0.096	-0.084	-0.303	0.104
Difference	-0.009	-.0004	-.161	.157

Notes: We report the summary statistics for our model implied $\Delta \ln \tau_{mn} + \Delta \ln \tau_{nm}$ and the counterpart from the observed Head-Ries trade cost using ICIO dataset between 2002 and 2007. The last row displays the summary statistics of the difference

Figure C.4: Model implied Trade Cost and Head-Ries Trade Cost



Notes: The scatterplot compares our model implied $\Delta \ln \tau_{mn} + \Delta \ln \tau_{nm}$ to the counterpart from the observed Head-Ries trade cost using ICIO dataset.

BIBLIOGRAPHY

S. Aiyar, J. Chen, C. Ebeke, C. H. Ebeke, R. Garcia-Saltos, T. Gudmundsson, A. Ilyina, A. Kangur, T. Kunaratskul, S. L. Rodriguez, et al. *Geo-economic fragmentation and the future of multilateralism*. International Monetary Fund, 2023a.

S. Aiyar, A. Presbitero, and M. Ruta. *Geoeconomic Fragmentation: The Economic Risks from a Fractured World Economy*. CEPR Press, 2023b.

L. Alfaro and D. Chor. Global production networks: The looming "great reallocation". *Structural Shifts in the Global Economy*, page 213, 2023.

F. Alvarez and R. E. Lucas. General equilibrium analysis of the eaton-kortum model of international trade. *Journal of Monetary Economics*, 54(6):1726–1768, September 2007.

M. Amiti, S. J. Redding, and D. E. Weinstein. The impact of the 2018 tariffs on prices and welfare. *Journal of Economic Perspectives*, 33(4):187–210, 2019.

J. E. Anderson and E. van Wincoop. Gravity with Gravitas: A Solution to the Border Puzzle. *American Economic Review*, 93(1):170–192, March 2003.

J. E. Anderson and E. van Wincoop. Trade Costs. *Journal of Economic Literature*, 42(3):691–751, September 2004.

S. T. Anderson, R. Kellogg, and S. W. Salant. Hotelling under pressure. *Journal of Political Economy*, 126 (3):984–1026, 2018.

P. Antràs. De-globalisation? global value chains in the post-covid-19 age. NBER Working Paper No. 28115, National Bureau of Economic Research, 2020.

R. Araujo, F. Costa, and M. Sant'Anna. Efficient forestation in the brazilian amazon: Evidence from a dynamic model. 2022.

C. Arkolakis and C. Walsh. Clean growth. Technical report, National Bureau of Economic Research, 2023.

E. Artuç, S. Chaudhuri, and J. McLaren. Trade shocks and labor adjustment: A structural empirical approach. *American Economic Review*, 100(3):1008–45, June 2010.

S. Asher, T. Garg, and P. Novosad. The ecological impact of transportation infrastructure. *The Economic Journal*, 130(629):1173–1199, 2020.

J. Assunção, C. Gandour, R. Rocha, and R. Rocha. The effect of rural credit on deforestation: evidence from the brazilian amazon. *The Economic Journal*, 130(626):290–330, 2020.

M. G. Attinasi, L. Boeckelmann, and B. Meunier. The economic costs of supply chain decoupling. ECB Working Paper No. 2023/2839, European Central Bank, 2023.

M. A. Bailey, A. Strezhnev, and E. Voeten. Estimating dynamic state preferences from united nations voting data. *Journal of Conflict Resolution*, 61(2):430–456, 2017.

C. Balboni, R. Burgess, and B. A. Olken. The origins and control of forest fires in the tropics. 2020.

C. A. Balboni. *In harm's way? infrastructure investments and the persistence of coastal cities*. PhD thesis, The London School of Economics and Political Science (LSE), 2019.

M. Blanga-Gubbay and S. Rubínová. Is the global economy fragmenting? Staff Working Paper: Research ERSD-2023-10, World Trade Organization, 2023.

M. A. Bolhuis, J. Chen, and B. R. Kett. Fragmentation in global trade: Accounting for commodities. Working Paper 2023-073, International Monetary Fund, 2023.

B. Bonadio, Z. Huo, A. A. Levchenko, and N. Pandalai-Nayar. Global supply chains in the pandemic. *Journal of International Economics*, 133:103534, November 2021.

B. Bonadio, Z. Huo, A. A. Levchenko, and N. Pandalai-Nayar. Globalization, structural change and international comovement. NBER Working Paper No. 31358, National Bureau of Economic Research, June 2023a.

B. Bonadio, Z. Huo, A. A. Levchenko, and N. Pandalai-Nayar. User manual for the bonadio-huo-levchenko-pandalai-nayar (bhlp) global network model version 1.0. mimeo, NYUAD, Yale, Michigan, and UT Austin, September 2023b.

N. Borlaug. The green revolution revisited and the road ahead. Special 30th Anniversary Lecture, The Norwegian Nobel Institute, Oslo., September 2000.

C. P. Bown, E. Jung, and E. Zhang. Trump has gotten china to lower its tariffs. just toward everyone else. *PIIE Trade and Investment Policy Watch*, 12, 2019.

J. Brander and S. Taylor. International trade and open-access renewable resources: The small open economy case. *The Canadian Journal of Economics*, 30(3), 1997.

J. A. Brander and M. S. Taylor. Open access renewable resources: trade and trade policy in a two-country model. *Journal of International Economics*, 44(2):181–209, 1998.

C. Broda and D. E. Weinstein. Globalization and the Gains from Variety. *Quarterly Journal of Economics*, 121(2):541–585, 2006.

S. Brown and D. Zarin. What does zero deforestation mean? *Science*, 342(6160):805–807, 2013.

R. Burgess, F. Costa, and B. A. Olken. The brazilian amazon's double reversal of fortune. 2019.

L. Caliendo, M. Dvorkin, and F. Parro. Trade and Labor Market Dynamics: General Equilibrium Analysis of the China Trade Shock. *Econometrica*, 87(3):741–835, May 2019.

T. Carleton, L. Crews, and I. Nath. Agriculture, trade, and the spatial efficiency of global water use. 2024.

D. A. Cerdeiro, R. Mano, J. Eugster, and S. J. Peiris. Sizing up the effects of technological decoupling. IMF Working paper 2021-069, International Monetary Fund, 2021.

S. W. Chang. Wto disciplines on fisheries subsidies: A historic step towards sustainability? *Journal of International Economic Law*, 6(4):879–921, 2003.

R. Chetty, A. Guren, D. Manoli, and A. Weber. Are micro and macro labor supply elasticities consistent? a review of evidence on the intensive and extensive margins. *American Economic Review*, 101(3):471–75, May 2011.

G. Chichilnisky. North–south trade and the global environment. In *International trade and the environment*, pages 261–284. Routledge, 2017.

C. W. Clark. *Mathematical bioeconomics: the optimal management of renewable resources*. John Wiley & Sons, 1990.

C. Clayton, M. Maggiori, and J. Schreger. A framework for geoeconomics. NBER Working Paper No. 31852, National Bureau of Economic Research, 2023.

D. Comin, D. Lashkari, and M. Mestieri. Structural change with long-run income and price effects. *Econometrica*, 89(1):311–374, 2021.

B. Conte, K. Desmet, D. K. Nagy, and E. Rossi-Hansberg. Local sectoral specialization in a warming world. *Journal of Economic Geography*, 21(4):493–530, 2021.

B. Copeland, S. Taylor, and J. Shapiro. Globalization and the Environment. *Forthcoming Handbook of International Economics*, 2021.

B. R. Copeland. Pollution content tariffs, environmental rent shifting, and the control of cross-border pollution. *Journal of international Economics*, 40(3-4):459–476, 1996.

B. R. Copeland and M. S. Taylor. Trade, growth, and the environment. *Journal of Economic Literature*, 42 (1):7–71, 2004.

B. R. Copeland and M. S. Taylor. Trade, tragedy, and the commons. *American Economic Review*, 99(3): 725–49, 2009.

B. R. Copeland, J. S. Shapiro, and M. S. Taylor. Trade and the environment. *Annual Review of Economics*, 14:155–181, 2022.

C. Costello and S. Polasky. Spatial-dynamic models of renewable resource management. *Environmental and Resource Economics*, 39(2):101–116, 2008.

A. Costinot, D. Donaldson, and C. Smith. Evolving comparative advantage and the impact of climate change in agricultural markets: Evidence from 1.7 million fields around the world. *Journal of Political Economy*, 124(1):205–248, 2016.

J. W. Coulston, G. A. Reams, D. N. Wear, and C. K. Brewer. An analysis of forest land use, forest land cover and change at policy-relevant scales. *Forestry*, 87(2):267–276, 2014.

P. G. Curtis, C. M. Slay, N. L. Harris, A. Tyukavina, and M. C. Hansen. Classifying drivers of global forest loss. *Science*, 361(6407):1108–1111, 2018.

R. S. DeFries, T. Rudel, M. Uriarte, and M. Hansen. Deforestation driven by urban population growth and agricultural trade in the twenty-first century. *Nature Geoscience*, 3(3):178–181, 2010.

K. Desmet and E. Rossi-Hansberg. On the spatial economic impact of global warming. *Journal of Urban Economics*, 88:16–37, 2015.

K. Desmet and E. Rossi-Hansberg. Climate change economics over time and space. *Annual Review of Economics*, 16, 2024.

K. Desmet, R. E. Kopp, S. A. Kulp, D. K. Nagy, M. Oppenheimer, E. Rossi-Hansberg, and B. H. Strauss. Evaluating the economic cost of coastal flooding. Technical report, National Bureau of Economic Research, 2018.

S. Dhingra and T. Sampson. Expecting brexit. *Annual Review of Economics*, 14(1):495–519, 2022.

T. Dominguez-Iino. Efficiency and redistribution in environmental policy: An equilibrium analysis of agricultural supply chains. *Working Paper*, 2023.

D. Donaldson. Railroads of the raj: Estimating the impact of transportation infrastructure. *American Economic Review*, 108(4-5):899–934, April 2018.

J. Elliott, I. Foster, S. Kortum, T. Munson, F. P. Cervantes, and D. Weisbach. Trade and carbon taxes. *American Economic Review*, 100(2):465–469, 2010.

P. Fajgelbaum and S. Redding. External integration and internal development: Evidence from argentina, 1870-1914. NBER Working Papers 20217, National Bureau of Economic Research, Inc, June 2014.

P. Fajgelbaum, P. Goldberg, P. Kennedy, A. Khandelwal, and D. Taglioni. The us-china trade war and global reallocations. *American Economic Review: Insights*, 6(2):295–312, 2024.

FAO. Guide for country reporting for fra 2015. *FRA 2020 Working Paper 184*, 2020.

FAO. The state of world fisheries and aquaculture 2022. towards blue transformation. *The State of World Fisheries and Aquaculture (SOFIA)*, 2022.

FAO. Fishstatj, global fisheries and aquaculture production statistics, 2024a. URL https://www.fao.org/fishery/en/fishstat.

FAO. The state of world fisheries and aquaculture 2024. blue transformation in action. *The State of World Fisheries and Aquaculture (SOFIA)*, 2024b.

F. Farrokhi. Global sourcing in oil markets. *Journal of International Economics*, 125:103323, 2020.

F. Farrokhi and A. Lashkaripour. Can trade policy mitigate climate change? *Working Paper*, 2024.

F. Farrokhi and H. S. Pellegrina. Global trade and margins of productivity in agriculture. *American Economic Journal: Macroeconomics*, 14(3):256–308, 2022.

F. Farrokhi, E. Kang, H. S. Pellegrina, and S. Sotelo. Deforestation: A global and dynamic perspective. *Working Paper*, 2024.

S. Federici, F. N. Tubiello, M. Salvatore, H. Jacobs, and J. Schmidhuber. New estimates of co2 forest emissions and removals: 1990–2015. *Forest Ecology and Management*, 352:89–98, 2015.

E. P. Fenichel, E. T. Addicott, K. M. Grimsrud, G.-M. Lange, I. Porras, and B. Milligan. Modifying national accounts for sustainable ocean development. *Nature Sustainability*, 3(11):889–895, 2020.

J. Fernández-Villaverde, T. Mineyama, and D. Song. Are we fragmented yet? measuring geopolitical fragmentation and its causal effects. NBER Working Paper No. 32638, National Bureau of Economic Research, 2024.

A. D. Foster and M. R. Rosenzweig. Economic Growth and the Rise of Forests. *The Quarterly Journal of Economics*, 118(2):601–637, 05 2003.

C. Freund, A. Mattoo, A. Mulabdic, and M. Ruta. Is US trade policy reshaping global supply chains? World Bank Policy Research Working Paper 10593, World Bank, 2023a.

C. Freund, A. Mattoo, A. Mulabdic, and M. Ruta. US-China decoupling: Rhetoric and reality. *VoxEU Column*, 31, 2023b.

R. Froese, H. Winker, G. Coro, M.-L. Palomares, A. C. Tsikliras, D. Dimarchopoulou, K. Touloumis, N. Demirel, G. Vianna, G. Scarcella, et al. New developments in the analysis of catch time series as the basis for fish stock assessments: The cmsy++ method. *Acta Ichthyologica et Piscatoria*, 53:173–189, 2023.

S. Galle, A. Rodríguez-Clare, and M. Yi. Slicing the Pie: Quantifying the Aggregate and Distributional Effects of Trade. *Review of Economic Studies*, 90(1):331–375, January 2023.

C. Góes and E. Bekkers. The impact of geopolitical conflicts on trade, growth, and innovation. *arXiv preprint arXiv:2203.12173*, 2022.

P. K. Goldberg and T. Reed. Is the global economy deglobalizing? if so, why? and what is next? *Brookings Papers on Economic Activity*, 2023(1):347–423, 2023.

D. Gollin, C. W. Hansen, and A. Wingender. Two blades of grass: The impact of the green revolution. Working Paper 24744, National Bureau of Economic Research, June 2018.

G. Gopinath, P.-O. Gourinchas, A. Presbitero, and P. Topalova. Changing global linkages: A new cold war? IMF Working Paper 2024-076, International Monetary Fund, 2024.

H. S. Gordon. The economic theory of a common-property resource: the fishery. *Journal of Political Economy*, 62(2):124–142, 1954.

C. Gouel and D. Laborde. The crucial role of domestic and international market-mediated adaptation to climate change. *Journal of Environmental Economics and Management*, 106:102408, 2021.

J. Greenwood, Z. Hercowitz, and G. W. Huffman. Investment, capacity utilization, and the real business cycle. *American Economic Review*, 78(3):402–17, June 1988.

S. Hakobyan, S. Meleshchuk, and R. Zymek. Divided we fall: Differential exposure to geopolitical fragmentation in trade. IMF Working paper 2023-270, International Monetary Fund, 2023.

M. C. Hansen, P. V. Potapov, R. Moore, M. Hancher, S. A. Turubanova, A. Tyukavina, D. Thau, S. V. Stehman, S. J. Goetz, T. R. Loveland, A. Kommareddy, A. Egorov, L. Chini, C. O. Justice, and J. R. G. Townshend. High-resolution global maps of 21st-century forest cover change. *Science*, 342(6160):850–853, 2013.

G. Hardin. The tragedy of the commons: the population problem has no technical solution; it requires a fundamental extension in morality. *Science*, 162(3859):1243–1248, 1968.

B. Harstad. Contingent trade agreements. Technical report, National Bureau of Economic Research, 2024.

K. Head and T. Mayer. Gravity equations: Workhorse, toolkit, and cookbook. In K. R. Elhanan Helpman and G. Gopinath, editors, *Handbook of International Economics*, volume 4 of *Handbook of International Economics*, chapter 3, pages 131 – 195. Elsevier, 2015.

K. Head and J. Ries. Increasing returns versus national product differentiation as an explanation for the pattern of us-canada trade. *American Economic Review*, 91(4):858–876, 2001.

T. Hertel. Implications of agricultural productivity for global cropland use and ghg emissions: Borlaug vs jevons". Technical Report 69, GTAP, 2012.

T. W. Hertel. Applied general equilibrium analysis of agricultural and resource policies. *Handbook of agricultural economics*, 2:1373–1419, 2002.

M. Hoel. Should a carbon tax be differentiated across sectors? *Journal of public economics*, 59(1):17–32, 1996.

H. Hotelling. The economics of exhaustible resources. *Journal of Political Economy*, 39(2):137–175, 1931.

A. Hsiao. Coordination and Commitment in International Climate Action: Evidence from Palm Oil. *Working Paper*, 2024.

C.-T. Hsieh, E. Hurst, C. I. Jones, and P. J. Klenow. The allocation of talent and u.s. economic growth. *Econometrica*, 87(5):1439–1474, 2019.

L. Huang and M. D. Smith. The dynamic efficiency costs of common-pool resource exploitation. *American Economic Review*, 104(12):4071–4103, 2014.

Z. Huo, A. A. Levchenko, and N. Pandalai-Nayar. International comovement in the global production network. *Review of Economic Studies*, 92(1):365–403, 2025.

IPCC. 2006 ipcc guidelines for national greenhouse gas inventories. 2006.

IPCC. IPCC, 2014: Climate Change 2014: Synthesis Report. Contribution of Working Groups I, II and III to the Fifth Assessment Report of the Intergovernmental Panel on Climate Change. *Core Writing Team, R.K. Pachauri and L.A. Meyer (eds.)*, 2014.

B. Javorcik, L. Kitzmueller, H. Schweiger, and M. A. Yıldırım. Economic costs of friendshoring. *The World Economy*, 47(7):2871–2908, 2024.

S. Jayachandran, J. De Laat, E. F. Lambin, C. Y. Stanton, R. Audy, and N. E. Thomas. Cash for carbon: A randomized trial of payments for ecosystem services to reduce deforestation. *Science*, 357(6348): 267–273, 2017.

R. J. Keenan, G. A. Reams, F. Achard, J. V. de Freitas, A. Grainger, and E. Lindquist. Dynamics of global forest area: Results from the fao global forest resources assessment 2015. *Forest Ecology and Management*, 352:9–20, 2015.

S. Kortum and D. A. Weisbach. Optimal unilateral carbon policy. 2021.

D. A. Kroodsma, J. Mayorga, T. Hochberg, N. A. Miller, K. Boerder, F. Ferretti, A. Wilson, B. Bergman, T. D. White, B. A. Block, et al. Tracking the global footprint of fisheries. *Science*, 359(6378):904–908, 2018.

D. Lagakos and M. E. Waugh. Selection, agriculture, and cross-country productivity differences. *American Economic Review*, 103(2):948–80, April 2013.

L. Ljungqvist and T. J. Sargent. *Recursive macroeconomic theory*. MIT press, 2018.

K. G. MacDicken. Global forest resources assessment 2015: what, why and how? *Forest Ecology and Management*, 352:3–8, 2015.

J. R. Markusen. International externalities and optimal tax structures. *Journal of international economics*, 5(1):15–29, 1975.

J. McLaren. Globalization and labor market dynamics. *Annual Review of Economics*, 9:177–200, 2017.

I. B. Nath. The food problem and the aggregate productivity consequences of climate change. Technical report, National Bureau of Economic Research, 2020.

F. Noack and C. Costello. Credit markets, property rights, and the commons. *Journal of Political Economy*, 132(7):000–000, 2024.

W. D. Nordhaus. A review of the stern review on the economics of climate change. *Journal of economic literature*, 45(3):686–702, 2007.

G. Osherenko. New discourses on ocean governance: understanding property rights and the public trust. *Journal of Environmental Law and Litigation*, 21:317, 2006.

E. Ostrom. *Governing the commons: The evolution of institutions for collective action*. Cambridge university press, 1990.

H. S. Pellegrina. Trade, productivity, and the spatial organization of agriculture: Evidence from brazil. *Journal of Development Economics*, 156:102816, 2022.

A. S. Pfaff. What drives deforestation in the brazilian amazon?: Evidence from satellite and socioeconomic data. *Journal of environmental economics and management*, 37(1):26–43, 1999.

E. Sala, J. Mayorga, C. Costello, D. Kroodsma, M. L. Palomares, D. Pauly, U. R. Sumaila, and D. Zeller. The economics of fishing the high seas. *Science advances*, 4(6), 2018.

T. Sampson. Brexit: the economics of international disintegration. *Journal of Economic Perspectives*, 31 (4):163–184, 2017.

M. Schaefer. Some aspects of the dynamics of populations important to the management of the commercial fisheries. *Bulletin of the Inter-American Tropical Tuna Commission*, 14(1):25–56, 1954.

J. S. Shapiro. Trade costs, co2, and the environment. *American Economic Journal: Economic Policy*, 8(4): 220–54, 2016.

J. S. Shapiro. The environmental bias of trade policy. *The Quarterly Journal of Economics*, 136(2):831–886, 2021.

I. Simonovska and M. E. Waugh. The elasticity of trade: Estimates and evidence. *Journal of International Economics*, 92(1):34–50, 2014.

M. D. Smith. Linking the biological and human components of the fishery system: the role of economic instruments. *ICES Journal of Marine Science*, 66(6):1965–1973, 2009.

V. L. Smith. On models of commercial fishing. *Journal of Political Economy*, 77(2):181–198, 1969.

S. Sotelo. Domestic trade frictions and agriculture. *Journal of Political Economy*, 128(7):2690–2738, 2020.

E. Souza-Rodrigues. Deforestation in the amazon: A unified framework for estimation and policy analysis. *The Review of Economic Studies*, 86(6):2713–2744, 2019.

U. R. Sumaila, L. Teh, D. Zeller, and D. Pauly. The global ex-vessel fish price database. *Catch reconstructions: concepts, methods and data sources. Online Publication. Sea Around Us (www. seaaroundus. com). University of British Columbia*, 2015.

U. R. Sumaila, D. Skerritt, A. Schuhbauer, N. Ebrahim, Y. Li, H. S. Kim, T. G. Mallory, V. W. Lam, and D. Pauly. A global dataset on subsidies to the fisheries sector. *Data in brief*, 27:104706, 2019.

S. Taylor. Buffalo hunt: International trade and the virtual extinction of the north american bison. *American Economic Review*, 101(7), 2003.

F. A. Teti. Missing tariffs. Mimeo, ifo Institute, June 2024.

T. Tombe. The missing food problem: Trade, agriculture, and international productivity differences. *American Economic Journal: Macroeconomics*, 7(3):226–258, 2015.

V. Traag, L. Waltman, and N. J. van Eck. From louvain to leiden: Guaranteeing well-connected communities. *Scientific Reports*, 9(1):5233, 2019.

F. N. Tubiello, A. Pekkarinen, L. Marklund, N. Wanner, G. Conchedda, S. Federici, S. Rossi, and G. Grassi. Carbon emissions and removals by forests: New estimates 1990. 2020.

UN. United nations convention on the law of the sea. 1833 UNTS 3, 1982. URL https://www.un.org/depts/los/convention_agreements/texts/unclos/unclos_e.pdf. Opened for signature 10 December 1982, entered into force 16 November 1994.

UN. United nations agreement on marine biodiversity of areas beyond national jurisdiction, 2023. URL https://www.un.org/bbnjagreement.

D. A. Weisbach, S. Kortum, M. Wang, and Y. Yao. Trade, leakage, and the design of a carbon tax. *Environmental and Energy Policy and the Economy*, 4(1):43–90, 2023.

WTO. Agreement on fisheries subsidies, 2023. URL https://www.wto.org/english/tratop_e/rulesneg_e/fish_e/fish_e.htm.

Y. Yang and W. Liu. Free trade agreements and domestic value added in exports: An analysis from the network perspective. *Economic Modelling*, 132:106656, 2024.

D. Zeller and D. Pauly. Reconstructing marine fisheries catch data. *Catch reconstruction: concepts, methods and data sources. Online Publication. Sea Around Us (www. seaaroundus. org). University of British Columbia*, 2015.

J. Zhang. Behavioral response to stock abundance in exploiting common-pool resources. *The BE Journal of Economic Analysis & Policy*, 11(1), 2011.